Microwave technology ... in transition

In less than two decades, transistors and integrated circuits have revolutionized the electronics industry; microwave technology is now in the midst of similar transition.

A time of change is a time of opportunity: opportunity for an individual to advance his career and stature, opportunity for a business to revitalize, move into new markets, or expand its present base.

The ability to effect such changes is based upon knowledge. Continuous and vigorous growth of knowledge in new technology is a challenge which can best be met by fully utilizing the advantages which accrue from advanced engineering courses, professional meetings, technical journals, and discussions with colleagues.

Dr. H. J. Woll
Chief Defense Engineer
Defense Electronic Products
Moorestown, N.J.

Our Cover
Dr. Willard T. Patton of Advanced Microwave Technology, Missile and Surface Radar Division, Moorestown, N.J. examines one of the phased arrays for the Advanced Multi-Function Array Radar (AMFAR). The AMFAR array (surrounded by RF-absorbing material for testing) operates at S-band and represents several significant improvements in size, weight, cost, and switching energy requirements (see the Landry paper, p. 20).

Vol 15 | No 3
Oct | Nov
1969

RCA Engineer

A technical journal published by RCA Corporate Engineering Services 2-8, Camden, N.J.

RCA Engineer articles are indexed annually in the April-May Issue.

• To disseminate to RCA engineers technical information of professional value • To publish in an appropriate manner important technical developments at RCA, and the role of the engineer • To serve as a medium of interchange of technical information between various groups at RCA • To create a community of engineering interest within the company by stressing the interrelated nature of all technical contributions • To help publicize engineering achievements in a manner that will promote the interests and reputation of RCA in the engineering field • To provide a convenient means by which the RCA engineer may review his professional work before associates and engineering management • To announce outstanding and unusual achievements of RCA engineers in a manner most likely to enhance their prestige and professional status.

Contents

editorial input

plans and papers

Schedules . . . early research . . . design goals . . . objectives . . . approvals . . . deadlines . . . these words accentuate essential ingredients in planning any engineering task. Every step of the creative technical process requires a carefully laid plan. To deliver a successful product coincident with the market demand, engineers must determine exactly when and where the resources (materials, parts, manpower, final design, and documentation) must be brought together.

In the entire time cycle—from the embryo of a careful plan to the final design—there are usually no idle moments, no time for unrelated work. Thus, at the conception of any project one must define, and subsequently audit, each proposed step.

We submit that one of the vital steps in the research, design, and development cycle is the careful documentation of significant achievements resulting from the work. How else can technical associates, management, and marketing groups be given the information they need to make correct decisions? Thus, at the outset, time should be included in the plan for documenting the total effort.

Government agencies have long recognized this need; they include, with each contract, requirements for periodic status reports, design reports, and test reports in addition to the technical manuals and specifications required. Often in study programs, the only product is the documentation, and engineers on such projects find that they have abundant sources of information to be used in technical papers and society presentations as well as a background for future work. However, regardless of the actual documentation requirements, every engineer will benefit from a well-planned personal documentation program.

Making detailed entries in the engineering notebook is an excellent tool for day-to-day documentation. But if you wait until the end of the project to transcribe the notes into a technical report, you will probably miss (or forget) some of the more subtle points that are worth mentioning. However, when you supplement your notebook with periodic summaries of accomplishments, the task of collecting material for your technical report is lessened. Again, the important ingredient is planning; with proper planning, the technical report will evolve as the project progresses.

One other advantage to documenting your progress according to a plan is that it forces you to re-think the problems—to re-trace the steps as you record them. Thus, it reinforces your confidence that your approach is correct or, in some instances, gives you a second chance to do the job better.

After a technical report is completed, you are only a few steps away from a technical paper for presentation or publication. RCA recognizes the importance of this type documentation by providing several channels (e.g., *RCA Review, RCA Engineer)* and by encouraging publications and presentations in the recognized industry trade and professional literature.

A well-written technical paper reflects credit on your abilities, on your division, on your company, and on your profession.

Future issues

The next issue of the *RCA Engineer* features interdisciplinary aspects of modern engineering. Some of the topics to be discussed are:

Interdisciplinary communication

Multi-discipline engineering

Concept engineering

Metallurgical engineering

Ceramic engineering

Manufacturing engineering

Environmental engineering

Quality engineering

Discussion of the following themes are planned for future issues:

Lasers

RCA engineering on the West Coast

Linear integrated circuits

Consumer electronics

Computerized educational systems

RCA engineering in New York

Computers: next generation

Computer peripherals

Displays, optics, and photochromics

The RCA continuing engineering education program

Dr. J. M. Biedenbach

The need to accelerate the updating of an engineer's professional development in recent years has resulted in RCA initiating the CEE program. Courses in the CEE program are designed to keep pace with the special technical requirements of many RCA engineers. The program is constructed in such a manner to help them use their time allotted for educational pursuits in the most effective and efficient manner.

The Engineer and the Corporation

Dr. Joseph M. Biedenbach, Director
Engineering Educational Programs
Corporate Engineering Services
Camden, N.J.
received the BS in Engineering and the MS in Education from the University of Illinois in 1950 and 1951 respectively. He received the MS in Physics from the University of Michigan in 1957, and in 1964 he received the PhD in Higher Education from Michigan State University. In his present position Dr. Biedenbach is responsible for developing a continuing engineering educational program that can be given at all RCA plant locations at any time. Dr. Biedenbach came to RCA from the Indianapolis Campus of Purdue University where he served as the Assistant Dean for Administration since 1964. In addition, he was Acting Chairman of the Mechanical and Industrial Engineering Technology Department at the Indianapolis Campus. As Senior Technical Instructor at General Motors Institute from 1951 to 1960, Dr. Biedenbach taught college physics, wrote laboratory manuals, developed a Nuclear Physics Lab and published a section entitled "Radioactive Decay" in *Radioisotopes in Industry*, a book developed for the United Nations Peaceful Uses of Atomic Energy Program. As Senior Project Engineer in the Research Lab of A. C. Spark Plug Division of General Motors Corporation from 1960 to 1963, he served as Group Leader investigating encapsulation of gyro components, and high temperature ceramics. During this same period, he developed a film-type pocket dosimeter for use by the Armed Forces. Among his current memberships in professional societies are: American Association of Physics Teachers, American Society for Engineering Education, American Society for Training and Development, Adult Education Association, Phi Delta Kappa, and the Cooperative Education Association.

As members of a distinguished profession, engineers generally consider their career responsibilities to include a constant updating of technical competence. Although the work experience provides an opportunity for engineers to continue to learn and develop, no engineer can stay abreast of his profession by applying only the knowledge acquired while earning a baccalaureate or masters degree. Throughout a lifetime career, an engineer should supplement his learning through formal educational programs or self-guided study. It has been estimated that about 10% of an engineer's time should be spent on "re-learning" what he has forgotten and an additional 10% of his time on acquiring new technical information.

RCA, and other modern employers of engineers and scientists, assist in the professional development of their personnel in many ways. For many years, RCA has played an active role in continuing engineering education through such activities as the Graduate Study Program, the Tuition Loan and Refund Plan, and after-hours courses sponsored at most of its engineering locations.

The Continuing Engineering Education (CEE) program described in this article was developed primarily to meet the particular needs of practicing engineers in various RCA divisions. This special industry-centered program provides courses that are necessarily different from conventional graduate-level courses, theoretically oriented toward the needs of young men working toward engineering bachelors or advanced degrees. The college curricula, while suited for a basic educational foundation, is seldom the most efficient program for engineers working in their profession.

Reprint RE-15-3-21
Final manuscript received August 15, 1969.

Program objectives

Major program goals are to update and advance the technical knowledge of engineers and to help them maintain sound study habits so vital to the continuous advancement of engineers in their professions. The CEE program is designed to supplement each division's in-house training efforts by providing in-depth engineering courses of both general interest to a majority of engineers and specific interest to engineers at each location.

Program format

To permit course scheduling flexibility and facilitate wide distribution of the program to all locations, the material is presented using the TV tape media. The program takes advantage of the unique characteristics of the television medium by the elaborate use of companion visual aids. Major emphasis is on a very high standard of teaching by the course instructors (many of whom are practicing engineers capable of applying the theoretical material presented). The instructors are supported in this objective by modern educational methods, including an evolutionary approach of pilot runs and field tests before actually committing the material to tape Corporate-wide distribution. Because the concept of TV-taped instruction is relatively new and does not allow course participants to pose questions to the instructor appearing on the TV monitor the pilot runs or field tests provide the lecturer an advance opportunity to sample student reaction.

Such advance tests provide a "feel" for the academic level of the course and class acceptance of course content. Thus, the instructor can anticipate many of the questions that might be asked by a group of students during the actual taped version of the lecture.

An associate instructor, knowledgeable in the subject, is recruited from the division where the course is being offered. He acts as a coordinator and resource person for each class session. The associate instructor leads discussions, answers questions, collects homework, and works closely with the CEE staff in Camden on course content and mechanics of the class presentation. This local or divisional contact enables class participants to get answers to questions not anticipated by the lecturer (during initial taping, pilot run, or field test).

Each course is supplemented with textbooks such as one would normally find in a good college engineering classroom. Study guides that closely parallel the lecture are furnished to course participants so that a minimum of note taking is required by the engineer. Visual aids shown on the screen are included in the study guide so that the course participant need only make brief notes in the study guides, eliminating the necessity of drawing figures and sketches that are normally drawn on a chalkboard by an instructor during a typical college engineering lecture.

To help the learning process, TV-tape lectures are interrupted periodically so that short in-class exercises can be completed by the engineer to see if he has assimilated the material given in the lecture. In this way, he has instant feedback concerning his learning accomplishments. If necessary, a taped lecture can immediately be rerun when material has not been assimilated effectively by a group.

Quizzes given periodically throughout each course and a final comprehensive examination covering the entire course content also allow engineers to know how much of the presented material they have assimilated. Upon successful completion of the course, a certificate is awarded to those men who have met the requirements set forth by the CEE staff. This evaluation is based on a combination of factors including attendance in the course, homework material turned in, quiz scores and the score received on the comprehensive examination. Engineers who do an outstanding job in the course are awarded certificates bearing "with distinction" citations. A duplicate certificate is placed in each engineer's personnel folder who successfully complete a CEE course.

Classes are generally operated for approximately 20 to 30 students with operating costs being met by "tuition fees" assessed against each participant's division when he enrolls for a CEE course. Scheduling and timing of classes is left to the discretion of each operating division. Most Divisions are attempting to provide the courses using a company-engineer "time shared" arrangement where operating circumstances permit. Courses normally consist of twelve 2-hour sessions spread over a twelve week period.

Program curriculum

The CEE program provides a varied curriculum for the practicing engineer. Course topics are those recommended by engineers and engineering management from all the divisions and are subjects pertinent to their particular engineering education requirements. A survey taken throughout the corporation resulted in an initial proposed curriculum of approximately 36 program areas. Approximately fifteen courses have been developed to date and additional programs are planned for the future. The average "life" of each course is considered to be approximately 4 years with certain courses being revised at a more rapid rate because of the rapidly changing technology. An advisory committee consisting of a representative from each division, selected by the chief engineer of the respective division, recommends to the CEE Staff courses which they feel their engineers need.

Conclusion

Since September 1968, approximately 950 engineers have taken a CEE course. The overwhelming majority of these engineers feel that TV tape was used successfully as the teaching media and that the time and effort expended in the courses was worthwhile. The program enables Corporate Engineering Services to provide an effective educational program that brings the latest technology in new scientific fields to engineering activities throughout RCA. Brief capsule descriptions of the courses currently available and those in development are listed below:

Courses currently available

C1—Digital computer fundamentals

Course answers the question "How does a computer function?" It covers the basic digital computer system, its organization, machine language programming, binary arithmetic, basic gates, logic design, memory systems, and control circuits.

C2—Fortran programming

Course covers the use of subscripts, functions, subroutines, double precision, and complex and logical variables—with emphasis on writing programs.

C3—RCA basic time sharing system

Course describes the SYSTEM, COMPILER, and EDIT Commands in BTSS. It covers the mechanics of the teletype terminal, use of paper tape, use of the simulated magnetic tape operations, the stored SNODE program to solve differential equations.

E1—Microelectronics for design engineers I

The integrated circuit chip is examined for its unique properties, characteristics, and limitations. The course reviews critically the application of available microelectronic packages and design of new microelectronics from the standpoint of the design engineer. Digital circuits and analog or linear circuits are considered in detail.

E2—Thick-film hybrid circuits

Upon completion of the course, the engineer should have a practical knowledge of the process and materials technology used in the fabrication of thick film circuitry. This course covers topics involved in processing technology including the fabrication processes and design guides as well as applications of thick-film hybrid circuits.

E4—Transistor circuits: discrete and integrated I

Topics to be covered include transistor fundamentals, biasing and stability, audio frequency power amplifiers, small-signal low frequency analysis, multiple transistor circuits and feedback circuits.

E5—Transistor circuits: discrete and integrated II

Topics discussed in depth include integrated circuits, field-effect transistors, low

frequency response of RC coupled amplifiers, high frequency response of RC coupled amplifiers, tuned amplifiers, and frequency response of feedback amplifiers.

E6—Transistor circuits: discrete and integrated III

This course gives the background for the development of more advanced concepts in other courses. Topics covered include: discussion of low frequency response of RC coupled amplifiers, feedback-amplifier fundamentals, high frequency response of RC coupled amplifiers, and tuned amplifiers.

M1—Engineering mathematics I

Topics include calculus review, differential equations and engineering applications, determinants, matrices, vector and tensor analysis. Exercises emphasize practical problems.

M2—Engineering mathematics II

Topics treated include complex variables, Bessel functions, Legendre polynomials, Fourier series, integral and Laplace transformation. Examples from the fields of electromagnetic theory and electronic circuitry are emphasized.

M3—Engineering probability and statistics

Lectures include the concept of a sample space, probability, random variables, probability distributions, point and interval estimation hypothesis testing, analysis of variance, and the design of experiments.

P1-A—Engineering physics

This course is designed to be a comprehensive review of basic engineering physics and provide background for subsequent study. Topics include: statics, dynamics, special relativity, work and energy, impulse and momentum, rotation and harmonic motion.

P3—Modern physics I

Included in this course are relativity, photoelectric effect, photons, the nuclear atom, atomic structure, electron diffraction, deBroglie waves, introductory wave mechanics, energy levels, and X-rays.

P5—Semiconductor device physics I

Topics include crystallography, band theory, Fermi level, donors and acceptors, and optical properties of semiconductors. Types of diodes are presented, and a discussion of the transistor as a small signal device (bipolar, FET, MOS, and injection) is presented.

Courses being developed

C4—RCA time sharing operating system

To provide the engineer with the skills required to write and execute Fortran programs on the RCA Spectra 70/46, using a Teletype Terminal as an input device.

C6—Numerical methods for solution of engineering problems

To develop the skills required to select and to utilize numerical methods for the solution of engineering problems.

C9—Computer-aided circuit design

To provide the engineer with the skills required to utilize existing digital computer programs in the design of electrical and electronic circuits.

C20—Basic logic

This is a basic course in Boolean algebra and logic design. Logic blocks are introduced and a method is developed for translating word problems into Boolean algebra.

C21—Logic and digital computers

This is a course in the application of logic to the design of digital computers.

C22—Logic design and microelectronics

This course deals with the present state-of-the-art in the utilization of microelectronics in digital logic design.

E7—Pulse, switching, and logic circuits I

After a review of basic principles, the subject of linear waveshaping is taken up and pulse transformers and delay lines are examined. Switching, clipping, and clamping circuits are covered in detail.

E8—Pulse, switching, and logic circuits II

This course emphasizes logic circuitry. The basic logic functions and their circuit configurations are examined, along with the details of the circuit design.

E9—Pulse, switching, and logic circuits III

Time base generators are examined as well as sampling gates, counting and timing circuits, synchronization, and transient switching.

E10/11—Basic communication theory I and II

The two courses emphasize the fundamental role of system bandwidth and noise in limiting the transmission of information and stress the unifying principles underlying modern systems. The two courses cover the fundamental principles of analog modulation theory and systems.

E13—Digital filtering and spectrum analysis

The objective is to introduce the design engineer to the technique of accomplishing the filtering function with digital methods. After an introduction to discrete time analysis techniques, the fast Fourier transform is developed and applied to design situations.

E14/15/16—Microwave circuit applications and semiconductor devices I, II and III

A series of three courses aimed at providing the engineer with a comprehensive coverage of microwave semiconductor devices and their circuit application.

E17/18—Advanced amplifier design I, II

The objective of these two courses is to develop the mathematical tools and techniques necessary to design amplifiers with stringent bandpass and phase requirements.

E22/23/24—Feedback theory and control system design I, II, III

The objective of this sequence of courses is to develop a comprehensive background in the subject of feedback theory and servomechanisms from a design engineer's standpoint.

E25—Large-scale integration using MOS standard cells

The objective of this course is to provide the design engineer with the capability to produce custom MSI and LSI P-MOS arrays using circuits from a standard-cell family.

E26—Phaselock techniques

After an introduction into the nature and applications of phaselock, the various orders of loop types are considered and root-locus plots are drawn. The effect of noise is examined and tracking problems are reviewed.

H1—Applied heat transfer

Topics include: brief review of the modes of heat transfer and the systems of units; steady-state conduction through simple geometric surfaces, transient conduction, transfer by convection through extended surfaces, transfer by radiation, heat exchangers, body temperature profiles, and thermal testing.

M4—Elementary statistics

Topics included are: laws of chance, methods of describing incoming data, statistical models, sampling, statistical tests, and design of experiments.

M5—Engineering mathematics III

To develop a background in mathematical functions and complex variable theory. Special functions include gamma, beta and error functions, Bessel and Legendre functions, orthogonal curvilinear coordinates and solutions to Laplace's equation.

P1-B—Engineering physics

Course is designed to be a comprehensive review of basic engineering physics and provide background for subsequent study.

P2-A—Engineering physics

Course is designed to be a comprehensive review of basic engineering physics and provide background for subsequent study.

P2-B—Engineering physics

Course is designed to be a comprehensive review of basic engineering physics and provide background for subsequent study.

P4—Modern physics II

Included are the topics of radioactivity, nuclear physics and cosmic rays. These concepts, especially wave mechanics are then used to explain the mechanical, electrical, thermal, magnetic, and optical properties of the solid state.

Synthesis of phased-array radar systems

Dr. A. S. Robinson

Major future trends in phased-array radar systems are identified in this paper by exploring the relative roles of operational requirements, system design, science, and technology in achieving minimum life-cycle costs.

TRENDS EMERGE from a continuing interplay between problems that need solutions and tools from which these solutions can be forged . . . our knowledge of systems, of science, and of technology. To derive an optimum system, a criterion for measuring the relative effectiveness of different proposed designs must be determined. Over the past decade, minimization of *life-cycle costs* has emerged as a very practical and logical criterion for the selection of optimum defense systems.

First selection process

The selection process is shown in simplified form in Fig. 1. Problems to be solved appear initially in many forms —ranging from documented operational requirements to informal knowledge of customer needs. Early in the problem solving process, these needs must be defined more precisely—usually in terms of system performance requirements against a "threat" model. Initial temptations, seldom resisted, tend toward establishing very high performance levels against worst-case threat levels such as number, distribution and speed regimes of targets; for clutter, chaff and ECM levels.

In response to the performance and threat, so defined, various fundamental systems for coping with the problem are postulated; and, for each such system, alternate embodiments are conceived. Resultant equipment designs are weighed in the light of current and projected technology, including information gained in prior related equipment and system developments. From these considerations, life-cycle-cost models are evolved to define the full costs to the military. Such costs include developing, producing, operating, maintaining, supporting, and protecting the desired system in the field throughout its life, or for some fixed period of time.

Reprint RE-15-3-3
Final manuscript received August 1, 1969.

A second look

Having succumbed to initial temptations, these costs are usually substantially greater than the bounds established by budget constraints, and so compromises in system performance and/or in the level and complexity of threat become essential. While some elements of the threat, and some performance requirements, cannot be changed, other elements often represent desirable, rather than essential, constraints. Perturbation of these variable elements of performance and threat begins the second turn around the loop. Iterations continue until a suitable threat/performance/system/equipment/cost compromise is found, or until it becomes apparent that the degree of performance and threat level that can be met, does not merit the cost.

Sometimes the judgments involved in these decisions become a matter of national debate. More often, necessary compromises are made with full knowledge that the system selected is not the ultimate answer to the problem, but is simply the best answer within the constraints dictated by technology, the national economy, and national and military priorities.

Role of phased arrays

During the past twenty years, phased-array radars have appeared as candidates for the solution of many different problems. During most of this period, technology limitations have worked strongly against the success of these systems. Some early phased-array programs foundered on the rocks of optimistic estimates of technological capability and overly complex system designs—made necessary by unrealistically high levels of assumed threats. Other programs accepted the limitations imposed by technology, but then suffered from a level of performance that was not really adequate in certain critical problem areas. One of the most popular compromises was the use of frequency scanning, a technique intrinsically limited in bandwidth and susceptible to modest levels of electronic countermeasures.

During recent years, the phased-array technology/performance gap has slowly closed. As a result, high-performance phased-array radars have emerged as cost-effective sensors for a number of new defense systems, and loom as strong contenders for many future defense applications. Many such radars are based on variations of the design approach of Fig. 2. In this system, a single aperture is used for both transmit and receive. One or more

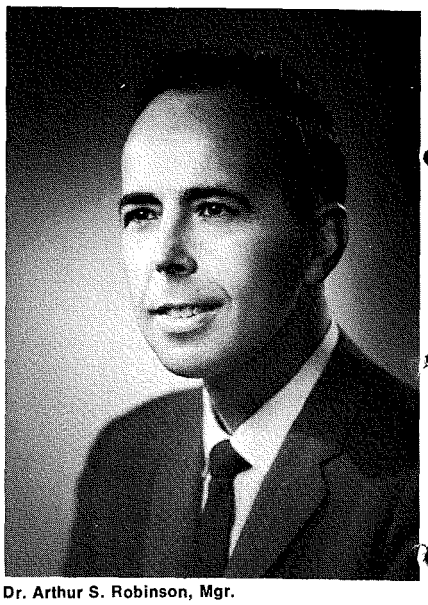

Dr. Arthur S. Robinson, Mgr.
Systems and Advanced Technology
Missile and Surface Radar Division
Moorestown, N.J.

received the BSEE from Columbia University, the MSEE from New York University, and the Doctor of Engineering Science degree from Columbia University. As Technical Director of RCA's Missile and Surface Radar Division, Dr. Robinson is responsible for the synthesis of both present and future systems, and for developing advanced technology consistent with these system goals. RCA's Missile and Surface Radar Division is active in the areas of air defense systems, surveillance, warning and control systems, range and reentry instrumentation, and tactical sensors. Before joining RCA, Dr. Robinson was Assistant Chief Engineer of the Bendix Eclipse-Pioneer Division and then Director of Kollsman Instrument Corporation's Research Division. He is a member of the Tau Beta Pi and has received 42 U.S. and foreign patents covering electronic sensing, signal processing, computing, and control systems.

transmitter tubes are used to generate RF power, with the energy from each tube distributed through an RF feed to thousands of high-power phase shifters, each in series with a radiating element. Each phase shifter is controlled by a phase shift driver, with the driver controlled by commands from a central beam-steering controller.

Need for subarrays

In radar designs requiring large apertures and wide bandwidths, the entire radar array is subdivided into a number of smaller subarrays, with each subarray driven from a single transmitter tube. The phase shifters in the main array steer the relatively broad subarray patterns to the commanded pointing angle, while time-delay units in series with the coherent exciters feed signals to each transmitter that "fine-steer" the narrow array beam to the precise commanded angle.

The time-delay units compensate for the differential path lengths encountered by energy emanating from each subarray. If technology could give us low-cost, high-power, low-loss, time-delay units, we would use them in wide bandwidth systems instead of phase shifters, and not bother with subarrays. Since such units are not yet within the state-of-the-art, we use available, relatively high-loss, high-cost, designs in modest quantities and at low-power levels to achieve reasonable bandwidth capabilities, even with large radar antenna apertures.

The subarray approach offers advantages even in moderate bandwidth applications, where fine-steering phase shifters can be used instead of time-delay units. The advantages stem from the fact that comparably located phase shifters in each subarray receive the same steering command. This feature can be used to minimize the cost and complexity of the beam-steering controller and the subarray phase-shift drivers.

Small-aperture systems

In some small-aperture systems, the entire radar can consist of a single tube, feed, and phase-shifter array. In these applications the bandwidth requirements are low enough and the aperture small enough that neither time-delay steering nor subarrays are needed.

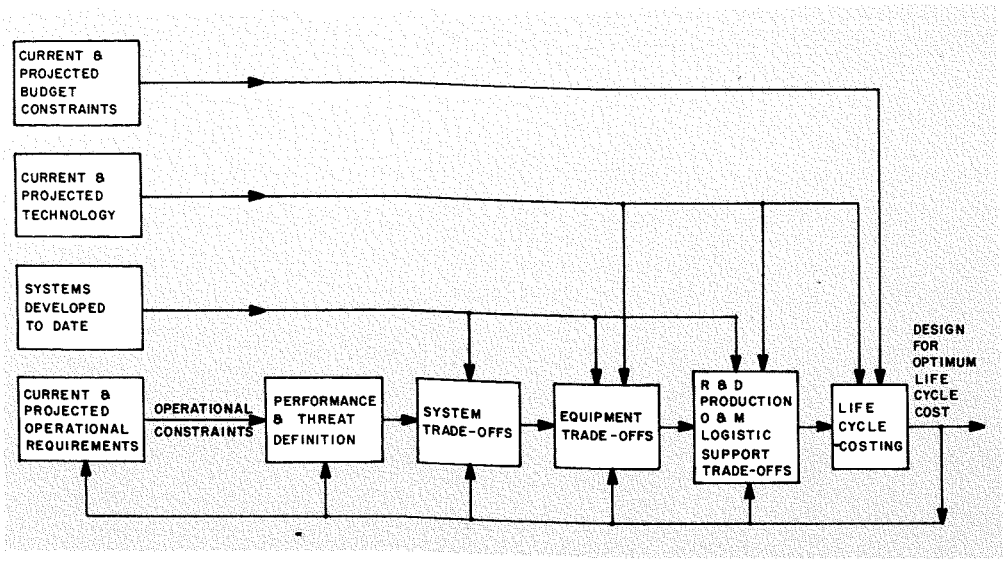

Fig. 1—Some functional factors affecting the design of next generation radars.

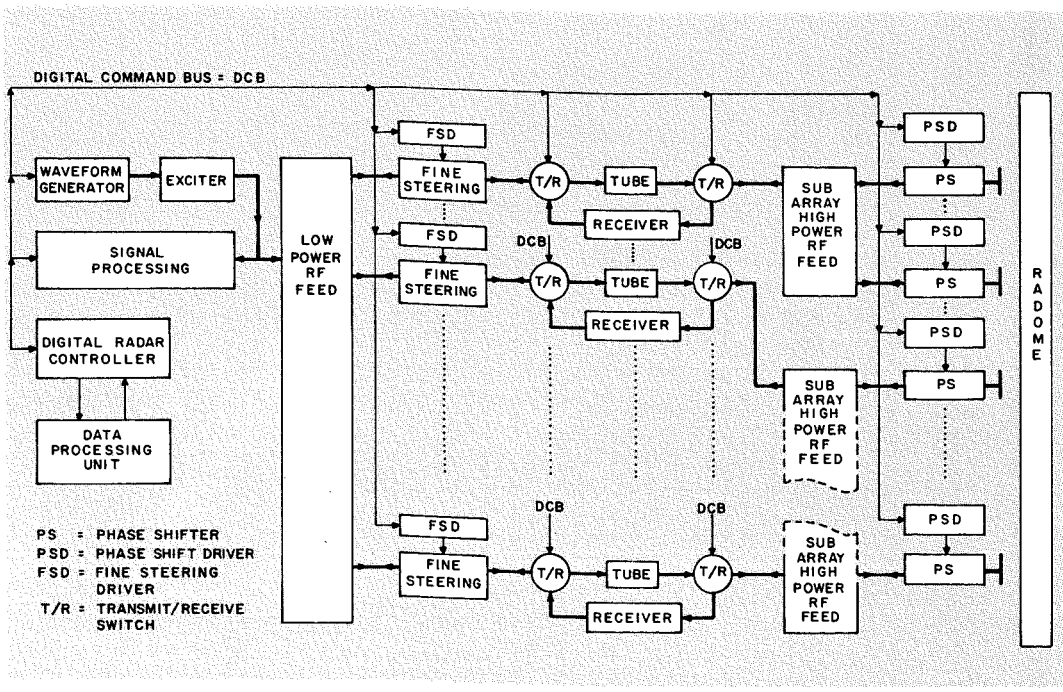

Fig. 2—Simplified block diagram—typical tube-driven phased array radar.

No attempt will be made here to show the many variations on this basic theme. The important point to be made is that tube-driven radars using high-power, low-loss phase shifters following the transmitter are a significant class of phased arrays that have only recently broken the cost/performance barrier. Such phased arrays *will represent a major trend in phased array design for at least the next decade.* We can expect to see arrays of this type implemented for land, sea, air, and space applications in the years ahead.

Science had a major role to play in this achievement—through improvements in tube elements, making possible superior transmitter designs, and even more important, through materials research that pointed the way to economical, efficient, high-power phase shifters. Technology gave us the actual design of the transmitters and phase shifters, as well as economical hybrid digital/analog phase-shifter drivers; compact, efficient feeds; and superior radomes and radome-phased-array design tech-

niques. The hardware shown in Fig. 3 illustrates some of these advances. Signal processing and data processing have also advanced significantly as part of this technology progress package.

These improvements are by no means complete. The years ahead will see continuing refinements and enhancements of this class of system, with particular emphasis on system producibility and on techniques for decreasing both hardware and software costs.

New technology—tubes vs. solid state

Phased array design, after twenty years of slow progress, is now profiting from a burst of new technology—some of it directly benefiting tube-driven phased arrays, and some applicable only to new phased-array design concepts.

Some of the technology pacing the new array design trend is suggested in Figs. 4 and 5. Fig. 4 highlights progress in solid-state RF power sources and receivers, while Fig. 5 shows typical devices, packaged with their associated circuitry in hybrid microwave integrated-circuit form. Power curves are based on average power from a single active chip. Typical power-amplifier modules will combine in the order of 2 to 10 such active elements on a single substrate.

In comparing transistor, bulk, and avalanche power sources, it is important to remember that in many applications transistors cannot be operated at their full average power ratings, due to system duty cycle constraints. A derating factor of 5 to 10 is often necessary, depending on the permissible transmitter duty cycle. Bulk and avalanche sources, on the other hand, generate substantially higher peak than average power, so no such derating is necessary.

Rough cost figures have been included to provide an insight into the problem. If RF power alone determined the cost of a phased array, then solid-state systems would not currently be in the running. But the fact is that completely solid-state phased-array designs are becoming increasingly competitive in many applications — when compared on a life-cycle cost basis.

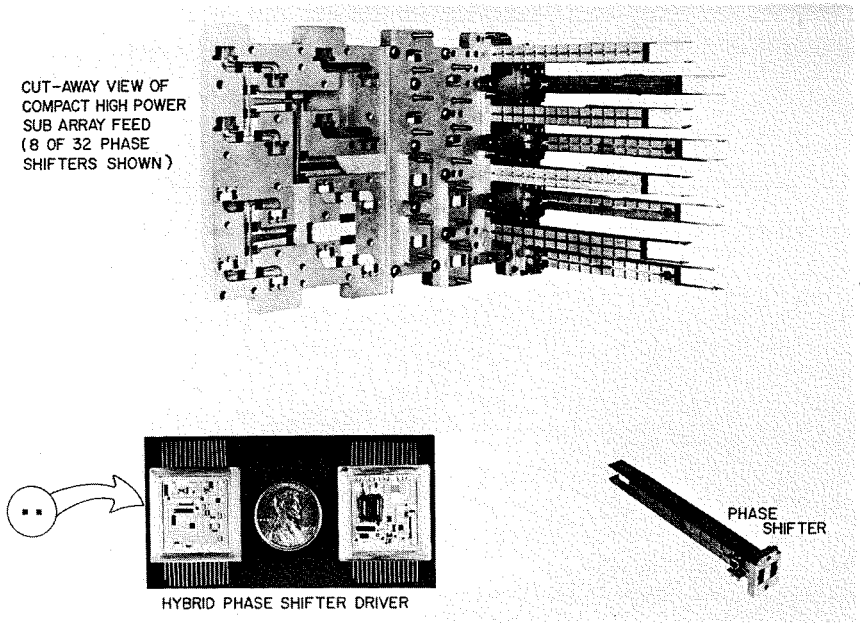

Fig. 3—Typical high-power phased-array radar sub-array components.

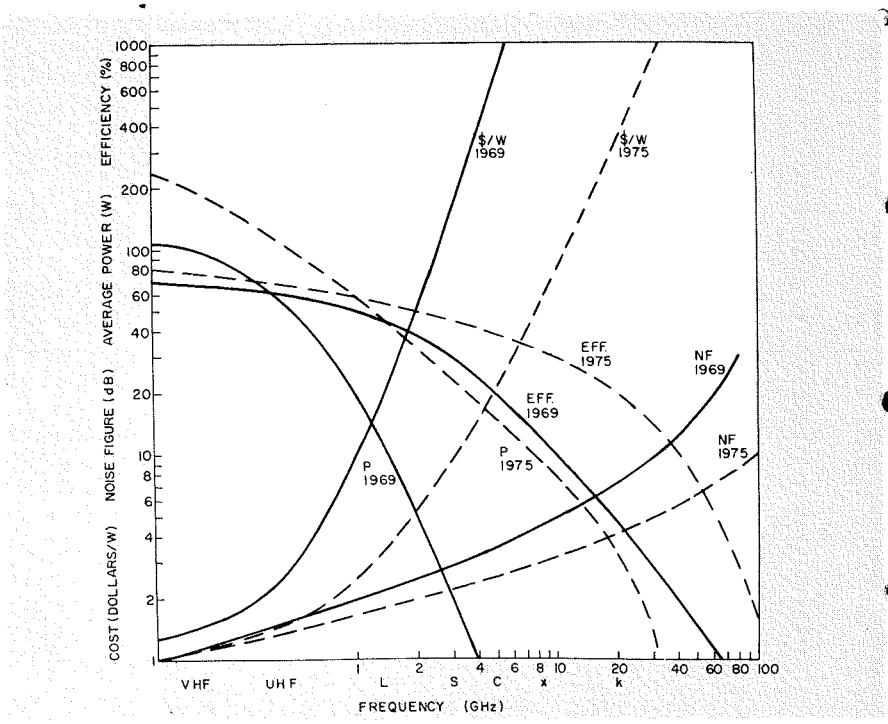

Fig. 4—Solid-state device trends.

The typical solid-state phased-array radar design of Fig. 6 illustrates factors that tend to counterbalance the higher initial cost of solid-state RF power. Each radiating element is driven by a phase shifter in series with a power amplifier. Some designers feel that tubes can compete with solid-state power amplifiers in this type of duplexed array, but the trend seems strongly toward solid state. In a conventional tube-driven phased array, about half the RF power is lost in the feed and high-power phase shifters, on its way to the radiating elements. In the solid-state design, the power amplifiers drive the radiating elements directly. Losses in the feed and phase shifters occur at low power and therefore have negligible effect on efficiency. Lightweight, low-cost, compact feeds and phase shifters become feasible in exchange for losses at a point where radar system performance is not significantly affected. In conventional tube designs, the high-power phase shifters require relatively high-power drivers to set them on command, while substantially lower-power, higher-speed, drivers do the job in the solid-state design. This increased switching speed is of particular importance in high-density tracking applications.

In the conventional tube design, all of the power lost in the phase shifters

has to be carried away by an integral cooling system, above and beyond the transmitter cooling requirements. The solid-state design requires cooling only for the solid-state power amplifiers. In lower frequency applications, the net solid-state power-amplifier efficiency will be substantially better than the efficiency of a competing tube transmitter. On "receive," the solid-state system amplifies the signal before it passes through phase shifters; this minimizes the effect of phase-shifter losses, and introduces a new flexibility for handling received RF signals. Because the signals are amplified immediately, they can drive a variety of lossy microwave circuits without significantly affecting system noise performance. Thus, lossy microwave time-delay devices such as microwave acoustic-delay lines become serious long-term contenders to replace phase shifters; multiple "receive" beams can be formed simultaneously; and circuits can be so configured that pilot signals received from anywhere within the antenna field-of-view automatically point the antenna beams at the pilot tone sources

Think about the rich variety of antenna designs that have emerged in the past using essentially only passive components. As these new active RF devices evolve, we can expect many new and exciting improvements in the design of solid-state antennas.

But this is only part of the tube vs. solid-state story. An overview of the relative cost distributions in a typical trade-off between two such systems is shown in Fig. 7. It has become clear that the actual life-cycle costs of many defense systems are strongly affected by the ease with which they can be operated, maintained, supported, and protected in the field. Reduction in the number of military personnel required to perform these functions is an area of great potential cost savings—for each individual so reduced proportionately decreases the service personnel and facilities needed to maintain that man and his functions in the field. The most intriguing aspect of solid-state phased arrays is their potential ability to meet high levels of threat, while simultaneously requiring substantially less field support due to their increased reliability.

In some applications these cost savings more than compensate for higher initial solid-state system costs. However, solid state is not a panacea; for example, it is not yet a serious contender for high-power applications at or above S-band. It is a contender for high-power applications at L-band and below, and for low-power applications in all microwave frequency bands. The only way to really know whether a solid-state design is sensible for a given application, is to go through preliminary designs of the best competing solid-state and tube approaches for that use, and to then compute their relative life-cycle costs.

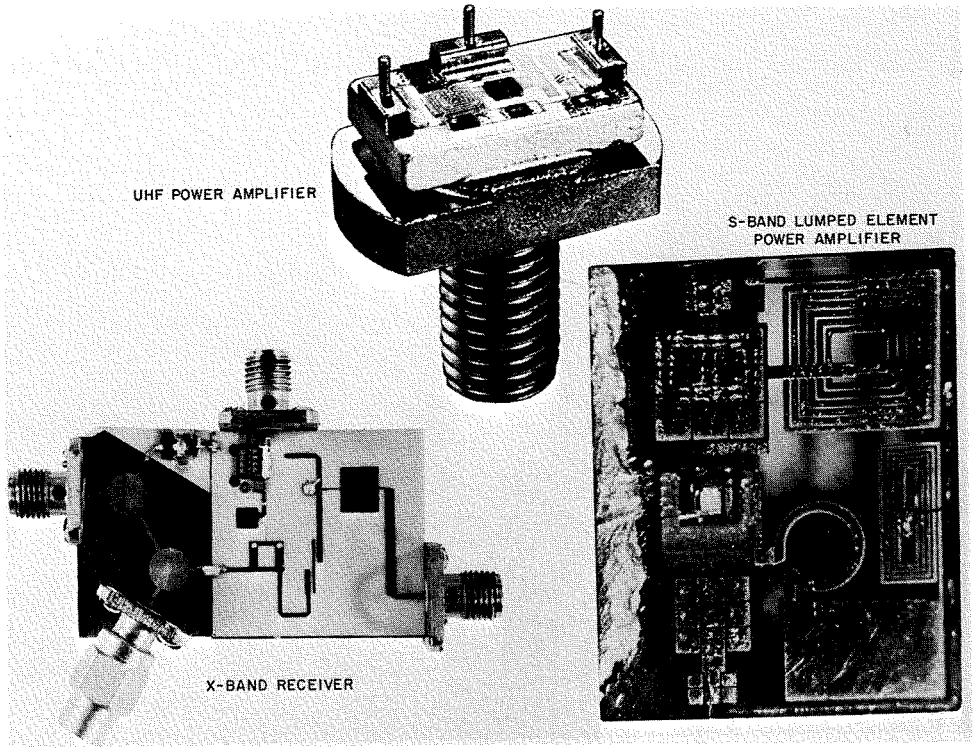

Fig. 5.—Typical solid-state microwave integrated circuits and devices.

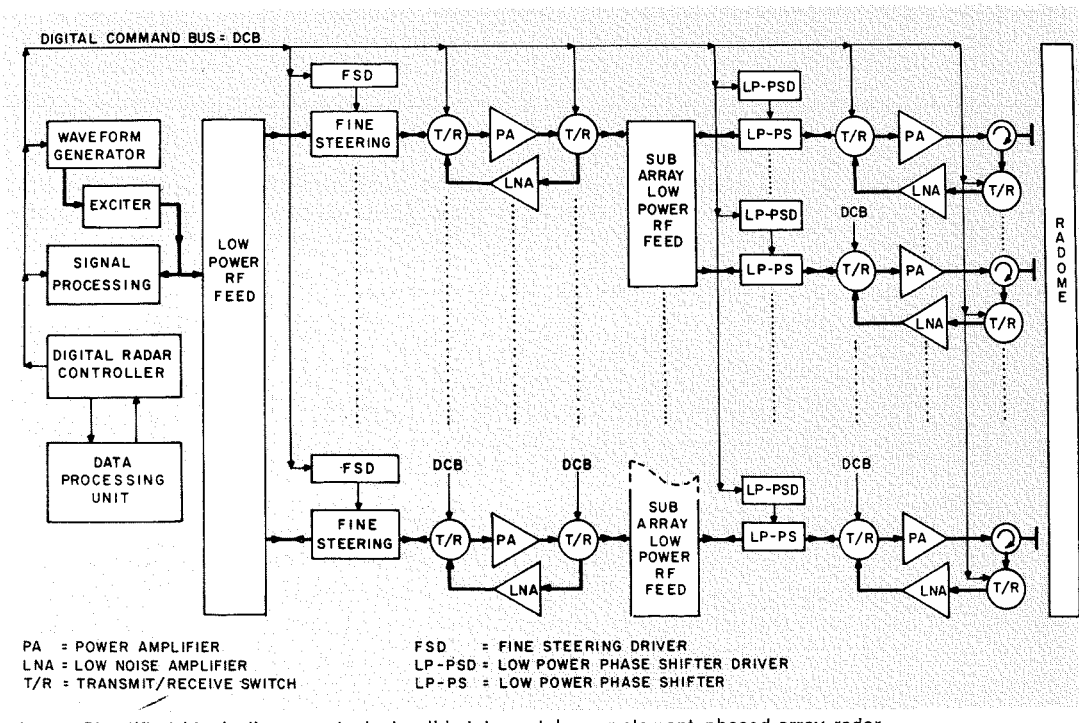

Fig. 6—Simplified block diagram—typical solid-state or tube-per-element phased-array radar.

A trend to digital signal processors

A technology trend of importance for both solid-state and tube applications

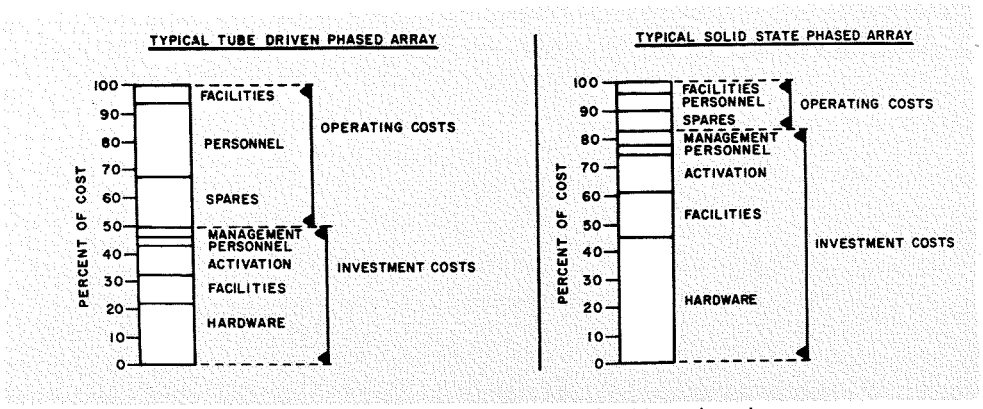

Fig. 7—Typical distribution of cost—solid state and tube-driven phased arrays.

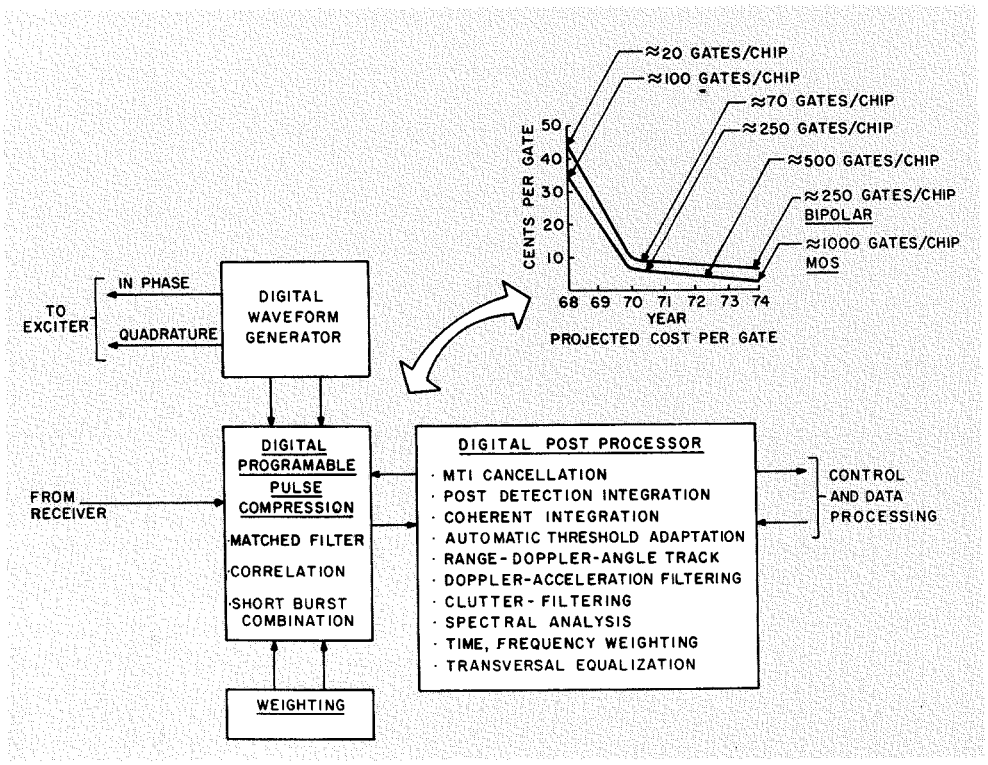

Fig. 8—Digital signal-processing functions.

is illustrated in Fig. 8. We can expect the projected price break in medium and large-scale digital arrays to have a significant impact on phased-array radar signal and data processing. In signal processing, more functions will be implemented in digital form, while analog-to-digital conversion functions will move progressively up the RF chain. Highly adaptive techniques will thus become an economic reality as signal-processor action comes increasingly under programmable software control.

The structure of a typical high-speed-digital signal processor is suggested in Fig. 9. For applications involving wide bandwidths and time-bandwidth products, conventional digital time-shared data buses will give way to non-time-shared networks, switchable under computer control. Extensive paralleling and pipeline processing will compensate for data-rate limitations of individual conversion and computing elements. Many variations on this theme are to be expected. For example, in applications requiring processing of only a limited number of range cells, it will be possible to minimize digital signal-processor functions by loading analog-to-digital converter outputs into a high-speed memory, and, using the system data processor, to operate on such data at lower speeds. At the other end of the spectrum, it should prove feasible in some applications to digitize data directly after amplification at the antenna receiving elements, and thereby include antenna beam forming as part of the digital signal-processing function.

The flow of data and commands between the signal processor, radar controller, system data processor and the overall radar system is illustrated in Fig. 10. In essence, the radar controller performs all functions necessary to match the signals flowing to and from the data processor to the rest of the radar system.

Role of data processing

Data processing remains a major problem in many phased-array radar applications. Complete weapons systems of which these radars are a part often require reaction times that make automatic operation essential. For demanding applications, establishing the computer architecture best suited to the threat is a major problem. Once the computer architecture is established, developing software to cope with the constantly shifting spectrum of targets, clutter, chaff, jamming, decoys, and interference is a monumental challenge. We can expect this area to assume increasing importance over the years, with a greater share of system investment going into improving real-time programming, as well as into developing the programs themselves.

For complex applications, data processing architecture is moving toward the simultaneous use of a multiplicity of processors. Figs. 11 and 12 present one of the many competing architecture concepts in this area to provide plexity of these machines.[1] The computing modules (Fig. 11) all operate under control of an executive computer; the executive allocates portions of the data processing task to individual modules, and establishes appropriate data routing, consistent with these tasks. Adjacent modules communicate through local data exchanges, while all modules can exchange data and instructions with one another and the executive over time-shared data and instruction buses. It is possible to configure hardware and software for this system so that the executive computer function can be assumed by any module.

Each computing module consists of many digital processors (Fig. 12). These processors can communicate with their adjacent neighbors within

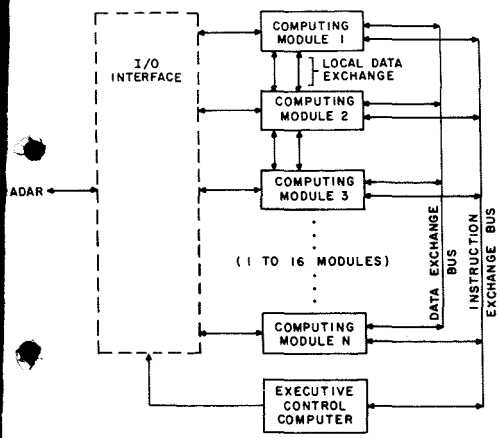

Fig. 11—Modular array data processor.

the module and to their neighbors in adjacent modules. In the example shown, a total of 16 processors are used in a computing module, while 16 computing modules are combined in the data processor—a total of 256 computers operating simultaneously on a common problem.

Conclusions

There is a final trend that I would like to call to your attention—the need for multiple-function, multiple-frequency, phased-array antenna complexes, capable of servicing all of the antenna requirements for a given vehicle. This need is particularly acute in aircraft, spacecraft, and ship applications, and in certain tactical Army systems where the available space for well situated antennas is extremely limited; at the same time, the number of subsystems requiring antenna access is constantly growing. Expect a trend, then, toward unified designs of the phased-array antennas for such systems, consistent with the frequency and time conflicts arising in any time-shared operation. Such conflicts will make the utilization of a single antenna for all functions extremely difficult when multiple systems are involved. Thus, a small cluster of arrays is a more likely possibility. There is every reason to believe, however, that time and frequency sharing of phased-array antennas between a family of systems will come into widespread use in the years ahead.

Acknowledgment

The assistance of M. Breese, H. Halpern and J. Kelble in the preparation of figures is appreciated.

Reference

1. This architecture is closely related to the University of Illinois, ILLIAC IV

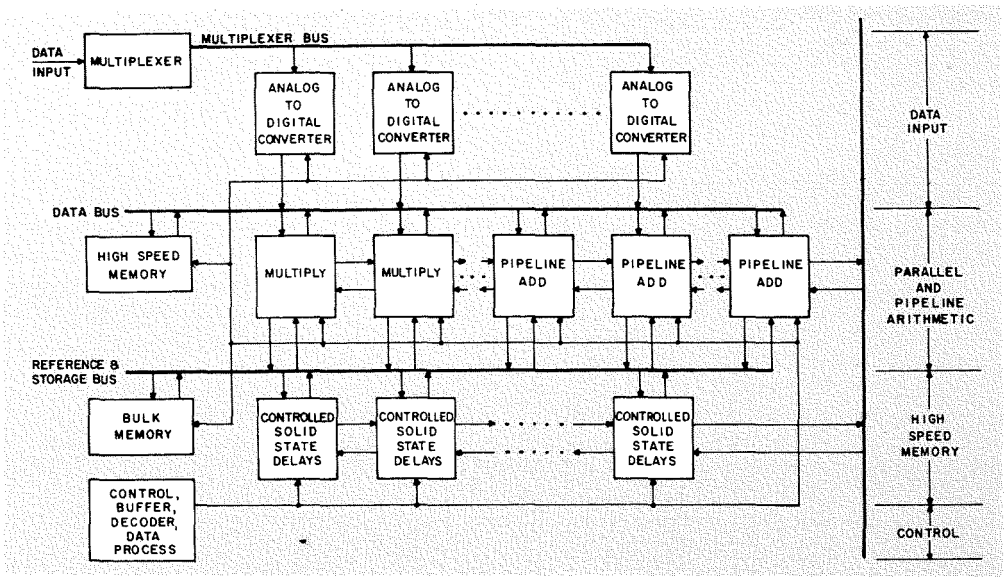

Fig. 9—Parallel, pipelined, digital signal processor.

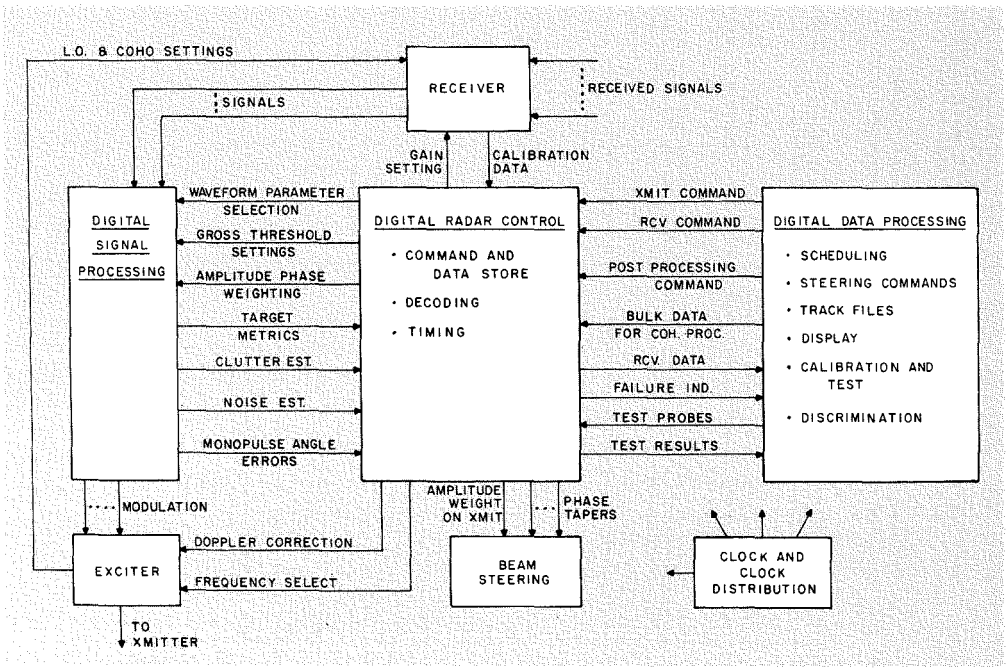

Fig. 10—Inter-relationships between digital sub-systems.

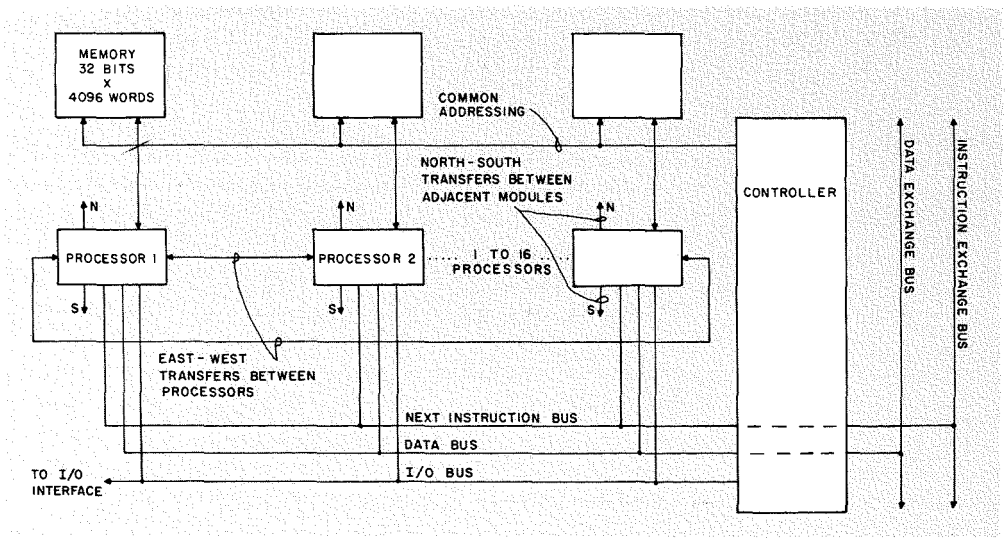

Fig. 12—Typical computing module.

Solid-state microwave antenna systems

F. Klawsnik

Recent advances in solid-state technology at microwave frequencies are having a tremendous impact on the design of radar systems. Specifically, microwave phased-array radar systems can now be designed to operate at many frequency bands and perform several functions simultaneously. It is possible to replace several existing conventional systems in a given location by a single multifunction system at a considerable savings of cost and space. This versatility of a single radar is achieved through the flexibility of modules of microwave integrated circuits.

THE CHARACTERISTICALLY SMALL SIZE of microwave integrated circuits permits increased packing density of a variety of microwave microelectronic circuits behind each radiating element in a phased-array antenna system. This permits the antenna to be simultaneously operated in several frequency bands and to perform many functions (e.g., radar, communication, etc.) through a common radiating aperture. Such systems are presently being developed for early application in high-performance aircraft to provide radar, communications, and electronic warfare functions. In addition, studies are in progress to replace the many radar systems currently in existence on naval combatant vessels with multipurpose integrated antenna systems carefully selected for compatibility with the vessel environment and located to optimize the functional operation of the vessel by reducing superstructure height, increasing ship stability, and making the vessel less visible to eye and to radar. Another advantage of performing a multiplicity of functions through a common radiating aperture is an improvement in the utilization of the few optimal antenna positions on the vehicle so as to obtain a clear field of view for a large number of antenna beams, and thereby eliminating the shadowing of the antenna beam by vehicle structure and other antennas.

The modular organization inherent in microwave integrated circuits also provides for orderly expansion and contraction of radar functions in order to fit a variety of vehicles or missions. In addition to the aforementioned system advantages, microelectronics have the intrinsic advantages of a decrease in volume, weight, power drain, heat dissipation, and operating voltages plus high reliability permitting maintenance-free operation and reduced life-cycle cost.

An example of a microwave module for a dual-function two-frequency-band phased array is shown in Fig. 1. This *L*- and *S*-band module is designed to feed microwave power to one *L*-band radiating element and nine *S*-band radiating elements in physically the same phased-array aperture. The *L*-band array is electrically smaller than the *S*-band array and, therefore, has a broader beamwidth. Also, the *L*-band portion of the module is more efficient because it does not contain the 3:1 multiplier. The *L*-band array is, therefore, comparatively speaking, more suited for the search function where high average power is required and angular resolution is not a severe problem.

For tracking functions, on the other hand, high average power can be sacrificed for the required angular accuracy and resolution. This is obtained because the common array aperture is electrically larger at *S*-band. The *S*-band energy is derived from the *L*-band power chain and the 3:1 multiplier. Although the search and tracking transmitted pulses are programmed so as not to occur simultaneously, the search and tracking functions in effect are performed concurrently.

An example of a dual-frequency-band phased array is shown in Fig. 2. Here the radiating element is a probe-fed slot. The *S*-band probes are located at the base of the slots in septum-divided sections. These are isolated from the *L*-band signal by the cutoff nature of these sections. The *L*-band signal is excited by probes located near the mouth of the slot. These probes are tuned to present an open circuit at *S*-band to provide high isolation between *S*-band and *L*-band operation. If higher power operation at *L*-band were required, more *L*-band radiators and more modules could be used in a similar design without sacrifice of performance. The design can also be extended to operation in three frequency bands by similar techniques or by using an orthogonal polarization in one of the frequency bands.

The design of multi-frequency phased array has become feasible because the integrated microwave transmitter and receiver circuit can be placed directly behind the radiating element. In conventional phased arrays, where a single high power RF source is used to feed many radiating elements, small-size feed networks are not practicable because of the large loss in expensive RF power.

RCA reprint RE-15-3-10
Final manuscript received September 8, 1969.

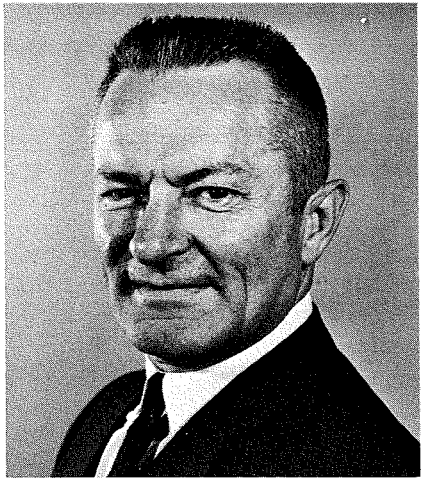

Frank Klawsnik, Mgr.
Advanced Microwave Technology
Missile and Surface Radar Division
Moorestown, N.J.

received the Bachelor of Social Science in 1946 from Brooklyn College and the Bachelor of Electrical Engineering in 1949 from the Polytechnical Institute of Brooklyn. He started his business career in electronics in 1945, and by 1951 he attained the position of Senior Engineer at Sperry Gyroscope. In 1953, he was promoted to Engineering Section Head having the managerial responsibility of the microwave engineering in charge of the development of air, surface, and counter-measure radars. He is presently the Manager of Advanced Microwave Techniques Engineering for M&SR. Mr. Klawsnik is a Senior Member of the IEEE; past Chairman of the Professional Group on Microwave Theory and Techniques and the Professional Group on Antennas and Propagation in Philadelphia. He has been Chairman of the Program Committee for the Philadelphia Section Meeting of the IEEE; advertising Manager of the PGMTT Transactions. Presently he is US Technical Advisor on Transmission Lines and Fittings to TC-46B of the International Electro-mechanical Commission; Chairman of Electronic Industries Association on Waveguides and Fittings; and a member of the USAS committee on Techniques and Instrumentation for Evaluating Radio Frequency Hazards to Personnel.

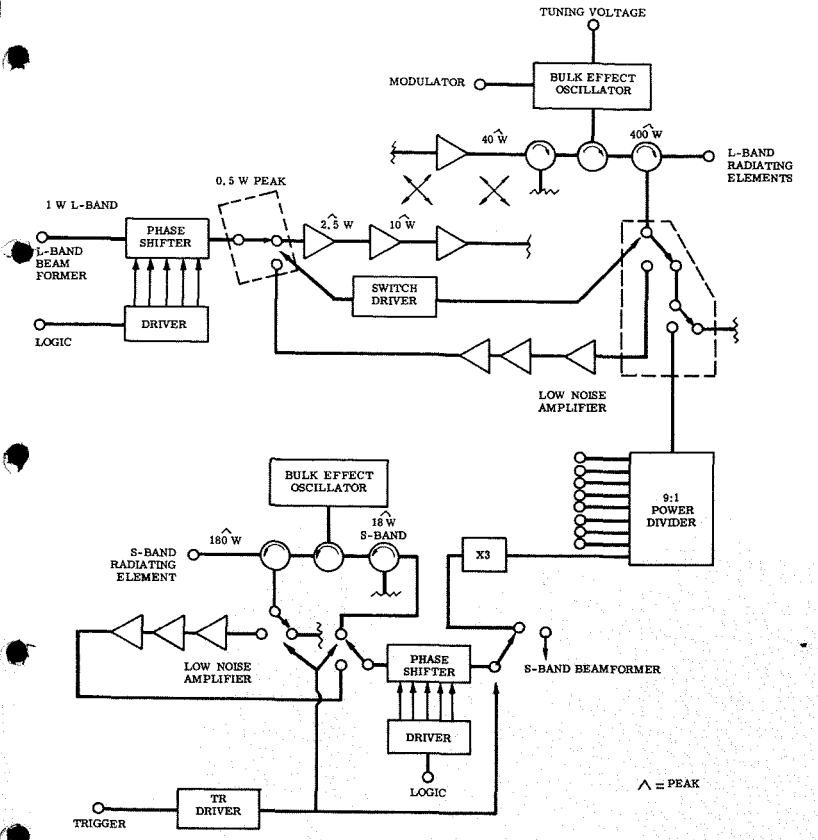

Fig. 1—S/L-band microwave module.

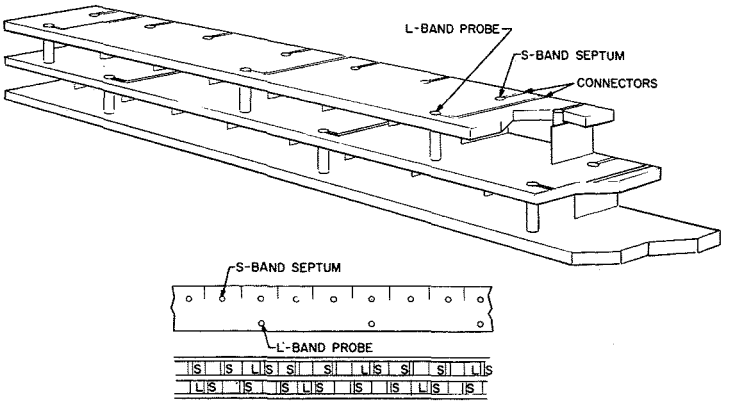

Fig. 2—S/L-band phased array.

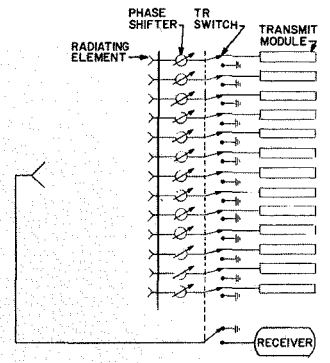

Fig. 3—Transmission-reflective array.

To generate very high RF power density per unit area of antenna aperture, a large number of microwave solid-state sources are required. This requirement prompted the development of arrays of electrically-small densely-packed radiating elements. In this case, power summation occurs in free space, in the radiated beam, and all power combiners are eliminated. It was long thought that arrays of electrically-small closely-spaced elements were highly reactive and nearly impossible to match over a useful band. RCA has developed a technique which circumvents this difficulty and, in fact, provides more bandwidth than arrays of half-wavelength spaced radiators.[1] Two developments—the flexibility of array aperture design afforded by the "closely-spaced element" concept and the practice of obtaining solid-state power at the upper microwave frequencies by multiplication from lower frequencies—spark the present development of multi-frequency apertures. These developments are expected to allow solid-state radars to develop greater capability through RF power programming.

Transistors are peak power limited, and for economic reasons, it is advisable to utilize long pulse widths. Long pulse widths necessitate sophisticated signal processing tecnhiques for clutter suppression and high resolution. Advanced techniques in digital processing are being developed which economically solve these problems.

Present solid-state array radar systems such as RCA's Blue Chip and Texas Instruments' MERA incorporate power combiners for combining the received RF energy for processing. These combiners provide aperture distribution so as to suppress receive side lobes. In addition, the receive combiner (beam former) also provides a monopulse capability for tracking. Since the same antenna system is used for transmit and receive, a compromise must be drawn between these two functions rather than separate optimization of each function. Future systems in which separate optimization of the transmit and receive functions are possible, might take the form of a transmission-reflective array or a transmission lens. This is shown schematically in Fig. 3. On transmission, the RF energy is generated and amplified by a multiplicity of solid-state sources, phase delayed for beam steering, and radiated. On receive, the plane wave impinges on radiating elements, goes through the phase shifter, and gets reflected by a short circuit on an alternate throw of the T/R switch. The reflected energy is re-radiated for pick up by the monopulse receiver horn. It is, therefore, necessary to have one rather than many receivers. An alternate version would be to have the receive horn on the opposite side of the array if the antenna designer wants to pay for the cost of another set of radiators in order to eliminate the blockage of the pick-up horn and thereby reduce the sidelobes.

Paralleling the evolution which has occurred in the computer industry, the attributes of microwave solid state bring highly complex and sophisticated systems within the realm of practicability. The man-pack systems comprise another category of equipment in which these features are extremely important. Here, a comparison might be drawn to the impact of solid state upon the proliferation of portable broadcast receivers. Although such microwave systems are of principal interest now to the military, the size, weight, and eventual cost of radar, beaconing, and other systems may indeed lead to similar high volume commercial markets.

Reference

Staiman, D., Breese, M., and Patton, W., "New technique for combining solid-state sources," RCA reprint RE-15-2-20.

Current applications of microwave integrated circuits

Dr. W. C. Curtis | H. Honda

Rapid strides have been made in the application of integrated circuit techniques to the microwave field. In this paper, the current state of the art and the applications of hybrid microwave integrated circuits (MIC) are discussed. Some functional components and their performances are first discussed briefly; their applications to radar and communication systems follow.

THE TERM HYBRID MIC as used here consists of chips, such as transistors and diodes, bonded to microstrip networks on planar ceramic substrates. The passive elements in the networks may be in distributed line form, where the electrical characteristics are functions of the running length, or they may be lumped-elements, which are minute and fabricated by the IC processes [1,2]. Use of integrated-circuit techniques makes the design approach to a particular application that of bonding (solder or otherwise) together functional components and sub-systems, rather than the more basic *R, L, C* elements.

Applications to components

In applying MIC's, the system designer must, of course, utilize their capabilities and take into account their limitations. Generally speaking, MIC components are reliable, have functional versatility, and are lower in cost and smaller in size in large quantities compared to the conventional microwave components.

Present limitations which may be mentioned are the relatively low power output of the individual devices, spurious output, and higher loss and noise outputs in some of the components.

Filters and matching networks operating at microwave frequencies can be built utilizing distributed components or as lumped-constant circuits, the former performing better. However, in recent months, the quality of the dielectric has been greatly improved and *Q*'s of the order of 400 at *S*-band and 100 a *X*-band have been achieved, resulting in lumped-constant components which are very much smaller than distributed circuits and which perform well. Fig. 1 shows the microstrip layout for a composite filter. These filters have been batch-fabricated and have excellent characteristics. The letters show the equivalent electrical points. If the circuit is interconnected using the components up to point *F*, one has the schematic circuit shown at the top of Fig. 1 with the series *m*-derived section omitted.

Power and signal amplifiers have been built as microwave integrated circuits from 400 MHz to *S*-band, with power outputs for a single integrated transistor at 1500 MHz of 5 watts and at 2500 MHz of 4 to 6 watts. With hybrid couplers two to four transistors can be paralleled giving much higher power outputs. Fig. 2 shows a schematic and layout for a 2.25-GHz power amplifier using a 7487 transistor. This amplifier is intended as a driver for a PA chain; its performance is 9-dB gain, 1-watt power output and 34% efficiency.

Varactor multiplier chains are often used in tandem with power amplifiers to produce frequencies and power levels not available by direct amplification.

In addittion to power amplifiers and multipliers as power sources, bulk effect oscillators are useful as a free running oscillator controlled by a resonant circuit and as a locked oscillator. Microstrip circulators have been developed at *L, S,* and *X*-bands. They are WYE junction type fabricated on 0.025-inch ferrimagnetic substrates. Three microstrip lines emanate from a circular junction. A platinum-cobalt magnet is placed under the ground plane of the junction. The characteristics of circulators are shown in Table II.

Microstrip balanced mixers using quadrature hybrid couplers and Schottky barrier diodes have been built to op-

Reprint RE-15-3-22
Final manuscript received September 4, 1969.

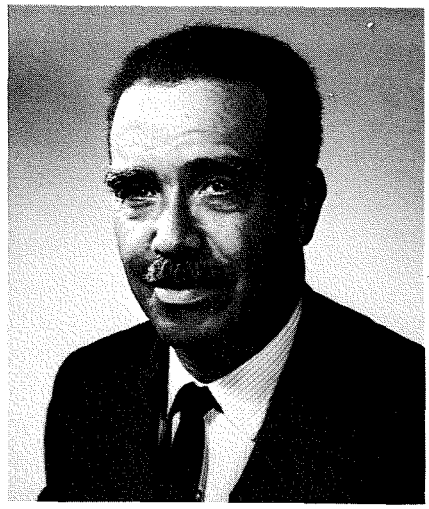

Dr. W. C. Curtis, Mgr.
Radar Systems Analysis
Aerospace Systems Division
Burlington, Mass.
received the BSEE in 1934 and the MSEE in 1935. both from U. of Illinois. At the Industrial Education Department of Tuskegee Institute, he was an instructor of electrical design in 1935 and became Director of the School of Mechanical Industries in 1940. In 1945, he left Tuskegee to attend Harvard where he received the MS in Communications Engineering in 1945 and the PhD in engineering sciences and applied physics in 1949. While a student at Harvard, he was employed at the Raytheon Company where he was in charge of Frequency Modulation Engineering for commercial transmitters. He returned to Tuskegee Institute as Dean of the School of Engineering in 1949. In 1954, he joined RCA and since has been responsible for the direction of theoretical and experimental analysis of new radar techniques. In one of his most recent responsibilities, Dr. Curtis directed a group of engineers responsible for the synthesis, analysis, and specifications for an airborne multifunction radar using microwave and digital microelectronics.

Hajime Honda
Systems Simulation
Aerospace Systems Division
Burlington, Mass.
received the BSEE from U. of Pennsylvania and the MSEE from Drexel Institute of Technology. Mr. Honda worked for four years on the design and development of microwave and UHF antennas for radar, communication sonobuoy systems, and in the analysis of communication antennas from the standpoint of anti-jam capabilities. For two years, Mr. Honda supervised the development of low-cost microwave relay systems and printed microwave circuitry. He has also applied microwave techniques to computer systems. He investigated optical radar processing techniques for ICBM detection and advanced microwave antenna techniques, including integrated circuit active element phased array. He has analyzed monopulse systems, particularly as related to antenna systems from standpoint of boresight shift and spurious responses.

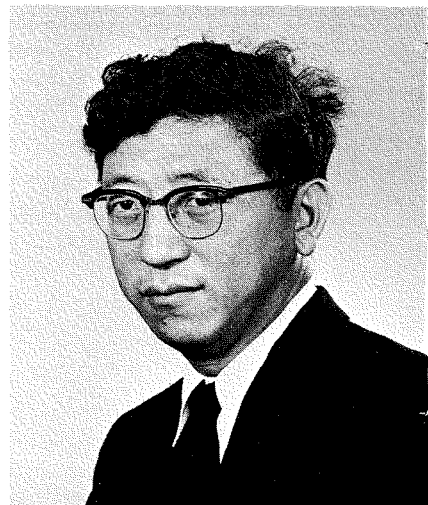

Table I—Power amplifiers.

Device	Freq(GHz)	P_{out}(W)	Gain(dB)	Class
7003/2NS470	2	1	6	C
7487	2	2	10	C
	3	1.75	5	C
7205	2	5	7	C

erate at many points in the microwave range. Table III shows current capabilities.

Paramps fabricated in microstrip and utilizing varactors cover the lower microwave region. The principles of operation are exactly those of the waveguide type and will not be discussed except to give performance in Table IV.

A number of 360° phase shifters have been developed using switched line lengths in four-bit digital form giving 22.5, 45, 90 and 180° steps. PIN diodes are used for switching. Insertion loss is 4 dB and phase error is ±2° at *S*-band. Digital phase shifters using quadrature hybrids and switched lumped components or PIN diode terminated lines have also been constructed. In the latter case about half the number of diodes are used; however, there are difficult matching

Table II—Circulator characteristics.

f_o (GHz)	Isol (max;dB)	Isol (BW20dB)	Insertion loss(dB)
1.8	>50	20%	0.4
3.5	>50	20%	0.4
9.0	>50	20%	0.4

problems. Phase tolerances are a problem in the lumped constant circuits while size is the problem in the switched line components.

Phased array applications

The application which utilizes the largest number of MIC's per system is the active-element phased array. Here the functional components are bonded together into larger units, or modules. In the array, the transmitter, receiver, duplexer, and phase shifter modules are associated with each radiating element. The modules may be arranged in a number of ways, three of which are shown in Fig. 3 (where the interconnections are from left to right for the transmitter and the reverse for the receiver). The first arrangement permits the use of phase shifters with relatively high insertion loss, such as those using diodes, since the phasers are located in the low power level network. This arrangement is currently being applied to the phased-array module. Various configurations for the phase shifters may be used. Two phase shifters, one for the transmitter and the other in the LO line, or one phase shifter, switched during the interpulse period, has been used. The transmitter may take any of the forms discussed previously. The receiver configurations used are low-noise transistor amplifier, applicable at *S*-band or lower, and one using balanced mixer, IF amplifier and LO multiplied up from a lower frequency, applicable at *X*-band. The duplexer can be a circulator or a diode switch.

A block diagram of the entire transmit-receive module currently being built is shown in Fig. 3c. The transmitter and

Table III—Microwave mixer characteristics.

f(GHz)	f_{IF}(MHz)	NF(dB)	NF_{IF}(dB)
1.8	30	6.2	1.5
3.5	30	6.5	1.5
4.2	30	6.5	1.5
4.4-5.0	30	6.8	1.5
9.0	30	7.2	1.5

LO drive use a common input. These signals, at *S*-band, are applied sequentially to a T/R switch which directs them to the appropriate line. The phase shifters are one of multi-bit PIN diode type, complementarily set to direct and receive signal from the same direction in space.

A multi-stage power amplifier drives a quadrupler, to provide an *X*-band output, which is directed through a circulator to the radiating element. Any reflected energy due to mutual coupling between radiating elements is directed into a resistive-load-terminated T/R switch in the receive line. The receive signal is directed to a balanced mixer. The tunnel diode amplifier is optional. The local oscillator drive is applied to the balanced mixer through a quadrupler.

Table IV—Paramp characteristics.

f_o (GHz)	f_p (GHz)	P_P (mW)	Type pump osc.	NF (dB)	BW (MHz)	G(dB)
1.9	8.5	5	G-A	1.3	50	13
2.25	8.5	5	A	1.8	50	17
3.5	11.5	15	A	2.0	50	17
4.2	13.5	20	G	2.2	50	17

G—Gunn; A—Avalanche

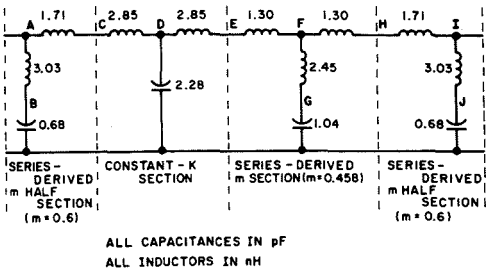

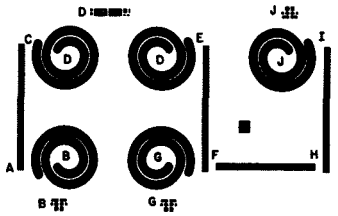

Fig. 1—Microstrip circuit layout for a composite filter.

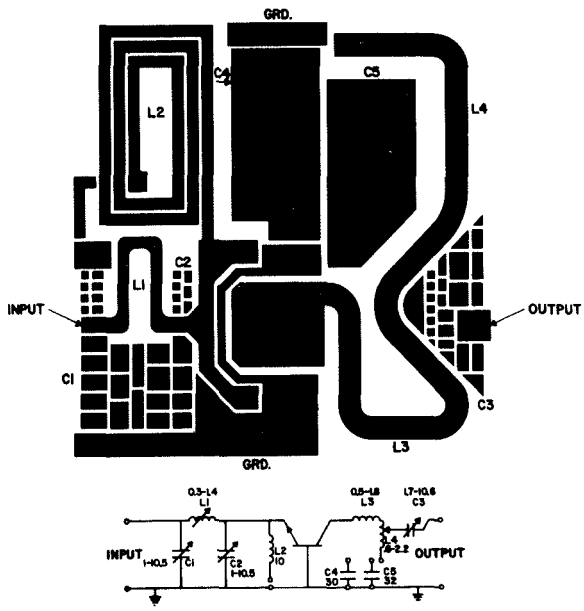

Fig. 2—Schematic and circuit layout for a 2.25-GHz power amplifier.

In the array, the effect of any coherent noise or spurious signals introduced through the LO line may be negated by use of an off-set phase taper in the LO drive network and a compensating phase taper in the receive signal combiner network.

The second arrangement in Fig. 3b utilizes a single phase shifter located in the high power line. Such a configuration requires a low phase shifter, such as that using latching circulators. These units are relatively bulky however.

Retrodirective array application

Another recent application of microwave integrated circuits is the space transponder for the Data Relay Satellite System. As currently configured the

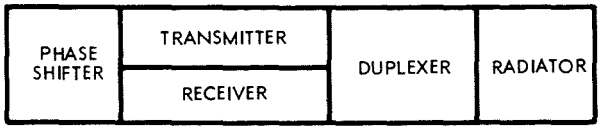

(A) ARRANGEMENT NO.1 FOR MIC MODULE

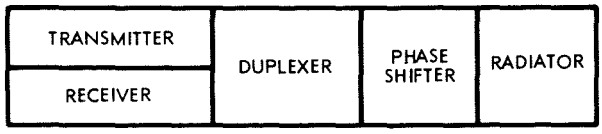

(B) ARRANGEMENT NO.2 FOR MIC MODULE

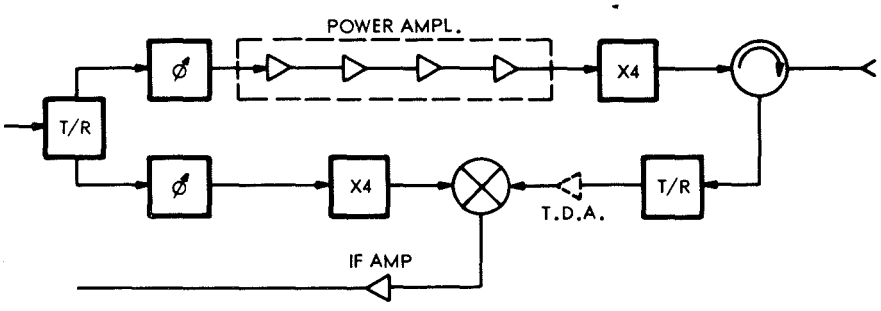

(C) A MODULE CONFIGURATION

Fig. 3—Three module arrangements for phased-array-radar modules.

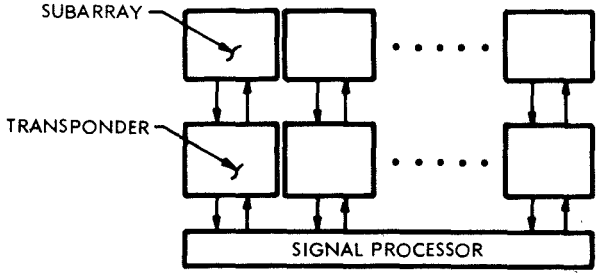

(A) RETRODIRECTIVE TRANSPONDER

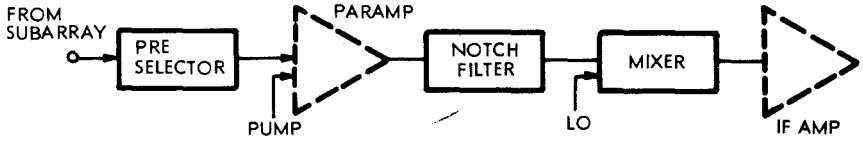

(B) TRANSPONDER RECEIVER

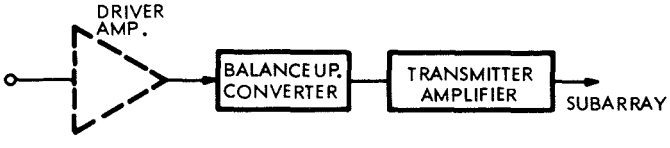

(C) TRANSPONDER TRANSMITTER

Fig. 4—Transponder arrangement for Data Relay Satellite.

transponder is retrodirective and a user can command the services of the orbiting satellite relay by sending a pilot tone. It is not the purpose of this paper to discuss the signal processing operations of this unit. For our purposes it is only necessary to state that the receiver is in *S*-band centered at approximately 2.2 GHz and that this signal is sidestepped to 1.8 GHz for retransmissions.

Fig. 4a shows a conceptual schematic of the transponder. The array is composed of subarrays containing 25 radiating elements which are in turn combined to form the array. A transponder is associated with each subarray.

Fig. 4b is a schematic of the transponder receiver. The pre-selector is a three-section (half-wave-length resonator) parallel-coupled, microstrip filter. This has a ±30-MHz 0.5-dB bandwidth at the signal frequency of approximately 2250 MHz with an insertion loss of 0.9 dB. The rejection at the transmitter frequency is 38 dB.

The parametric amplifier uses a four port circulator. The characteristics are 3 dB bandwidth of 90 MHz, and pump power of 35mW at 8.8 MHz.

The noise figure of this amplifier is 2.2 dB. A two-section notched filter to reject the image noise is deposited in microstrip and has a rejection of 15.6 dB and an insertion loss of 0.45 dB. The mixer is a quadrature hybrid coupler balanced mixer with a 6.6 dB noise figure feeding a 100-MHz bandwidth IF amplifier centered at 80 MHz.

The input to the transponder transmitter (shown in Fig. 4c) is a 140- to 230-MHz driver amplifier for the balanced varactor up-converter which in turn drives a five-stage power amplifier.

The PA consists of three transistor amplifier stages; the first two being 7003 devices operating class-*A* and *AB* respectively, and a 7487 transistor as a class-*C* amplifier. An additional 7487 transistor operates as a class-*C* driver amplifier for a final 7205 amplifier with an output of 5 watts. The overall gain of the amplifier is 37 dB with an overall efficiency of greater than 20%.

References

1. Sobol, H., "Extending IC Technology to Microwave Equipment," *Electronics, 40,* 112 (Mar 20, 1967).
2. Moroney, W. J., "Microwave IC's: part 1. New problems, but newer solutions," *Electronics, 41,* 100 (Jun 10, 1968).

Potential of integrated electronics for microwave systems

Dr. L. S. Nergaard

Integrated microwave systems . . . the subject has aroused great interest, and many are making a substantial investment in such systems. Why? The question has a number of answers depending on the level at which it is asked. For the research man, it provides a host of new problems in materials, devices, and technology. For the development man, it provides an area in which to exploit devices and technologies, familiar and unfamiliar, in new ways. For the systems man, it opens new vistas in systems—systems of greater utility, versatility, and hopefully, in a more cost-effective manner. The ultimate justification, of course, lies in the utility (including the cost-effectiveness) of the systems. This paper explores the potential of integrated microwave systems.

BECAUSE NO FIELD IS BORN FULL-BLOWN, it is desirable to examine its beginnings; the beginnings in part shape its future growth. A field is also shaped by the state of the art; in this instance, by the things available for integration; these things are reviewed briefly. Finally, the field is shaped by its promises, and these promises are the focus of our attention.

The beginnings

Work on integrated microwave systems stemmed from a variety of factors, the most important of which are:

1) *The state of the art in solid-state devices.* Diodes and transistors have become a common-place in a host of applications. They are used by the thousands in computers.

2) *Integration in computers.* The solid-state devices in computers do not appear as discrete components but as parts of functional blocks (modules) that contain not only the devices but the circuitry required to perform particular functions. Because a computer requires thousands of identical modules performing identical functions, these modules are now fabricated in integrated form by batch fabrication techniques so they can be made in the required quantities at an acceptable cost.

3) *Microwave solid-state devices.* Except for the crystal detector, solid-state devices came more slowly to the microwave field. This transition is natural; it takes time and a more-highly-developed technology to raise the cut-off frequency of any device. However, about ten years ago, the varactor reached a point where it was quite acceptable in parametric amplifiers, and the discovery of the tunnel-diode made possible low-noise tunnel-diode amplifiers. More recently, the operating frequency of transistors has been pushed into the gigahertz region and it has become possible to build all-solid-state transmitters with transistor sources and diode multiplier chains to achieve the required frequency. Now new devices, Gunn and avalanche diodes, have appeared on the scene and bid fair to make their impact as power generators.

4) *Microwave systems.* With the advent of solid-state transmitters, it became possible to build all-solid-state systems. There are a number of these in the field: mobile equipment, microwave communication systems (such as the CW-60), and sophisticated radar systems (such as the LEM radar). While none has accumulated the life required to verify its predicted mean time to failure, all have performed well as to reliability and freedom from service calls.

5) *Power.* All of the systems referred to above have been low-power systems, a watt or less. With the success of these systems, it was natural to inquire as to what might be done to achieve higher power systems. To assay this problem requires an examination of the state of the art, a matter to be discussed shortly. It suffices here to say that it requires a lot of paralleled devices to achieve a kilowatt, and when a lot of devices are required it is natural to think of integration.

6) *Phased-array radars.* For some time, there has been much interest in phased-array radars. Spadats, SAM and SAM-D are well-publicized systems. One of the attractive features of such systems is that the radiated beam can be made very agile without mechanical motion of the antenna. Such systems require a large number of identical, individually-driven antenna elements. The drive can be supplied in a number of ways. The power output of a large power tube can be sub-divided and distributed to the antenna elements via phase shifters or the elements can be driven by individual power sources appropriately phase-locked. The latter case prompts an examination of the use of solid-state devices as sources and of constructing the radiating elements and their drivers as integrated modules. Thus, phased-array radars have had their impact on microwave integrated system thinking from the beginning.

In summary, the integration already achieved in computers, the advent of microwave solid-devices and systems employing them, the search for higher power, and the modular approach to modern radar systems—all have spurred an examination of the potentials of integrated microwave systems.

State of the art

As to the state of the art in microwave power generation, it is displayed in Fig. 1. The "wedge" was drawn in 1962 and shows the state of the art

Reprint RE-15-3-11
Final manuscript received June 12, 1967.

Dr. Leon S. Nergaard, Director
Microwave Research Laboratory
RCA Laboratories, Princeton, N.J.

attended the University of Minnesota and received the BSEE in 1927. He received the MSEE from Union College, Schenectady, N.Y., in 1930 and the PhD in physics from the University of Minnesota in 1935. From 1927 to 1930 Dr. Nergaard was associated with the research laboratory and vacuum-tube engineering department of the General Electric Company. He held a teaching assistantship in the Department of Physics at the University of Minnesota from 1930 to 1933. Dr. Nergaard joined the RCA Manufacturing Company in 1933 and transferred to RCA Laboratories as a research physicist in 1942 where he worked on pulse-radar tubes until the end of the war. Since then he has worked on transmitting tubes and television transmitters, then switched to solid-state physics, particularly the semiconducting properties of oxide cathodes. He assumed responsibility for the microwave work at RCA Laboratories in 1957. In 1959 he was appointed associate laboratory director, Electronics Research Laboratory. He assumed his present responsibility in 1961. He is responsible for 24 issued patents and 23 papers, has received two RCA Achievement Awards and the David Sarnoff Award for Outstanding Achievement in Science. Dr. Nergaard is a Fellow of the American Physical Society and the IEEE, a member of the American Association for the Advancement of Science. He has been active in numerous committees of the IEEE, URSI, and a member of Theta Kappa Nu, Gamma Alpha and Sigma Xi.

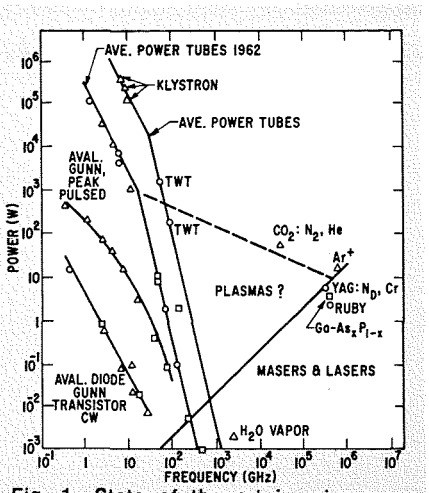

Fig. 1—State of the art in microwave power generation.

FREQUENCY BAND	SYSTEM	FREQUENCY GHz	PEAK POWER WATTS	BEAM WIDTH DEGREES
S-BAND	INTERPLANETARY	2	50-100	< 5°
	MICROWAVE RELAY	2	3-10	30
	TELEMETRY GROUND STATION	2	10^3	3
C-BAND	COMMUNICATIONS	4-6	20-50	6
	MICROWAVE RELAY	4-8		2
	TROPOSCATTER	4-5	10^3	3
	RADAR	5	10^3	3
X-BAND	AIRBORNE	9	10^3	3
	GROUND STATION (SPACE)	7-8	10^3	4
	RADAR	9	5×10^3	<3

Fig. 2—Medium power systems, typical requirements.

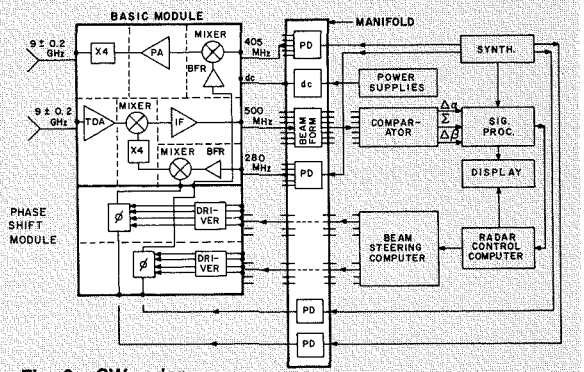

Fig. 3—CW radar.

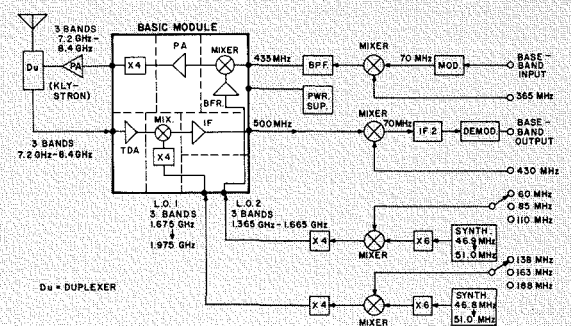

Fig. 4—Communications system.

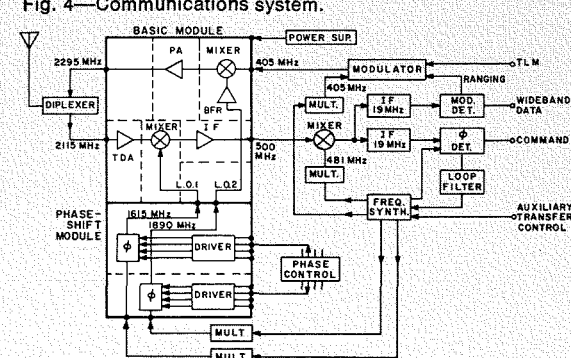

Fig. 5—Spacecraft range and range rate transponder.

as of that time plus some points that were added as time progressed. The center curve shows the progress in tubes as of June 1966, at which time the points on the maser and laser curve were also added. In the center, the writer noted speculatively "Plasmas?" because he felt that nature had not so contrived things that no substantial power could be obtained at 300 GHz and thereabouts. Gas-discharge lasers seem to be encroaching on this area. In 1962, solid-state devices did not show at all. Now it is necessary to up-date the curves almost every week. Perhaps solid-state devices will show the same progress shown by tubes from 1962 to 1966. Below 10 GHz, tubes will produce an average power given by P_o (watts) f^2 (GHz) $\sim 10^7$. Transistors, in the same terms, will do about $P_o f^2 \sim 4$; so there are about 6 orders of magnitude between them. The transistor curve shows avalanche and Gunn diodes as giving about the same average power. There have been isolated reports of Gunn and avalanche diodes with $P_o f^2 \sim 200$. Even with such a figure of merit, it takes many solid-state devices to equal one tube.

Systems—present and future

At this point, it is pertinent to inquire what kinds of powers are required for various systems. Typical systems are shown in Fig. 2 by frequency band. Note that these systems, with few exceptions, call for a beamwidth of about 3°. Now the beam width is about $\theta = 100°/n$ where n is the number of half-wavelengths in the antenna aperture. Thus to get a beam with 3° spread in both azimuth and elevation requires an array of about 30x30 elements or a total of about 1000 elements. For the systems listed, it turns out that the power required divided by the number of half-wave elements required yields a few watts per element, at most. Such powers are available from solid-state devices now at the lower frequencies and certainly will be available at the higher frequencies in the near future.

Modular approach

It appears that these systems can be implemented by combining the power coherently in space. Are there alternatives to this approach? Certainly, the power of a number of devices can be combined in a circuit and delivered to a common load. A power output of 1.1 kW at 300 GHz and of 0.55 kW at 450 GHz has been obtained by combining the power of 64 overlay transistors.[1] The choice of means depends on the system.

If systems using thousands of modules are to be constructed, these modules must be produced by mass-production techniques if their cost is to be reduced to within gunshot of the $12/watt or so of initial investment in tube radar systems of conventional design. It can be argued that solid-state systems require less maintenance, hence a higher initial cost is justified. This contention remains to be demonstrated; although, as noted above, things look hopeful on this score. Nevertheless, cost considerations require that integration and batch fabrication techniques be used in the construction of the modules if they are to have a chance of competing with tube systems. Whether the volume of modules required for future systems can justify the capital investment required to produce them is another matter, one to which we will return after an examination of the promises of integrated microwave systems.

These promises pertain to large systems using the modular approach and are in brief:

1) The required power is achieved by combining the power output of many power sources in space.
2) The required beamwidth is achieved by virtue of many elements.
3) The beam can be steered by phasing the drive to individual elements.
4) Individual modules can be highly reliable; available data bear this out.
5) System performance degrades gracefully. If there are random failures of modules in the array, nothing catastrophic happens; the beam degrades somewhat, the noise level rises a little, the radar range is practically unaffected, and the system goes on playing.
6) Multi-function systems are possible. By proper signal processing and distribution to modules a number of radar and communication functions can be performed by one and the same system.

Thus, the solid-state phased-array approach to modular systems promises a number of advantages, not the least of which are long life and high reliability. So far, modular systems and their attributes have been discussed in general terms. Now it may be advantageous to look at some possible systems to put "meat on the bones." Several such systems are delineated in Figs.

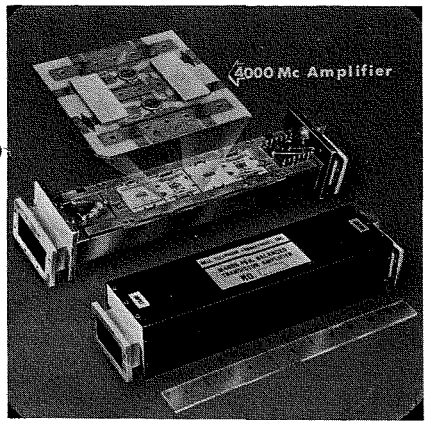

Fig. 6—Three-range, 4-GHz, repeater amplifier [Courtesy of Bell Telephone Laboratories, Murray Hill, N.J.].

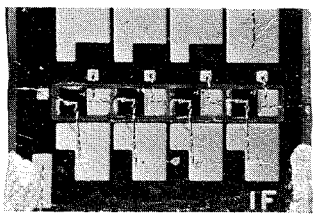

Fig. 8—Four-stage hybrid-integrated IF strip. The transistors run down the middle; decoupling capacitors run down the two edges (0.140 x 0.160 inches).

3, 4 and 5. These figures should not be taken too literally; they are merely intended to illustrate ways in which a basic integrated module can be used in a number of systems. In each of the figures, the basic module is in the upper left-hand corner, the signal-processing equipment at the right. The basic module shown has a transmitter at the top comprising a mixer fed by a local oscillator and a subcarrier that carries the modulation, whether pulse, AM, or FM. The output of the mixer, shown as at about 2 GHz, is then amplified by a power amplifier and then multiplied up to the required output frequency. The receiver consists of a tunnel-diode amplifier feeding a mixer that in turn feeds the IF strip. For phased-array systems, phase coherence between receiver and transmitter must be maintained. Hence, the local oscillator for the receiver mixer is obtained by mixing a signal obtained from the transmitter local oscillator and an offset-frequency signal, then multiplying the sum-frequency signal by the same factor as in the transmitter multiplier. Thus, phase coherence is maintained.

Fig. 4, which illustrates a possible troposcatter communication system, shows a klystron output stage with an integrated module as a driver. Hence, this system illustrates the use of a combination of tubes and solid-state

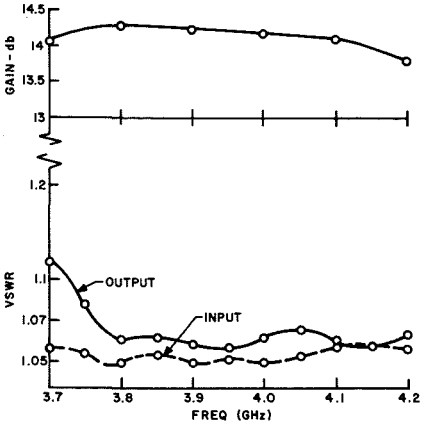

Fig. 7—Performance of the 4-GHz transistor amplifier of Fig. 6.

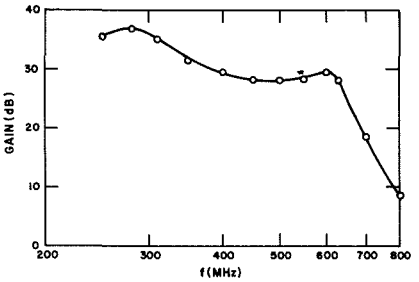

Fig. 9—Performance of the IF strip of Fig. 8 with output peaking.

devices; in the writers opinion, an interim solution to the power problem. Obviously, for microwave relay systems, the klystron may be omitted.

The signal processing in each case is conventional and lends itself to the integration techniques now common in computers.

Cost effectiveness

Now to return to the question of whether the number of modules required for even a number of large systems will justify the capital investment required to make them. From a systems point of view, it would be desirable to integrate an entire microwave module, both transmitter and receiver, for particular systems. Two factors militate against this approach. First, while the number of modules required for particular systems seems large at first blush, it does not compare with the number of transistors produced per month, i.e., this number is a far cry from the volume required to bring fabrication costs down to the level possible with real mass production.[2] Second, the circuit and power dissipation requirements within a module may be such that it is desirable to subdivide functions and use monolithic blocks for some and hybrid blocks for others. Fig. 6 shows a beautiful example of what is meant by hybrid blocks. The figure, kindly loaned by Mr. R. Engelbrecht of Bell Telephone Laboratories, shows a three-stage, 4-GHz repeater amplifier, with 5 dB of gain/stage using transistors as active devices and thin-film passive components. Each stage is a block of the kind in question. The performance is shown in Fig. 7. Since this amplifier has been described elsewhere[3,4] it is not discussed here, except to note that the computed mean time to failure is 10^6 hours and that failure means a departure by 1% from any prescribed characteristic.

The subdivision of modules into blocks offers the possibilities of spin-offs that may well find application in systems that could advantageously use modules or parts of modules but do not offer the volume that alone would justify them. Possible examples of such spin-offs are power amplifiers and IF strips. These are potentially so useful in a variety of applications that they may be the first to be available in integrated form. Fig. 8 shows such an IF strip, developed under RCA's Blue-Chip Program. The dimensions of this four-stage amplifier are 0.140 by 0.160 inches; its performance is shown in Fig. 9. In the meantime all of the components required for complete systems are under close scrutiny and time alone will tell which form the various blocks take.

Conclusion

Low-power all-solid-state microwave systems are operating in the field. Their performance is such that one has been led to examine the possibilities of higher power systems. Kilowatt systems using integrated modules seem in the cards in the near future, and these systems offer performance not now available. The next generation of devices will prompt an examination of megawatt systems, and with the present rate of progress in devices, the next generation may not be far off.

References

1. Private communication from I. E. Martin, RCA Electronic Components and Devices, Lancaster, Pa .
2. For an analysis of cost trade-off and the business potential of integrated microwave modules, see Webster, W. M., "Integrated Microwave Modules—A Prospectus," *IEEE Transactions on Electron Devices*, Vol. ED-15, no. 7 (Jul 1968) pp. 446-450.
3. Engelbrecht, R. S. and Wise, J. W., "Microwave Integrated Circuits," *Bell Laboratories Record*, Vol. 34, no. 9 (Oct-Nov 1966) pp. 329-333.
4. Saunders, T. E. and Stark, P.D., "An Integrated 4-GHz Balanced Transistor Amplifier," *IEEE Journal of Solid-State Circuits*, Vol. SC-2, no. 1 (March 1967) pp. 4-10.

Microwave phase shifter

N. R. Landry

A modern radar system requires agility in the positioning of its antenna beam, and the microwave phase shifter is instrumental in giving it this capability. One type of phase shifter consists of a rectangular toroid of ferrimagnetic material which is mounted in the longitudinal center of a waveguide, is matched for a low reflection coefficient, and is switched by a suitable electronic circuit. The design of this microwave assembly is discussed in this paper, and performance characteristics of several designs are given. The final design uses a ceramic with a dielectric constant of 50 in the rectangular slot of the toroid. This improves performance over the more conventional $K=16$ design by reducing size, weight, cost and switching energy requirements.

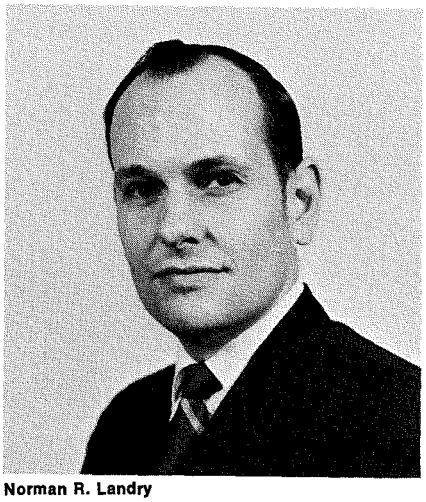

Norman R. Landry
Advanced Microwave Techniques
Missile and Surface Radar Division
Moorestown, N.J.

received the BSEE with High Distinction from Worcester Polytechnic Institute in 1957 and the MSEE from Drexel Institute of Technology in 1965. Prior to joining RCA, Mr. Landry served two years in the U.S. Army as an electronics instructor. His first assignment with RCA was to help in the design, fabrication and checkout of a very high power, high-frequency radar transmitter. He was then associated with a full-scale radar range where he designed system improvements and wrote several technical articles on radar cross-section measurement techniques and results. His major designs were the microwave system of an L-band cross-section measurement range and, at a later date, a coherent transmitter using microwave pulse shaping and travelling wave tube amplification to fifty kilowatts of peak power. With this equipment, the phase and amplitude of the backscattered radar energy could be simultaneously measured. Mr. Landry has done applied research into an L-band super-cooled Tunnel Diode Amplifier which operated at cryogenic temperatures and has designed and built a low loss, high isolation PIN diode limiter for C-band. For the past three years, he has been involved in the design of ferrite phase shifters for use in microwave phased array radar systems. Two designs have reached pilot production and have been reported in recent radar system proposals. Mr. Landry is a member of Eta Kappa Nu, Sigma Xi, and the IEEE.

Reprint RE-15-3-5
Final manuscript received May 23, 1969.

A MICROWAVE PHASE SHIFTER (PHASER) is a device that is capable of changing its electrical length (insertion phase) in a predictable manner in response to a proper command signal. One of the primary applications for a microwave phaser is in phased array antenna systems. A typical radar system requires four of these antenna systems with a total of about 16,000 phase shifters.[1] The radiation pattern of each antenna system is determined by the vector sum of the fields that are radiated from each of its elements. These fields can be made to add constructively in any desired direction by phasing the phase shifters to achieve the proper phase taper across the array face. Radiation in other directions is low because of the destructive interference of the element patterns. Thus, by controlling the electrical length of these phasers (hence the phase taper across the array) the radar beam can be made to point in any desired direction, and this direction can be changed several thousand times per second.

Microwave phase shifters can be fabricated using either diodes[2,3] or ferrites[4,5] as the switched material and either can be used in coaxial, stripline, microstrip or waveguide construction. To compare the various designs, several factors bearing on the system requirements must be evaluated: phaser size, weight, cost, reliability, VSWR, insertion loss, temperature sensitivity, power handling capability, switching energy requirements, frequency characteristics, and reproducibility. When this is done with present technology, diodes in a stripline configuration and ferrites in a waveguide housing usually emerge as the serious competitors. In general, diodes are superior at low frequencies and ferrites have the advantage at high frequencies. A recent tradeoff study selected ferrites for operation in the 3.1- to 3.5-GHz frequency band. This paper is limited to the design, construction, and performance of the ferrite type of phaser, using an S-band design as the primary example.

Phaser construction

The ferrite phase shifter consists of a rectangular toroid of ferrimagnetic material which is mounted in the longitudinal center of a rectangular waveguide. A sketch of a ferrite phase shifter and a list of the microwave parameters of interest is given in Fig. 1. The toroid slot contains one or two magnetizing wires and is otherwise filled with dielectric material. The ferrimagnetic material has a high fixed permittivity which is used to concentrate the microwave energy and a variable anisotropic permeability which is used to develop the useful differential phase shift. Each of the parameters—voltage standing wave ratio, insertion loss, insertion phase length, and differential phase shift—is a function of operating frequency, ambient temperature, and incident power level.

Referring to Fig. 1, the approximate equations for maximum VSWR and insertion loss are given in terms of incident, transmitted, reflected, and dissipated power levels. The equation for insertion phase (IP) includes ε_1 and ε_2 as the phase errors contributed by reflections at the two ends of the device (see Glossary). Differential phase shift, $\Delta\phi$, is the difference in insertion phase when the magnetization is switched from one state to another—e.g., from state A to state B. If ε_1 and

Glossary

AMFAR	Advanced Multi-Function Array Radar
a	Waveguide-to-ferrite separation
B	Flux density
C-band	4 to 8 GHz
f	Frequency
G-1004	Garnet designation of Trans-Tech, Inc.
H	Magnetic field intensity
IL	Insertion loss
IP	Insertion phase
K	Dielectric constant
k_a	Transverse wave number in air
k_e	Transverse wave number in dielectric
k_m	Transverse wave number in ferrite
k_o	Free-space propagation constant
L	Inside waveguide width
P	Power
$\gamma_{1,2}$	Reflections at Port 1, 2
S-band	2 to 4 GHz
State A	Initial Phaser Magnetization
State B	Final Phaser Magnetization
X-band	8 to 12.4 GHz
Z	Generalized impedance
Z_f	Impedance of ferrite loaded waveguide
Z_o	Impedance of empty waveguide
Z_1	First matching impedance
Z_2	Second matching impedance
$4\pi M$	Magnetization in gauss
β	Phaser propagation constant
δ_1	Width of toroid leg
δ_2	One-half dielectric thickness
$\Delta\phi$	Differential phase shift
ε_1	Transmission phase discontinuity at port 1
ε_2	Transmission phase discontinuity at port 2
θ	Function of magnetic susceptibilities
λ_g	Wavelength in waveguide
ρ	Function of magnetic susceptibilities

ε_2 remained the same for states A and B, the differential-phase-shift error would be zero. This is not the usual case and, in fact, this error can be as large as ±10.4° for a VSWR of 1.2 in each of the two states. Fortunately, it is usually less than ±3° which is essentially negligible. Impedance matching transformers are used at each end of the ferrimagnetic toroid to improve phaser performance over the desired frequency range.

The two competing waveguide ferrite-phase-shifter designs are usually referred to as *multiple bit* and *flux drive*[6]. Design of the toroid and waveguide cross-sections is the same for both types, but the multiple-bit approach divides the toroid length such that each physical piece is related to a particular differential phase shift, while the flux-drive concept adjusts the magnetization in the entire toroid for the desired insertion phase. In effect, the multiple-bit phaser is a digital device while the flux-drive phaser is an analog device that is used in a digital fashion. Both types are non-reciprocal in that the insertion phase for any given level of magnetization is different for the two directions of propagation. This is caused by the different amounts of microwave-ferrite interaction for right and left circular polarizations and these polarizations change with direction of propagation or direction of magnetization.

The driver circuits for these two types of phase shifters are considerably different. For the multiple-bit phaser, the driver must switch each ferrite toroid between its maximum positive and its maximum negative remanent states. For a four-bit phaser, then, four separate driver circuits are required, and each must be capable of supplying the saturating current pulses. However, the amplitude of these current pulses is not critical since the phase shift is primarily determined by the ferrite dimensions and material parameters. For the flux drive phaser, only one driver is required, but this driver must control magnetization by accurately controlling the voltage-time product applied to the toroid winding. One of the maximum remanent states is used as a reference point and increments of flux are metered into the toroid for the various flux levels required. Lack of precision in the applied voltage-time product appears as an error in the amount of differential phase shift obtained.

Phaser design

The analytical model used to calculate ferrite phase shifter performance has been described by Ince and Stern[7]. A sketch of this model with a list of the variants is given in Fig. 2. Note that in the model, the top and bottom bridges between the twin ferrite slabs are ignored and internal magnetization is generated with external fields; whereas in the actual device, internal magnetization is generated through hysteresis effects and the applied field is zero. Interaction between the DC magnetization and the propagating RF field causes the propagation constant to either increase or decrease over what it would be if only the dielectric

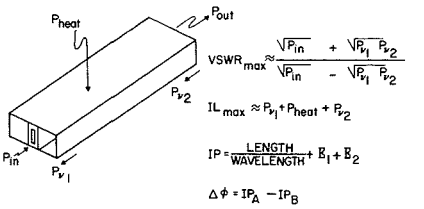

Fig. 1—Phaser description.

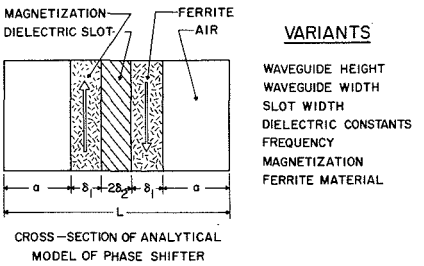

Fig. 2—Cross-section of analytical model of phase shifter.

properties of the material were considered. The amount of interaction is a function of the level and direction of magnetization and the direction of propagation. The interaction of the two slabs with the microwave energy is the same for a given direction of propagation since both the sense of circularly polarized **H** fields and the direction of the magnetization fields are different for the two slabs. For a given design, differential phase shift is obtained by changing the remanant magnetization to the value required for the desired change in propagation constant.

The equation relating material parameters, device dimensions, and propagation constant can be derived by incorporating the ferrite tensor permeability into Maxwell's equations and solving the appropriate boundary value problem. A set of equations result from matching boundary values at each of the four interfaces in the cross-section of the model. These interfaces are the sidewall of the waveguide, the air-to-ferrite interface, the ferrite-to-dielectric interface, and a plane in the center of the dielectric which is equivalent to a mirror image of the second half of the model. For a nontrivial solution, the determinant of the four equations is set equal to zero, and the resulting characteristic equation is

$$\tan(k_a a) = \frac{k_a\left[\frac{k_e}{\rho^2} - \frac{j\beta}{\rho\theta}\cot(k_e\delta_2) - \frac{k_m}{\rho}\cot(k_m\delta_1)\cot(k_e\delta_2)\right]}{\left(\frac{\beta^2}{\theta^2} - k_m^2\right)\cot(k_e\delta_2) - \frac{k_m k_e}{\rho}\cot(k_m\delta_1) + \frac{j\beta k_e}{\rho\theta}} \quad (1)$$

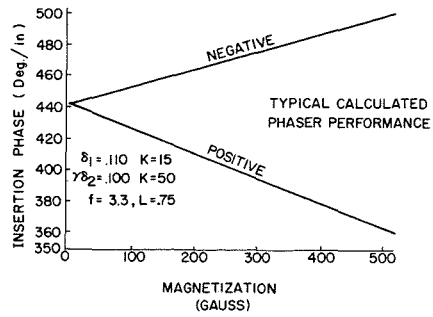

Fig. 3—Insertion phase as a function of magnetization for a typical toroid.

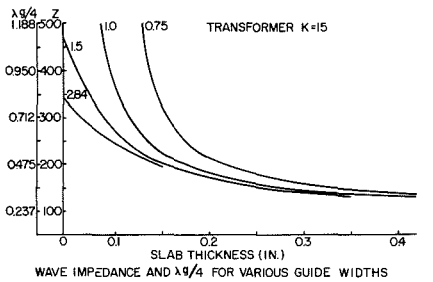

Fig. 4—Wave impedance and $\lambda_g/4$ for various guide widths.

For latching ferrite devices, the diagonal components of the tensor susceptability are zero since there is no applied magnetic field intensity. The off-diagonal component, however, is directly proportional to the remanant magnetization of the material and it is this component which is responsible for the behavior of the device.

Computer calculations

Eq. 1 is a transcendental equation with the propagation constant, β, as the parameter of interest. With the aid of a computer, a value of β is calculated for the maximum positive and negative remanent magnetizations; the difference of the two propagation constants is the maximum useful differential phase shift—usually calculated in degrees/inch of length. Each of the variants listed in Fig. 2 is given a range of interest, and the propagation constant and maximum differential phase shift are calculated for selected combinations of the variants. Consider, for example, an S-band design that is required to have a nearly constant differential phase shift versus frequency characteristic over the 3.1- to 3.5-GHz frequency band. One set of calculations for a waveguide width of 0.75 inches is given in Table I. This table gives maximum differential phase shift as a function of frequency and slot loading for several toroid designs.

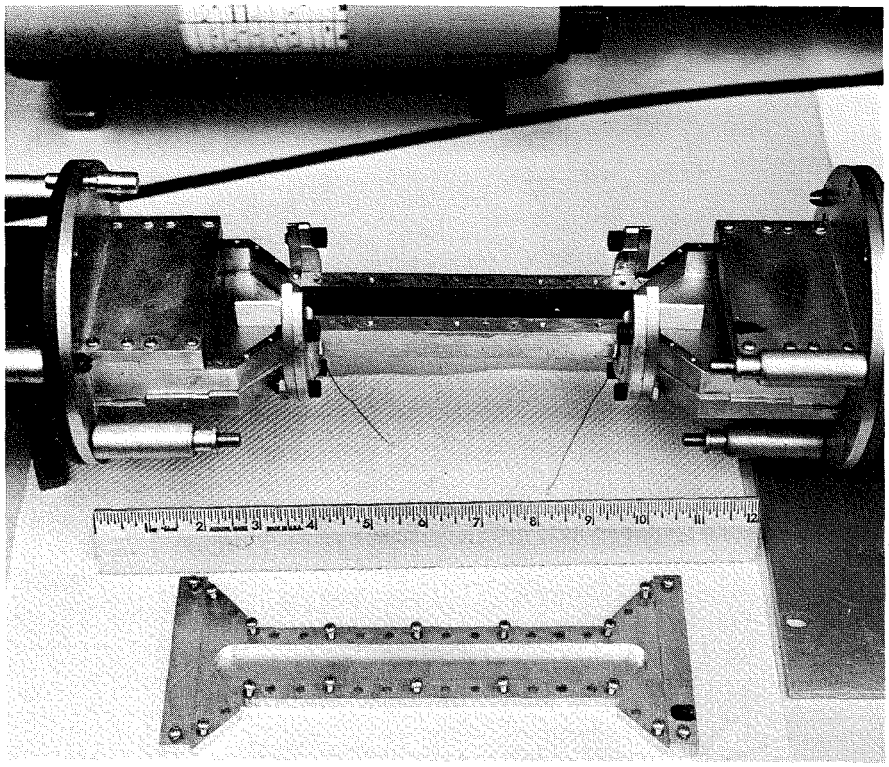

Fig. 5—Phaser and radiating horn.

Table I—Differential phase for various geometries (degrees/inch).

Toroid Description	*Freq.*	$\Delta\phi$ *K=16*	$\Delta\phi$ *K=23*	$\Delta\phi$ *K=30*	$\Delta\phi$ *K=40*	$\Delta\phi$ *K=50*	$\Delta\phi$ *K=60*	$\Delta\phi$ *K=70*	$\Delta\phi$ *K=80*	$\Delta\phi$ *K=90*
$\delta_1=0.090$	3.1	59.67	70.44	80.92	95.47	109.59	122.68	134.62	145.68	155.43
$2\delta_2=0.100$	3.2	59.52	70.44	81.21	96.05	110.17	123.26	135.20	145.97	155.43
$2(\delta_1+\delta_2)=0.280$	3.3	59.23	70.44	81.50	96.49	110.75	123.70	135.49	145.97	154.99
	3.4	59.09	70.58	81.79	97.07	111.33	124.14	135.78	145.82	154.55
	3.5	58.94	70.73	81.93	97.51	111.77	124.57	135.78	145.53	153.68
$\delta_1=0.100$	3.1	64.91	75.68	86.45	101.29	115.41	128.65	140.87	151.79	161.69
$2\delta_2=0.100$	3.2	64.47	75.38	86.45	101.58	115.84	129.09	141.17	151.79	161.25
$2(\delta_1+\delta_2)=0.300$	3.3	63.89	75.38	86.59	101.87	116.28	129.38	141.17	151.64	160.52
	3.4	63.60	75.24	86.74	102.16	116.57	129.67	141.02	151.21	159.79
	3.5	63.31	75.09	86.74	102.45	117.01	129.81	141.02	150.62	158.48
$\delta_1=0.110$	3.1	69.42	80.48	91.39	106.38	120.65	133.89	145.97	157.03	166.78
$2\delta_2=0.100$	3.2	68.84	80.19	91.25	106.53	120.79	134.03	146.11	156.74	166.20
$2(\delta_1+\delta_2)=0.320$	3.3	68.25	79.75	91.10	106.53	120.94	134.18	145.82	156.16	165.18
	3.4	67.82	79.46	90.96	106.67	121.23	134.18	145.68	155.57	164.01
	3.5	67.24	79.31	90.96	106.82	121.23	134.03	145.24	154.70	162.56
$\delta_1=0.120$	3.1	73.64	84.84	95.90	110.89	125.16	138.40	150.48	161.54	171.29
$2\delta_2=0.100$	3.2	72.91	84.26	95.32	110.89	125.16	138.40	150.33	160.96	170.27
$2(\delta_1+\delta_2)=0.340$	3.3	72.18	83.68	95.18	110.75	125.16	138.25	149.90	160.23	168.96
	3.4	71.31	83.24	94.89	110.60	125.01	137.96	149.46	159.21	167.51
	3.5	70.73	82.95	94.60	110.60	125.01	137.82	148.88	158.05	165.91
$\delta_1=0.090$	3.1	60.69	71.31	81.79	95.47	108.13	119.48	129.23	137.82	
$2\delta_2=0.120$	3.2	60.25	71.16	81.64	95.61	108.28	119.34	128.65	136.80	
$2(\delta_1+\delta_2)=0.300$	3.3	59.96	71.02	81.64	95.61	108.28	119.04	128.21		
	3.4	59.52	70.87	81.64	95.61	107.98	118.61	127.34		
	3.5	59.23	70.73	81.64	95.61	107.98	118.03			

Table II—Phase versus magnetization for typical S-band design.

40°F			*160°F*		
$4\pi M$ *(gauss)*	*IP (deg/in)*	$\Delta\phi$ *(deg/in)*	$4\pi M$ *(gauss)*	*IP (deg/in)*	$\Delta\phi$ *(deg/in)*
−500	499.3		−400	489.4	
−400	489.4	9.9	−300	478.7	10.7
−300	478.7	20.6	−200	467.4	22.0
−200	467.4	31.9	−100	455.3	34.1
−100	455.3	44.0	0	442.2	47.2
0	442.2	57.1	+100	428.2	61.2
+100	428.2	71.1	+200	413.4	76.0
+200	413.4	85.9	+300	397.5	91.9
+300	397.5	101.8	+400	380.8	108.6

The effects of the bridges at the top and bottom of the toroid and the void surrounding the magnetizing wires have not been corrected for in this Table. In general, these effects cause the actual differential phase shift to be lower than that calculated, and the discrepancy becomes larger for the higher dielectric constant slot loadings. There are several observations that can be made based on Table I:

1) The differential phase shift can have a slight positive or a slight negative slope with frequency;
2) The differential phase shift increases with toroid leg width for the same slot width and loading;
3) The differential phase shift continues to increase with increasing slot dielectric constant; and
4) The performance of the 0.280-inch-wide toroid with the 0.100-inch slot is about the same as that of the 0.300-inch-wide toroid with the 0.120-inch slot.

Experimental results (presented later in the paper) confirm the above observations.

The flux-drive type of phase shifter utilizes remanent magnetization values intermediate to the maximum positive and negative values. Eq. 1 can be used to calculate insertion phase as a function of magnetization and the results for a typical toroid design are plotted in Fig. 3. Note that the insertion phase is a function of the direction as well as the magnitude of magnetization. Since the calculations are for the twin-slab approximation of the toroid, the curves are labeled negative and positive. In practice, the toroid is magnetized in a clockwise or counter-clockwise direction. The flux-drive phaser uses the maximum negative remanent state as a reference and differential phase shift is calculated from it. Tables of insertion phase and differential phase as a function of magnetization can be constructed from Fig. 3, but since the maximum remanent magnetization is a function of temperature, each table will be valid at only one temperature.

For example, assume that the maximum remanence is 500 gauss at 40° F and 400 gauss at 160° F; Table II can be constructed for a three-bit phase shifter. Note that since the maximum insertion phase is reduced at the higher temperature and the minimum insertion phase is increased (see Fig. 3), the maximum available differential phase shift is lowered for the multiple-bit phaser, while Table II shows differential phase shift being increased for the flux-drive phaser. Basically, the calculations predict that a temperature change from 40° F to 160° F would decrease the differential phase of all bits in a multiple-bit phaser by about 20% and increase the differential phase shift of all bits in a flux-drive phaser by about 7%. Fig. 3 shows the desirability of having a large value of maximum remanent magnetization. This value is limited, however, by the problem of low field losses and the squareness of the *B-H* loop of the material. To eliminate low field losses in a moderate power (5 kW peak) S-band phaser, the saturation magnetization of the ferrite must be less that 850 gauss at all operating temperatures. This value scales directly with frequency and must be decreased as the power handling requirement is increased.

Impedance matching

The dielectric loading of the filled toroid produces waveguide impedances which are considerably below that of empty waveguide; therefore, matching transformers are needed to maintain a low reflection coefficient. The model is the same as that in Fig. 2 except that the width of the ferrite sections is set equal to zero. Solving the resultant boundary value problem yields the following transcentenial equation:

$$(k_0^2-\beta^2)^{1/2}\cot\left[a(k_0^2-\beta^2)^{1/2}\right] = (Kk_0^2-\beta^2)^{1/2}\tan\left[\delta_2(Kk_0-\beta^2)^{1/2}\right] \quad (2)$$

With the aid of a computer, the wave impedance and quarter-guide wavelength have been computed for various waveguide widths, dielectric thicknesses, and dielectric constants. A sample of the data ($K=15$) is given in Fig. 4. Maximally flat transformer response is obtained by calculating two intermediate impedances, Z_1 and Z_2, as defined in the following equations.[8]

$$Z_1=(Z_0^3\ Z_f)^{1/4} \quad (3)$$

$$Z_2=(Z_0\ Z_f^3)^{1/4} \quad (4)$$

The values of Z_1 and Z_2 are used with Fig. 4 to determine the thickness and length of a K = 15 slab required to produce the desired quarter-wavelength impedance in a known waveguide width.

Typical application

A recent S-band requirement was to develop a ferrimagnetic phase shifter for the Advanced Multi-Function Array Radar (AMFAR) model. The requirement to be operational in any ambient temperature between 40° F and 160° F led to the decision to use a temperature stabilized garnet rather than a ferrite which is generally less expensive and less stable with temperature. The final choice was G-1004 which is manufactured by Trans-Tech, Inc. A flux-drive design was chosen over a multiple-bit design because a flux-drive phaser is more tolerant to material variations and is easier to assemble. Design of the waveguide and toroid cross-sections was limited by the requirements that the peak driver current be 12 amperes or less and that differential phase shift be nearly independent of frequency over the 3.1- to 3.5-GHz band. The 12-ampere limit in conjunction with the coercive force of G-1004 (0.9 oersted) led to the decision to fix the toroid height at 0.550 inches. Several of the designs listed in Table I were then investigated in detail. A picture of the brass test fixture with its transitions from standard S-band waveguide to the 0.75 x 0.55 inch phaser cross-section is given in Fig. 5.

Two magnetizing wires were used in the toroid slot so that identical driver amplifiers could be used to switch the toroid magnetization to any desired level. Only one amplifier was driven at any given time, and during this time, the second wire acted as a secondary winding from which a feedback control voltage was derived. The magnetizing wires are in the microwave circuit and were found to be a strong coupling mechanism to undesired higher order modes. These modes propagate within the phaser and create VSWR and insertion-loss spikes at certain resonant frequencies[9]. The eventual solution to the mode problem was to shield the magnetizing wires with a fine wire that was wrapped in a spiral around them. This spiral wrapped wire presents a larger resistance and inductance to longitudinal RF currents and effectively suppresses the undesired mode.

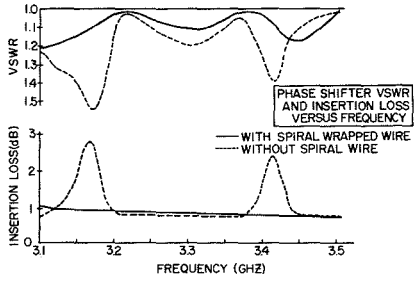

Fig. 6—Phase shifter VSWR and insertion loss versus frequency.

Typical swept frequency results with and without the spiral are shown in Fig. 6.

Test results

Once the garnet toroids could be matched for a low VSWR without mode spikes, the various toroid geometries and slot loading dielectrics could be measured for differential phase shift and insertion loss. Test results for 6-inch-long toroids are summarized in Table III. Observe that the top and bottom toroids have the same toroid wall thickness (0.090 inch) and that the performances are about the same.

Under the heading of $K = 50$ as the toroid wall thickness was increased, both the differential phase and insertion loss increased. Also note that for a given toroid width, the use of higher dielectric constant inserts increases both of the measured parameters.

Since the dielectric and magnetic properties of the toroid and ceramic inserts vary with temperature, phaser performance must be evaluated over the temperature range of interest. Results of the temperature tests on the final design are shown in Fig. 7. The final design was a six-inch-long toroid that was 0.300-inch wide and had a 0.120-inch slot that was loaded with a $K = 50$ ceramic. The data in Fig. 7 was taken with the driver circuit at room temperature and shows the characteristics of the G-1004 and $K = 50$ materials in the phaser geometry. The results show that differential phase shift of a multiple-bit phaser with this geometry would vary ± 9% while the flux-driver phaser reduces this to ± 3%. Insertion phase over the full temperature range varied ± 3°. This insertion-phase state was reached by a saturating current pulse in the magnetizing wires that flowed in a direction opposite to that of the propagating RF energy.

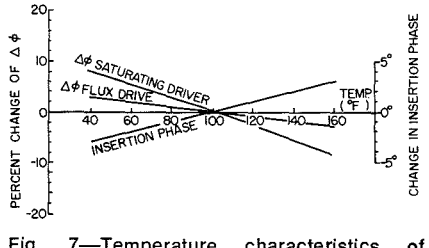

Fig. 7—Temperature characteristics of phaser.

One of the design goals was to make differential phase shift insensitive to the operating frequency by the proper selection of toroid and waveguide geometries. The final design accomplished this within ±2.0° which is close to measurement accuracy and fabrication repeatability. Referring to Table II, the calculations at either temperature show that differential phase shift is approximately linear with magnetization. The departure from linear, however, is enough that driver compensation is required to provide smaller than calculated amounts of flux change for the larger differential phase increments. Overall linearity of the phase shifter and driver has been measured for the final design. Variations from linear have been found to be different for each unit but are usually less than ± 4.0°. In fact, the combined linearity and frequency errors are usually less than ± 5.0°.

This phaser was required to handle 1.2 kW of peak power and 12 watts of average power. This is a relatively low power level for a ferrite phase shifter and is one of the reasons why a compact phaser using high dielectric constant ceramics could be used. The final design has been tested at 4.4-kW peak and 36.5-W average power with no degradation. The peak power of 4.4 kW was found to be below the critical power level where coupling to spin waves results in increased insertion loss. To check for voltage breakdown, the phasers were operated into a short circuit with 4.4-kW peak power applied. This effectively applied 17.6-kW peak to parts of the toroids and no breakdown occurred.

Production

For the AMFAR subarray, 128 phase shifters had to be built and tested with their respective drivers. The G-1004 toroids and the $K = 50$ inserts were purchased in 1½ inch lengths. Each of the 579 toroids was measured for maximum remanence, and those with a low remanence were paired with those that had a high remanence so that the total switchable flux was about the same for each phase shifter. Average remanence for the 579 toroids was about 530 gauss and the maximum variations were about ± 8%. Two inserts were picked at random for each toroid, and these were held in position at the top and bottom of the toroid slot by a compressed teflon tube between the inserts. A spiral wrapped wire pair was then fed through the four toroids chosen for a particular phase shifter. The wire assembly fit between the two inserts and next to the compressed teflon tube. The four toroids and two matching transformers were joined on the sides with a pressure-sensitive glass adhesive tape. The waveguide housing was partially fabricated by electron-beam welding four precision-formed aluminum parts together. It was designed to limit the

Table III—Summary of differential phase and insertion loss tests (toroid in low-loss state).

Toroid Width	*Slot Width*	*K=16*	*K=30*	*K=50*	*K=81*
0.280	0.100	320° 0.63 dB		434° 0.63 dB	
0.300	0.100		387° 0.67 dB	446° 0.67 dB	493° 0.90 dB
0.320	0.100		417° 0.67 dB	466° 0.70 dB	524° 0.83 dB
0.340	0.100			473° 0.73 dB	
0.300	0.120			443° 0.63 dB	

pressure applied to the garnets at about 10 lbf/in^2. The toroid assembly slipped into the housing and was held at one end by a small waveguide flange. During assembly of the subarray, this flange attached to a stripline power divider which fed 32 phasers. The other end of each phaser was matched to a radiating horn which was very similar to the tapered matching sections in Fig. 5.

Testing of the 128 phase shifters and drivers was facilitated by the Hewlett-Packard Automatic Network Analyzer[10]. This analyzer is capable of measuring the reflection and transmission characteristics of microwave devices and displaying this information on a meter, an oscilloscope, a teleprinter, and/or a punched paper tape. The analyzer measures both amplitude and phase, and with the computer, it can process data to remove directivity and cross-talk errors. A special computer program and interface with the phase shifter driver was developed for this application. With these interfaces, the analyzer can automatically measure the insertion phase and maximum differential phase shift at each of nine frequencies and then measure the VSWR, insertion loss and differential phase shift for each of sixteen bits and nine frequencies (Table IV). The test results showed that

1) The differential phase shift is nearly constant with frequency;

2) The insertion loss increases with bit setting;

3) The insertion loss decreases with increasing frequency;

4) The insertion loss indicates the absence of mode spikes;

5) The differential phase is nearly linear with bit settings;

6) The VSWR at each frequency changes only slightly with bit settings;

7) The average VSWR and insertion loss are 1.17 and 0.69 dB respectively; and

8) The Figure of Merit as usually defined is 459.6/.69 = 665°/db.

PHASES WITH SATURATING DRIVERS

FREQ	PHI-NEG LATCH	PHI-POS LATCH	DPHI
3100.0	6.60	110.80	464.20
3150.0	6.00	108.30	462.30
3200.0	5.70	107.20	461.50
3250.0	5.90	106.30	460.40
3300.0	5.90	105.50	459.60
3350.0	5.60	104.10	458.50
3400.0	5.50	103.70	458.20
3450.0	5.30	103.90	458.60
3500.0	6.40	104.60	458.20

VSWR, LOSS, AND PHASE FOR ALL BIT SETTINGS

FREQ	3100	3150	3200	3250	3300	3350	3400	3450	3500
BIT									
0 VSWR	1.003	1.437	1.191	1.138	1.041	1.154	1.241	1.045	1.185
LOSS	.67	.67	.56	.47	.79	.59	.54	.54	.58
PHI	.0	.0	.0	.0	.0	.0	.0	.0	.0
1 VSWR	1.005	1.417	1.204	1.146	1.058	1.139	1.244	1.048	1.179
LOSS	.79	.78	.66	.58	.90	.73	.66	.65	.67
PHI	23.3	22.5	22.4	22.4	22.2	22.4	22.4	22.4	22.5
2 VSWR	1.031	1.398	1.223	1.155	1.072	1.135	1.245	1.054	1.175
LOSS	.81	.79	.68	.62	.93	.79	.68	.67	.65
PHI	45.3	44.4	44.1	44.0	43.9	44.2	44.1	44.3	44.4
3 VSWR	1.100	1.378	1.228	1.160	1.083	1.115	1.244	1.058	1.171
LOSS	.77	.77	.65	.61	.89	.78	.65	.62	.63
PHI	68.6	67.8	67.2	67.2	67.1	67.4	67.5	67.4	67.4
4 VSWR	1.128	1.362	1.225	1.166	1.093	1.108	1.244	1.057	1.169
LOSS	.73	.74	.62	.58	.86	.77	.64	.61	.62
PHI	91.0	90.1	89.4	89.5	89.3	89.6	89.5	89.5	89.4
5 VSWR	1.153	1.351	1.240	1.173	1.101	1.100	1.241	1.064	1.169
LOSS	.71	.73	.61	.59	.86	.78	.65	.61	.62
PHI	114.6	113.7	112.8	113.0	112.9	113.1	113.0	112.9	112.9
6 VSWR	1.170	1.340	1.244	1.177	1.107	1.094	1.239	1.063	1.169
LOSS	.72	.72	.59	.55	.84	.78	.64	.60	.61
PHI	138.4	137.4	136.6	136.7	136.7	136.8	136.7	136.6	137.0
7 VSWR	1.179	1.334	1.246	1.180	1.111	1.088	1.237	1.066	1.170
LOSS	.71	.72	.57	.56	.80	.76	.63	.59	.61
PHI	162.7	162.1	161.2	161.4	161.4	161.5	161.3	161.5	161.4
8 VSWR	1.179	1.334	1.247	1.184	1.110	1.091	1.236	1.063	1.172
LOSS	.72	.72	.57	.55	.78	.77	.64	.61	.61
PHI	181.4	180.4	179.6	179.8	179.8	179.7	179.8	179.8	179.9
9 VSWR	1.173	1.335	1.233	1.182	1.108	1.091	1.239	1.059	1.173
LOSS	.72	.75	.59	.56	.78	.76	.65	.63	.62
PHI	205.4	204.1	203.5	203.6	203.6	203.4	203.6	203.7	203.6
10 VSWR	1.120	1.342	1.231	1.181	1.105	1.097	1.242	1.059	1.174
LOSS	.76	.78	.62	.58	.81	.77	.66	.66	.65
PHI	227.3	225.7	225.2	225.3	225.3	225.0	225.1	225.2	226.1
11 VSWR	1.139	1.350	1.237	1.178	1.095	1.106	1.241	1.061	1.174
LOSS	.72	.79	.64	.56	.81	.76	.67	.67	.65
PHI	250.8	249.2	248.8	248.8	248.9	248.4	248.5	248.7	249.0
12 VSWR	1.118	1.361	1.224	1.172	1.087	1.120	1.245	1.057	1.175
LOSS	.73	.80	.66	.57	.80	.73	.65	.68	.66
PHI	271.1	269.6	269.5	269.3	269.4	268.8	268.8	269.0	269.5
13 VSWR	1.089	1.375	1.220	1.163	1.074	1.126	1.246	1.055	1.174
LOSS	.76	.86	.71	.60	.84	.75	.69	.70	.70
PHI	295.0	293.2	293.2	293.0	292.9	292.0	292.3	292.9	292.8
14 VSWR	1.037	1.392	1.203	1.153	1.067	1.141	1.248	1.050	1.174
LOSS	.77	.89	.75	.63	.86	.76	.70	.71	.68
PHI	318.1	316.0	316.1	315.8	315.6	314.7	314.9	315.8	316.1
15 VSWR	1.032	1.406	1.196	1.143	1.051	1.147	1.246	1.047	1.175
LOSS	.75	.88	.75	.61	.84	.72	.68	.73	.71
PHI	344.0	342.0	342.2	341.7	341.5	340.4	340.5	340.8	341.1

AVG VSWR= 1.17 AVG LOSS= .69DB

Table IV—VSWR, insertion loss, and differential phase shift.

Conclusion

Although the design model ignores the magnetizing wires and the top and bottom of the toroid, it is useful in predicting the relative merits of many designs. The phaser design example met a particular requirement with special input and output geometries. One advantage of this S-band phaser is that its cross-section is about the same as that of standard X-band waveguide. It has been demonstrated that spiral-wrapped magnetizing wires can be used to eliminate higher order mode spikes and that high dielectric constant ceramic inserts can be used to significantly improve phaser performance. Ferrimagnetic phase shifters of this type have also been built at C-band and X-band and phasers for frequencies as high as 60 GHz are being investigated. The C-band application was of the multiple-bit variety and 224 of these phasers are in operation in a 10-foot diameter antenna model.[11]

Acknowledgement

The author expresses his gratitude to the management and staff of the Advanced Microwave Techniques Group of the Missile and Surface Radar Division for their assistance in this work. Special thanks are extended to Dr. W. T. Patton, W. H. Sheppard, R. J. Mason, E. H. Poppel, H. C. Goodrich, and R. J. Tomsic.

References

1. Cheston, T. C., "Phased Arrays for Radars," *IEEE Spectrum*, Vol. 5, No. 11 (Nov. 1968) pp. 102-111.
2. Burns, R. W. and Stark, L., "PIN Diodes Advance High-Power Phase Shifting," *Microwaves* (Nov. 1965) pp. 38-48.
3. White, J. F., "Review of Semiconductor Microwave Phase Shifters," *Proceedings of the IEEE*, Vol. 56, No. 11 (Nov. 1968) pp. 1924-1931.
4. Whicker, L. R. and Jones, R. R., "Design Guide to Latching Phase Shifters," *Microwaves* (Nov. 1966) pp. 31-39 and (Dec. 1966) pp. 43-47.
5. Frank, J., Kuck, J. H., and Shipley, C. A., "Latching Ferrite Phase Shifter for Phased Arrays," *Microwave Journal* (Mar. 1967) pp. 97-102.
6. Ince, W. J. and Temme, D. H., "Phasers and Time Delay Elements," Project Report RDT-14, Contract AF19(628)-5167, MIT Lincoln Laboratory, (Jul. 11, 1967).
7. Ince, W. J. and Stern, E., "Nonreciprocal Remanence Phase Shifters in Rectangular Waveguide," *IEEE Transactions on Microwave Theory and Techniques*, Vol. MTT-15, No. 2 (Feb. 1967) pp. 87-95.
8. Cohn, S. B., "Optimum Design of Stepped Transmission-Line Transformers," *IRE Transaction-Microwave Theory and Techniques* (Apr. 1955) pp. 16-21.
9. Collin, R. E., *Field Theory of Guided Waves* (McGraw-Hill Book Co., New York, N.Y., 1960) pp. 224-256.
10. Hackborn, R. A., "An Automatic Network Analyzer System," *Microwave Journal*, (May 1968) pp. 45-52.
11. Patton, W. T., and Klawsnik, F., "Hybrid Radar Antenna Pedestal-Mounted Electronic Scanning Array," RCA reprint RE-13-6-16.

RCA's newest coherent instrumentation radar

M. R. Paglee

RCA's leadership in the design and manufacture of Instrumentation Radars for use in worldwide tracking stations is reemphasized by the new AN/MPS-36 just shipped to the White Sands Missile Range. This mobile radar includes a new antenna and pedestal, digital range tracker, coherent local oscillator and transmitter, built-in computer and digital tape station, and doppler velocity extraction system. This paper reports the significant technical features and the departures from prior radar designs.

M. Robert Paglee, Ldr.
Signal Processing Engineering
Missile & Surface Radar Division
Moorestown, N.J.
received the BSEE from Purdue University in 1944. There he was a member of Tau Beta Pi, Eta Kappa Nu, Sigma Delta Chi, and Lambda Chi Alpha. His past experience with RCA includes Field Engineering on radar and sonar equipments, Broadcast and Television Equipment Sales, technical advising to NATO groups attached to the U.S. Embassies in Brussels, Belgium and Rome, Italy. He joined the Missile and Surface Radar Div. in 1956, where he performed project and design engineering assignments on AN/FPS-16, AN/FPQ-6, AN/TPQ-18, AN/MPS-25, and ASIR Instrumentation Radars. He was responsible for the design of early pulse doppler modifications to several instrumentation radars, and coordinated the design development and integration of four signal processing subsystems in the AN/MPS-36 Radar. He is holder and co-holder of two patents, has two other disclosures in process. He is a member of IEEE, and the Delaware Valley Council's Commercial Aviation Committee.

RECENT delivery of the first AN/MPS-36 radar system to White Sands Missile Range signals the birth of a new generation within the RCA family of precision instrumentation radars. This latest addition to the AN/FPS-16, AN/MPS-25, AN/FPQ-6, AN/TPQ-18 and CAPRI radar (AN/FPS-105) series includes many unique features—one of the most significant being its capability for direct measurement of target velocity by pulse-doppler signal-processing techniques.

The primary tasks of such sensors are to perform range safety and trajectory measurements at missile ranges throughout the free world and to provide the basic structure for a worldwide satellite tracking network. Position data gathered by these radars has enabled scientists and engineers to monitor (within a few feet) the location of our satellites from the beginning of our space programs.

The AN/MPS-36 was designed and developed by a team of engineers at the Missile and Surface Radar Division, headed by Mr. J. C. Volpe, Project Manager. This new system represents the first time an instrumentation radar has been developed from the outset to be fully coherent. In effect, the pulsed-transmitter frequency and the local-oscillator frequency are both derived from the same one-megahertz standard; great care is taken to preserve the phase relationships of the signal through the transmitter, the local-oscillator chain, the receiver, and the doppler processor—as required to realize the benefits of coherency.

General description

The AN/MPS-36 radar is a mobile system contained in two units—a van which houses the major electronics components, and a flat-bed trailer which carries the antenna and support pedestal. It has been designed for rapid transport from one site to another at White Sands Missile Range so that radar coverage over a large area can be provided in accordance with individual test mission requirements. The "electronics van" is air conditioned for operator comfort and equipment cooling, an important consideration in the White Sands desert.

Extensive use of integrated circuits was made throughout the design of the electronics equipment, with digital techniques taking preference over analog circuits wherever possible. This approach has permitted repetitive use of standard modules, minimizing the need for new designs. Important advantages are improved precision, space reduction, less heat dissipation, increased equipment reliability, reduced alignment time, ease of maintenance, and simplified spare-parts logistics.

The instrumentation radar exterior, the interior layout of the electronics van, and the hardware supplied are shown in Figs. 1 and 2. The digital range tracker is shown in Fig. 3.

Antenna and receivers

The solid 12-ft.-diameter antenna reflector is constructed of foam-filled fiberglass, and its surface is metalized to provide electrical conductivity. Tolerances of 0.050-inch RMS are maintained in the forming of the parabolic surface. The lightweight materials represent a significant mass reduction over previous RCA 12-ft.-diameter instrumentation radar designs.

The microwave system utilizes a unique five-horn monopulse feed which provides complete choice of polarization, including horizontal, vertical, left-circular, or right-circular. Through an ingenious arrangement of miniature electro-mechanical switches mounted in stripline for low-level signals and of waveguide transfer switches for high-power signals, the console operator can instantly select the desired polarization. This feature is useful when tracking targets through varying geometrical aspects, particularly those equipped with transponders (radar beacons) and their related transponder antennas.

The AN/MPS-36 provides a two-channel monopulse system instead of the three channels used in past instrumentation radar designs wherein azimuth error, elevation error, and reference were carried separately through the microwave and receiver systems. In this two-channel system, successive pulses are switched in a microwave sampling system and combined in hybrids with the reference signal. Thus, the two channels carry reference signals and one of the angle-error signals simultaneously (but with opposite phase between channels) as shown in

Reprint RE-15-3-2
Final manuscript received August 1, 1969.

the simplified microwave block diagram (Fig. 4); the information contents of four successive pulses are shown in parenthesis.

This information is amplified by paramps to obtain the specified system noise figure, is converted to 30-MHz IF in the first mixers, and passed through a two-channel, RCA-designed solid-state receiver. It is subsequently summed and differenced to provide separate reference, azimuth-error, and elevation-error signals for the range tracker and angle servos. Separate skin- and beacon-track receivers, each comprising two channels, are provided.

The two-channel system offers an advantage in hardware reduction and in operational reliability. Should one of the channels fail, the radar can continue tracking, although with reduced signal-to-noise ratio and accuracy. With the more conventional three-channel system, a failure of one channel causes loss of track.

Angle-positioning system

The antenna is mounted on a newly designed pedestal whose position is servo controlled in azimuth and elevation for acquisition and automatic target tracking. The two axes rotate on cross-roller bearings driven directly by single -speed DC torquers instead of the more conventional geared electric or hydraulic motors. Direct-drive DC tachometers mounted integrally with the torquers close minor rate-loops around the servo drives. The major position-loop closure is Type II with variable bandwidth control in the auto-track mode. Elimination of drive gearing permits a smooth "closed-loop" tracking performance at all tracking rates, including both low and high speeds. In past designs using gear drives, smooth performance over a wide speed range has only been attainable with hydrostatic main bearings and dual preloaded gear trains.

Eliminating the compliance (springiness) of the conventional gear train results in high mechanical stiffness. The antenna backup structure is especially designed for rigid mechanical coupling. The lightweight foam-filled fiberglass reflector exhibits a high damping characteristic and low inertia. The torquers have an inherently high torque-to-inertia ratio; the combined antenna and motor inertia totals only 2200 slug ft^2, compared to 3500 slug ft^2 for a previous equivalent geared-drive design (a reduction of almost 40%).

Such factors combine to increase damping, hence reduce resonance peaking or ringing, and increase the resonant frequency of the antenna pedestal, which is well removed from the servo bandpass. Special compensation techniques employing notch-lead networks have aided in producing a servo whose gain and phase margins are better than those of geared-drive systems applied to the same size pedestal having the same servo bandwidth. The problems of gear-train backlash and variation of resonance with signal amplitude (a condition of geared drives) are eliminated. The bandpass characteristic is exceptionally flat, and the servo exhibits excellent transient response with a complete absence of backlash, stick-slip friction, and other forms of deadzone limit-cycle oscillations which can occur with Type II control.

At speeds up to 1.0 radian/sec, servo noise has been observed to be only 0.05 mils RMS. Position and velocity resolution better than 0.01 mil and 0.01 mil/sec respectively have also been observed, with less than 10% tracking velocity jitter (smoothness) at the very low rate of 0.01 mil/sec (one revolution in 7½ days).

Maximum (wide) servo position-loop bandwidths of 4.0 Hz (at 3.0 Hz crossover) and K_a (acceleration error coefficient) of 115/sec^2 have been achieved in both axes. This represents an improvement of four times in bandwidth and ten times in K_a over that reportedly obtained by other pedestals of comparable size and power which also use direct drive torquers. Although comparable pedestals using geared drives may exhibit equal bandwidth capability, their typical K_a is only ½ to ¼ as great. The improvement in the direct-drive system results from superior phase margin at the servo crossover frequency, which permits the design of greater low-frequency loop gain without stability problems.

The torquer (Fig. 5) used for the azimuth drive is a 32-pole device, 45 inches in diameter; two 18-pole torquers, 29 inches in diameter, are used at each end of the trunnion shaft for elevation drive. The rated torque in each axis is 2000 lb-ft average, 3000 lb-ft peak. The peak torques can be developed at maximum speeds of 1.0 radian/sec in azimuth and 0.5 radian/sec. in elevation.

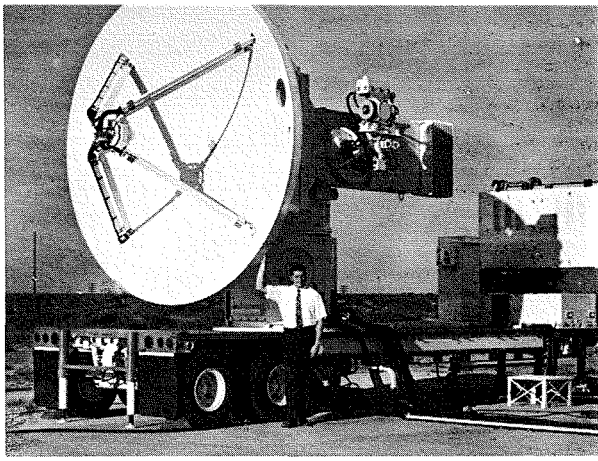

Fig. 1—AN/MPS-36 Instrumentation Radar.

Range tracker

The range tracker is a digital, all-electronic system capable of "n^{th} time around" tracking up to a range of 32,000 nautical miles while maintaining a high information rate. Since as many as 256 pulses may be in transit before the first target return is received, an ambiguity resolution process must determine which target return is related to a particular transmitted pulse. This is accomplished through a coded-pulse delay technique which automatically "finds" the correct "zone" for the range counter. The basic pulse repetition frequency (PRF) is maintained in this process to avoid interference from "running rabbits" in case other radars are also tracking the same target.

Since the target range is ambiguous due to the high PRF, it is necessary to prevent interference between the transmitter pulse and the target when the range of the target approaches the end of an ambiguous range interval (interference region). Depending on the "zone" of the target, a series of delayed and undelayed pulses is transmitted so that the target always appears at a time which is free of the transmitted pulse and close-in ground clutter. Corresponding delays are provided for the range gate, so that continuous tracking is performed through any of the 256 interference regions. The basic PRF is unaffected by this process.

Automatic transmitter phasing prevents "beacon stealing" which could occur whenever radar PRF timing, or the radar/target geometry are such that the target beacon would need to reply to more than one radar at the same

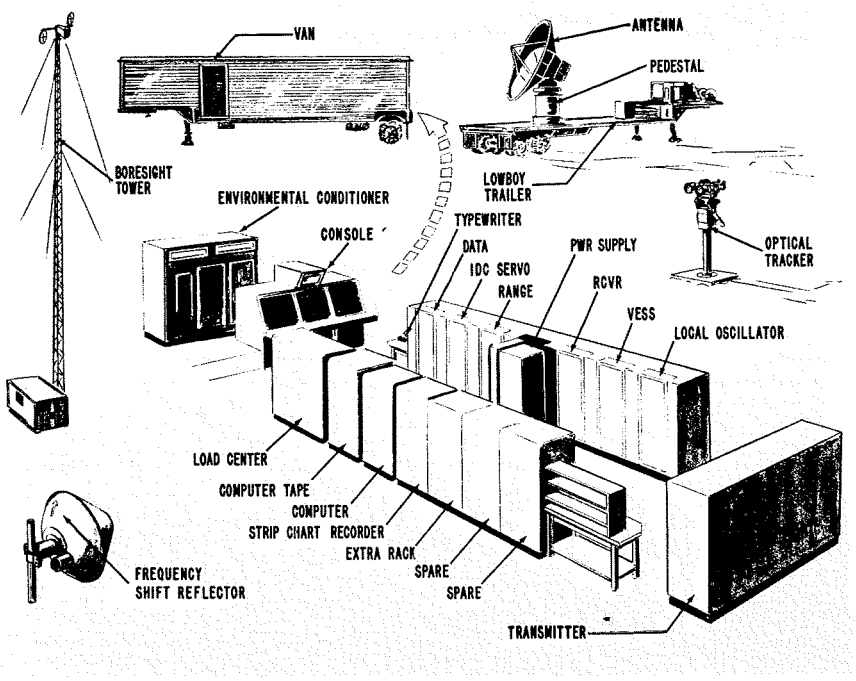

Fig. 2—AN/MPS-36 equipment supplied.

instant. Within a chain-radar system, several radars may track the same beacon simultaneously, but to prevent "running rabbits" their interrogations must be performed at the same PRF (or an integral multiple thereof). They must be spread out in time (at the beacon) so that spacing between pulses is always greater than the beacon's recovery time (that time delay required before the next pulse can be transmitted).

The range tracker senses the entry of a target return into either of two "guard gates" located on each side of the range gate. When an interfering target is detected, the radar's timing is rephased so that the desired target return moves to a new time position, clear of the potential interference.

A beacon coder is also built into the range system. If desired, a group of up to four additional closely-spaced pulses can be transmitted immediately following each "main bang", providing a 5-pulse code. The number of pulses and spacings is adjustable for compatibility with beacon decoders.

The Type II servo is designed with a K_a of about 3000/sec², and its K_v (velocity error coefficient) is almost infinite, resulting in very nominal dynamic tracking lag errors. The granularity of the 26-bit range word is 1-yard per bit (nominal).

Data system

The MPS-36 is the first RCA mobile instrumentation radar to include a general purpose digital-data processor and a digital tape recorder. The computer is a compact 24-bit word machine using integrated circuit techniques. It has a 8192-word memory with a 1.75-microsecond cycle time; a typewriter and paper-tape reader and punch are included for ease of instruction or program input. Programs can be stored in the magnetic tape recorder, or this equipment can be used to record radar metric data.

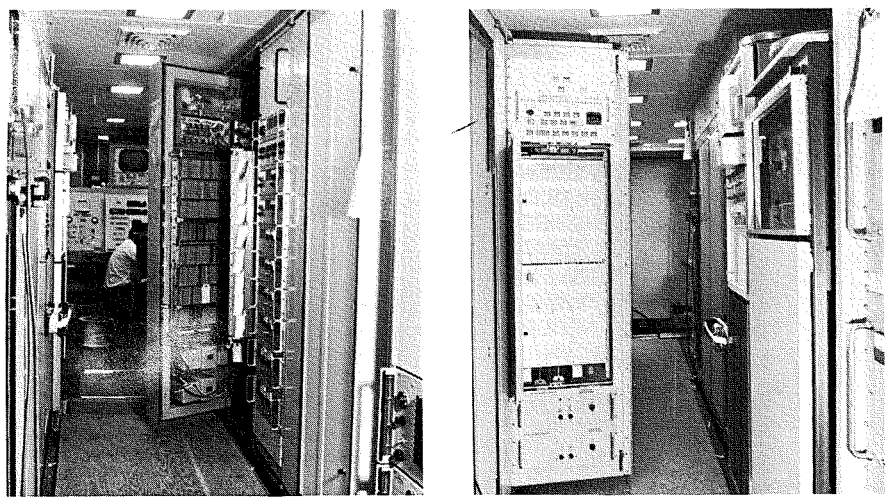

Fig. 3—Left photo is a rear view of the range tracker subsystem as it swings open for servicing. The receiver and doppler processor are on the right (with cover panels closed), and a portion of the console is visible at the rear. Photo at right shows the front of the range tracker (with cover panel open); computer and tape station are on the right.

The computer has been integrated with the radar to perform many functions previously requiring hardware implementation. Azimuth, elevation, range and doppler binary-data are converted into decimal numbers for console presentations. Angle servo bandwidths are adjusted in accordance with tracking error. Both standard deviation and lag errors are assessed; if standard deviation is excessive, bandwidth is decreased; if lag error is successive, bandwidth is increased to achieve an optimum compromise. Output data is corrected in azimuth and elevation virtually eliminating the effects of angle servo lag errors. Corrections for encoder bias (pedestal orientation with respect to grid North), pedestal leveling and antenna droop are also performed.

The computer performs many functions required in conjunction with the velocity extraction (doppler) subsystem described later. To assist the doppler tracker in the acquisition process, the computer provides coarse designation in velocity and acceleration based on the first and second derivatives of range position.

Doppler ambiguities in the fine-line spectrum are quickly resolved based on an advanced technique known as "invariant imbedded smoothing"; this method uses both ambiguous (but smooth) doppler information and unambiguous (but rough) range derivative information. Once resolved, the computer periodically verifies that the system is tracking the correct (central) spectral line, and automatically redesignates if a line shift occurs. It scales the doppler frequency (Hz) into velocity data (yards per second) based on the radar's operating frequency.

The computer also programs the doppler simulator while performing range simulation. The simulated velocity matches that of the moving range target, and the RF frequency of the simulated target includes the corresponding doppler shift. The radar is thus able to acquire and track a simulated target that represents a real target in range and range rate.

The computer stores a continuous se-

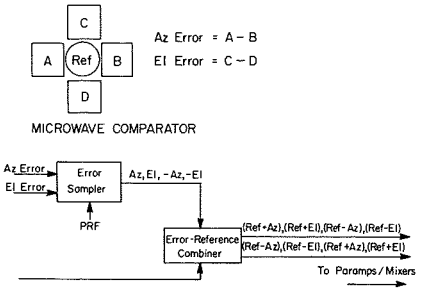

Fig. 4—Microwave block diagram.

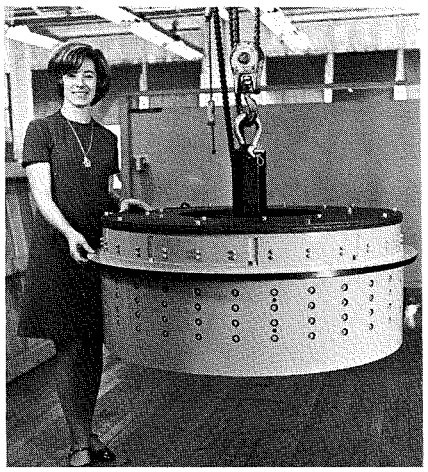

Fig. 5—Azimuth torquer (photo courtesy of Inland Motor Corp.).

quence of several angle, range, and doppler data words, then calculates and prints out the standard deviations of angle, range and doppler-tracker outputs. Such data provides an excellent check of system performance both during dynamic simulations of range and doppler, or under actual target-tracking conditions.

Transmitter

The AN/MPS-36 transmitter presented several new design challenges. For example, a more compact and lighter weight equipment suitable for the trailer was indicated. To accomplish weight reduction, a new type cross-field amplifier was designed for the final stage of the coherent chain. Transformer coupling of the modulator to the final stage was undesirable due to the requirement for pulse coding, and because of demanding space and weight considerations.

The resultant design has reduced the required space by a factor of 50%, compared with the previous noncoherent design of the AN/MPS-25 trailerized instrumentation radar. The final cross-field amplifier (CFA) is the first of a family of DC-operated CFA's. The amplifier is capable of one megawatt output at *C* band (5400 to 5900 MHz) with a system duty cycle of 0.001. The tube and its related 29-kV power supply are liquid-cooled through a heat exchanger in the radar's cooling equipment.

The DC-operated CFA exhibits several interesting properties; because it operates directly from a −29-kV DC supply, the usual bulky high-power modulation transformer is eliminated. Transformer storage and saturation characteristics with their limitations on pulse-code minimum spacing, pulse-to-pulse amplitude variations, and pulse-shape distortion are also eliminated.

Although the CFA can be "turned on" by application of signal to initiate the pulse, the amplifier cannot be "turned off" by cutting off the drive without creating spurious oscillations. To avoid this problem, a control electrode in the CFA receives a high-voltage pulse that clears the free electrons out of the CFA's interaction space and turns the amplifier off.

Careful attention was given throughout the transmitter design to considerations required for coherent system operation. Spurious signals are suppressed in excess of 30 dB; DC operated heaters are required for the two IPA's and the first IPA switch tube; DC supplies are carefully regulated to avoid undesirable phase modulation; and great care is taken to minimize pulse jitter so that range tracking accuracy can be maintained.

Doppler-tracking system

One of the most interesting features of the AN/MPS-36 in comparison with predecessor instrumentation radars is the inclusion of pulse doppler capability in the original design. Although several existing instrumentation radars have been upgraded by the addition of doppler modification kits, the AN/MPS-36 is the first RCA instrumentation radar to initiate this design feature as part of the basic radar.

The doppler-tracking system performs three principal functions:

1) It derives the "C" band local-oscillator signal and the transmitter-excitation signal from the frequency standard, and related coherent-frequency synthesizers, multipliers, mixers, and amplifiers.
2) It performs acquisition information processing to assist the doppler tracker in locking on to a spectral "fine-line."
3) It provides the doppler-tracking servo from which the doppler frequency of the target can be read into the computer for conversion into velocity data.

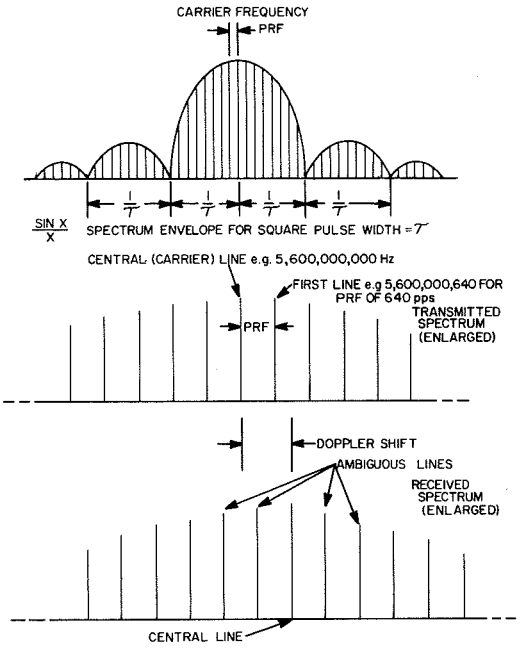

Fig. 6—Transmitted and received spectrum.

The typical fine-line spectrum of a pulsed signal in the frequency domain is shown in Fig. 6. The amplitude of the envelope corresponds to a (sin X/X) shape, and is composed of a large number of lines separated in frequency by the radar's PRF (see expanded diagram). To provide correct output data, the doppler system must track the central (carrier) spectral line of the target's return pulse, which has been shifted in frequency from the transmitted carrier line in proportion to the target's radial velocity.

After the gross-spectrum signal has been acquired, and the radar is automatically tracking in azimuth, elevation, and range, the received 30-MHz range-gated pulse is provided to the doppler processor. Based on first and second differences of range-position data, the computer provides coarse velocity and acceleration designation to the doppler tracker.

Any one of the ambiguous lines can then be acquired by the doppler tracker provided the signal can be maintained within its narrow-band fine-line filter for a time interval sufficient to allow the doppler servo to respond and lock-on. This process requires that the doppler acquisition system match approximately the target's acceleration and velocity before

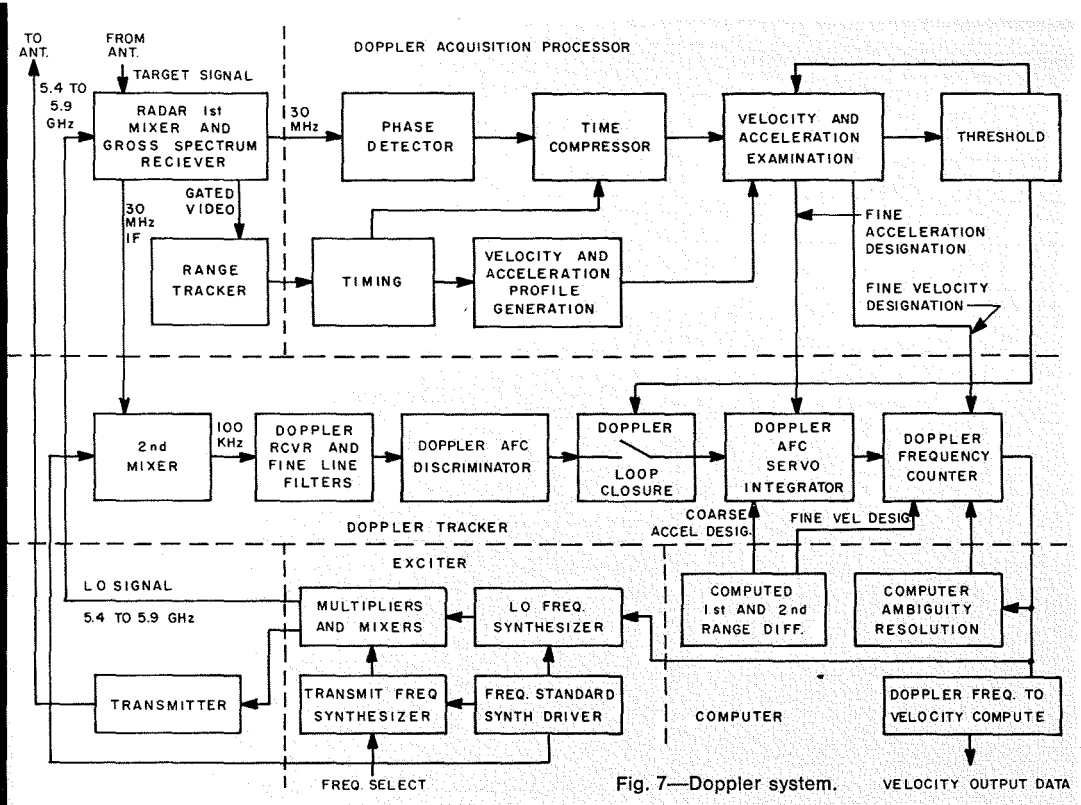

Fig. 7—Doppler system.

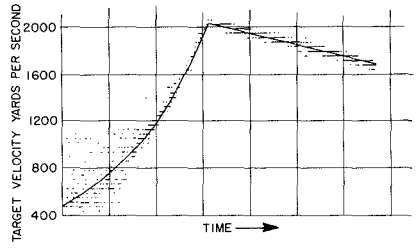

Fig. 8—Doppler velocity (solid line) vs. range first derivatives.

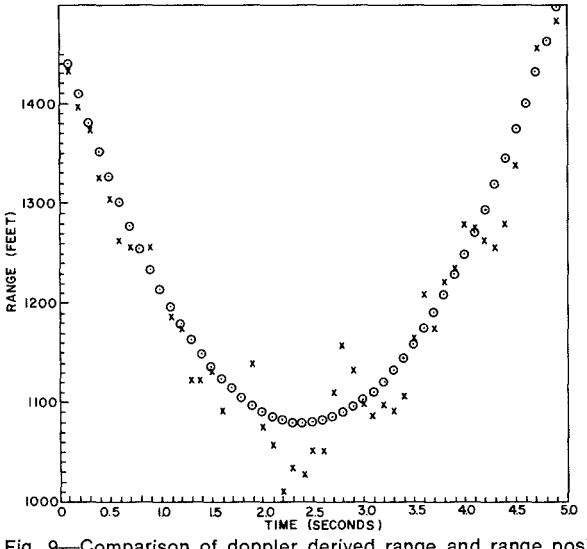

Fig. 9—Comparison of doppler derived range and range position (direct measurement).

the doppler servo loop can be closed. After doppler tracking has been initiated, the computer resolves the doppler ambiguity by calculating the number of lines (velocity offset) by which the doppler data differs from computed range velocity, and inserts an appropriate digital correction into the doppler counter.

A simplified block diagram (Fig. 7) shows the doppler exciter, acquisition system, and tracker, as well as their interrelationships with the gross-spectrum receiver, range tracker, computer, and transmitter.

The doppler acquisition processor represents the most complex part of the doppler system. Within the coarse velocity and acceleration region designated by the computer, the processor searches the time-compressed information very rapidly through a series of velocity and acceleration "profiles" for the particular velocity and acceleration which best "match" the actual target characteristics. The corresponding "fine" values of velocity and acceleration are then inserted into the doppler counter and servo integrator respectively, while the doppler tracking servo loop is closed.

The error sensed by the doppler discriminator is integrated and applied to an analog-to-pulse-rate converter which drives the doppler up-down counter. The data in the doppler counter sets the frequency of the digital frequency synthesizer from which the local oscillator frequency (of approximately 5 x 10^9 Hz) is derived with 1 Hz granularity, and the doppler loop is closed through the radar's first mixers. The Type II doppler servo includes fine-line filter bandwidths of 160 and 40 Hz, which relate to 3 dB servo bandwidths of approximately 40 and 10 Hz respectively; design values of K_a are 2920/sec^2 and 230/sec^2 for the respective servo bandwidths (K_v is essentially infinite for a Type II servo). Laboratory tests of the doppler subsystem alone indicate standard deviation of tracking error to be in the order of 0.02 yards/sec for accelerating targets having 12-dB signal-to-noise ratio.

Two interesting examples of the improvement in information capabilities made possible by pulse doppler radars are apparent in Figs. 8 and 9 which are data plots obtained from an instrumentation radar previously modified for doppler tracking.

The doppler velocity time plot (Fig. 8) is superimposed on a plot of velocity data obtained from first differences (first derivative) of range position. Note the wide dispersion of the latter data, and the uncertainty at the instant the target motion changed from acceleration to deceleration (jerk). In contrast, the doppler velocity plot shows a well-defined corner.

Two plots of range position points (Fig. 9), as obtained during a satellite track, are superimposed on one another. The X marks represent position points measured by the range tracker. The circled points show range position data computed from time integration of doppler velocity data.

Conclusion

This paper has discussed some of the outstanding design accomplishments of RCA's newest Instrumentation Radar product, which was delivered on schedule to White Sands Missile Range in August, 1969. At this writing, the first AN/MPS-36 is undergoing evaluation tests at White Sands. It provides many capabilities never before available in a fully mobile instrumentation radar, and promises to enhance RCA's leadership in this field.

Acknowledgment

The author acknowledges the contributions of his associates who made the preparation of this article possible. Some of the major contributors are: J. C. Volpe, Program Manager; W. H. Beckett, System; J. J. Wonderlich, Angle Tracker; H. D. Young, range tracker; B. J. Matulis, Data System and Computer; T. C. Royer, Programs; W. W. Powell, Microwave System; A. K. McGee, Transmitter; W. L. Mays, and H. A. Ulrich, Doppler Processor.

Using tests and analyses to achieve reliable microwave equipment

H. H. Anderson, Jr. | V. Stachejko

Those aspects of microwave devices, commonly used in radar applications, which affect system reliability are identified and appropriate tests are recommended. Included in the discussion are RF amplifiers of various classes, duplexers, antennas, and other microwave devices.

APPLICATION OF RELIABILITY ENGINEERING TECHNIQUES in the design and development of large-scale radar systems has resulted in marked improvement in the long-term performance of many critical subsystems. In particular, those equipments employing familiar mass-produced components in lumped-parameter circuits have received the most attention and have derived the greatest benefit.

In some cases, the reliability of these low-frequency equipments has improved to the point where the microwave subsystem has become limiting in terms of system reliability. The time therefore appears ripe for more emphasis on reliability in microwave equipments.

Admittedly, this is not an easy task for several very important reasons:

1) Microwave devices generally employ distributed parameter techniques which are often unfamiliar to many reliability engineers;
2) Microwave devices often involve peculiar electrical-mechanical interfaces and interrelationships;
3) Production quantities of microwave components and devices are often so low and the unit cost so high that statistical evaluations are impractical;
4) Vendors of newly produced components, pressing the state of this rapidly-advancing-art often do not know, or fail to fully state, all of the significant performance limitations pertinent to the myriad applications of the devices.

In view of such conditions, how can reliable microwave equipment be achieved? At present, by the extensive use of electrical and mechanical testing in an environment which duplicates (as nearly as possible) the intended end-item application of the device and by painstaking analysis of failures or performance degradations.

In general, the microwave subsystem of a typical radar will begin at the output of the transmitter, will interface with the ultimate propagating medium (generally free space) at the antenna, and will end at the input to the IF receivers. Included within these boundaries will be such components and/or devices as: RF transmission lines (typically waveguide or coaxial); isolators; rotary joints; duplexers; antennas or antenna feeds; RF amplifiers; RF switches, attenuators and phase shifters; mixer/frequency converter/IF pre-amplifier assemblies; and the associated local oscillator, LO distribution network and peripheral test and monitoring equipments.

RF amplifiers

Among the most troublesome microwave devices employed in a modern radar are the low-noise RF amplifiers required to achieve high sensitivity to enable long-range detection of small targets. The principal problem is the susceptibility of this class of device to burn out or long-term degradation caused by leakage of RF energy spikes through the duplexer. As a result, the reliability of solid-state amplifiers often fails to live up to expectations and in some cases is even lower than competing tube-type devices.

There are wide variations, however, between the various types of amplifiers and some may be protected more easily than others.

Reprint RE-15-3-13
Final manuscript received September 2, 1969

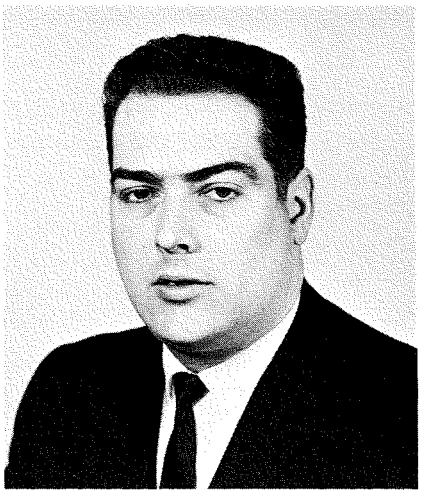

H. H. Anderson, Jr., Ldr.
Antenna/Microwave Design
Missile and Surface Radar Division
Moorestown, N.J.
received the BSEE from the University of Pennsylvania in 1960 and the MSEE from U. of Pa. in 1967. Since joining RCA in 1960, Mr. Anderson has concentrated on development of antenna and microwave systems for a variety of applications. He has been active in study programs for advanced antenna systems, including space-erectable antennas. One of his assignments involved design work on the rendezvous radar for the Apollo LM lunar-landing vehicle. Mr. Anderson held the post of Antenna Skill Center Engineer, an internal consultant position, for over a year; during this time, he was responsible for the synthesis of advanced microwave and antenna subsystem configurations for a wide range of programs. Mr. Anderson became Leader of an Antenna/Microwave design group in 1966 and is currently responsible for the RF sub-system of the AN/FPS-95 radar and several other major antenna and microwave R & D programs. Mr. Anderson is a member of IEEE (PGAP, PGMTT, & PGAES) Tau Beta Pi, and Eta Kappa Nu. He has filed a number of patent disclosures and recently taught a Company-sponsored after-hours course on antenna theory.

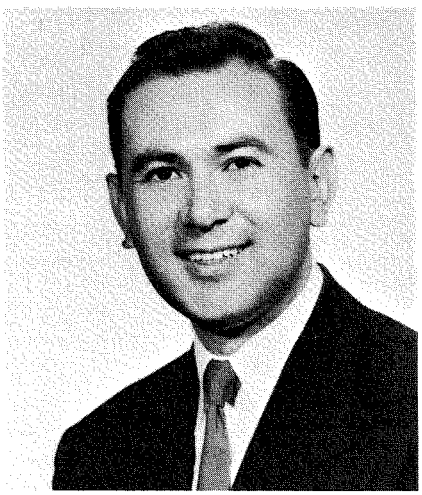

Vitaly Stachejko
Antenna/Microwave Design
Missile and Surface Radar Division
Moorestown, N.J.
received the BSEE and MSEE from the University of Pennsylvania in 1958 and 1963, respectively. Since 1958 he was employed by the Missile and Surface Radar Division as a design and development engineer. He has been engaged in development of low-noise solid-state microwave amplifiers, Gunn-effect microwave oscillators, and high power diode duplexers. Mr. Stachejko is a member of IEEE.

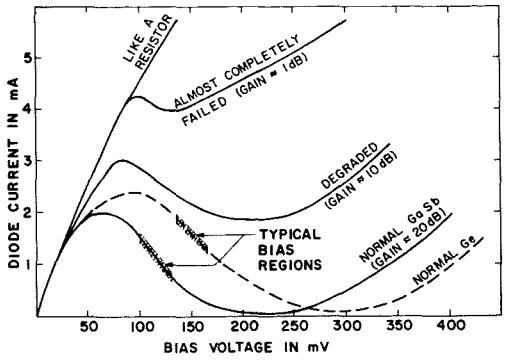

Fig. 1—Progressive failure of typical tunnel-diode amplifiers.

Tunnel diode amplifiers

Based on recent observations, tunnel-diode amplifiers apparently can tolerate only 0.03 to 0.10 erg RF spike leakage and 20 to 30 mW flat leakage during the radar pulse for Gallium Antimonide (*GaSb*) and Germanium (*Ge*) types respectively if long term degradation is to be held to an acceptable level. This value currently represents a lower limit of leakage obtainable with PIN diode limiters backing up a typical duplexer. The long-term effect of excessive spike leakage as revealed by changes in the tunnel diode *I-V* characteristic (Fig. 1).

Since the operating bias voltage is normally on the order of 80 to 150 mV with 1.0 to 1.5 mA typical bias current, the device is quite subject to damage by transients and the need for filters and fast acting clamps in the bias input circuit is obvious. In addition, the performance of tunnel diode amplifiers is temperature dependent, often requiring thermal stabilization.

To achieve a reliable tunnel diode amplifier design, it is necessary

1) To determine by testing the adequacy of the RF spike leakage suppression,
2) To demonstrate transient immunity,
3) To perform within specified limits under extended periods of temperature cycling, and
4) To survive shock and vibration testing commensurate with the intended operating environment.

After installation in the field, the amplifier gain and noise figure should be measured frequently to detect the onset of diode degradation and permit corrective action prior to total failure.

Parametric amplifiers

Parametric amplifiers can tolerate up to approximately 1.0-erg spike leakage with approximately 100 mW permissible flat leakage during the radar pulse without appreciable long-term degradation. This leakage level can be obtained with conventional gas duplexers without the need for back-up limiters, if a DC keep-alive voltage is employed in the TR device. Bias voltage is typically in the range of 0 to 1.0 volts which results in under 3.0 μA bias current and a considerably reduced susceptibility to transients. Thermal variations are still significant, although not to the same degree as with tunnel diode amplifiers. Testing of these devices should however be equally thorough and rigorous and the same parameters must be monitored as with TDA's. In addition, parametric amplifiers employ RF pump sources such as klystrons with peripheral equipment (such as power supplies) which also must be tested and monitored.

Transistor amplifiers

Transistor amplifiers are useful up through *L*-Band (in some cases to *S*-Band if noise figure is not paramount) and are far more rugged than either TDA's or Paramps. Transistor amplifiers will typically survive spike and flat leakage levels of 0.1 to 1.0 Watt. Since the bias voltage will typically run from 10 to 20 V with only milli Amps of current resulting, the device is highly insensitive to damage by conducted transients. Verification of these characteristics by testing is still necessary however before considering the design to be final. In the field, an occasional gain and noise figure check will usually suffice to verify normal operation of the device.

Other RF amplifiers

Other types of RF amplifiers exist which are even less subject to RF leakage effects than the foregoing. These would include traveling wave tubes (TWT's), diftron's, and masers. In general, however, these devices require complex power supplies and peripheral support equipment which must be carefully evaluated from a reliability standpoint. The TWT's and diftrons must be tested for the effect of nearby magnetic fields and/or ferromagnetic materials while the cryogenic cooling equipment and millimeter-wave pump source associated with the maser must be carefully evaluated.

In general, although there are differences between the various devices described above, certain common tests are involved. In all cases involving the relatively unforgiving solid-state devices, the tolerance to RF spike leakage must be thoroughly explored. The vulnerability of the device to conducted transients on bias or control leads must be determined by simulation of "worst case" expected field conditions and performance effects due to thermal changes must be measured. In some instances (as with *TDA*'s) an extended period of thermal cycling may be required before the characteristics of the device stabilize. Vibration and shock testing is required to assure diode/holder compatibility and survival of the device under field conditions including accidental mishandling. All peripheral equipments—such as RF pump sources, power supplies, and refrigerators—must be evaluated with respect to both their own reliability and to the degree of performance variation permitted by the design margin.

Duplexers

The duplexer serves to direct high power RF energy from the transmitter toward the antenna during the transmit period and to direct low-level RF signals from the antenna toward the receiver during the quiescent period. It is this device which, through finite isolation, causes the RF energy leakage discussed in preceding paragraphs which can be damaging to the sensitive RF amplifiers. The duplexer itself has also been a frequent source of radar failure. There are several different types in use today incorporating gas, ferrite, and diode devices and combinations thereof.

Gas duplexers

Perhaps the oldest form of duplexer is the gas type. A quantity of gas capable of being readily ionized is contained within a transmission line. The incidence of a high RF field causes ionization of the gas and presents a short circuit across the line thereby inhibiting the flow of RF energy beyond the cell and reflecting it back down the transmission line. By means of the microwave circuit structure involving branch lines or hybrids, the energy is routed toward the antenna. When only low-level signals are present, the gas de-ionizes and energy is free to propagate toward the receiver.

To encourage rapid ionization of the gas and limit the quantity of energy which passes through the TR device to the receiver prior to its firing, a high-voltage electrode known as a "keep-alive" is often inserted into the cell to assure a ready supply of free electrons. Since ionization of the gas within a TR tube is essentially a random process, the actual spike leakage energy passing through the tube will vary from pulse-to-pulse. Fig. 2 shows a typical spike energy distribution for both single TR's and balanced gas duplexers. There will be virtually no spikes having energy less than the minimum value required to ionize the gas. However, there may be occasional spikes having energy considerably greater than the maximum levels indicated by the graph although the frequency of occurrence will be extremely low. It has been observed that the first sign of an incipient TR tube failure is a change in the keep-alive current which is typically on the order of 100 μA. As typical TR tube life is on the order of 500 to 1000 hrs, this parameter should be measured often to permit replacement of the device before it fails completely with an attendant damaging effect on RF components in the low-level receive chain.

There are also available on the market, TR devices without keep-alive electrodes which are augmented by solid-state limiters to suppress the RF spike leakage. It is said that this technique results in extended life of the device although the resulting insertion loss is somewhat higher. Without a keep-alive current to monitor, incipient failure is much more difficult to detect and a direct measurement of spike leakage is indicated on a regular basis.

Ferrite duplexers

Non-reciprocal ferrite devices such as circulators are frequently used in radar duplexing applications. Since the available isolation is on the order of 20 to 25 dB and is dependent on the impedance match of the antenna, the circulator is generally backed up by another device such as a gas TR tube, ferrite limiter, or diode switch.

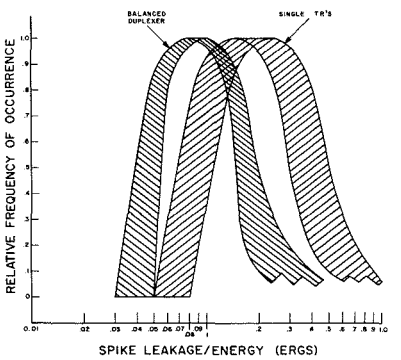

Fig. 2—Spike leakage characteristics for typical gas duplexer.

The ferrite circulator is often large, heavy, and dissipates appreciable amounts of RF energy thereby often requiring liquid cooling. The ferrite material is brittle, temperature dependent, and is usually hygroscopic. The device therefore presents mechanical problems and should be subjected to shock, vibration, and environmental testing at low and high power before use in a field installation. Also in the event of an antenna arc or failure, full transmitter power may appear at the backup TR device at least momentarily. This must be taken into account in sizing and evaluating this component.

Diode duplexers

A class of solid-state duplexers employing high power silicon PIN diodes in a single-pole switch configuration are currently under development for several radar applications. Although long-term life data is not yet available, several of these devices have been subjected to severe high-power RF testing at peak power levels in excess of four Megawatts (twice the design level) and average power levels up to one hundred Kilowatts in a balanced duplexer configuration. To make the test even more severe, the antenna was caused to arc intermittently, reflecting the RF power back toward the duplexer without failure. In a final desperate attempt to cause a failure, 50% of the diodes were removed from the TR device and the tests were repeated. No failures occurred. Fig. 3 shows the measured and calculated diode junction temperature rise as a function of the applied RF power level.

As with any high-power RF component, testing at full power or above is an absolute necessity before completion of the design phase. It is not always necessary to have the actual transmitter available for this purpose as resonant ring testing is quite adequate for most low-loss, one- or two-terminal dominant-mode RF devices. The solid-state driver circuit used to switch the PIN diode bias current before and after each transmitter pulse

EXPERIMENTAL AND CALCULATED DIODE JUNCTION TEMPERATURE RISE AS A FUNCTION OF AVERAGE RF INPUT POWER AT 26 MHz WHEN THE DIODES WERE FORWARD BIASED TO 2 AMPERES PER DIODE

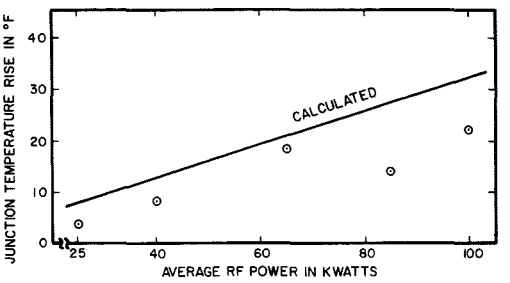

Fig. 3—Diode junction temperature versus average RF power level.

must be carefully evaluated from a reliability standpoint; but this should not be difficult as it is basically a conventional switching circuit using standard components. As for the RF diodes, a safe rule of thumb is that reliable operation requires that the junction temperature be maintained below 100°C, although some claim that 175°C represents a safe upper limit.

Antennas

When used in stringent applications, extraordinary testing of antennas may also be required to achieve a reliable design. In addition to high power, shock, vibration, gain, pattern and other conventional tests, it may be necessary to expose an antenna intended for space application to extended periods in a thermal-vacuum chamber. Certain materials acceptable for ground-based applications may out-gas or sublime in space.

Antennas intended for undersea use may require testing under high pressure and certainly extended exposure to salt water. Antennas intended for airborne applications must be high-power tested at worst-case pressure-altitudes to evaluate multipactor breakdown effects. Defense-related antenna systems must sometimes be exposed to blast overpressures.

Conclusion

The variety of special tests required to assure reliable equipment design is limited only by the number of different applications one can find for the equipment. The main point to be made is that there is no acceptable substitute at this time for a well-conceived carefully-formulated and executed testing program if reliable microwave equipment design is to be achieved.

Various methods of determining the gain of a proposed TV antenna

R. N. Clark | Dr. M. S. Siukola

The quest for maximum radiated TV power and optimum coverage with practical transmitter power levels often calls for sophisticated high-gain directional antennas. Such custom designs have many interrelated characteristics; however, gain, because of its obvious relationship to radiated power, is the most scrutinized. This paper brings into perspective all the factors influencing gain such as beam tilt, null fill, and directional patterns. These factors influencing gain must be observed so that the simplified gain equations in this paper can be applied; similarily, to guarantee antenna specifications, all radiation parameters must be studied and power losses considered. Although the design philosophy and methods discussed may result in antennas with somewhat larger apertures than those based on over-simplified approaches, there is greater assurance that custom antennas will possess the desired characteristics.

IN THE DESIGN of any television broadcast antenna system the attainment of high gain is nearly always desirable. But, for custom-antenna radiation requirements (involving special patterns, directional antennas, unusual terrain conditions, and extremely high- or super-power), the provision of high gain can be of paramount importance. To appreciate the role of gain in the successful design of antennas to meet such rigorous requirements, it is appropriate to describe and define antenna gain.

What is gain

Antenna gain is defined very simply by Eq. 1, which compares the antenna under consideration with an ideal dipole when both radiators are producing the same field in the desired polarization at a given distance in the far field.

Here, P_D is the power into the ideal dipole and power to the antenna under consideration is represented by P_{IN}, which can be separated into radiated power and antenna power losses.

Another basic relationship to be discussed later involves the RMS, peak, and horizontal gains of an antenna; it is expressed in Eq. 2.

Determination of the power radiated from any source involves a complete summation of the power radiated in all directions. The reason for this may be more apparent when the operation of the antenna is visualized in its true sense as a multiport network such as that shown in Fig. 1. Here, the antenna is a radiating source at the center of a sphere in space; the sphere is divided into a finite number of segments, or ports, which pass radiated power. Through one such port, we will have a power of P_1 out, through another, P_2 out, etc. The sum of the power from all ports will equal the power to the antenna, P_{IN}-losses, or:

$P_{IN} = P_1 + P_2 + P_3 + \cdots + losses$ where N is the total number of ports.

Summation of radiated power in terms of relative field is given in pattern integral form by Eq. 3.

The relative field, E, is a function of the angles of azimuth and elevation. K includes the radiated power of a dipole, while P_L, normalized to the K factor shown, is the power lost in the antenna.

In Eq. 3, the relative field is not specified as to polarization, since for a TV antenna, the gain must be in terms of the horizontally polarized field, thus any vertically polarized field produces energy that is considered lost. Since most radiators do radiate some vertically-polarized energy, Eq. 3 is expanded to a general gain equation (Eq. 4). Eq. 4 separates horizontal from vertical polarization and relates them both field, $E^2_{HP(MAX)}$. Thus, there are two sur- to the maximum horizontally-polarized

Reprint RE-15-3-20
Final manuscript received May 8, 1969.

Dr. Matti S. Siukola, Ldr.
Advanced Development
Commercial Electronic Systems Division
Gibbsboro, N.J.

holds the degrees of Diploma Engineer (MS) in Electrical Engineering from the Finland Institute of Technology, Helsinki, and Doctor of Philosophy in Electrical Engineering from Oregon State University (1952). From 1946 to 1949 he was employed as a Design Engineer by the Finnish Broadcasting Corp. to work mainly on AM and FM transmitters and antenna. He also acted as Technical Advisor for the Finnish Government and the City of Helsinki on VHF communications equipment. In 1952, Dr. Siukola joined RCA as a design and development engineer on television transmitting antennas. He has continued in this field and is presently technical consultant to the TV Antenna Engineering section and leader of the Advanced Development group. He has been instrumental in developments familiar to the TV Broadcast Industry, such as: high-gain Superturnstile antennas, Traveling Wave antennas, Zig-Zag antennas, "Candelabra" installations, and RF pulse analysis of antenna system performance. Dr. Siukola who is listed in the American Men of Science, has presented and published several papers in his field. He is a member of IEEE, the Professional Group on Antennas and Propagation, Professional Group on Management, Institution of Electrical Engineers, England, Franklin Institute, Phi Kappa Phi, Eta Kappa Nu, and Pi Mu Epsilon.

R. N. Clark
TV Transmitting Antennas
Commercial Electronic Systems Division
Gibbsboro, N.J.

began his career in radio in 1946 with radio station KCRS. After three years in the U.S. Air Force he entered Southern Methodist University and received the BSEE in 1952. He received the MSEE from Drexel Institute of Technology in 1956. Mr. Clark has been employed by RCA since 1952. He has contributed to the development of high powered radar, television, and broadcast transmitters; he holds three patents in this field. He is presently concerned with the development of television transmitting antennas.

face integrations, one being that of the horizontally-polarized energy, and the other that of the vertically-polarized energy. Further, losses are separated into two components: those in the antenna radiator and those in the feed system of the antenna.

To constitute a complete surface integration, the horizontally-polarized field related to the radiator, E_{HP}, can be represented by horizontal and vertical patterns of the antenna.

Factors affecting gain

The general gain equations, Eq. 4, is rewritten as Eq. 5 to show all the factors affecting gain, and to identify the portions of the equation influenced by such factors. G, of course, represents the directional gain of the antenna.

The factors influencing the directional antenna gain, G, which are described in detail later, are listed with Eq. 5. Shown alongside the factors are percentages indicating the general range of influence, the mid-values being typical. The high extremes are rare, but they can and do exist in certain applications that require special variations in antenna designs.

Horizontal gain

The effect of horizontal gain on directional gain was first expressed in Eq. 2 and is now expanded here as Eq. 6 to illustrate the relationship in integral form.

The horizontally-polarized relative field is expanded into two terms; which for a first approximation is generally possible. The first term (E_θ) is represented by the vertical pattern of the antenna since it is the relative field as a function of the elevation angle; and the second term (E_ϕ) is represented by the horizontal pattern since it is the relative field as a function of the horizontal angle. The integral of E_ϕ is seen to be $2\pi/G_H$. Since $E_{\phi MAX}$ represents the

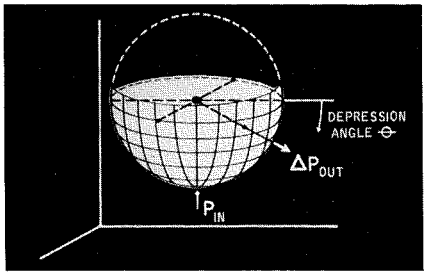

Fig. 1—Antenna as a multiport network.

$$G=\frac{P_D}{P_{IN}}=\frac{P_D}{P_{RADIATED}+P_{LOSSES}} \quad (1)$$

$$G_{RMS}=\frac{G}{G_H} \quad (2)$$

$$G=K\left[\frac{1}{E_{MAX}^2}\int_\phi\int_\theta E^2(\theta,\phi)\cos\theta\,d\theta\,d\phi+P_L\right]^{-1} \quad (3)$$

where $P_L=\frac{K}{P_D}P_{LOSSES}$.

$$G=K\left[\frac{1}{E_{HP(MAX)}^2}\left[\underbrace{\int_\phi\int_\theta E^2_{HP}(\theta,\phi)\cos\theta\,d\theta\,d\phi}_{\text{radiated power horizontal polarization}}+\underbrace{\int_\phi\int_\theta E^2_{VP}(\theta,\phi)\cos\theta\,d\theta\,d\phi}_{\text{radiated power vertical polarization}}\right]+P_{LR}+P_{LFS}\right]^{-1} \quad (4)$$

(P_{LR}: radiator losses; P_{LFS}: feed system losses)

$$G=K\times(SF)\left[\frac{1}{E_{HP(MAX)}^2}\left[\underbrace{\int_\phi\int_\theta E^2_{HP}(\theta,\phi)\cos\theta\,d\theta\,d\phi}_{G_H\,NF_E\,NF_A\,BT\,PV}+\int_\phi\int_\theta E^2_{VP}(\theta,\phi)\cos\theta\,d\theta\,d\phi\right]+P_{LFS}\right]^{-1} \quad (5)$$

(SF; VP; FS)

G	*directional gain*	
G_H	*horizontal gain*	
NF_E	*null fill by element*	*(typical 0 to 20 to 30%)*
NF_A	*null fill by array factor*	
BT	*beam tilt*	*(typical 0 to 5 to 20%)*
PV	*vertical pattern variation*	*(typical 0 to 3 to 15%)*
VP	*vertically polarized energy*	*(typical 1 to 3 to 10%)*
FS	*feed system losses*	*(typical 1 to 3 to 10%)*
FS	*safety factor*	*(typical 2 to 5 to 10%)*

$$G=K\left[\frac{1}{E_{HP(MAX)}^2}\left[\underbrace{\int_\phi\left(\frac{E_\phi}{E_{\phi MAX}}\right)^2 d\phi}_{\text{equals }\frac{2\pi}{G_H}}\cdot\underbrace{\int_\theta E^2_\theta\cos\theta\,d\theta}_{NF_E\,NF_A\,BT\,PV}+\int_\phi\int_\theta E^2_{VP}(\theta,\phi)\cos\theta\,d\theta\,d\phi\right]+P_{LFS}\right]^{-1} \quad (6)$$

(VP; FS)

$$G=(G_V)_{RMS}\,(G_H)\,(SF) \quad (7a)$$
$$(G_V)_{RMS}=(D_V)\,(\eta)$$
$$(D_V)=1.22\,(A\lambda)\,(NF)_A\,(BT)$$
$$(\eta)=(NF)_E\,(PV)\,(VP)\,(RL)\,(FS)$$

$$G=1.22\,(A\lambda)\,(NF_E)\,(NF_A)\,(BT)\,(PV)\,(VP)\,(RL)\,(FS)\,(G_H)\,(SF) \quad (7b)$$

$A\lambda$	*aperture in wavelengths*	
NF_E	*element null fill factor*	*(typical .7 to .8 to 1)*
NF_A	*array null fill factor*	
BT	*beam tilt factor*	*(typical 8. to .95 to 1)*
PV	*vertical pattern variation factor*	
VP	*factor for vert. pol.*	*(typical .9 to .97 to .99)*
RL	*radiator loss factor*	
FS	*factor for feed system efficiency*	*(typical .9 to .97 to .99)*
G_H	*horizontal gain*	
SF	*safety factor*	*(typical .9 to .95 to .98)*

$$G_{RMS}=N\,(G_L)\,(NF_A)\,(BT)\,(FS)\,(SF)\,(\textit{omnidirectional})$$
$$G=N\,(G_L)\,(NF_A)\,(BT)\,(PV_A)\,(G_H)\,(FS)\,(SF)\,(\textit{directional}) \quad (8)$$

$$G_{RMS}=N\left(\frac{G_{PANEL}}{G_{H(PANEL)}}\right)(NF_A)\,(BT)\,(PV_A)\,(FS)\,(SF)\,(\text{omni}) \quad (9)$$
$$G=(G_{RMS})\,(G_H)$$

$$G_{RMS}=N\left(\frac{G_{PANEL}}{M\,G_H{}^1}\right)(NF)_A\,(BT)\,(FS)\,(SF) \quad (10)$$

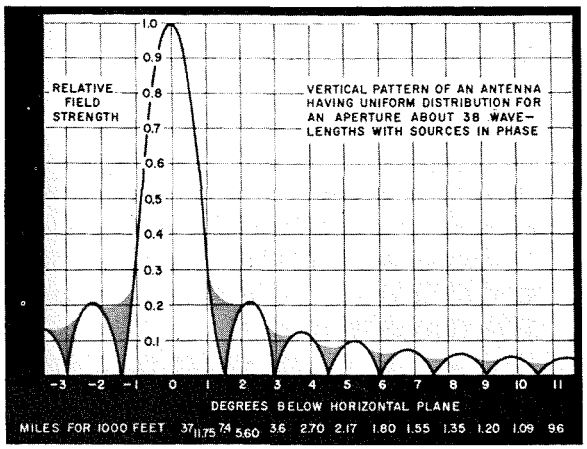

Fig. 2—Null fill increases power integral.

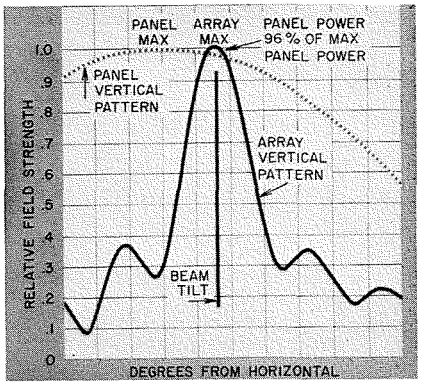

Fig. 3—Beam tilt factor illustration.

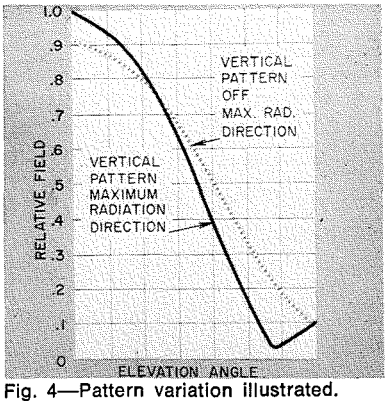

Fig. 4—Pattern variation illustrated.

maximum gain, and the integral of E_ϕ^2 represents the area of the horizontal pattern, and results in the average gain, then the horizontal gain G_H may be defined as the ratio of peak gain-to-average or RMS gain. Wherever the horizontal gain is brought out as a separate factor, the remaining factors represent the RMS gain of an antenna. Thus, in general, the RMS gain includes the various factors that affect the directional gain.

Null fill

Null fill, in general, consists of two factors: null fill by the element and null fill by the array. When the radiator is one of high gain such as a zig-zag element on a panel, there is a null-fill factor due to the natural illumination on the element. When an array of radiators has a power distribution or relative phasing so that the various nulls are filled to the desired level, a reduction of gain occurs; this may be defined as the array null-fill factor The influence of this factor upon gain is illustrated in the vertical pattern of Fig. 2. Here we see a series of complete nulls that occurs when all the radiating elements are driven with equal power and equal relative phase. To introduce pattern distribution and phasing to fill the nulls, as represented by the shaded areas, requires additional energy, of course. Thus, the array null-fill factor is generally derived when the vertical pattern of the proposed antenna is computed or synthesized. Possible values of null-fill factor ranges from 0 to 30 percent, but 20 percent is typical.

Beam tilt

Beam tilt is a factor that often influences the gain of arrays made up of high-gain radiating panels. This factor is illustrated by the two vertical patterns in Fig. 3, one being that of the radiator mounted to produce maximum radiation in the horizontal direction, and the array pattern that is tilted to an angle below the horizontal. It can be seen that, in the direction of beam tilt, or maximum radiation of the array, the relative field of the panel pattern is below its maximum field, and in this case the gain is only 96% of its maximum. This emphasizes the importance of the beam-tilt factor in determining the gain of such antennas.

Pattern variations

Vertical pattern variations in the horizontal direction from the main lobe of radiation are illustrated in Fig. 4; we see a typical vertical pattern of a panel-type radiator, measured in the maximum direction of radiation. Now, when the vertical pattern is measured in directions off the main lobe (as shown by the dashed pattern), considerable variation appears in the vertical pattern. It is a broader pattern in which energy is radiated in the elevation angle where a null normally exists, particularly in the main lobe. This condition illustrates the importance of considering radiation characteristics not only in the main lobe but in all directions.

An exception is the type of antenna which utilizes slots arranged in phase about a pole, such as the Pylon antenna. The pattern variation of the Pylon antenna is negligible. Every configuration of radiators, however, should be evaluated for this factor prior to use in a system. Other aspects of vertical pattern variation are considered later when methods of predetermining gain are discussed.

Vertical polarization

Vertically-polarized energy, considered as lost in TV antennas, may be kept to within one to three percent of the total power into the antenna in good designs. The vertically-polarized energy radiated is controlled by the design of the radiating elements. This energy loss, of course, effectively reduces the gain of the antenna by the same percentages.

Feed-system losses

Feed-system losses are readily determined by calculating the losses in the transmission line and radiator. Typical values, which are a function of transmission line and radiator size, range from one to three percent.

Safety factor

Safety factor is introduced in antenna-gain calculations to compensate for manufacturing tolerances that exist in the radiating elements and feed system components. This factor is added on top of those previously determined.

Predetermining antenna gain

Antenna gain may be predetermined by any of three general approaches:

1) By complete measurements;
2) By calculations; and
3) By measurements supplemented with calculations.

In the first method, by measurement, a full-size or scale-model antenna may be fabricated and complete horizontal and vertical patterns taken to derive the gain. In the second and purely arithmetical approach, the relative field in all directions would be derived from either the complete volume integral, the maximum gain per aperture, or from the product of horizontal and RMS gains where they have been pre-

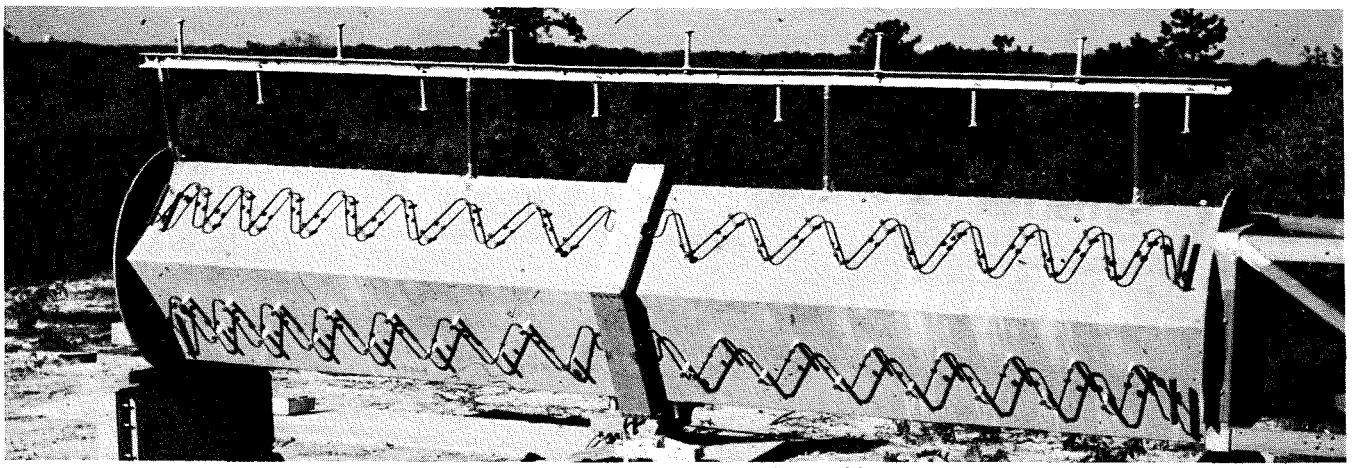

Fig. 5—Polygon antenna made up of several layers.

determined. The third method, partial measurements supplemented with calculations is the most practical approach for new custom antennas when the layer gain or panel gain is known. It is the method used in this paper to illustrate the steps in some of the methods used in predetermining antenna gain.

As expressed in Eq. 7a, the gain formula often may be reduced to a simple approximate product form.

The gain is the product of the RMS and horizontal gain, with the introduction of the safety factor. Now the RMS gain may be determined as the product of the array directivity, D_V and the various factors associated with the radiating element gain that have been previously discussed, such as element null-fill, vertical-pattern variation, vertically-polarized radiation, radiation losses, and feed-system losses. D_V is a resultant of other factors that are pertinent to the array. The 1.22 factor is the maximum gain per vertical aperture of the antenna, and A is the effective vertical aperture in wavelengths.

The peak gain in complete product form is seen in Eq. 7b with all the factors including typical values.

When the antenna is made up of several layers, such as the Polygon layer shown in Fig. 5, the gain formula is given in Eq. 8, where $G_L = 1.22$ $(A\lambda/\eta)$ (NF_E) (PV_L) (VP) (RL) and in the mutual coupling vertically small N=number of layers.

Here we gave the RMS-gain equation and the directional-gain equation, which includes the horizontal gain. The RMS layer gain, G_L, will be predetermined by a complete measurement and used as a building block in the design of the array. The gain per layer for the directional antenna would be the omnidirectional gain per layer; when the layer is redesigned for a desirable horizontal gain, the mutual coupling between adjacent panels on the layer could introduce a vertical pattern variation factor which must be considered.

An array with panels mounted close together around a small tower to achieve a desired horizontal pattern is illustrated in Fig. 6. Of course, the pattern may be either directional or omnidirectional. This is an example where there could be an infinite variety of arrangements to consider. The RMS gain as well as the directional gain of the array can be predetermined from the factors given in Eq. 9, where G_{PANEL} includes (NF_E) (VP) (RL) (PV_E) and in the mutual coupling horizontally non-zero N = number of layers.

The pattern variation factor of the array, PV_A (not as well defined as in the case of layer gain), is a function of the mutual coupling between panels, horizontally, and is generally based on experience with previous arrays with similar configurations. Since both RMS and horizontal gains of the panel are predetermined for a panel in free space, conceivably there will be pattern variations due to mutual coupling, and back lobes to be considered when it is placed in an array.

Panels mounted around a large tower as illustrated by the vee-zee array

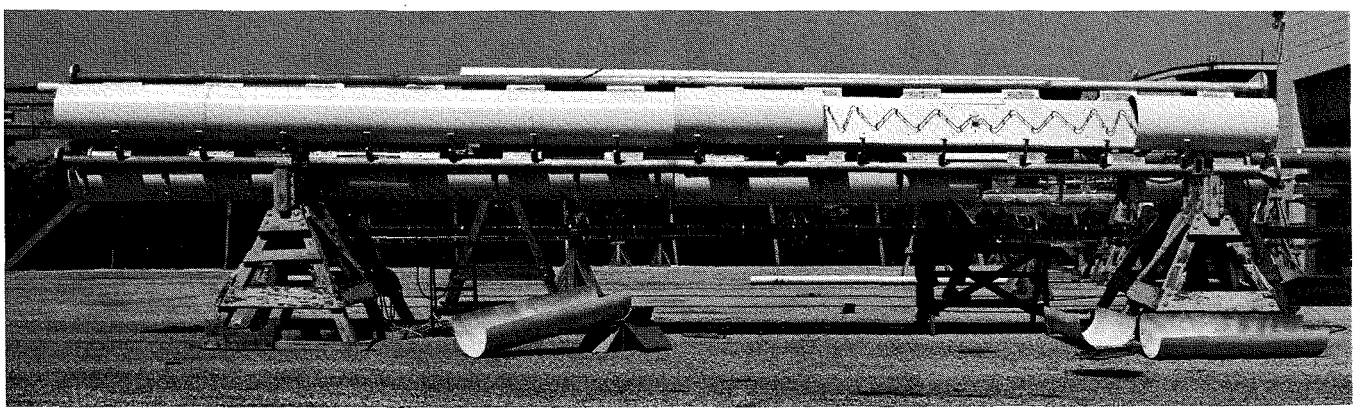

Fig. 6—Antenna designed with arrays of panels for horizontal pattern.

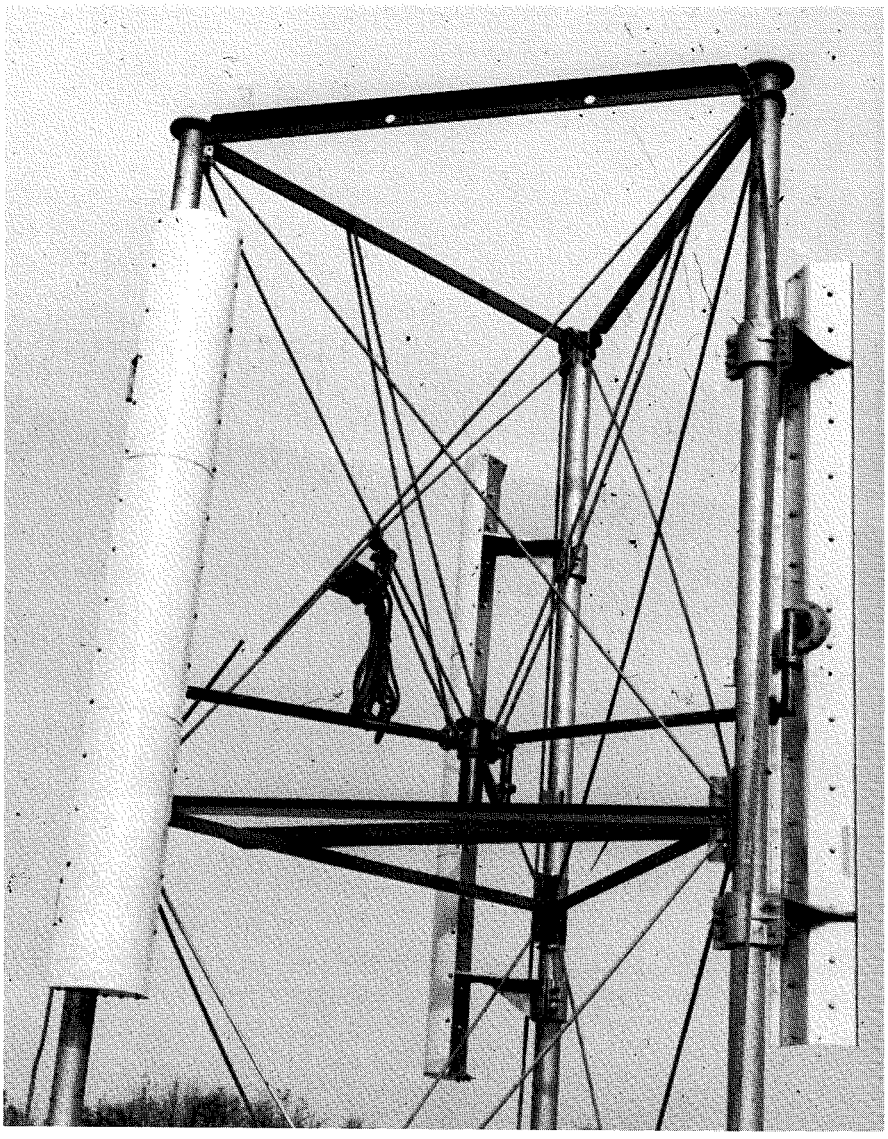

Fig. 7—Vee-Zee array with panels mounted around large tower.

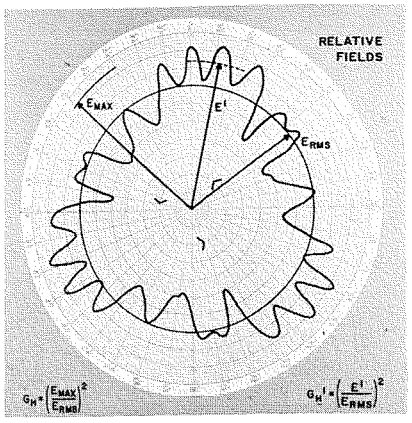

Fig. 8—Horizontal pattern of three VZ-panels around relative fields.

shown in Fig. 7 produce the typically complex horizontal pattern illustrated in Fig. 8. This pattern, achieved by a special skewed arrangement of the a panels, represents excellent horizontal coverage for the case where the panels must be mounted on such a tower. In establishing a gain formula for this array, the following is assumed: the peak directional gain of the single vee-zee panel is predetermined by measurement and since the panels are mounted far apart, mutual coupling is negligible.

Now, in observing the horizontal pattern in Fig. 8, note the relative field value of E'; this represents the maximum field produced by a single panel of the array. The serrations about E' represent the scattering effect of the tower and adjacent panels. Thus, the relative field, E', is established by the peak gain of the panel. The RMS gain is established by integration and the horizontal gain, G_H, is obtained; further, the horizontal gain G_H' is defined to represent the horizontal gain for the E′ field.

The gain formula for the vee-zee panels around the large tower is then given in Eq. 10, where $G=(G_{RMS})\ (G_H)$; G_{PANEL} includes $(NF)_E\ (VP)\ (RL)\ (PV_E)$; $(PV_A)=1$; M=number of panels in a layer; and N=number of layers.

Here it can be seen that the gain-per-layer of panels may be described as the peak-gain-per-panel divided by M, the number of panels in the layer, and G_H'. This factor represents the RMS gain-per-layer, since the peak gain in the direction of E' is the peak gain of a panel divided by the number of panels around; in this case, $M=3$. The RMS gain, of course, must include G_H', so we obtain the factor for RMS gain per layer, which may be used in a fashion similar to the previous equation where the layer gain is known. Thus, the gain formula is the number of layers, times the gain-per-layer, times the factors pertinent to the array. Where the array is being used as a directional antenna, the peak gain would be determined by the RMS gain, times the horizontal gain of the particular pattern desired.

Conclusion

In describing the nature of gain and discussing the many factors that influence gain in the antenna system, extensive reference has been made to panel antennas used in TV broadcast installations. The previous discussion illustrates all the design factors that must be considered.

The gain equation in product form was expanded to include three special cases involving custom arrays, and the relationship between panels for different spacings were reviewed. Means were prescribed for determining the gain in each case, and their differences pointed out. When an antenna is designed to meet a specified null fill and beam tilt, it is necessary to consider the radiation characteristics of the antenna in all directions. Since gain, null fill, and beam tilt are generally contractual items, and gain and relative field are often considered minimums, it is very important to establish their correct values. Utilizing all of the factors discussed in this paper, the designer should be able to build an antenna which will meet the customer's specifications.

Time-division multiple-access communication satellite system

V. F. Volertas

Frequency-Division-Multiplexing or Code-Division-Multiplexing schemes have several limitations when used for simultaneous access to a communications satellite. Because of the poor power-control, high intermodulation noise, and limited capability for network interconnectivity inherent in these techniques, the Time-Division-Multiple-Access technique was investigated. The method compares favorably in efficiency with the others; in addition, it has the major advantage of flexibility and is feasible for commercial and military uses. A means, however, must be provided within the time format to permit an earth station to accurately locate itself within its assigned interval. Two acquisition concepts are considered in this paper: 1) special code patterns without overlap and 2) time-overlapping signals.

TIME DIVISION MULTIPLE ACCESS (TDMA) is defined as the time-sequenced entry at the satellite of information-modulated RF signals which emanate from different earth sources.[1] Power sharing in the time-division system is accomplished by changing either the transmission rate from each station or its burst length, or both. The intermodulation is avoided by the time-guard bands between channels. The guard bands and the time required for synchronization determine the efficiency of the system which is the ratio of the information-transmission time to the total station burst time. Efficiencies of 95% are achievable with TDMA.[2,3] Although analog modulation may be possible, digital modulation is more compatible. There are a number of alternate approaches to demand-assignment systems design. For example, a central channel-assignment station (or an autonomous network) could be used to allow stations to appropriate channels on a first-come, first-served basis.

Other multiple access methods

Presently, satellite repeaters are hard limiting and are limited in output power. The same situation is expected in the near future. The multiple-access problem is then that of devising signal modulation techniques that permit simultaneous access to a power-limited, hard-limiting satellite repeater by a number of geographically separated stations with a minimum amount of co-channel interference. Numerous other considerations may affect the multiple-access modulation technique:

1) The amount of network control required in terms of network synchronization and up-link power control;
2) The link synchronization required;
3) The message modulations which can be used with multiple-access modulation;
4) The ease of obtaining access to the repeater; and
5) The efficiency of the multiple-access modulation in terms of usage of the channel capacity.

One of the most difficult situations in choosing a multiple-access modulation scheme arises when there is a mix of large and small stations which use a single repeater simultaneously. Unless up-link power control is used, a signal from a large station can capture the repeater and suppress signals from small stations.

Frequency division multiple access

The multiple carriers of a Frequency Division Multiple Access (FDMA) system are transmitted at different frequencies and are ultimately demodulated by frequency-selective receivers. The bandwidth of the repeater is divided into a number of non-overlapping frequency slots which constitute the access channels. Each link is assigned an access channel.

The FDMA technique has the disadvantage that intermodulation products are formed since the signals are simultaneously present in the repeater. The intermodulation noise subtracts from the power available to the desired signals at the repeater output. Further, unless the access channels are widely and properly spaced in the repeater, bandwidth intermodulation products will fall within access channels and cause interference with desired signals.

In FDMA, the number of access channels obtainable is a function of message modulation, receiver sensitivities, and up-link power control. Access to the repeater is simple since transmitting stations can monitor a given frequency slot to determine whether or not it is occupied. The quality of each channel is a function of the number of active users.

Code division multiple access

In Code Division Multiple Access (CDMA) systems, an access channel consists of a carrier waveform distinguished by distinct wideband angle modulation which spreads the spectrum over the entire repeater bandwidth. The carrier RF bandwidth is large relative to the message bandwidth. All active users transmit simul-

Reprint RE-15-3-12
Final manuscript received April 9, 1969

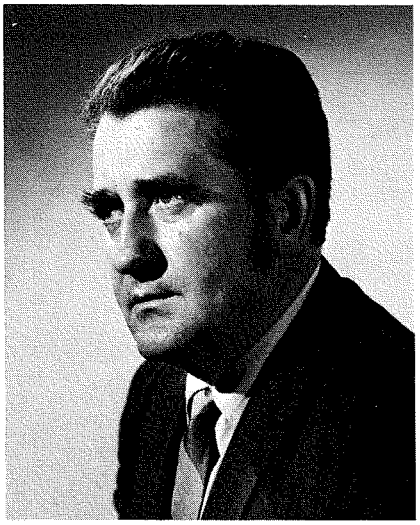

V. F. Volertas
Space and Special Systems
Defense Communications Systems Division
Camden, N.J.

was graduated from the University of Kaunas, Lithuania in 1943 with the BS and from the University of Pennsylvania in 1954 with the MA; he also did graduate work in E.E. and Math. at U. of Maryland and the U. of Pa. He joined RCA's Communications Systems Division in 1961 and began work on passive satellite communcations studies. Later, his assignments included satellite and tropo systems analysis, electrical and optical correlation techniques, antijam techniques, analog and digital modulation, and filtering methods. Prior to his RCA employment, he was a Project Engineer on communications systems and performed airborne radar performance analysis at Westinghouse. From 1943 to 1949, he taught mathematics and physics at European secondary schools. Mr. Volertas is a member of the IEEE and the American Mathematical Society.

taneously, and coherent-synchronized receivers employing correlation detectors with locally stored phase codes are required. Since all signals occur simultaneously in the repeater, intermodulation products are created. These appear as Gaussian noise at the receiver output due to the large correlator processing gain which is ideally the ratio of the RF bandwidth to the message bandwidth. Network synchronization is not required. Link synchronization must be obtained and maintained; this involves chip synchronization, i.e., the synchronization of the pseudo-random code. The keying rate must be high to obtain a large RF bandwidth with its resultant large processing gain. The higher the keying rate the more difficult the link synchronization problem becomes. Furthermore, unless a strict up-link power control is used, signals from weaker stations will be lost.

Pulse address multiple access

Pulse Address Multiple Access (PAMA) systems are similar to CDMA systems in that they use a pulsed coded waveform for each access carrier. The pulse lengths (intervals between pulses) and carrier frequency of each pulse constitute a distinct pattern for each access. The duty factor of each carrier is small and the same patterns are used to carry each message sample. Most PAMA systems have the advantages of rapid link synchronization, a large number of access channels, and no requirement for network timing. The disadvantages are relatively low information capacity and operational problems with a fully loaded network.

Time division multiple access

In TDMA, the transmissions of different links are separated in time such that each link has sole use of the repeater at specified times. The simplest scheme is a repetitive sequence of time slots where an access-channel consists of the same time slot in each frame. Any form of angle modulation, compatible with the pulsed nature of the waveform such as PSK or FSK, may be used.

The TDMA scheme requires network synchronization in the form of a time-reference signal which can be generated at, or repeated by, the satellite repeater. This time reference is needed by transmitting terminals to accurately pulse their transmissions so that they occur during their allocated time slot. Receiving terminals require the time reference to synchronize the gating of their receivers to the allocated time slot. The timing inaccuracy must be kept small to maintain a high efficiency, since the guard time provided between time slots must be greater than or equal to the timing inaccuracy.

The TDMA technique has the advantage that no power is lost or no interference is produced due to intermodulation products, since only one signal is present in the repeater at any time. This exclusive use of the total repeater power by a single link at any one time also permits a wide disparity in up-link power and receiver sensitivities in separate links without the requirement for up-link power control or modification of data rates. This also results in high efficiency in the use of satellite repeater power or, equivalently, a high information rate for a given satellite output power when all the channels are used. The capacity of each access channel is independent of the number of access channels being used. Because the major problems of simultaneous access (power control, satellite nonlinearity, network connectivity) are circumvented, TDMA receives much emphasis.

Frame and burst formats

The primary consideration in the synthesis of a TDMA system is the arrangement of individual station bursts in a format which maintains high transmission efficiency. To achieve this, attention must be given to the processing delay, information storage efficiency, and acquisition. Processing delay is implicit in every burst transmission. For real-time channels, this delay must be insignificant compared to the transport delay. The selected format should not require an extraordinary large memory for information storage. Because guard bands are required between station bursts, and also some time is consumed for synchronization and control, the individual bursts must be relatively long to maintain high transmission efficiency. Finally, a means must be provided within the format to permit a station to determine accurately the range and time so that it can locate itself properly within its assigned time interval.

The commonly used method divides time into relatively short intervals or frames. The frame, in turn, is divided into shorter intervals or slots (bursts) where each time slot is a possible access. The duration of the frame, t_f, cannot be arbitrary. It is usually chosen to be a multiple of the Nyquist rate for those input signals which constitute the major portion of the input traffic. If the voice-band signals are considered to be major inputs, and if the sampling rate, f_s, is 8.0 kHz, the frame duration equals n/f_s. For n selected to be one, the frame length is 125 μs, and the system is called a real-time system, since no storage is required.[2] If t_f is made longer, quantized samples of each channel must be stored, but the efficiency of the system improves at the cost of storage. Each station, before information transmission, must have some time devoted for synchronization and operational purposes (e.g., identifying and addressing the station being called). This time is allocated immediately after the guard time in each burst. Signals in this portion of the burst are called preamble (Fig. 1).

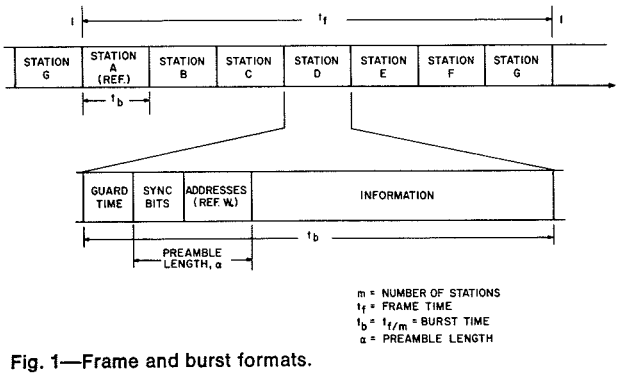

Fig. 1—Frame and burst formats.

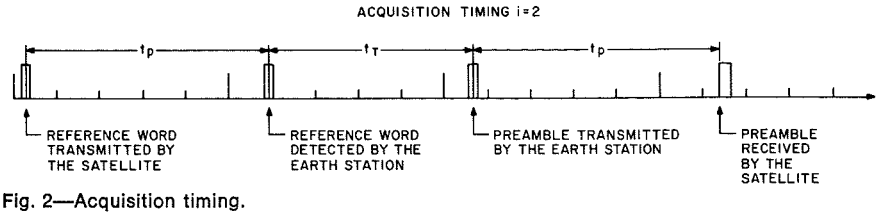

Fig. 2—Acquisition timing.

Synchronization

Before transmitting, a user of the TDMA system is concerned with time synchronization of his transmitter. Synchronization is required at three levels: the first level is called the time slot or network synchronization; the second level is the bit and word synchronization (data sync); and the third level for coherent RF detection schemes is the carrier synchronization. Network timing is achieved by receiving the frame synchronization signal of the satellite beacon. The user adjusts his network timing by varying the phase of his frame signal oscillator until his ranging signal and the network timing signal received from the satellite exactly coincide in time. Ranging signals can be pulse or pseudo-random signals transmitted by the user initiating the call on his selected TDMA channel. The returned signal from the satellite repeater is correlated with the beacon framing signal for adjusting the transmitted signal to arrive at the satellite within the assigned time slot. Present estimates of ranging circuit capability indicate that a network timing frame accuracy of at least 0.5 μs is possible.[4]

In fact, the apparent difficulty of establishing and maintaining network synchronization with the requisite accuracy has been, up to the present, a major obstacle to the implementation of TDMA systems. The concept of TDMA operation through a communication satellite involves synchronization of multiple signals received in the repeater channel; however, to be derived at the earth terminals. This can be accomplished in principle if each terminal corrects for its own propagation range (and doppler) to the satellite. With respect to a common reference, each terminal advances its transmitter timing and retards its receiver timing. Each terminal, thus, must have a timing reference in synchronism with all others. Therefore, the required information for synchronization of timing is a common clock and range to the satellite, continually updated.

To permit the efficiency which is the major advantage of TDMA, transmissions must be synchronized to less than 10% of the burst length. If the burst length is likely to be between 10 and 100 μs for voice links so that network synchronization to the order of 1 to 10 μs will be required. To achieve this precision, the transmitting station must be able to lock a receiver to its ranging signal retransmitted by the satellite, and the ranging signals must not seriously interfere with operating links. Using sidetone ranging from an earth station to a spacecraft, accuracy of ± 100 feet or better can be achieved when signal-to-noise ratio is high. But not all earth stations have sidetone ranging. Using good tracking data, satellite range can be predicted as much as 30 days in advance within ± 1 nautical mile.

One possible procedure for acquisition, without interfering with other bursts already present within the frame, is aiming the preamble bits at the center of the assigned time slot, using computer-predicted satellite range and monitoring the reception time of the reference word, transmitted by the satellite beacon. Say, the slot number one in the time frame (station A of Fig. 1) is used for controlling purposes, and the beacon reference word occupies the same position in the burst as the preamble. Let the station desiring to acquire be the i^{th} station in the frame. Let γ be the duration of the guard time. Thus, the start of the i^{th} time slot in the frame is $(i-1)t_b$ from the reference burst. Let propagation time, computed from predicted range, be expressed in terms of frame time: $t_p = kt_f + \beta$, where k is an integer, and $0 < \beta < t_f$. To enter the center of the assigned time slot, one would start transmitting the preamble burst at time t_T relative to the detection time of the reference word of the satellite beacon. Time t_T is given by

$$t_T = (r-2k)t_f + (i-1)t_b + \frac{t_b - \alpha}{2} - (\gamma + 2\beta)$$

where r is the smallest integer which satisfies the limits $0 \le t_T \le t_f$; these limits assure the entrance of the preamble in the nearest time frame and avoids unnecessary delays.

After the preamble has been placed in the assigned time slot and retransmitted by the satellite to the earth station that sent it, the position of the preamble can be compared with the reference word of the beacon in the same frame, and the necessary correction can be made. The detected time errors are due to the error in predicted range and range rate, frequency instability of the equipment, etc. The acquisition timing is shown in Fig. 2.

Once the preamble is placed in the assigned time slot, the synchronizer will automatically move the preamble bits to the beginning of the time slot (leaving the guard time unoccupied), the information bits are added, and normal operation commences (Fig. 3).

RCA efforts

The described acquisition procedure limits the minimum duration of a time slot. To avoid interference with transmissions of other stations during the acquisition mode, the duration of the time slot must be at least twice as long as the time uncertainty. Thus, if range is known with ± 1 n. mi., the acquisition uncertainty is ± 12 μs, and the time slot must be >24 μs.

For this reason, a search for other acquisition methods is needed. Presently RCA is involved in studies of very narrow or very wide bandwidth synchronization signals. In the first case, the total power of the synchronization signal is negligible to the total power of transmission; in the second case, the power density of the signal is very small in comparison to the power density of regular signals. Hence, the effects of interference are annihilated, and no restrictions on the duration of the time slot are imposed.

References

1. Hultberg, R. M., Jean, F. H., and Jones, M. E., "Time Division Access for Military Communications Satellites," *IEEE Transactions on Aerospace and Electronic Systems* (Dec 1965).
2. Schmidt, W. G., "An Efficient TDMA System For Use by Emerging Nations with the Intelsat IV Satellite," *Eascon 1968 Record.*
3. Sekimoto, T., and Puente, J. G., "A Satellite Time-Division Multiple-Access Experiment," *IEEE Trans. on Com. Tech.* (Aug 1968).
4. Gabard, O. G., "Design of a Satellite Time-Division Multiple-Access Burst Synchronizer," *IEEE Trans. on Com. Tech.* (Aug 1968).

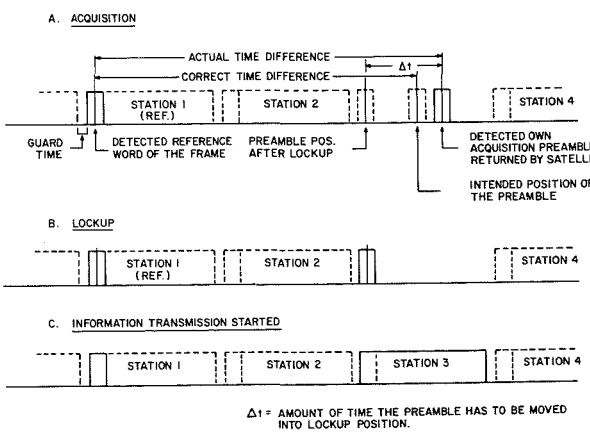

Fig. 3—Acquisition and burst synchronization.

Three-channel C-band maser for radar installation

B. R. Feingold | A. L. Polish | D. J. Miller

This paper describes a three-channel traveling-wave maser to be used in a C-band monopulse radar system. The maser system is unique in that each channel contains a separate, electronically-controllable simultaneously-operating skin (for normal radar mode) and beacon amplifier, each tunable from 5.4 to 5.9 GHz, and also a unique "noiseless" magnetic duplexer. The maser is housed in a closed-cycle helium refrigerator (CCR). This article is mainly a description of the measured electrical characteristics and physical aspects of the device which would interest an applications engineer.

THE THREE-CHANNEL C-BAND MASER SYSTEM is part of the modification program on the RF receiver of the AN/FPQ-6 tracking radar at Wallops Island, Virginia. This radar is being modified to increase the total loop gain by 12 dB, thereby doubling the tracking range in the normal radar mode. This increase in gain is being accomplished by incorporating improvements to the antenna feed and RF receiver portions of the system. The maser is replacing the parametric amplifier in the present radar.

The AN/FPQ-6 monopulse radar can track a target in either the normal radar mode (skin tracking) or the beacon mode, where the radar acts as a passive receiver, receiving signals originating from the target. In a typical mission, the radar must switch from one mode to the other in milliseconds. Therefore, the amplifier must amplify at both the skin and beacon frequencies simultaneously. Consequently, each of the three channels of the maser amplifier must contain two amplification bands (one skin and one beacon per channel) resulting in six independent maser amplifiers.

The primary system advantage of a maser preamplifier in a radar is its extremely low noise temperature. The incorporation of this maser (along with the associated peripheral equipment, such as low-noise duplexers) will lower the system noise temperature from the present value of 943°K to approximately 130°K. This is an improvement of 8.6 dB, or approximately 65%, in the radar (skin track) mode.

Maser System

Maser amplifiers

There are six independent masers in the maser package—a beacon maser and a skin maser in each of three channels. Each maser can be tuned from 5.4 GHz to 5.9 GHz and each was designed to have 30 dB of gain and 10 MHz of bandwidth.

Each channel is contained in a separate slow-wave structure surrounded

Reprint RE-15-3-14
Final manuscript received April 10, 1969.

A. Polish
RCA Laboratories
Princeton, N.J.
received the BS in Physics from Pennsylvania State University in 1965 and the MS in Physics from Purdue University in 1967. He joined the Applied Physics Group of the Advanced Technology Laboratories in July of 1967 to work on the development and application of traveling wave masers. He has participated in the development of broadband masers at *S* and *C* bands, an ultra broadband tunable masers, and a three-channel C-band maser. He is now working at the RCA Laboratories.

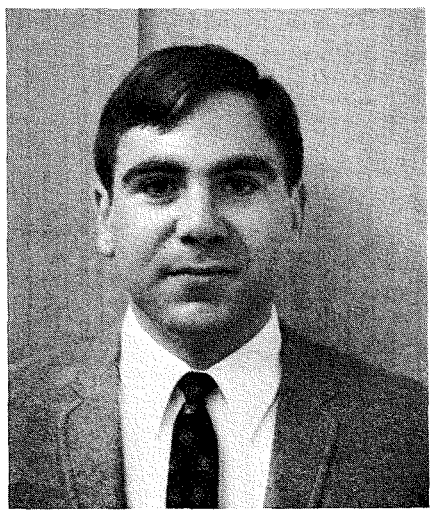

D. J. Miller
Maser Group
Advanced Technology Laboratories
Camden, N.J.
received the BA in Physics from the University of Pennsylvania in 1959 and the MS in Physics in 1963. He worked on the design of microwave components for airborne radars and ground-based-phased arrays in the Microwave and Antenna group of the Philco Corporation from 1959 to 1961. Since November of 1961, he has been employed by RCA in the Advanced Technology Laboratories, where Mr. Miller has been primarily concerned with the development of traveling wave masers from *S* to *Ka* band. Mr. Miller has published several papers and letters on antennas and traveling wave masers. He is an active member of the IEEE and has served as Chairman of the Philadelphia Chapter of the PTGMTT-AP.

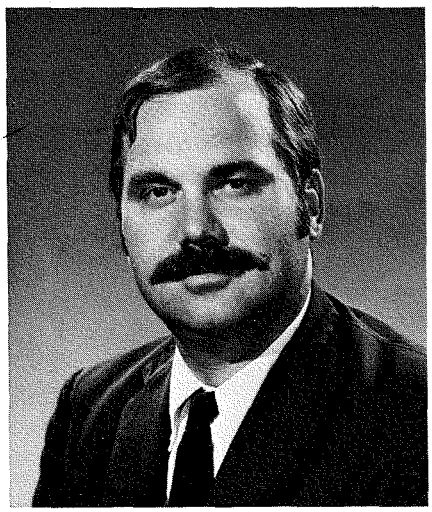

B. R. Feingold
Maser Group
Advanced Technology Laboratories
Camden, N.J.
received the BS in Engineering-Physics from Columbia University in 1965, the MS in Physics from the University of Pennsylvania in May 1967 and is now well into his course work for the PhD. In 1965, Mr. Feingold joined the Maser Group of RCA Advanced Technology Laboratories. He has participated in programs for development of high frequency traveling wave masers (35 GHz); development of a three-channel maser for radar applications; EPR studies of Fe^{3+} in rutile to broaden its bandwidth; and an optically pumped maser utilizing rare earth ions (Tm^{2+}, Dy^{2+}) in CaF_2. He is presently engaged in the study of millimeter-wave imaging systems.

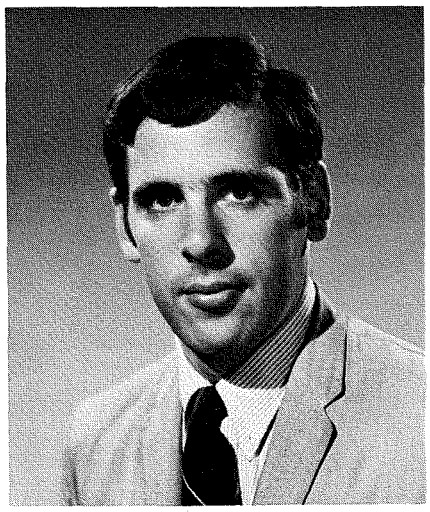

by its own superconducting magnet. The skin and beacon amplifiers are in cascade, with the skin amplifier followed by the beacon. The slow-wave circuit is a meander line which is folded so that 14 inches of crystal fit into a 7-inch length (see Fig. 1). The crystal is irondoped rutile, containing 0.33% Fe^{+3} by weight.

The maser is tuned across the frequency band by varying the DC magnetic field. Therefore, each skin and beacon amplifier needs a separate, electronically controllable DC field. Each field has a small trimmer which enables the gain or the bandwidth of each amplifier to be varied independently. The upper magnetic field corresponds to the skin-track mode while the lower field corresponds to the beacon amplifier of each channel. The three channels, with their associated magnets, are placed side by side so that the magnets lie against each other, forming a 2 x 4½ x 9-inch package.

Operation of this radar requires that the three skin amplifiers be tuned to the same frequency and that the three beacon amplifiers be tuned to another frequency (which is at least 70 MHz away from the skin frequency). The gains of the three skin amplifiers must be the same for all three channels; the same condition is required of the beacon amplifiers. This is accomplished by designing the masers to have more than 30 dB of gain so that it is possible to trade gain and bandwidth of the masers until all three have identical gain, in both the skin and beacon modes.

Superconducting magnet

One of the major innovations in the maser system was the development of a superconducting magnet which could provide two uniform and completely independent fields in an extremely small package. To conserve space, the magnets are rectangular in cross section. Each magnet has two main coils to produce the two fields corresponding to the skin and beacon amplifiers (see Figs. 2 and 3). A trimmer coil on each main coil facilitates trading gain for bandwidth to equalize gain among channels. The proximity of the magnets imposes severe requirements on the superconducting shielding, which must contain fields as high as 2400 gauss. The shielding configuration developed for this maser prevents fringing, thereby allowing field uniformity of 10 parts in 10,000, and isolates the channels so completely that independent tuning is achieved. These magnets have produced fields as high as 4000 gauss.

Each coil is equipped with a superconducting persistent-current switch which closes the coil to form a superconducting loop after the desired operating current has been introduced into the coil. The current will continue to flow in the coil forever, preventing any instabilities in the current supplies from affecting the maser and thereby allowing very good maser gain stability. After the loop is closed, the current supply may be removed; in fact, each channel is tuned separately and then placed in the persistent mode, allowing the same four current supplies to tune all three channels (a total of 12 coils)—one channel at a time.

Saturation protection switch

Previous applications for masers (radio telescopes and satellite communication ground stations) were in passive receiver systems only. Radars, however, use the same antenna to transmit and receive, and leakage from the transmitter pulse is so large that it saturates the maser. Since a maser requires about 10 ms to recover from saturation, unprotected masers are impractical for radar use. A device is therefore required to protect the maser from saturation. Such a device was developed for this maser system.

The protection switch detunes the maser quickly, just before the transmitter pulse. The transmitter then cannot saturate the maser (since it can no longer induce downward transitions in the maser) and cannot affect the inversion condition. At the end of the transmitter pulse, the maser is returned to the operating frequency and is ready to amplify the echo signal.

Detuning is achieved by changing the magnetic field at the maser crystal. This change is accomplished by sending current down a series of wires located above the crystal over the length of the maser structure (see Fig. 4). Approximately 9 amperes are required to produce a field of sufficient magnitude to completely detune the maser. The recovery time (time required for the magnetic field to return to its normal value after the current is removed) is typically 60 μs.

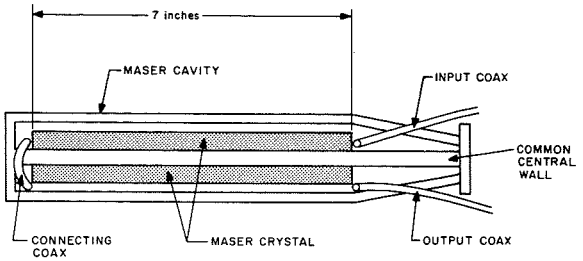

Fig. 1—Folded slow-wave circuit.

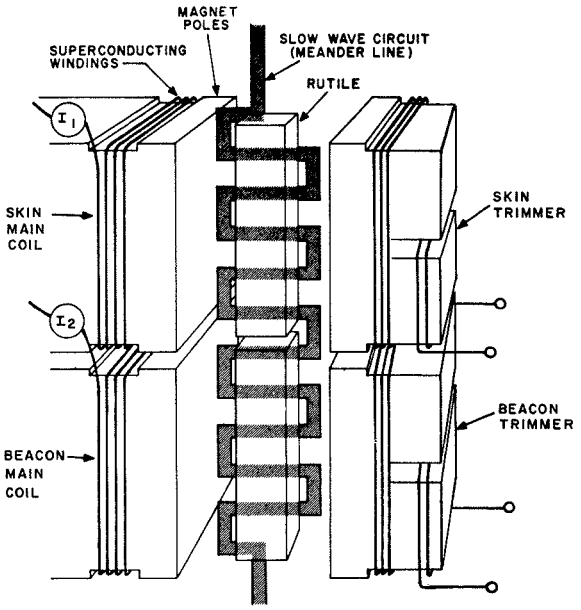

Fig. 2—Schematic of superconducting magnet.

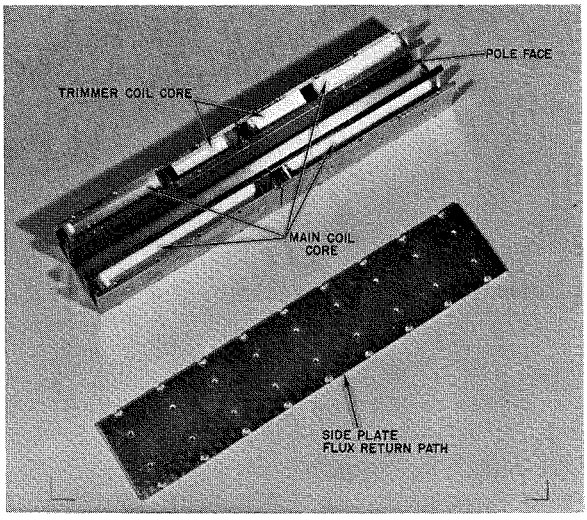

Fig. 3—Superconducting magnet cores.

Cryogenics

The maser-magnet assembly was packaged in an Air Products & Chemicals Model E-311 closed-cycle refrigerator, which has a measured thermal capacity of 1.6 watts at 4.2°K—the operating temperature of the maser. The unit was designed for the strenuous mechanical environment of the tracking radar antenna.

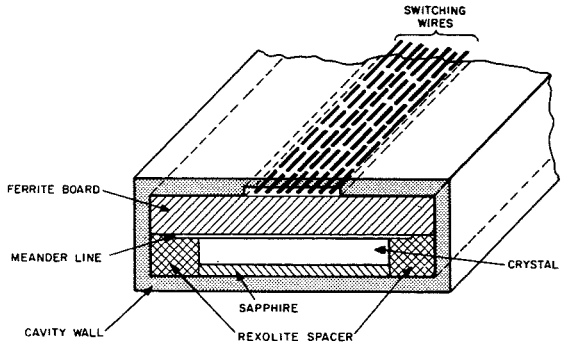

Fig. 4—Cross-section of maser and protection switch.

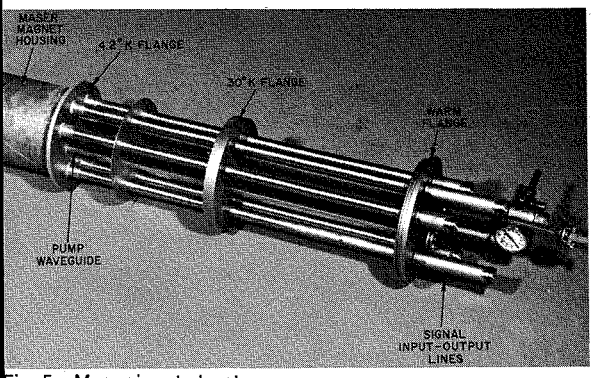

Fig. 5—Maser input structure.

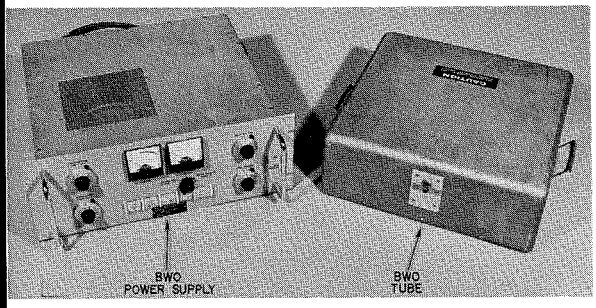

Fig. 6—Backward-wave oscillators and power supply.

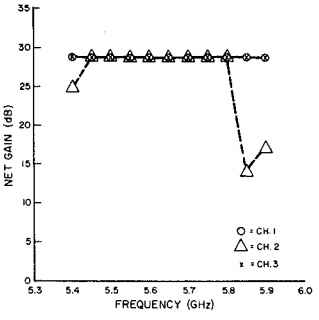

Fig. 7a—Maser gain vs. frequency—skin masers.

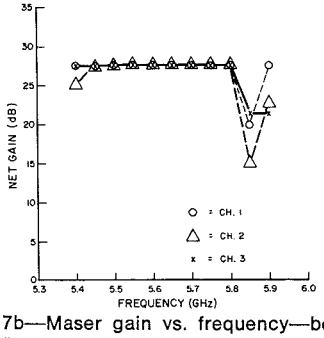

Fig. 7b—Maser gain vs. frequency—beacon masers.

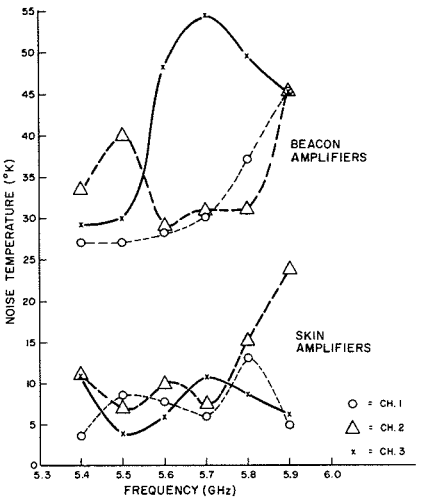

Fig. 8—Measured noise temperatures.

Input Structure

A special low-noise, low-thermal-transfer, input structure utilizing GR900 series connectors was constructed for the maser (see Fig. 5). This structure contains the input and output coax lines, the three pump waveguides, the magnet control leads, helium gas lines, and nitrogen precool lines.

Backward-wave oscillators

Two backward-wave oscillator (BWO) tubes and the controlling power supplies were built by Hughes Aircraft Corporation to provide pump radiation. One BWO inverts the skin masers, and the other inverts the beacon masers (see Fig. 6). Each tube has an output of approximately 5 watts over the required band. The outputs of the two BWO's are combined, with the resulting two-frequency radiation being equally divided to provide pump power for each of the three masers.

Measured Characteristics

Gain-bandwidth

Fig. 8 shows the gain for each channel's skin and beacon amplifiers over the tunable range. The gain, in many cases, was higher than 30 dB, but any gain greater than 30 dB was reduced by magnet trimming. The bandwidth was nominally 10 MHz over the band.

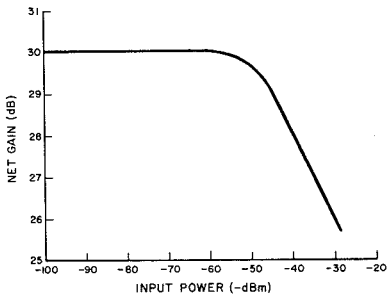

Fig. 9—Typical maser dynamic range.

Fig. 9 shows noise temperatures that were measured by the hot-cold load *Y*-factor method, where the hot load was a 373°K load and the cold load was a liquid nitrogen load.

Successful radar operation requires very good relative phase and gain stability among channels. Relative gain stability better than ±0.10 dB for 10 minutes was measured. Relative phase stability better than ±1° over 10 minutes was also measured. Relative phase stability was also measured over a six-hour period; stabilities better than ±1.5° were observed.

An important characteristic for this radar is the phase change over the 10-MHz bandpass of the maser. Phase variations between the 3-dB points were measured to be in the order of ±3°.

The dynamic range of the maser amplifier is a function of the radar pulse width and pulse repetition rate. For 10-μs pulses at a rate of 700 pulses per second, the maser's 1-dB gain compression occurred at approximately −50 dBm (see Fig. 10).

The maser has a number of additional properties that add to its desirability as a radar amplifier. The maser is immune to RF interference at any frequency in the tunable band except those frequencies enclosed in the two 10-MHz gain slots, thereby acting as a bandpass filter, since the maser attenuates signals outside the amplifying bands by 35 dB.

Preliminary measurements show that the maser has no spurious responses and no intermodulation between skin and beacon amplifiers, properties that are expected from maser theory.

Conclusions

The construction of this maser has demonstrated that a three-channel maser can be built with all the properties needed for successful operation in a radar environment. In fact, the maser amplifier has shown characteristics beyond extremely low noise that could improve radar performance. The installation of this maser in the Wallops Island antenna may well point out highly beneficial aspects of "secondary" properties such as ultra-fine phase stability or interference immunity. The use of the maser will stimulate the development of lower-noise devices in the amplifier system, such as duplexers and antenna feeds.

The requirement for maintainable electronics on long-duration manned space missions

M. L. Johnson

Must electronics systems be maintainable on long duration space missions? The literature on the subject assumes so. This is supported by the theories of failure causes and failure rates of conventional reliability techniques. Yet, in hindsight, these techniques cannot account for the remarkable successes of some of our space programs, such as TIROS. A better understanding of the causes of failure might provide an explanation and might also indicate that long-duration missions can be undertaken without resorting to maintenance.

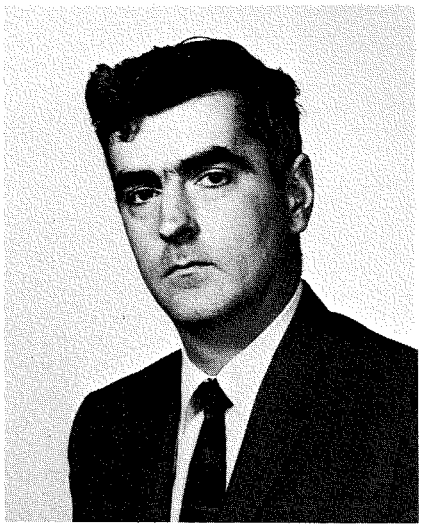

Michael L. Johnson
System Effectiveness
System Design Support
Aerospace Systems Division
Burlington, Massachusetts
received the BSEE from Northeastern University in 1959 and the MSEE from Northeastern in 1967. Before joining RCA in 1965, Mr. Johnson was employed by Sanders Associates and the Raytheon Company. At RCA, Mr. Johnson is responsible for the reliability aspects of electronic equipments for manned space ventures. In this capacity, he has conducted studies on reliability and maintainability aspects of long duration missions. Prior to this, he was responsible for the production reliability program on the Lunar Module Rendezvous Radar Program.

TO ASSESS THE DEGREE OF RELIABILITY IMPROVEMENT required for a long-duration mission, the Apollo mission was chosen as a baseline. A typical electronic black box was selected for study; the Lunar Module (LM) Attitude and Translation Control Assembly (ATCA). The ATCA was designed and manufactured by the Aerospace Systems Division of RCA for Grumman's Lunar Module.

The LM ATCA

The function of the LM ATCA is to accept 800-Hz attitude-error signals and commanded rate signals which are summed, amplified, demodulated, and dead-banded to produce vehicle rotation commands. It combines these signals with vehicle translation commands in decision logic networks and determines which of 16 pulse ratio modulators and jet solenoid drivers to energize. Thus, by analog processing of basic yaw, pitch, and roll input data, it actuates the proper combination of any of the 16 thrusters to achieve the commanded vehicle motion.

The LM ATCA is packaged in a flange-mounted aluminum case having dimensions of 17.8 x 5.1 x 7.4 inches and is penetrated by three electrical connectors. The assembly has ten removable subassemblies designed for factory maintenance. In-flight service maintenance is not a design requirement. The removable subassemblies are seven electronic subassemblies, a power conditioning subassembly, a wiring subassembly, and a cabling subassembly. The power conditioning subassembly services other LM items in addition to providing ATCA bias levels. The inclusion of a multipurpose power conditioning subassembly is considered atypical for an electronic black box of this type and for this reason it is excluded from the analysis. The electronics analyzed include four identical output subassemblies and one each of physically and functionally similar pitch, roll, and yaw subassemblies. The parameters and specifications of the packaged electronics pertinent to this analysis are presented in Table I.

Table I—LM ATCA parameters.

Weight	20 pounds
Complexity	2500 piece-parts
Predicted failure rate	$100f/10^6$ hours
Probability of success, P_s	0.9999 (design goal) 0.999 (predicted)
Mission length	10.25 hours

Reliability improvement calculations

Since a space station will be considerably more complex than Apollo, the required probability of success for the ATCA function will be higher. For this study, it has been set at 0.99995. Mission duration has been set at five years (50,000 hours).

The average piece-part failure rate for the LM ATCA (λ_{LM}) is:

$$\lambda_{LM}=\frac{100\times10^{-6}}{2500}=0.04\times10^{-6}\ \text{failures/hr}$$

The required piece-part failure rate for the space station (λ_{SS}) is:

$$\lambda_{SS}=\frac{(1-P_s)/t}{2500}=0.4\times10^{-12}\ \text{failures/hr}$$

where t is the space-station mission duration (50,000 hours) and P_S is the probability of space-station success (0.99995).

The required improvement factor is:

$$\frac{\lambda_{LM}}{\lambda_{SS}}=\frac{0.04\times10^{-6}}{0.4\times10^{-12}}=10^5$$

The improvement factor is the product of the following three components:

1) Increased mission duration—50,000 hours versus 200 hours, or 250;
2) Increased complexity because of a more sophisticated mission—complexity increase by a factor of 2 to 4; and
3) Increased duty cycle—100% versus 5% or 20.

In the foreseeable future, reliability achievements may increase by a factor of ten, but the three to five orders of magnitude improvement required appear unachievable unless the space station is configured to tolerate malfunctions.

Quantitative argument for maintenance

There are two ways of configuring the space station to tolerate malfunctions:

1) Additional hardware may be wired in for automatic switchover or repro-

Reprint RE-15-3-16
Final manuscript received April 14, 1969.

gramming upon failure. This is defined as *redundancy.*

2) Additional hardware may be provided for manual replacement upon failure. This is defined as *maintenance.*

Redundancy

The required P_S for the ATCA may be met by providing redundancy at various levels of complexity. Three of these are compared below on a total-weight basis.

Redundancy at the black-box level

The number of standby LM ATCA's required to meet space-station longevity requirements can be found by iterative solution of the following equation:

$$P_S = \exp(-N\lambda t) \sum_{j=0}^{k} \frac{(N\lambda t)^j}{j!} \quad (1)$$

where P_S is the required probability of success (0.99995); λ is the predicted failure rate (100 x 10^{-6}); t is the mission duration (50,000 hours); N is the number of identical active elements, (1 in this case); and k is the number of standby elements required.

In this case, the solution is k = 14. Thus, assuming either perfect switching or positive connectors, one active and fourteen standby LM ATCA's are required to achieve the required service life. Since the 20-pound LM ATCA is a tractable package, it could be spared for manual replacement at a total weight penalty of 300 pounds. If wired-in switching is required in a redundant configuration, a weight penalty for switching circuits must be added.

Redundancy at the piece-part level

At the other end of the spectrum from black-box redundancy is piece-part redundancy. Comparing the average LM ATCA failure rate with the required space-station failure rate, and converting these to the probability of failure (Q) in 50,000 hours, it is found that Q_{LM} = 2 x 10^{-3} failures in 50,000 hours/part, whereas Q_{SS} must be 2 x 10^{-8} failures in 50,000 hours/part. Therefore, each LM part must be triplicated based on the mathematical analysis.

However, when using redundancy at the part level, part failure modes become very important. One must consider circuit tolerance effects, and modes of single failures resulting in loss of circuit function. When these are accounted for by quading semiconductors, and providing enough parallel resistors or (typically) series capacitors to overcome tolerance effects of a single failure, the average number of parts to perform a single part's function becomes eight.

There is an additional drawback in piece-part redundancy. To have sufficient protection (reliability) each of the eight parts must be good, yet it is next to impossible to test such parts individually once assembled into a circuit.

Modular redundancy

Standby redundancy may be employed at a module level to obtain a signicant weight saving and, at the same time, avoid a large increase in complexity. An optimum module is one that is large enough to be relatively insensitive to mode, yet small enough to have a reasonably low failure rate. Redundancy at this level would require a complexity increase of more than three, since this increase is numerically required for piece parts and less than eight, since this level is required to deal with failure modes. Optimum redundancy would require a complexity increase on the order of five.

Maintenance

Both the black-box redundancy and the modular redundancy can be implemented within a maintenance concept, simply by having the crew perform the switching function, most probably by modular replacement. In this manner, the maintenance approach is weight effective, since switching circuits need not be supplied. At the same time, redundancy is time effective since repair is instantaneous and the crew need not be involved.

Maintenance can also take advantage of commonality of modules. Where a specific module is used in several different locations in the spacecraft, a single set of spares can simultaneously support all of these locations.[1]

Table II—Summary of maintainable modularized—ATCA configurations.

Module type	*Failure rate* ($f/10^6$ hr)	*Apportioned probability of success* (P_S)	*Number of modules assembly*	*No. of spares (not utilizing commonality)*	*No. of spares (utilizing commonality)*
Input limit amp	2.5	0.9999990	3	12	5
Demod & deadband	2.5	0.9999990	3	12	5
Vertical sum amp	3.0	0.9999985	1	4	4
Horizontal sum amp	7.0	0.9999965	1	5	5
Logic pack	9.5	0.9999950	1	6	6
Bias & reference	1.0	0.9999995	1	3	3
Output	6.0	0.9999970	8	40	11
Totals			18	82	39

The advantages of commonality are quite impressive as shown below. Again the ATCA has been used as a realistic model. In this case, the ATCA has been reconfigured into 18 modules which are close in complexity to the optimum module discussed under modular redundancy. Twenty-five percent was added to the baseline ATCA weight and failure rate to account for additional packaging and complexity for checkout of the modularized design.

Spares were added to each type module using Eq. 1. When the commonality was not considered, 82 spare modules were required. When the inherent commonality was considered only 39 spare modules were necessary (see Table II.)

In Table III, several of the configurations discussed are summarized. All of the entries in Table III are based on LM failure rates. Table IV indicates the sensitivity of the results to a different failure-rate assumption. The factor-of-10 improvement in failure rates is felt to be the very best that can be expected over the next several years.

Table III—Weight of various ATCA configurations.

Configuration	*Maintenance concept*	*Weight w/spares*
Baseline ATCA	Black box replacement	300 lbs. and switch if desired.
Piece-part redundant	N/A	160 lbs.
Module redundant	Module replacement w/o considering commonality	139 lbs. and switch
Module replacement	Module replacement considering commonality	79 lbs.

Table IV—Sensitivity to failure rate.

Configuration	*Relative failure rate*	*Total weight including spares*
Baseline LM ATCA	1	300
Baseline LM ATCA	0.1	120
Maintainable ATCA (18 Modules)	1	79
Maintainable ATCA (18 Modules)	0.1	48

Conceptually, maintenance and redundancy differ only in the manner of switching. To implement module replacement, considering commonality on the ATCA, would require a switching circuit containing at least 3300 piece parts. Restated, the switch would be at least 125% as complex as the baseline ATCA. (This does not include circuitry for detecting and isolating the fault, which would be the same in both the redundant and maintainable concepts.)

Reliability prediction techniques

The above discussion is based on the standard reliability prediction model. When starting any new project by relying on the techniques of the past, the underlying assumptions must be examined to see if they remain acceptable approximations.

The standard reliability prediction technique has been in use with little modification for about a decade. Simplified, it states the equipment failures result from piece-part failures; and that piece-parts fail at constant rates dependent on their usage. The necessary assumptions are:

1) The design will function as intended;
2) Good workmanship will virtually preclude initial defects;
3) Debugging will detect any initial defects that are introduced;
4) Wearout items will be replaced before the wearout mechanism is significant.

When this technique first gained popular acceptance, these assumptions were very good approximations. Since then, Reliability Engineering has been constantly improving reliability. The most dramatic improvements have come in piece-part reliability. High-reliability piece-parts, with their stringent controls and demanding screening tests, are indeed highly reliable. While advances have been made in other areas, similar improvements have not been attained. At this point in time, the assumptions upon which reliability predictions are based are relatively poor approximations.

Bean and Bloomquist have analyzed all in-flight spacecraft reliability data and their conclusion is:

> ". . . even if part failure distributions were known with a certainty, the reliability models currently used in the industry to predict performance could not account for a large proportion of the difficulties encountered in attaining 'successful' spacecraft performance."[2]

Why should this be so? Consider an article in *Electronic News* concerning "reliability problems" with Minuteman II. It states:

> "Minutemen II was highly touted for extreme reliability. Its component specs were widely adopted as the ultimate in high reliability standards throughout the military and NASA. Subsystem problems have been traced to random workmanship errors and not to component problems . . . "[3]

Workmanship errors are not restricted to subsystems or assemblies. Troxel and Tiger of RCA's Central Engineering have found that integrated circuit reliability is dependent on "screening effectiveness" and "quality related failure mechanisms" and "is not primarily a function of usage factors".[4]

The Aerospace Systems Division has had considerable experience on high reliability programs, which is summarized in Table V. Included in Table V are all failure events at the black box level of test, representing several thousand system test hours. Most of the failures are initial defects; two-thirds of the vendor defects are also initial defects.

Thus, while the existing reliability prediction model defines away initial defects, these several examples show that they are a real part of observed unreliability, even into the useful life period of the equipment.

Table V—High-reliability failure summary by cause.

	%
Human error	50.0
Non-failure	17.2
Vendor defect	13.2
Design error	11.3
Test equipment malfunction	4.3
Unknown	4.0
	100.0

Conclusions

Standard reliability prediction techniques point towards maintenance as the most effective approach to long duration electronics. However, these techniques have a weakness in that they do not consider initial defectives. With the advent of high-reliability piece-parts, initial defectives are now a significant proportion of the in-use failure population.

While this discussion does not offer an alternative prediction technique, there are three general conclusions based on the presence, even in mature equipments, of initial defectives:

1) Electronics become more reliable as they age (excluding those isolated wearout items). As initial defectives identify themselves as failures and are replaced, the new population has a lower number of defects, and is more reliable.

2) Reliability must be designed in—high reliability must be tested in. To achieve higher reliability, the unreliability represented by initial defects must be revealed by test so it can be eliminated. High reliability programs require longer and more severe screening and debugging testing at *all* levels of assembly.

3) We do not know enough about failure causes to generalize upon the design technique to use to tolerate malfunctions.

a) In some areas, failure causes and distributions are very well understood. One of these is solar cells, where a redundant design is obviously preferred.

b) Other areas may not require or allow for additional hardware. Major structural members are in this class.

c) In still other areas (the bulk of the electronics), due to a lack of knowledge, the approach is not obvious. Since a repairable design is required to approach the inherent reliability during all levels of prelaunch testing, it may be desirable to extend the concept to inflight repair. This has the advantage of deferring the decision on the level of protection (number of spares) until actual experience is available. However, the penalties one must pay to design for capability to repair in the space vehicle environment must be examined carefully for individual cases versus the mission requirements and various redundancy schemes. For optimization of a complex spacecraft, there may not be a "general solution."

References

1. Frumkin, B., *System Effectiveness Through Interchangeability*, 1967 AIAA Fourth Annual Meeting
2. Bean, E. E. & Bloomquist, C. E., *Reliability Data From In Flight Spacecraft*, 1968 Symposium on Reliability, pp. 271-279
3. *Electronic News* (7 August 1967) p. 35
4. Troxel, D. I. & Tiger, B., *Predicting Integrated Circuit Reliability Via Failure Mechanisms*, 1968 Symposium on Reliability, pp. 217-225

A dispersed-array mobile-radio system

Dr. H. Staras | Dr. L. Schiff

The radio spectrum, especially for the land-mobile service, is extremely congested and relief is urgently needed. The FCC has conservatively estimated that the number of licenses for mobile use will triple by 1980.[1] Even in plans to set aside an additional 40 MHz of bandwidth for land-mobile use, the FCC admits that "the 40 MHz is appreciably less than the amount of additional spectrum space considered necessary to meet the anticipated 1980 demands of private land-mobile systems." This paper describes a dispersed-array, common-user, mobile-radio system which can provide an order of magnitude improvements in spectrum utilization over the conventional private-user approach and which, therefore, can meet the expected growth in the mobile-radio market, even beyond 1980, within the 40-MHz bandwidth proposed by the FCC.

THE URBAN AREA to be covered by the dispersed-array, common-user, mobile-radio system is divided into a number of non-overlapping cells or zones. In the center of each zone is a fixed base station, and mobile units in the zone can communicate with this local base station. All these base stations are connected to a central processing unit (CPU) by leased land lines (or by SHF short-range, point-to-point radio links). Each of the non-mobile subscribers (or dispatchers) to the system is also connected, by leased line, to this CPU. This allows for a complete connection between any mobile unit and any fixed subscriber. [In this simple form, the system makes no provision for mobile to mobile communication, but from the configuration described above it is obvious that this too can be done.] The CPU is, in effect, a switching center, switching dispatcher calls to the proper local base station. To do this, the CPU must be aware of the location of the mobile unit so that the call can be switched to the correct base station. In one embodiment of this system the "locating" function is accomplished with an "electronic fence" around each zone. Zones are laid out and zone boundaries slightly modified so that zone boundary lines cut through streets near their centers. At each intersection of street and zone boundary line a short-range sensor is installed. All mobile units have low power transmitters that periodically emit the units identity. When the unit gets within range (perhaps 100 feet) of a receiver this identity is picked up. By having two antennas, back-to-back, that look down the street in each direction, the receiver (with the aid of some internal storage) can not only tell which vehicle crossed the boundary but also in which direction. All such receivers are connected to the CPU by leased lines and transmit vehicle number and direction of crossing. To save on the cost of line rental, a number of receivers time share one voice circuit, since the low incidence of zone crossings implies low data rate transmitted for each receiver. The arrangement is similar to the arrangement of polled teletype machines with the CPU being the polling source.

Because of interference, two adjacent zones cannot use the same frequency channel simultaneously. If a base station (designed to give a nominally circular plane pattern in free space) is used with enough power to reliably cover its zone, its radiation pattern will probable spill over to cover major portions of adjacent zones and at least some portions of zones beyond those. Fig. 1a shows a typical pattern that might result; the zones in this drawing are hexagonal in shape. Based on some experimental data,[2] it is felt that essentially interference-free communication can be provided if a "two-ring" buffer is placed around any active base station. That is, the same frequency cannot be used at the same time in any of the zones forming two rings about the central zone. This amounts to 18 hexagonal zones "blocked out" for any given frequency. Using square zones, the corresponding result is 24 zones. For this reason, the zones are designed

Reprint RE-15-3-15
Final manuscript received April 17, 1969.

Dr. Harold Staras
Communications Research Laboratory
RCA Laboratories
Princeton, N.J.
received the BS from CCNY in 1944, the MS from NYU in 1948, and the PhD in Physics from the U. of Md. in 1955. He joined the National Bureau of Standards in 1948 and served as group leader in radio-propagation research and in the performance evaluation of radio systems. He joined RCA in 1954 and was engaged in tropo-scatter propagation studies and in the systems design of tropo-scatter circuits. He has participated in basic studies of electromagnetic theory including "meteor-burst" communication, an island as a natural VLF slot antenna, and dipole characteristics in magneto-ionic media. He performed analyses of the effect of high-altitude nuclear explosions on communication systems, and conducted radar studies of re-entry vehicles. Dr. Staras is the author of 18 technical papers. During 1961-62 he was a Guggenheim Fellow and visiting professor at the Technion-Israel Institute of Technology.

Dr. Leonard Schiff
Communications Research Laboratory
RCA Laboratories
Princeton, N.J.
received the BEE from City College of New York in 1960, the MSEE from New York University in 1962, and the PhD from the Polytechnic Institute of Brooklyn in 1968. From 1960 to 1966 he was employed by Bell Telephone Laboratories, Inc., Murray Hill, N.J., where he was concerned with various aspects of electronic switching systems. Since 1967, he has been employed by RCA Laboratories, Princeton, N.J. working in the field of communication theory. Dr. Schiff is a member of Eta Kappa Nu, Tau Beta Pi, and Sigma XI.

to be nominally hexagonal. This buffering will still allow a frequency to be used simultaneously in many different parts of a metropolitan area.

One method of assuring this buffering of 18 zones around an active base station is to provide adjacent base stations with different frequency channels. However, from Fig. 1b it can be seen that the minimum number of frequency channels to do this is 7. This implies that each mobile unit must have capability on at least 7 frequency channels to insure communications capability in all zones. In our system, however, a different approach is used. The switching and location update facilities at the CPU are assumed to be computer controlled. This computer can also keep track of what frequencies are being used in each zone and refuse to use a base station on a frequency that is simultaneously in use in one of the 18 surrounding zones. Each base station is thereby equipped to communicate on all frequency channels assigned to a given metropolitan area but mobile units need only be given capability on one channel. This is especially important since the major cost of the system is for mobile units. While mobile units need only be equipped for one channel, they may also be equipped for more. The desirability of this multi-channel access is well known. For a constant traffic per channel, multi-channel capability gives a better grade of service; alternately for a given grade of service, the traffic load per channel can be increased. Further, complete flexability can be had by offering units with one or more channel capability. A customer can then purchase or rent a more expensive unit to provide better service.

Since the entire system is computer controlled, a number of desirable features can be implemented rather easily; e.g., giving vehicle location (i.e., what zone) on request. It must also be pointed out that many interconnections accomplished via land lines can also be done with radio links. The main reason for using cable connections in this system is that it makes the cost analysis (to be discussed later) easier.

Traffic-carrying capability

Aside from cost considerations, the system proposed here can only be considered effective if it demonstrates

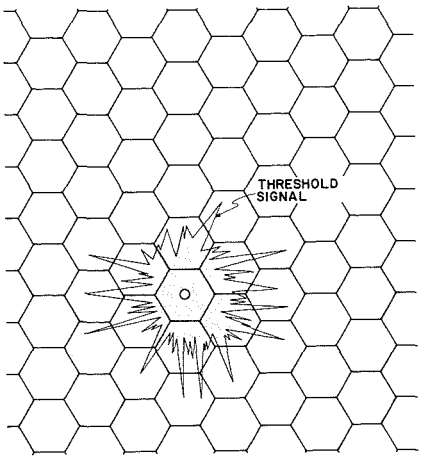

Fig. 1a—Typical coverage from any one zonal transmitter.

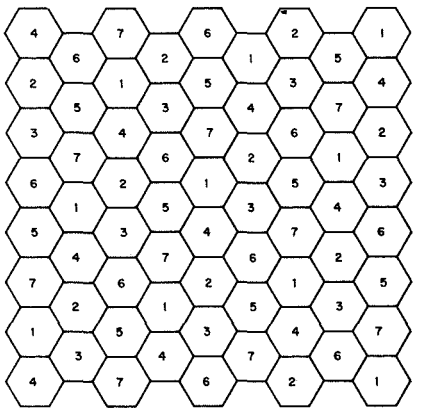

Fig. 1b—Repetition pattern for tightest packing.

increased traffic-carrying capacity over present private-user systems and also over relatively simple common-user systems with a central base station and multi-channel mobile units. Figs. 2a, 2b, and 2c indicate the amount of improvement. These are plots of the *relative* number of vehicles that can be served per channel (or equivalently per unit bandwidth) as a function of the grade of service provided. The grade of service is defined by 1-p, where p *is* the probability of initial blocking. Using a simple first-in, first-out queueing mode, p determines the average delay suffered in completing a call (in units of τ, the average time of a message). This is shown on the top scale. The three plots show the system performance in an urban area of 19, 37 and 91 zones respectively for 1, 4 and 10 channels plot gives the performance of a private user system (N = 1, m = 1) and a multi-channel mobile unit common user system (N = 1, m = 10). The relative number of mobile units served per channel (plotted on the vertical axis) is identical to the erlang load carried per channel. This can, of course, be greater than unity in the system described here since the same frequency channel is reused several times in the city. It should be specifically noted that the shorter the average duration of a typical conversation, the more is gained by using a dispersed-array approach such as is proposed here and the less is gained by multi-channel trunking. This results from the fact that the shorter the average message duration, the higher the blocking probability can be in order to provide the same quality of service as measured by the average time delay before a call can be put through.

The analysis on which these plots are based is approximate. It is based on the probability that a given zone is occupied at a given frequency is exactly equal to the erlang load. Many calculations were made assuming both equal traffic loads in all zones and graded traffic load with the zones and the perimeter of the city carrying substantially less traffic than zones in center city. The curves obtained were relatively independent of the assumed traffic load distribution in the city. The curves presented in Figs. 2a, 2b, and 2c are based on the assumption of equal traffic load in all zones. By assuming independence between occupancies in all cells and at all frequencies, it is simple to calculate blocking probability by noting that if the mobile unit has access to m channels, blocking can only occur if—on all m channels—the cell or any of the surrounding 18 cells are occupied. Of course, occupancies are not independent, but a more exact analysis demonstrates the validity of the approximation in the important range defined by grade of service greater than 0.5.

The nature of the approximate analysis is essentially as follows: assume the traffic carried per channel in each zone is given by a (i.e., a is the fraction of time that a given channel in a given zone is carrying traffic). Therefore, if the whole city were considered as one zone, the probability, p, that a call arriving at random would be blocked is given by $p = a$. If on the other hand, there are N zones in the city (N is a large number) then the probability that a randomly arriving call to a given zone is not blocked, 1-p, is given by

$$1-p=(1-a)^{19} \qquad (1)$$

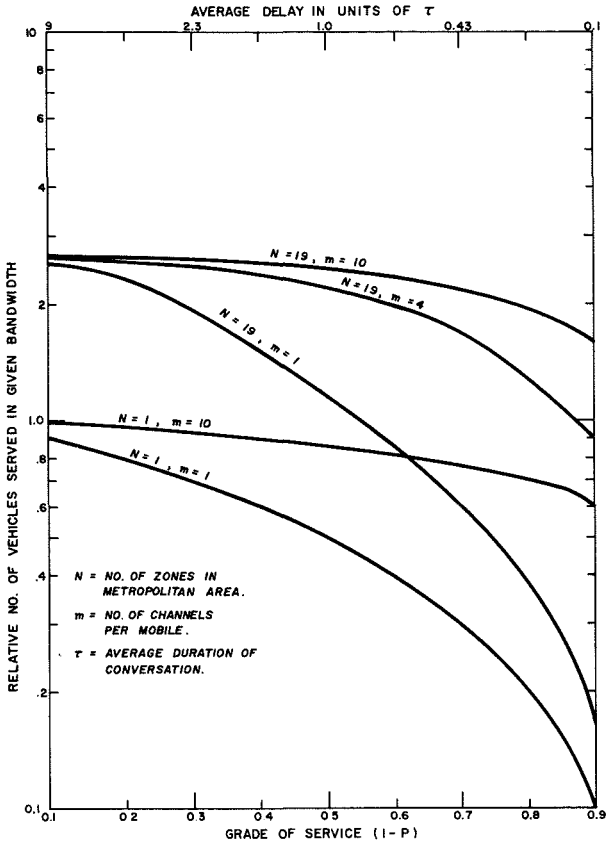

Fig. 2a—Comparison of radio traffic carried between dispersed-array technique and present one-zone technique.

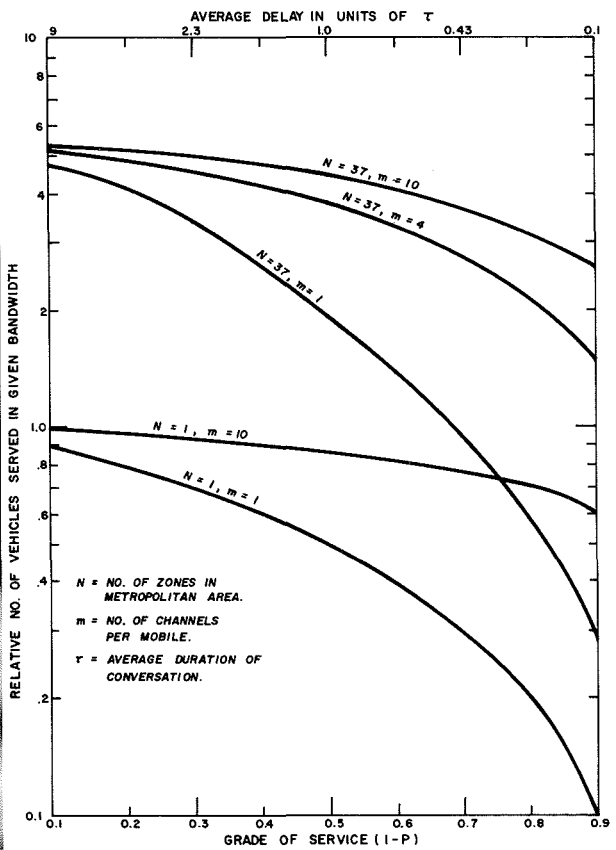

Fig. 2b—Comparison of radio traffic carried between dispersed-array technique and present one-zone technique.

Table I—Estimated number of additional radio-equipped surface vehicles expected by 1980 (based on FCC Docket #1862).

City	*Rank*	*Mobile radio service area (sq. mi.)*	*Additional radio-equipped vehicles (1980)*
New York	1	600	345,000
Los Angeles	3	900	150,000
Chicago	2	440	160,000
Philadelphia	4	260	90,000
St. Louis	9	120	40,000
San Francisco	12	90	30,000

where $(1-a)^{19}$ represents the probability that the channel is not in use in the given zone and is also not in use in the two rings (18 zones) surrounding the given zone. From Eq. 1, we can easily derive the average traffic carried per channel per zone, a, in terms of the probability of blocking.

$$a = 1 - (1-p)^{1/19} \qquad (2)$$

Neglecting edge effects on the outer perimeter of the city, the total traffic carried per channel in the city would be Na. This formula is clearly invalid (since it is based on the assumption of traffic carried in each zone being independent) when p approaches unity (e.g., Eq. 2 indicates that when $p = 1$, $Na = N$). This result states that the total traffic carried per channel in the city would be equal to the number of zones in the city which violates the contraint that there must be two-zone buffering between co-channel operation. Inspection of Fig. 1b indicates that for tightest packing ($p \rightarrow 1$) $Na \approx N/7$. A plot of Eq. 2 for $p < 0.5$ and interpolation between that point and the limiting value of $N/7$ for $p \rightarrow 1$ would yield a good approximation for the traffic carried per channel in the entire city if N were large enough, perhaps a 150 or 200. For smaller N, the traffic carried per channel in the city is a little better than that because two-ring buffering does not block out a full 19 zone on the edges of the city. The curves presented in Figs. 2a, 2b, and 2c include these edge effects.

To show the implications of these plots, consider Table I which shows the additional radio-equipped vehicles in some large cities by 1980. It is instructive to consider how this traffic per mobile unit. For comparison, each can be serviced. If one can attach an easily identifiable number to any point on the ordinates of Figs 2a, 2b, and 2c, the entire ordinate scale becomes determinate. It appears reasonable to assume that the traffic associated with any one vehicle is approximately 1/250 erlangs. With this assumption, we can associate 250 vehicles per radio channel with the ordinate value of 1.0. A system design goal might be to provide a grade of service $(1-p)$ of the order of 0.8. This implies a blocking probability of 0.2; assuming for the Business Radio Service an average conversation of one minute, this would imply an average delay of about 15 seconds before a call can be placed.

In connection with the 40-MHz band under consideration, the FCC, in Docket Number 18262, indicates that the minimum bandwidth per channel would probably be 30 kHz. Consistent with the present usage at 450 MHz, this would mean that a total of 60 kHz would be assigned for each two-way channel: 30 kHz for transmission and 30 kHz for reception. Therefore, the 40-MHz band can provide a maximum of 666 two-way radio channels. Since some channels would have to be available for communities surrounding the large cities, only about 75% of these (or 500 channels) can be provided on an interference-free basis in any given city if a private-user system or common-user system with only multichannel capability is implemented.

On the other hand, if the system described here is implemented, the full 666 channels could probably be made available. To evaluate the traffic capacity on a private user basis, we would use the curve $N = 1$, $m = 1$ in Fig. 2a (or 2b or 2c). From this curve, we see that to provide a grade of service given by 0.8 one can accommodate approximately 50 vehicles per channel. Thus, the 500 available channels can serve at most 25,000 vehicles. From Table I, we observe that this would not be sufficient for at least the top 12 urban areas by 1980. Furthermore, a common user system which would provide a multichannel capability to each vehicle but which would not use a cellular array approach can increase the traffic-handling capacity of each channel by a factor of about 3½ or a maximum of 105,000 vehicles per urban area (see

curve $N = 1, m = 10$ in Figs. 2a, 2b, or 2c). Again from Table I, we see that this would definitely not be sufficient for the three largest cities (in 1980) and probably should be considered marginal for the fourth largest city, (the Greater Philadelphia area). On the other hand, the system described in this paper can provide service in a very large city to at least 1,500 vehicles per channel (see curve $N = 91, m = 10$ of Fig. 2c). This implies a total capacity of at least one million vehicles.

Cost estimate

We are clearly dealing here with a very complex system involving many possible ways of implementing the system. For example, there are several substantially different types of radio location schemes that could be considered. There are also considerations of whether one uses a minimum number of radio channels at each transceiver site at the expense of more expensive multichannel equipment in the vehicles. There is, also, the question of whether the central computer should be connected to the transceiver sites by X-band radio links or by telephone cable. No real studies of the tradeoffs among these possibilities have yet been undertaken. However, estimates of the order-of-magnitude of the costs involved have been made for several cities—both large and small. We here cite the results appropriate to the Greater San Francisco area which is a relatively small system. Based on Table I, it was assumed that Greater San Francisco will have 25,000 mobile-radio-equipped vehicles in the system and that 19 hexagonal zones of 5 sq. mi. each would cover the city. From the curve labeled $N = 19, m = 1$ in Fig. 2a, we estimate that to provide a grade of service ≈ 0.8, each radio channel would be able to service approximately 100 vehicles. A grade of service ≈ 0.8 was chosen because, as seen from the upper horizontal scale on Fig. 2a, it corresponds to an average service delay of approximately 0.25 of a typical conversation period. Assuming a typical conversation length to be one minute, the grade of service chosen would imply an average delay in service of 15 seconds, a number which appears reasonable. Should more accurate data indicate that the average length of conversation is substantially less than a minute (which appears entirely likely) a grade of service ≈ 0.5 or even 0.4 may turn out to be most appropriate.

For the present calculation, however, a grade of service ≈ 0.8 was chosen and, as already indicated, this grade of service implies that each radio channel could adequately service approximately 100 vehicles. Therefore, a total of 250 transceivers would be required at each base station of the dispersed array. The cost analysis was based on these assumptions.

The dispersed-array mobile-radio system consists of three major subsystems:

The central processing unit,
The zonal base stations,
The vehicle-locator system.

In this cost analysis it was assumed that the interconnections between these subsystems are by means of telephone cable for which a rental charge was computed. Table II presents a rough estimate of the fixed-installation hardware costs associated with this dispersed-array mobile-radio system.

Table II—Fixed-installation hardware costs.

CPU	$3 million
Base stations	4 "
Vehicle locator	1 "
Dispatcher panels	1 "
Total	$9 million

The monthly fee for amortization, maintenance, and a reasonable profit for the above fixed costs is approximately $150,000/mo. In addition, the telephone-line leasing costs were estimated at $87,500/mo. Distributed over 25,000 vehicles, the above cost/vehicle would be just under $10/mo. The cost of the radio equipment for the vehicle itself, even at 900 MHz, would probably be less than $700 because of the low power requirement on the transmitter. When converted to an equivalent monthly charge, the vehicle equipment cost is approximately $12/mo. This brings the expected costs for service to $22/mo. per vehicle. It is of interest to compare the above cost estimate with the expected cost for a private-user system at 900 MHz. The high-power radio equipment in the mobile would probably be about $1,000 and each base station $3,000. When prorated over 10 vehicles per base station, the total radio equipment cost per vehicle would be about $1300 and, amortized over 7 years, would result in a monthly cost of about $18.00. To this must be added the cost of a private line from office to base station, maintenance for the mobile and the base stations, and rental costs associated with the base station real estate. These are estimated to add about $17/mo. per vehicle or a total cost to a private user of $35/mo. per vehicle. Thus we see that not only does the dispersed-array mobile-radio system provide for the anticipated growth of the mobile-radio market, but does so at a lower cost than the private-user approach.

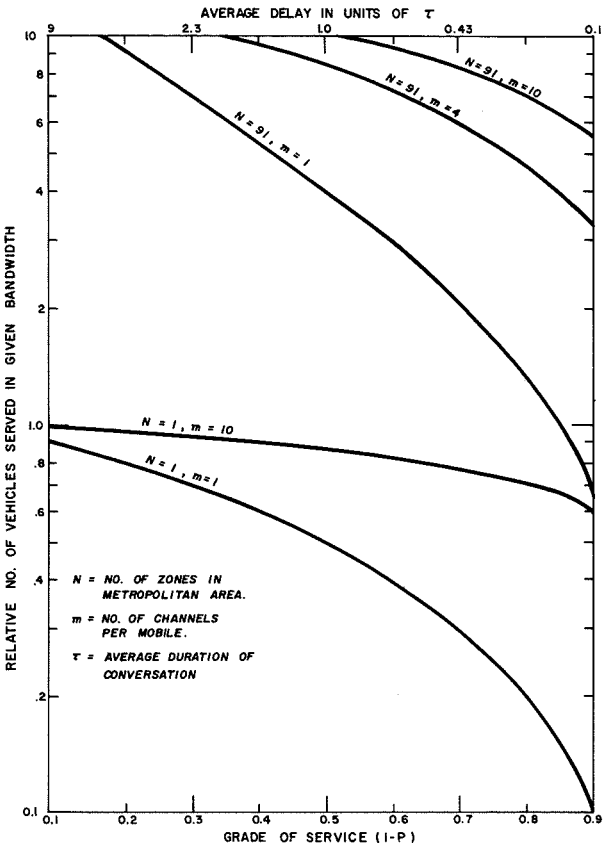

Fig. 2c—Comparison of radio traffic carried between dispersed-array technique and present one-zone technique.

Conclusion

The dispersed-array mobile radio system represents a radical new approach to the problem of spectrum congestion in the land-mobile radio service. This new approach provides a very substantial improvement in spectrum utilization over the present mode of operation and at a cost to the user of about 20% to 30% less. Spectrum efficiency is achieved by a dynamic combination of space, time, and frequency diversity. Cost reduction is achieved because the mobile radio unit is a compact, low-power, short-range, all-solid-state transceiver.

References

1. *FCC Docket Number 18262.*
2. Young, W. R., Jr., "Comparison of mobile radio transmission at 150, 450, 900 and 3700 Mc.", *Bell System Technical Journal, 31* (Nov, 1952) pp. 1068-1085.

Strategic/transportable frequency-division-multiplex equipment—AN/UCC-5(V)

N. E. Edwards | E. J. Sass

Many frequency-division-multiplex (FDM) systems in current service suffer from lack of commonality of interface parameters in equipment that comprises the system. This degrades performance, maintainability, and reliability. The RCA-built FDM equipment described in this paper has sufficient flexibility to overcome current interface difficulties yet is a strategic and transportable equipment substantially more compact and lighter than previous equipments.

IN THE EARLY DAYS OF TELEPHONY, a separate transmission line was required for each voice communications channel. With the rapid growth and expansion of telephony, a more efficient means of voice transmission was desired. This requirement resulted in the technique whereby a number of voice-frequency signals could be combined into a composite signal and transmitted over a single communications circuit. Frequency-division multiplexing (FDM) provides multichannel capability in a wideband transmission circuit by accepting voice frequency information from several voice frequency channels, translating each channel to a different frequency band, then combining them, one frequency band above the other, to provide a baseband signal suitable for transmission by a radio or wide band coaxial cable system. The equipment is used in a similar manner to separate the received baseband signal into individual voice frequency channels for distribution to the local wire lines. Transmission of digital data is accomplished by utilizing any one or more of the available voice frequency channels to convey the output of a teletype multiplex or a data modem.

Most frequency-division-multiplex equipment in the United States is affected by one or both of two worldwide communication system interface standards—commercial and military. Commercial international communications standards have been established by agreement among the various nations through the International Telegraph and Telephone Consultative Committee (CCITT) as part of the International Telecommunication Union. U.S. military global communications standards have been established by the Department of Defense through the Defense Communications Agency. This agency, by means of DCA Circular 330-175-1, specifies standards for interface of Defense Communications Systems and DCS-connected facilities.[1] This military specification, which provides more stringent control of FDM multiplex interface and operational parameters than the CCITT commercial standards, was established by DCA to prescribe interface standards so that proper systems control could be maintained.

There currently exists within the Defense Communications Agency a number of non-complying multiplex systems which were either inherited by DCA or purchased due to urgencies of installation schedules. Through these equipments operate satisfactorily by themselves, there is little commonality between them, creating difficult and troublesome interface problems.

Today's problems

Fig. 1 shows a typical system deployment in Southeast Asia where a wide variety of equipment is encountered with little commonality of interface parameters. Different modulation plans, pilot frequencies, input/output levels and impedances, and signalling facilities dictate interface at the channel level and the need for substantial line conditioning equipment. This not only degrades circuit performance and reliability but greatly adds to the cost and complexity of the system.

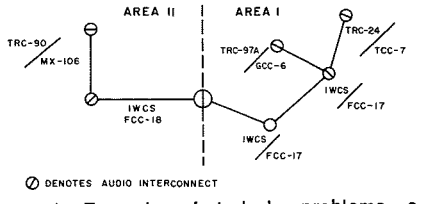

Fig. 1—Example of today's problems—a typical system deployment in southeast Asia.

As Fig. 1 shows, a number of multiplex systems are deployed; some utilizing lower sideband modulation while others utilize twin sideband. Further, group pilot frequencies at 64, 68, 84.08, 92 and 104.08 kHz are used while line pilots at 16, 60, 64 and 96 kHz are employed. These interface elements alone greatly hamper interconnections—not to mention the incompatabilities of levels, impedances, signalling facilities, and other parameters. System interconnection can be —and in fact has been—implemented at the channel level but at a cost of increased system complexity and reduced end-to-end reliability and quality.

RCA approach

For any difficulty there is usually a number of approaches to effect a proper remedy. RCA considered the future requirements of the Defense Communications Agency as well as the past installations and their inherent interface difficulties. The approach followed, then, is twofold:

1) An FDM system fully compliant with DCAC 330-175-1 for new circuits.
2) An FDM system which provides *flexibility* beyond DCAC 330-175-1 to allow effective interface with existing circuits, thus protecting all the inventory as well as providing efficient and substantially less costly interface with it.

Another primary design goal was to develop an equipment which offered measurable cost effectiveness. To this end, we considered both direct effectiveness in that we knew the final product offered must be competitively priced, as well as the indirect effec-

Reprint RE-15-3-4
Final manuscript received April 16, 1969.

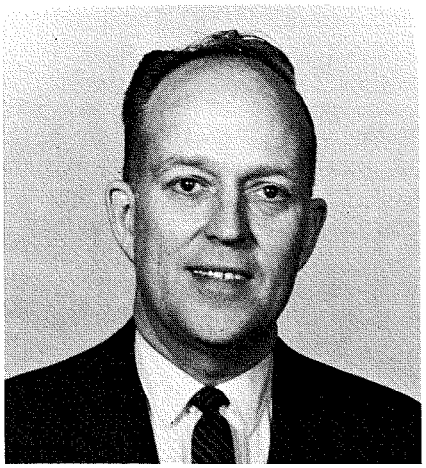

Earl J. Sass, Ldr.
Communications Equipment Engineering
Defense Communications Systems Division
Camden, N.J.
received the BSEE in 1945 from the University of Nebraska; and the MSEE in 1954 from the University of Pennsylvania. He joined RCA in 1945, and worked on RF and IF coils and transformers and the first RCA printed-circuit television tuner. He transferred to the Home Instruments Division in 1951, and was responsible for product design of picture and sound IF amplifiers for RCA's first commercial color television receivers. In 1957, he supervised half of the electrical design of commercial color television receivers and remote control receivers. He transferred to CSD in 1961, where he was responsible for the design 1) of the ground receiving equipment for the DYNA-SOAR Project and 2) a part of the GRC and 744 project. In 1963 he was responsible for the design and development of the AN/TRC-97 exciter, receiver, and shelter. At present, he is Group Leader in charge of the development and design of military frequency division multiplex terminal equipment and is responsible for the 60-channel FDM equipment, AN/UCC-5(V)1. He holds three U.S. patents and is the co-author of two published articles. He is a Senior Member of the IEEE and is a member of Sigma Tau and Pi Mu Epsilon.

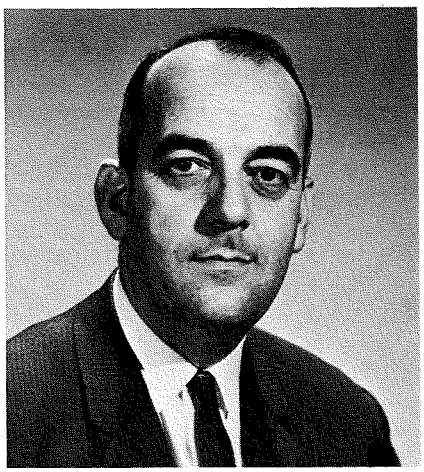

N. E. Edwards, Mgr.
Communications Equipment Engineering
Defense Communications Systems Division
Camden, N.J.
attended Romford Technical College in England from 1932 to 1937. From 1949 to 1953 Mr. Edwards was responsible for various engineering and supervisory activities in the planning and development of international HF and VHF systems for Cable & Wireless Ltd. Mr. Edwards joined RCA in 1953 and was responsible for the design of telecommunications systems and equipment. He became Leader of Communications Systems Design in 1957 and Manager of Microwave and Communications Systems Design in 1958. From 1962 to 1965 Mr. Edwards was Manager, Microwave and Troposcatter Communications Engineering. From 1966 to present Mr. Edwards has been Manager of Technical Control, Communications Equipment Engineering with major responsibility for TACSATCOM Satellite Ground Stations for USASCA, UCC-5 developments for STRATCOM, MMCSA, a 1 KW airborne C-Band transmission system for ESD, and various fixed plant Troposcatter equipments. Mr. Edwards holds two U.S. patents and has presented several papers on communications systems. He is a Senior Member of the IEEE and a Member of the American Management Association.

tiveness offered by a system of reduced size and weight, universal flexibility, and higher reliability.

System

The RCA FDM multiplexer, the AN/UCC-5(V)1, was developed as a solid-state, 60-voice-channel, frequency-division-multiplex, carrier equipment for use in microwave radio or line carrier systems. The AN/UCC-5(V)1 is a versatile 60-channel mutliplexer in that it is conforms to DCAC 330-175-1 for fixed-station applications and Military Standard 188B for tactical applications[2]. Further, the equipment is designed to MIL-E-16400 for environmental service conditions and component requirements.[3]

The equipment has been designed to operate on a continuous basis with a minimum of maintenance or adjustment. This has been achieved through the use of transistors and integrated circuits in a conservative design, with 96% of all components mounted on plug-in printed circuit boards for ease of maintenance and system expansion.

The system uses a two-step modulation process from voice frequencies to a 12-channel 60-to-108-kHz base group. The formation of this channel group is either inverted sideband (CCITT basic group B) or twin sideband. The group formation is a field option selected by a single switch. Five 12-channel groups are further modulated to give a standard 60-channel supergroup from 312 to 552 kHz (CCITT supergroup 2). The 60-channel standard supergroup is then remodulated in the supergroup translation equipment to form the baseband of 12 to 252 kHz or 60 to 300 kHz. Higher capacity systems of 300 or 600

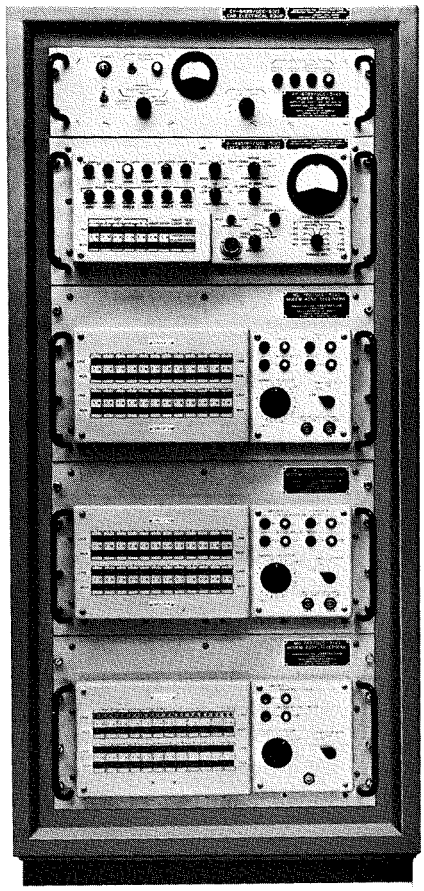

Fig. 2—60-Channel AN/UCC-S(V)1

voice channels are constructed in a similar manner by choosing the appropriate supergroup translation frequencies.

All channel modems are identical and completely interchangeable, providing great maintenance flexibility and allowing a substantial reduction in the number of spare modules required. The channel filter is identical in each modem and has been designed by the application of advanced filter techniques. This results in outstanding performance in channel amplitude and envelope delay response. The amplitude requirements of both DCAC 330-175-1 and MIL-STD-188B are met and the delay response permits the transmission of high-speed data.

Modem configurations are available with and without termination and in-band signalling. When included, the line termination provides a 2W/4W option and a three-position switched attenuator in both the transmit and receive paths. In-band signalling is selectable at either 2600 or 1600 Hz, and 20-Hz ringdown is also a part of the termination option.

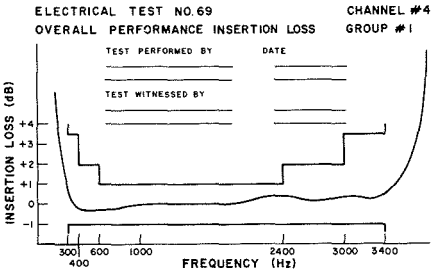

Fig. 3—Overall insertion loss of a typical channel.

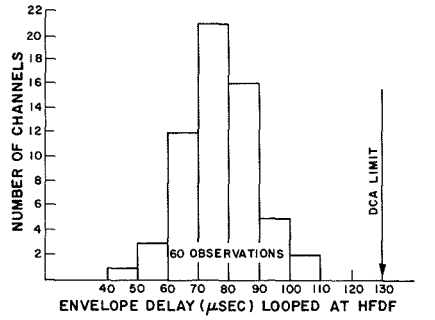

Fig. 4—Overall envelope delay (1000-2500 Hz).

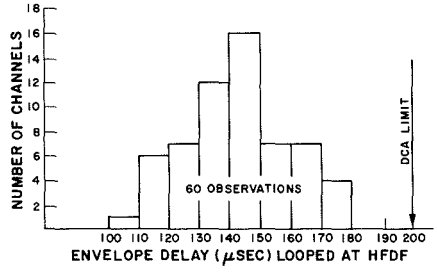

Fig. 5—Overall envelope delay (600-3200 Hz).

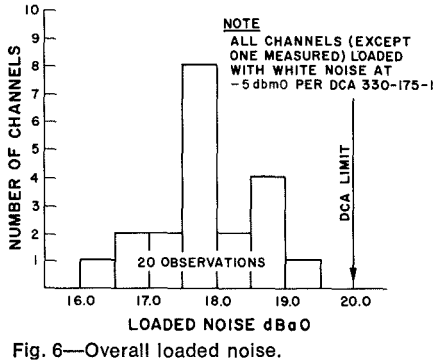

Fig. 6—Overall loaded noise.

Carrier frequencies for the different modulation stages are phase-locked to the 1344-kHz master oscillator. This oscillator is contained in a proportional oven and has a long-term stability of ±2 parts/million for 90 days. It is, therefore, capable of supporting a 600-channel system. System synchronization is maintained by a line pilot giving stable phase and frequency lock required for data transmission. Four group pilot frequencies are available by switch selection on a group basis. Various line pilot frequencies are available and can be field selected by plug-in module substitution.

Complete testing facilities are included as an integral part of the equipment. A switch is provided so the operator may talk or listen on any traffic channel with no degradation in channel performance. Indicator lights show the operational status of the equipment while malfunctions are indicated by both alarm lights and an audible alarm.

Each power supply handles up to 120 channels and operates on any AC frequency power source between 47 and 440 Hz. If operation from a battery is considered necessary, an alternative power supply is available which permits operation from 24 or 48 VDC. The equipment is protected by a circuit breaker on the AC side of the power supply, fuses in the unregulated DC voltage supply, and a short circuit protect circuit in each of the regulated DC voltage supplies. This protect circuit drops the output current to a minimal value in the presence of a short circuit. When the short circuit condition is eliminated, the circuit automatically resets to a "go" condition.

All modules plug into keyed multi-pin receptacles. This arrangement facilitates removal for inspection and service and prevents incorrect insertion of modules. A bank of break-jacks is provided which are used in conjunction with an integral test set to perform all necessary setup and routine maintenance tests. The AC voltmeter included in the test set is available for general use.

Equipment

Fig. 2 depicts a typical 60-channel terminal complete with termination and signalling equipment and field adaptable to either transportable or strategic applications. This terminal, as it stands, can efficiently interface with any of the existing multiplex systems in the field regardless of type of modulation, group or line pilot frequencies or supergroup assignment. The mean-time-between-failure (MTBF) for a single channel is 5683 hours at 50°C while the total MTBF for the entire 60-channel terminal is 553 hours.

Performance

The design program was governed by DCAC 330-175-1, MIL-STD-188B and environmental specification MIL-E-16400. We have recently concluded a successful test program on the AN/UCC-5(V)1 in accordance with DCAC 300-195-2.[4] The equipment was tested against the criteria set forth in DCAC 330-175-1. These tests were sponsored by the U.S. Army Strategic Communications Command (USASTRATCOM) and were witnessed by DCA/STRATCOM representatives.

Typical channel response

An actual insertion-loss curve for one of the equipment channels is shown in Fig. 3 and displays the margin provided beyond the DCA requirement.

The exceptional channel response characteristics of the AN/UCC-5(V) are due to a great extent to the unique channel filters employed in the system. Since both twin sideband and lower sideband modulation plans were to be accommodated, symmetrical channel filters were employed. This provided modulation flexibility and greatly improved channel response.

Envelope delay

The measured envelope delay in the 1000- to 2500-Hz region is shown in Fig. 4 while that for the 600- to 3200-Hz band is given in Fig. 5. In both cases, the channels measured considerably less delay than the limit.

Loaded noise

Loaded noise performance is one of the most difficult requirements imposed by DCA. Compliance is essential if the system is to be able to provide the 100% data-handling capability at a channel-input level of −5 dBm0 required by the military. As can be seen from Fig. 6, the AN/UCC-5(V) easily meets this specification and provides a 1-2 dB safety margin as well. Space does not permit a presentation of the other test results but a list of the AN/UCC-5(V)1 characteristics are given in Table I.

Operational compatibility

The AN/UCC-5(V)1 provides switch or module substitution selection of all important parameters affecting interface and thus can be simply and easily adapted to interface with any FDM equipment now developed.

Table I—AN/UCC-5(V)1 characteristics.

VF input	−16, −4, 0 dBm
VF output	+7, −4, −3 dBm
HF (trans.)	−45 dBm (DCA) −35 dBm (Tactical)
HF (rec.)	−15 dBm (DCA) −25 dBm (Tactical)
VF line imp.	600 ohms (balanced)
HF line imp.	75 ohms (unbalanced)
60-channel line group	60-300 kHz (DCA) 12-252 kHz (Tactical)
Attenuation versus frequency (looped at HFDF)	−1.0, +1.0 dB 600 to 2400 Hz −1.0, +2.0 dB 400 to 3000 Hz −1.0, +3.5 dB 300 to 3400 Hz
Envelope phase delay (looped at HFDF)	200 μsec 600 to 3200 Hz 130 μsec 1000 to 2500 Hz
Load handling capability	100% data loading, −5 dBm0 per channel
Idle noise	15 dBa0
Loaded noise	20 dBa0
Harmonic distortion	−40 dBm0
Intelligible crosstalk	−70 dBm0
Unintelligible crosstalk	—60 dBm0
Near-end crosstalk	−50 dBm0
Prime power	47 to 420 Hz, single or three phase, 120 V ±10%, 320 W (Additional 125 W required for signalling for 20 field phones)

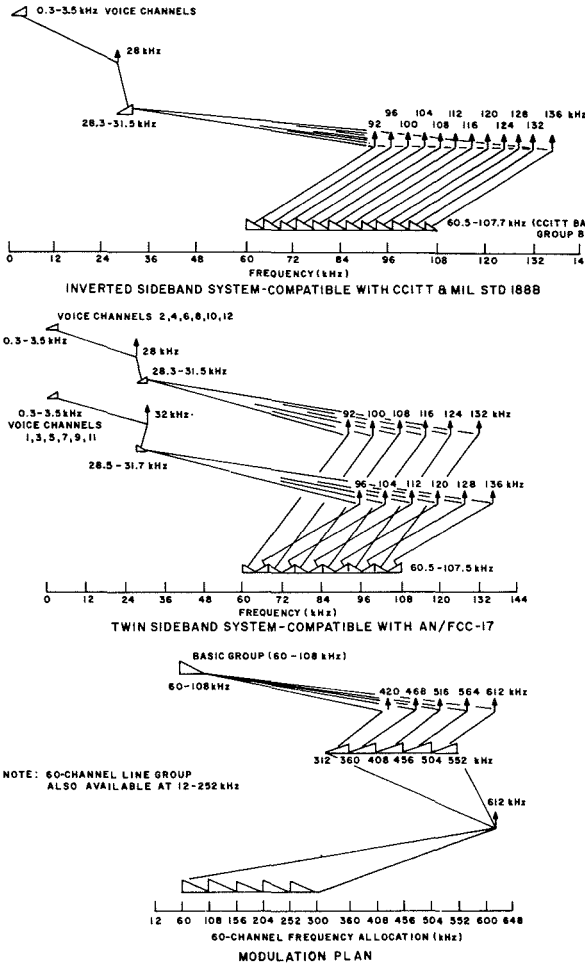

Fig. 7—Modulation plans for inverted and twin sideband syste

Modulation plan

Some FDM equipment currently in the military inventory uses both lower-sideband and twin-sideband modulation plans. This prevents group or supergroup interface between the various equipments and has forced interconnect at the channel level with its resulting increase in equipment and cost.

The AN/UCC-5(V) has been designed to provide either modulation plan (Fig. 7) on a group basis, and selection is made by a single front panel switch. This provides direct interface at the group or supergroup level with all twin-sideband equipment such as AN/FCC-17, AN/MCC-12 or AN/GCC-5, with all lower sideband equipments such as AN/FCC-18, AN/TCC-7, AN/UCC-4, AN/FCC-32, and with all CCITT type equipments.

Should the application demand, the AN/UCC-5(V) could interface with both plans simultaneously with some groups operating twin sdieband and the remaining operating lower sideband, all within the same supergroup.

Group and line pilots

Table II shows some of the inconsistencies encountered in the area of group and line pilot frequencies utilized by the various multiplex systems. As can be seen, four different group pilot frequencies are in use, while the line pilot inconsistencies are even greater with six being used. Let us first discuss the group pilot situation. In the AN/UCC-5(V) *all four* of the pilots listed are included in the basic package and are switch-connected to each group. This allows an AN/UCC-5(V) supergroup to utilize the same group pilot throughout or, in the case of multiple system interface, as many as four independent group pilot frequencies can be operating simultaneously in one supergroup.

The line pilot situation is slightly different in that module substitution is utilized to change frequencies. However, each of the line pilots listed is available by a single module change.

Signalling

Two separate signalling generators are provided with the capability of selecting the desired signalling frequency on a group basis—thus providing any combination of two signalling frequencies in the five groups of a supergroup. The desired frequency of the signalling detectors is obtained by a switch on each channel modem.

Supergroups

Transportable (12 to 252 KHz) and strategic (60 to 300 KHz) supergroup flexibility is achieved by changing one module.

600-Channel system

A typical 600-channel system is shown in Fig. 8. Only four basic drawers are needed. In this case, 25 identical channel modem drawers are included, each of which contains 24 identical and interchangeable channel translating modems. Five power supply drawers are utilized for increased reliability. The group and supergroup equipment as well as the automatic group regulators are contained in a total of five drawers. The complete carrier generation system requires only one drawer.

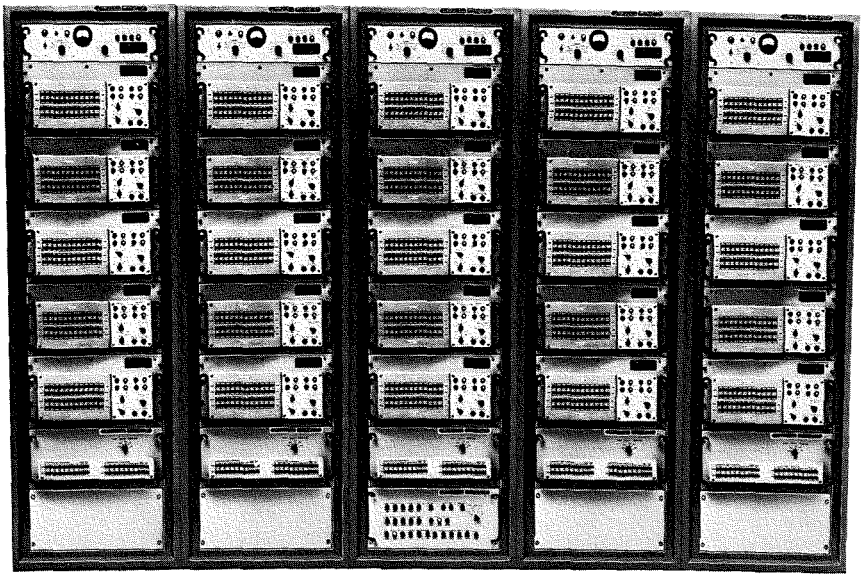

Fig. 8—600 Channel AN/UCC-S(V) FDM system.

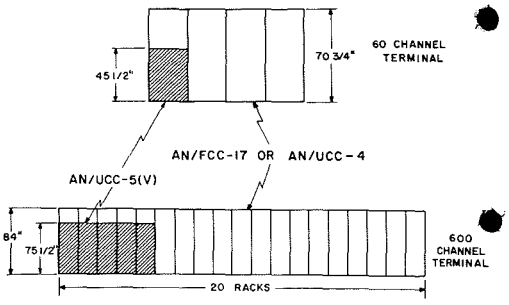

Fig. 9—Size comparisons between AN/UCC-S(V) type equipment and typical FDM equipment deployed in the field.

Size

Fig. 9 shows rather dramatically the size reduction offered by the AN/UCC-5(V). The upper portion represents a typical 60-channel FDM system as currently used and requires four racks greater than 70 inches high in comparison with the equivalent AN/UCC-5(V) 60-channel terminal provided in one rack less than 46 inches high.

The lower portion is a similar comparison of a 600-channel terminal. Here approximately twenty racks are needed with currently deployed multiplex to provide the same facilities contained in the AN/UCC-5(V) 600-channel terminal of but five racks. Transportation requirements, building requirements, and shelter sizes are all affected favorably by these reductions.

Weight

The 60-channel AN/UCC-5(V)1 weighs 540 pounds while the weight of comparable FDM equipments currently deployed is approximately 2200 pounds. As can be seen, the AN/UCC-5(V)1 offers better than a 4-to-1 reduction in weight. This weight reduction ratio continues to be maintained when comparisons are made with typical 600-channel systems.

Maintenance

Maintenance effectiveness is always a vital consideration for equipment of this nature. During the design phase the following enhancing features were included:

1) Unified functional grouping of circuitry on the modules;
2) All channel modems identical and interchangeable;
3) Built-in jackfield (no separate IDF required);
4) Channel monitoring;
5) Automatic switchover on redundant master and group oscillators;
6) Fault alarms;
7) Built-in test set;
8) Three basic drawer types for 60 channels—four types for systems from 120 to 600 channels;
9) Only twenty module types; and
10) Automatic reset on power supply.

By incorporating these features, the resultant mean-time-to-repair is 6.2 minutes.

Table II—Various group and line pilots presently in use.

Pilot	*AN/FCC-17 AN/UCC-4*	*AN/FCC-18*	*MX-106*	*AN/GCC-5 AN/GCC-6*	*Tactical 188-B*	*L. Haul 188-B*	*Bell "L"*	*AN/UCC-5*
	64							64
		84.08			No	84.08		84.08
Group				None				
		92	92		Spec.	92	92	92
	104.08					104.08		104.08*
				16				16
		60				60		60
Line		64	64				64	64
(sync)					68			68
	96							96*
		308					308	308

*DCA standards

Summary

The AN/UCC-5(V) Frequency Division Multiplex equipment meets the requirements of the Military where an FDM system, fully compliant with both DCAC 330-175-1 and MIL-STD-188B, is needed. In addition, the AN/UCC-5(V) has sufficient flexibility to overcome the current interface difficulties while maintaining commonality between strategic and transportable systems as well as offering substantial size and weight reductions.

Acknowledgments

The authors wish to acknowledge all those who made substantial contributions to this program, particularly Daryl Hatfield of DCSD Marketing. The efforts of those in Engineering and Marketing whose specific efforts and effective teamwork made this equipment possible are also gratefully acknowledged.

References

1. DCAC-300-175-1, *Defense Communications System Engineering — Installation Standards Manual.*
2. MIL-STD-188B, *Military Communication System Technical Standards.*
3. MIL-E-16400, *Military Specifications, Electronic Equipment, Naval Ship and Shore.*
4. DCAC-300-195-2, *Testing of Defense Communications Systems Equipments/Systems.*

Millimeter waves for communications systems

Dr. H. J. Moody

Millimeter-wave communications systems could provide relief from the spectrum congestion at frequencies below 10 GHz. This is due particularly to recent developments in power sources and detectors. This paper discusses the atmospheric problems inherent in millimeter-wave transmission, surveys recent developments in components, and gives several system applications.

Dr. Harry J. Moody
Research Laboratories
RCA Limited
Montreal, Canada
received the B. Eng. in 1948 from the University of Saskatchewan. He obtained a National Research Council Bursary and Studentship to continue work with the University of Saskatchewan Betatron. He obtained the M.Sc. in Physics in 1950 for studies of radioactive chlorine 39. He spent a year at the University of Illinois working with the 300 MeV Betatron, and then returned to Canada to take a position at the National Research Council. He received the PhD from McGill in 1955 for work on total cross sections for high energy neutrons. He then joined the Research Laboratory of the Canadian Marconi Company and worked in a number of fields, including component reliability, frequency modulation techniques, electron-beam-type parametric amplifiers, and crossed-field devices. In 1961, he joined the Research Laboratories of the RCA Limited, in Montreal as a member of Scientific Staff to work in the field of millimeter waves. During the course of this work he made substantial contributions to four of a series of twelve review volumes put out by the Research Laboratories on the subject of millimeter waves. For some time he worked in the field of electronically scanned antenna arrays, during which he determined the systematic design techniques for the Butler Matrix and made detailed studies of waveguide slot parameters. Recently he has extended his interest in the electromagnetic spectrum to the infrared, and is working on an infrared system study. He is a member of the Canadian Association of Physicists.

FOR MANY YEARS, millimeter waves have been proposed for various applications, particularly as a means of relieving the spectrum congestion at frequencies below 10 GHz. This promise of usefulness has been thwarted by the lack of a complete line of components, particularly by the lack of adequate power sources and sensitive receivers. In addition, the millimeter wavelengths have been handicapped by certain basic limitations such as high atmospheric absorption and the requirement that antenna gains be higher to compensate for the loss due to smaller receiving aperture areas.

In the last few years, the limitation due to the lack of adequate components has been largely removed. System designers are now able to make a concerted effort to find applications where millimeter waves can provide a real advantage in terms of performance or cost.

Atmospheric effects

Air absorption

At millimeter wavelengths, the atmosphere has higher attenuation than at microwave frequencies. The attenuation (dB/km) of the atmosphere is shown in Fig. 1, while the total atmospheric attenuation between the earth's surface and points outside the atmosphere is shown in Figs. 2 and 3. Note that at 35 GHz, the attenuation is about 0.12 dB/km. While this is large compared to lower frequencies it is still small compared to the space loss over short path lengths. This attenuation consists primarily of a number of resonance absorption lines with regions of lesser attenuation between. The windows between the lines exhibit continuously increasing attenuation with decreasing wavelength, at least in the millimeter and sub-millimeter wave regions.

The absorption band at 60 GHz is a composite of many individual lines. At ground level, these lines are pressure broadened so that they completely overlap forming a broad band of attenuation reaching a maximum of more than 14 dB/km. At high altitudes, the individual lines become narrow and completely separate from each other leaving regions of very low attenuation between. Fig. 4 shows the attenuation between 50 and 70 GHz at a number of altitudes. At an altitude of 32 kilometers, the lines are completely separate, and for a frequency between lines, such as 60 GHz, the horizontal attenuation is very low but the total attenuation to ground level would be more than 100 dB.

The total attenuation through the atmosphere depends upon the look angle measured from the vertical. This is illustrated in Fig. 2 for a number of specific angles and in Fig. 3 for certain specific frequencies and specific weather conditions. As the antenna beam gets closer to the horizon, the thickness of the atmosphere traversed increases, resulting in increased total attenuation.

In addition to reducing the signal strength the atmosphere introduces thermal noise in proportion to $(1-\tau)$ T_a where τ is the transmission and T_a is the ambient temperature.

Rain attenuation

For ground level use of millimeter waves, the attenuation due to rain is of more importance than clear-weather attenuation. Fig. 5 shows the attenuation due to rain and fog of various intensities. The rainfall rate is seldom constant over very great distances, particularly when heavy rates are involved. Storm centers are swept along by wind conditions. Thus, a pattern which appears in an instant of time over the path of the storm will appear, with some changes, at a specific point over a period of time. Fig. 6 shows a rain storm measured by the Bell Telephone Laboratories at a single point over a period of time.[1] The sampling interval was approximately 10 seconds. The maximum rainfall rate shown in about 11 in./hr and the average is just under 2 in./hr.

In calculating attenuation, the parameter of interest is the path-average

Reprint RE-15-3-1
Final manuscript received July 8, 1969.

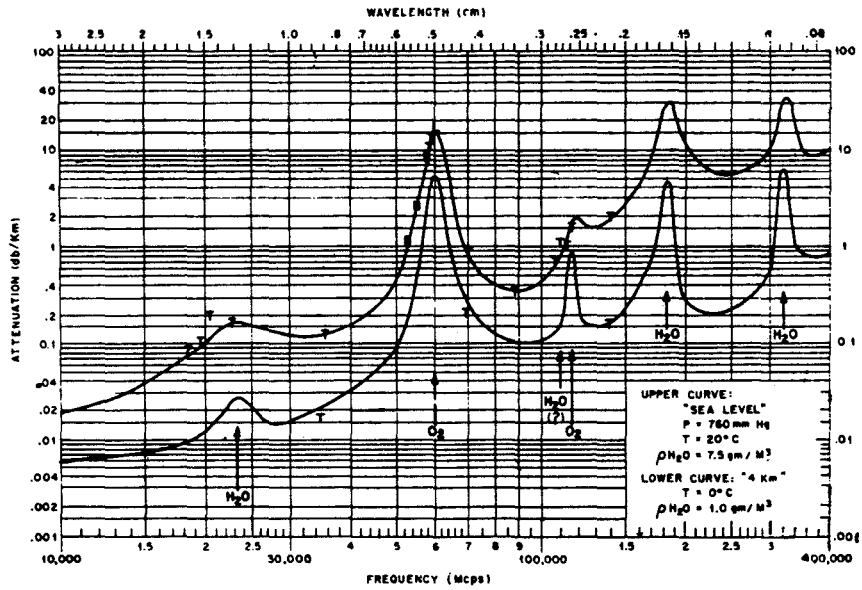

Fig. 1—Attenuation versus frequency for horizontal paths through the earth's atmosphere (after Rosenblum, Ref. 15).

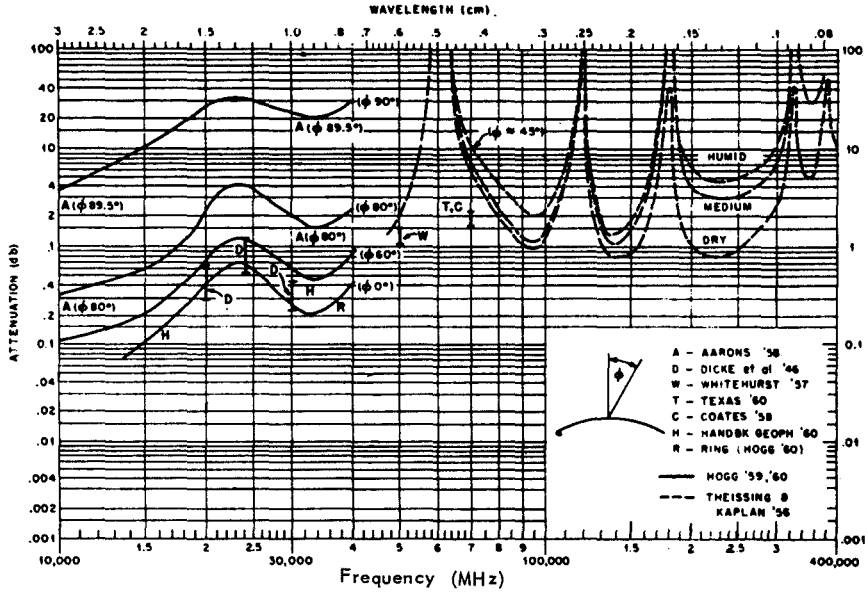

Fig. 2—Total attenuation versus frequency for a one-way transmission path through the earth's atmosphere (after Rosenblum, Ref. 15).

rate: the average of the point rainfall rates over the propagation path. Unfortunately, this is usually not available for a planned radio link, the available information usually being in the form of one-hour point rates for single stations in the region.

Bussey[2] has considered the problem of correlating point rates and path rates. Working with data obtained from the US Department of Agriculture, Soil Conservation Service, he established a relationship between 50-km path averages and one-hour point averages. This empirical relationship he justifies by the following picture. The storm giving rise to the rainfall is in motion with a ground speed which averages 45 to 50 km/hr. A fixed ground based gauge averaging for t hours measures rainfall originating from points in this storm covering about $50t$ kilometers. It seems reasonable that if the statistical characteristics of the storm remain more or less unchanged as it moves past the gauge, then the $t \times$ hour average of the gauge should be about the same as an instantaneous ($50t$ km) path average in the direction of the storm motion. (This might be looked upon as an assumption of ergodic behavior). It further seems reasonable that the long time distribution of these averages should be the same as for any other $50t$ km path exposed to the same storms. Thus, the distribution for hourly average and 50 km path average are equated, and similarly half hourly and 25 km path, ten minute and 8 km path, etc. Fig. 7 could be used to estimate distributions for other averaging periods from one hour average point rate distributions. If the prevailing average rate of storm motion in the region considered were higher or lower than 50 km/hr, a given averaging time would presumably be equivalent to a proportionately longer or shorter path.

This then gives us the distribution of occurrences of path average rainfall intensities for the path length in question. From these we can use the curves of attenuation versus rainfall to convert the distribution of occurrence of path average rainfall intensities to a distribution of path attenuations.

The Bussey method was used by Tsao, et al,[3] to calculate the power margin for a 35-GHz communication link required to ensure a specified maximum outage time with path length as a parameter. Tsao's curves are reproduced in Fig. 8.

Millimeter wave components

Transmission lines

The requirements of a transmission line for electromagnetic propagation are many and varied. The different lines that have been used or proposed are equally numerous and varied. At millimeter wavelengths, only two of these transmission lines have been developed extensively although at least two others are potentially useful. The two that have been developed to a considerable extent are the rectangular waveguide and the TE_{01} mode in circular (or spiral) guide. Two others that show potential promise are the quasi-optical and the H-guide.

The various properties desired of a transmission line vary from low loss to ease of component design and fabrication. Table I lists several properties

Table I—Rating chart for mm-wave transmission lines.

Property	*Rectangular*	*Circular TE_{01}*	*Quasi-Optical*	*H-guide*
Attenuation	1	3	2	3
Ease of launch	3	2	1	2
Freedom from interference	3	3	2	3
Component design	3	2	2	2
Moding or alignment problems	3	1	2	2

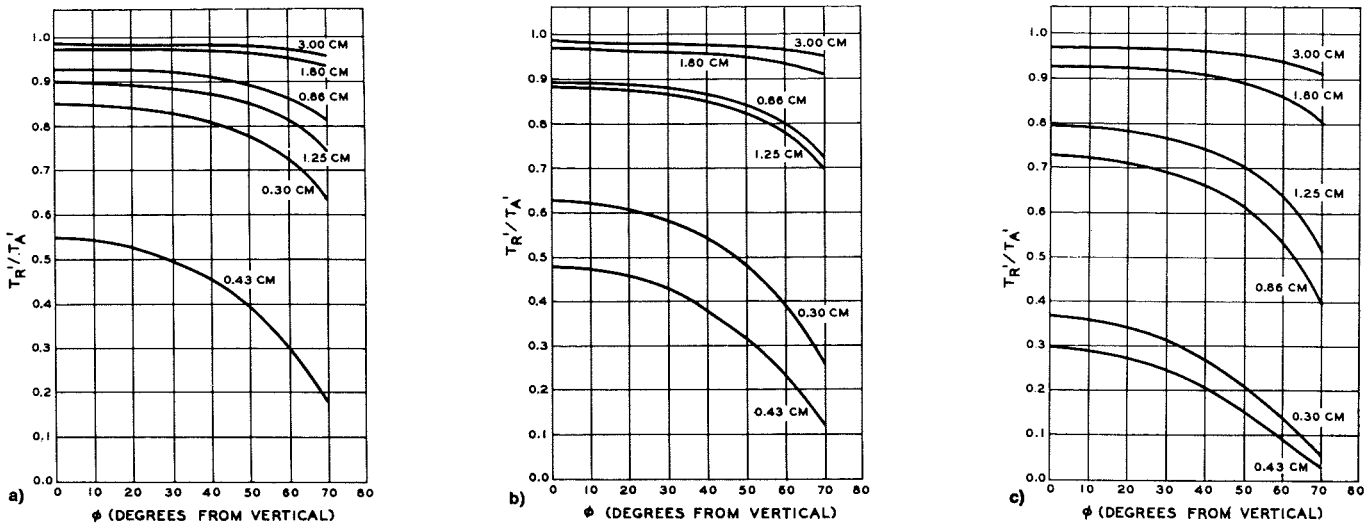

Fig. 3—Overall atmospheric attenuation factor (T_R'/T_A') as a function of vertical angle ϕ, and wavelength (Ref. 17). a) conditions: clear sky, 1% absolute humidity at sea level; sea-level temperature 290°K. b) conditions: moderate cloud cover (0.3 g water/m³) between 3000 and 6000 feet; 1% absolute humidity at sea level; sea-level temperature 290°K. c) conditions: moderate rain (4 mm/hour) between 0 and 3000 feet; moderate cloud cover (0.3 g water/m³) between 3000 and 6000 feet; sea-level temperature 290°K).

along with a number corresponding to the assigned rating of the type of transmission line, one for poor, two for fair, and three for good.

Table I is weighted toward rectangular waveguide partly because of a long history of design and development at lower frequencies but primarily because rectangular waveguide is almost ideally suited for the transmission of microwave energy. The H-guide also rates quite high. This is partly because the H-guide is similar to rectangular waveguide with a dielectric ridge down the center and therefore enjoys many of the same properties. However, very little work has been done on this type of transmission line and very little is known about launching problems or designing components for use in conjunction with it. If such experience were obtained, some of the ratings might go either up or down. The relative weightings will vary also from application to application. For some applications one or two properties will be of overriding importance. For instance, for long distance communications via transmission line it is vitally important that the attenuation per kilometer be a minimum. On the other hand, for a system using free space propagation the size of the terminal portion of the system decreases with wavelength and the loss for this portion will be roughly constant if the loss per wavelength is independent of wavelength. In this case, the availability of components is a more important consideration.

Fig. 9 gives a summary of the attenuation of these and other transmission lines as a function of frequency. It is seen that both H-guide (Duo-Dielectric, Parallel Plane Waveguide) and TE_{01} mode in circular waveguide have attenuations which decrease with increasing frequency. Thus very low attenuation factors can be obtained provided that the unwanted modes that can also propagate can be suppressed.

Microwave tubes

Many novel techniques have been proposed for generating millimeter wave energy. In spite of this, the types of generator that have been developed for use at lower frequencies have worked out best for millimeter wave generation. These types are klystrons, magnetrons, and various forms of traveling wave tube or extended interaction types. Low power klystrons (<0.5 W) have become available up to about 250 GHz. High power cw sources have been made that deliver 6 kW at 50 GHz.[4] This was distributed interaction klystron design and may be considered at the limit of the state of the art. It delivers, for instance, more power than can be handled by rectangular waveguide without special cooling arrangements, and is approaching the breakdown limit of air filled rectangular waveguide.

The evolution of extended interaction microwave tubes since 1940 is presented by Osepchuk.[5] He shows that,

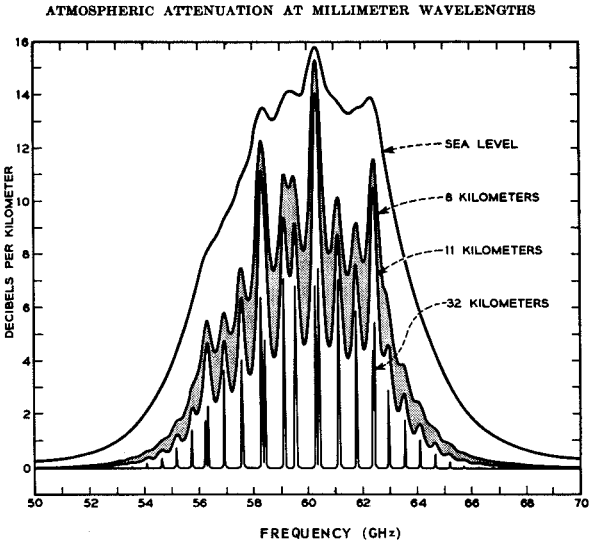

Fig. 4—Calculated curves of absorption by 5-mm oxygen line for different altitudes based on a line breadth constant $\Delta\nu$=600 Hz, (after Rogers, Ref. 16).

even in the past 10 years, since 1958, power level has increased at some freqeuncies by two orders of magnitude with the maximum frequency limit increasing by nearly one order of magnitude. This does not suggest that progress in microwave tube development is slowing down; however, a period of stagnation is likely unless some new innovation is forthcoming. Two suggestions that may provide further impetus to microwave tube development are

1) Extended interaction devices using periodic beams rather than periodic circuits[6]; and

2) An electron cyclotron maser[7].

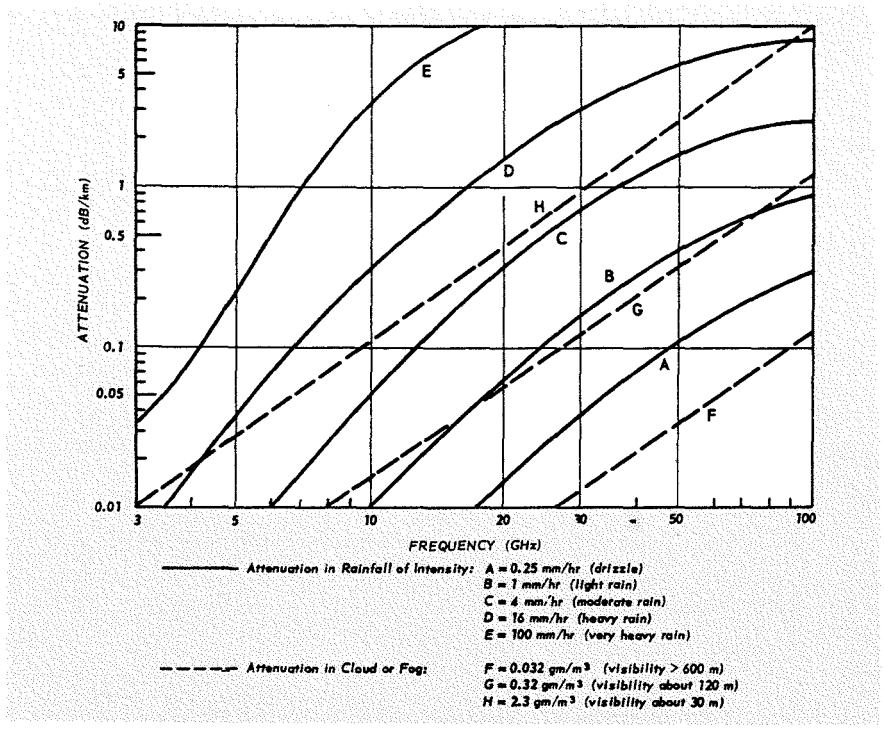

Fig. 5—Rain and fog attenuation (Ref. 18).

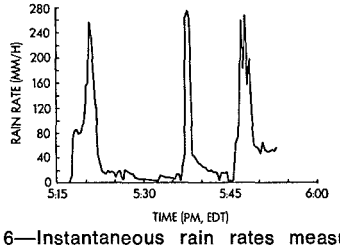

Fig. 6—Instantaneous rain rates measured with a ten-second sampling interval in central New Jersey. (Ref. 1).

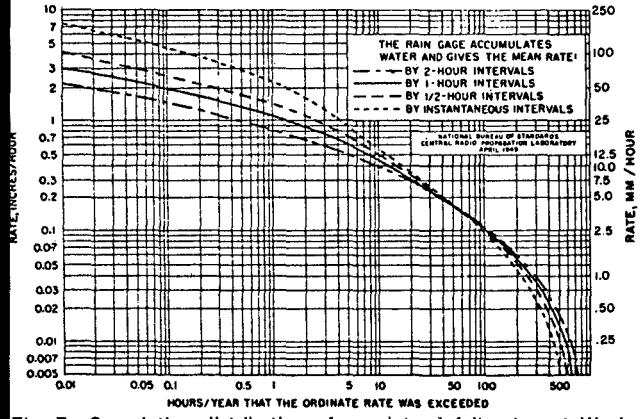

Fig. 7—Cumulative distributions for point rainfall rates at Washington, D.C. Only the one-hour curve is actually observed, the others being derived from it (Ref. 2).

Solid-state sources

The most significant change in the millimeter wave band is the recent development of solid-state oscillators which convert DC power directly into microwave and millimeter wave energy without an intermediate chain of frequency multipliers from a solid-state oscillator in the megahertz range. The first of these was the Gunn oscillator, named after the discoverer (and also called the Transferred Electron Oscillator or TEO), followed by IMPATT devices and various other avalanche diodes. Fig. 10 shows the evolution in solid state sources between 1958 and 1967. These devices have increased practically two orders of magnitude in frequency as well as in power. Thus, solid-state devices have been evolving somewhat faster than tubes. However, solid-state devices are approaching a theoretical limit for transit-time devices and new techniques may be required if much further progress is to be made.

Fig. 11 shows the state of the art, in February 1969, for various types of solid state devices. The IMPATT devices give the highest CW power output reaching about 0.5 W at 35 GHz. The next highest is a varactor Harmonic generator followed by CW GaAs transistors and tunnel diodes.

Fig. 12 compares tubes and solid-state devices. There are extensive regions in power and frequency where the microwave tube is still supreme. There are also regions where solid-state devices have completely taken over from tubes. In between, there is a region of competition where either solid-state devices or tubes may be selected depending upon the particular properties desired.

The efficiency of solid-state devices is also of importance. Fig. 13 shows the efficiency of an IMPATT oscillator as a function of frequency and for various load resistances.[8] A maximum efficiency of about 9% is indicated. Some devices have been operated at higher efficiencies. For instance, Fig. 11 shows a pulsed GaAs device with an efficiency of 29%.

Solid-state devices have higher noise levels than microwave tubes. The AM noise has been reported to be about 100 to 120 dB below the carrier level for IMPATT oscillators. The effect on receiver noise figure is shown in Fig. 14 when this oscillator is used for the local oscillator in a single-ended mixer. The noise figure is about 15 dB poorer when the IMPATT oscillator is used in place of a klystron. This difference is reduced to about 0.5 dB if a balanced mixer is used. The contribution to the noise figure due to the local oscillator can be calculated.[9] This contribution is shown in Fig. 15 as a function of the local oscillator noise temperature and the mixer suppression.

The FM noise of various oscillators is shown in Fig. 16. This shows the deviation of the carrier from its mean position to give the measured FM noise in a 1-kHz band at the indicated displacement from the carrier. It is seen that an IMPATT oscillator has about 20 dB higher FM noise than a low noise 2-cavity klystron, while that of a typical transistor multiplier chain is only slightly better than an IMPATT device. The AM and FM noise figures at kHz and 100 kHz from the carrier respectively are given in Table II. No figure is available for the AM noise from a reflex klystron, but it is probably of the order of 120 dB below the carrier. The noise content of microwave oscillators depends also upon the Q of the cavity and upon the sta-

Table II—AM and FM noise for a number of X-band oscillators.

Device	AM *noise 1-kHz band at 10 kHz from carrier (db below carrier)*	FM *noise 1-kHz band at 100 kHz from carrier (freq. deviation Hz)*
IMPATT oscillator	106	55
Gunn oscillator	117	25*
Reflex klystron		<10
2-cavity klystron	125	0.2
Transistor multiplier chain		6.7

bility of the 43 power supply. Since no information is available on the conditions under which the data of Table II was measured, the data itself must be considered only typical of what can be attained by the various devices.

It has been suggested that both AM and FM noise can be reduced by appropriate feedback circuits,[9] and some measurements have been made. The suggested circuits are shown in Fig. 17. Using an absorption type cavity as a discriminator, the FM circuit gave a 25 to 30-dB reduction in FM noise. It should be possible to apply the FM loop outside the AM loop and simultaneously reduce both AM and FM noise provided that the FM circuit did not affect the amplitude. Amplitude leveling and frequency stabilization by AFC have long been used with klystrons, and there is no reason why these techniques cannot be used with solid-state oscillators. Additional stability can be obtained by phase locking to a high stability crystal reference. Commercial circuits are available for phase-locking sources up to 40 GHz, and these should work equally well with the solid-state sources.

Receiver mixers

The recent development of GaAs Schottky Barrier diodes has made low-noise-mixer receivers possible at millimeter wavelengths. Commercially available single-ended mixers have the diode package in a wafer which is then inserted into a block containing the waveguide. A small section of the guide is contained in the wafer. A waveguide tunable short is provided, and a bias of 0.6 to 0.8 volts must be applied to the diode for optimum performance. Table III summarizes the performance of these mixers. Since noise figures for these units are similar to what can be obtained at lower frequencies, the receiver sensitivities should also be similar to those obtainable at lower frequencies.

When the local oscillator for a receiver is a solid-state Gunn or IMPATT oscillator, then balanced mixers should be used to ensure a minimum noise contribution from the local oscillator. The noise figure degradation ΔF_N due to local oscillator noise has been calculated[9] to be

$$\Delta F_N \text{ (dB)} = 10 \log\left[1 + \frac{t_{LO}\, G_c/S}{F_{IF} + 1/t_D}\right]$$

where diode noise temperature $t_D = 1.1$; IF noise figure, $F_{if} = 1.8$ (2.5 dB); and conversion gain, $G_c = 0.25$ (−6 dB). The oscillator noise ratio t_{LO} is the ratio of AM noise power—in a band (Δf)—at a frequency equal to the IF frequency off the carrier frequency to the thermal noise power in the bandwidth Δf. A plot of ΔF_N versus t_{LO} with S, the mixer noise supression ratio, as a parameter is shown in Fig. 15.

An alternative method of reducing the noise contribution from the local oscillator is to filter the local oscillator power with a high-Q band-pass filter and, at the same time, using a high intermediate frequency. In this way, the local oscillator noise content at a frequency of $f_{LO}+f_{IF}$ can be minimized. Scherer has reported satisfactory results in this way using a 120 MHz intermediate frequency.[9]

Parametric amplifiers

Another application of the Gallium Arsenide Schottky barrier diode is as a varactor in a parametric amplifier. Dickens has described a room temperature parametric amplifier giving a 3-dB noise figure, 15-dB gain over a 600-MHz band between 30.3 and 30.9 GHz.[10] It is a degenerate amplifier being pumped at 61.2 GHz with a power level of 40 mW. The noise temperature of 290°K was the combined noise temperature for the whole system, the estimated contribution from the diode alone was 110°K. It should be possible to extend this technology to an operating frequency of 100 GHz and bandwidths of 1 GHz.

Millimeter wave integrated circuits

Over the past number of years, a considerable amount of effort has been expended by various laboratories on the development of integrated microwave circuits in the frequency range below 10 GHz. Some of this effort has spilled over into the frequency range above 10 GHz as evidenced by recent papers by Battershall [11], Mehal[12], and Mao [13]. Battershall describes a phase shifter for operation between 15.5 and 17.2 GHz; Mehal describes the frabrication of active devices on a GaAs substrate for operation with a 94 GHz system; and Mao describes circuit design and testing techniques for the 94 GHz system.

The technique is to use a single crystal GaAs chip 0.004-inch thick as a substrate. When properly processed, the material has a conductivity low enough so that losses are small. At 94 GHz, the dimensions of the chip are very small, (0.03 × 0.03 inch for a complete balanced mixer), so that very little GaAs is required. In addition, a GaAs substrate has the advantage that active elements can be fabricated right on the substrate. The microstrip conductors and circuits are deposited at an appropriate point in the process. The active elements fabricated were a Schottky barrier diodes used in both a single-ended and balanced mixer configuration, and a Gunn oscillator

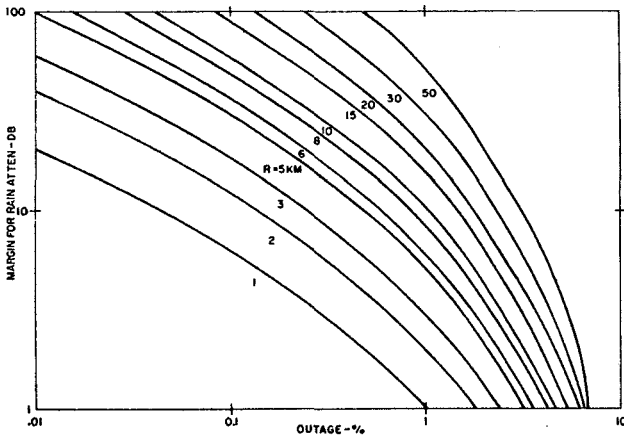

Fig. 8—The power margin for a 35-GHz communication link required to ensure a specified maximum outage time, due to rain, as a function of path length. (Ref. 3).

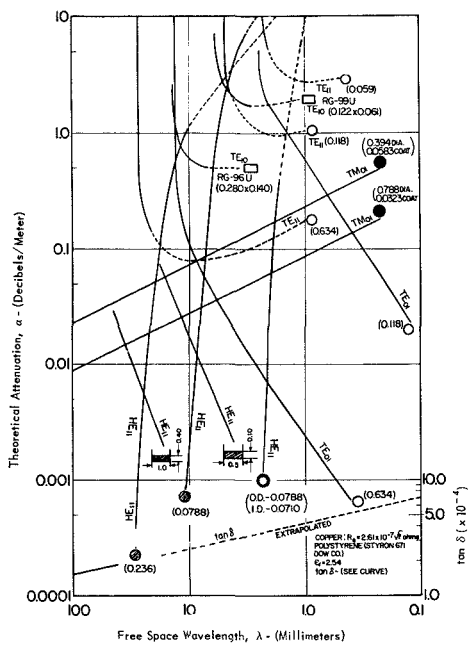

Fig. 9—Comparison of the theoretical attenuation characteristics of waveguide suitable for millimeter wavelength applications (Ref. 14).

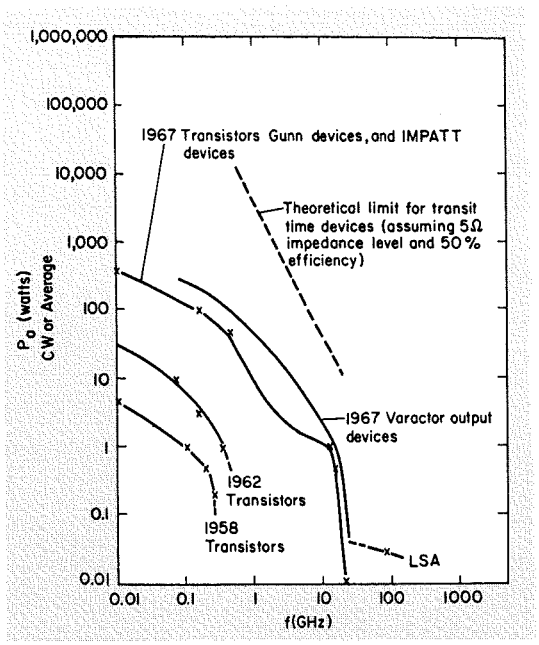

Fig. 10—Evoluation of microwave solid state power generators: 1958-1967 (Ref. 5).

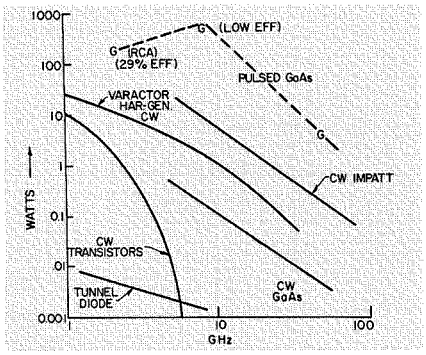

Fig. 11—State-of-the-art (1968) in solid-state power generators of various types (Ref. 19).

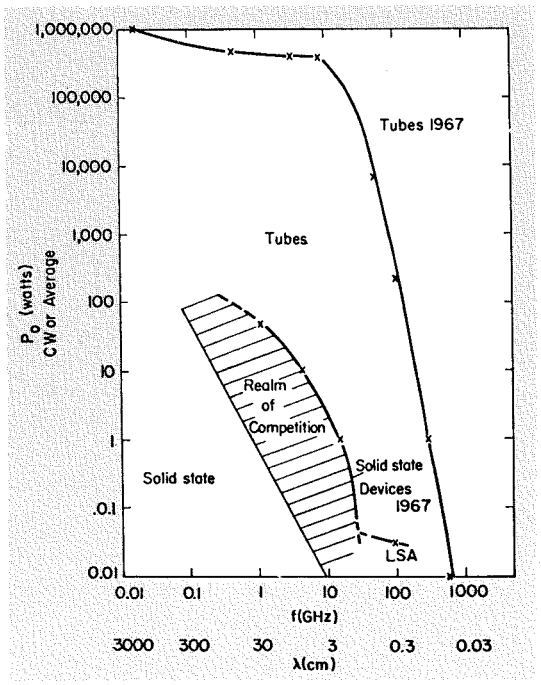

Fig. 12—Comparison of microwave power generators: 1967 (Ref. 5).

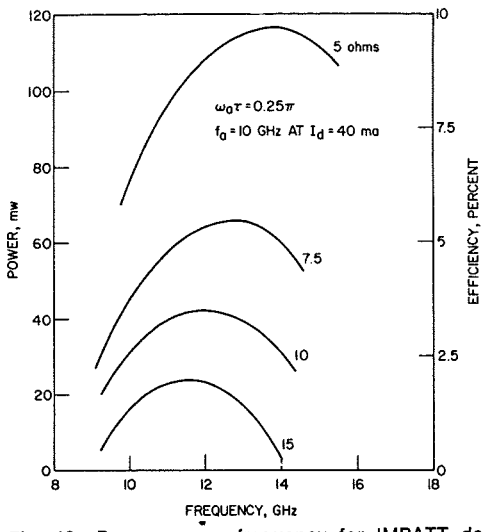

Fig. 13—Power versus frequency for IMPATT devices with fixed load resistance (Ref. 8).

for 30 GHz complete with deposited resonant structure.

While millimeter wave integrated circuits are still in a very rudimentary stage enough work has been done to indicate the possibility of further development.

Applications

Terrestrial communication networks

A very promising way of relaying messages from point to point is using Te_{01} mode in circular waveguide. By filling the waveguide by a suitable gas the loss due to the gas, can be kept to a minimum. In such a transmission line system, the radiation would be propagated in specially constructed circular waveguide consisting of a spirally wound conductor. The individual turns are non-contacting being separated by an absorbing media. The desired mode, having only circumferential wall currents, passes down the pipe with very low loss while other modes, with longitudinal wall currents, are highly attenuated.

The Bell Telephone laboratories are considering such a system operating between 40 and 115 GHz. This bandwidth is capable of accommodating 80 to 100 channels of 300 megabits each. With 75 GHz of usable bandwidth, the system would handle the growth in traffic for many years to come, and a major problem is providing economic justification to construct the system in the first place.

An alternative to a transmission-line system is free-space propagation along a line of repeater stations. As seen from Fig. 8, the margin at 35 GHz required to provide an acceptably low outage time due to rain for a link in the Washington area becomes excessive for path lengths of only a few kilometers. Thus a millimeter-wave relay system would be faced with repeaters spaced every few kilometers. An alternate approach being considered by the Bell Telephone Laboratories would be to provide redundant paths separated by a few kilometers. The reasoning is that the heavy rain rates require the very high power margins are confined to local storm centers. Thus when one of the paths is experiencing high attenuation, the alternate path will most probably have a much lower attenuation. The message would be routed by the path providing the lowest attenuation. By carefully selecting the system parameters, it may be possible to provide a system with the same percentage outage time with a fewer number of repeaters and lower overall cost than for a single line of non-redundant repeaters.

Synchronous satellite to ground

Although the number of synchronous satellites in orbit is still very small, the problem of traffic congestion in this facility is already being considered. This is because there is a very definite upper limit to the number of satellites that can be placed in synchronous orbit. The number is determined primarily by the ability of the ground stations to discriminate against radiation from adjacent satellites operating in the same frequency band. The minimum spacing between satellites is of the order of 3° to 3.5° but this might be reduced somewhat by careful ground station antenna design.

With a definite upper limit to the total number of channels in any one frequency band, the eventual need for other frequency bands is apparent. The frequencies suggested are 12 and 18 GHz with eventual use of 35 GHz. Examination of Fig. 3 shows that attenuation through the atmosphere increases rapidly with increasing angle from the vertical. At 35 GHz (8.6 mm), there is a 3-dB loss at 63° from the vertical with only 4 mm/hr rain rate. Since ground stations over most of Canada and all of Alaska have beam angles more than 63° from the vertical, the loss will be generally more than 3 dB any time it rains. This

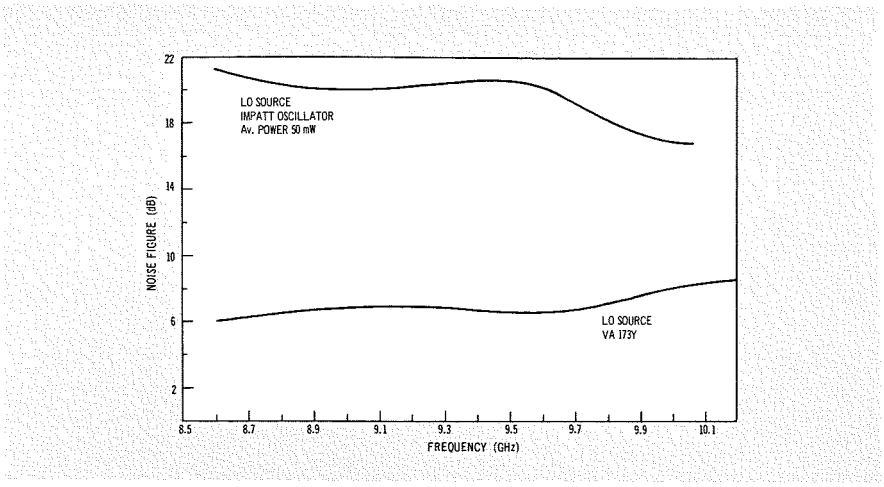

Fig. 14—The noise figure of a single-ended mixer showing the noise contribution of an IMPATT local oscillator compared to a klystron local oscillator.

Table III—Single-ended-mixer performance using Schottky barrier diodes.

Waveguide band	Waveguide RF bandwidth (GHz)	(GHz)	Conversion loss (dB) typical	max.	Noise ratio typical	max.	*Noise figure (dB) typical	max.
RG-96	26.5-40	4	5.5	7.0	1.2	1.3	6.1	7.9
RG-97	33-50	4	6.0	7.5	1.2	1.3	6.6	8.5
RG-98	50-75	5	6.5	8.0	1.2	1.4	7.1	9.3
RG-99	60-90	6	7.5	9.0	1.2	1.4	8.2	10.3
WR-10	75-110	7	8.5	10.0	1.2	1.5	9.2	11.6

*Calculated from $NF = tr(L_c - 1) + 1$ where tr is the noise ratio and L_c is the conversion loss ratio.

imposes a severe penalty on the satellite design and frequencies of 35 GHz or higher may prove unsatisfactory for any northern area.

Systems providing freedom from interference

The high attenuation of the atmosphere for millimeter waves can be used to advantage to prevent interference or cross talk between nearby systems using the same frequency. In the military sense, it provides freedom from interception or jamming of sensitive communications. Over short path lengths, communications can be established in the vicinity of 60 GHz wher air absorption is very high (up to 14 dB/km). With this high attenuation rate, the signal quickly attenuated beyond the receiving station allowing the spectrum to be reused for other message service in another part of the metropolitan area.

Another possible application of this principle is in communications between high flying aircraft or between two spacecraft without any danger of interference with ground-based systems using the same frequency.

Antenna sizes at millimeter wavelengths are generally smaller than at longer wavelengths. This allows more freedom on the part of the antenna designer to provide narrower beam widths, lower side lobes, or both. In this way, some additional isolation can be obtained between nearby systems as compared to lower frequencies.

References

1. Bell Telephone Laboratories advertisement, *Microwave Journal,* Vol. 10, No. 12 (Nov 1967) p. 124.
2. Bussey, H. E., "Microwave Attenuation Statistics Estimated From Rainfall and Water Vapour Statistics" *Proc. IRE,* Vol. 38 (1950) p. 781-785.
3. Tsao, et al, "Design of Millimeter Communication System" *Microwave Journal* (Nov 1968) p. 47.
4. Forster, D. C., "High Power Sources at Millimeter Wavelengths" *Proc. IEEE* Vol. 54 (Apr 1966) pp. 532-539.
5. Osepchuk, J. M., "Towards A Renaissance in Microwave Tubes" *Microwave Journal* Vol. 10, No. 10 (Sep 1967) p. 18.
6. Kulke, B., "Millimeter Wave Generation With Electron Beam Devices", NASA Technical Note NASA TM D-3727.
7. Hirshfield, J. L., and Wachtel, I. M., "Electron Cyclotron Maser" *Phys. Rev. Letters* Vol. 12, (1964) p. 533-536.
8. Evans, W. J. and Haddad, G. I., "Power and Efficiency of Impatt Oscillators" *1968 GMTT International Symposium Digest* (May 1968) p. 54.
9. Scherer, E. F., "Circuit Techniques for Noise Reduction and Frequency Stabilization of Avalanche Diode Oscillators" *1968 G-MTT International Symposium Digest* (May 1968) p. 63.
10. Dickens, L. E., "A Ka Band Paramplifier Using Planar Varactors" *1968 G-MTT Symposium Digest* (May 1968) p. 164.
11. Battershall, B. W., and Emmons S. P., "Optimization of Diode Structure For Monolithic Integrated Microwave Circuits" *IEEE Journal Solid State Circuits* Vol. SC-3 (Jun 1968) p. 107.
12. Mehal, E. W. and Wacker, R. W., "GaAs Integrated Microwave Circuits" *IEEE Journal of Solid State Circuits* Vol. SC-3 (Jun 1968) p. 113.
13. Mao, S., Jones, S., and Vendelin, C. D., "Millimeter Wave Integrated Circuits" *IEEE Journal of Solid State Circuits* Vol. SC-3 (Jun 1968) p. 117.
14. Coleman, P. D. and Becker, R. C., "Present State of the Millimeter Wave Generation and Technique Art—1958" *IRE Trans.* MTT-7 (1959) p. 42.
15. Rosenblum, E. S. "Radiation Absorption of 10-400 GHz Radiation" *Microwave Journal* Vol. 4 (Mar 1961) p. 91.
16. Rogers, T. F., "Factors Effecting the Width and Shape of Atmospheric Microwave Absorption Lines," Air Force Cambridge Res. Center, Mass. (Oct. 1951).
17. Weger, E., "Apparent Thermal Noise Temperatures in the Microwave Region," *IRE Trans* AP-8 (Mar 1960) p. 213-217.
18. Ryde, J. W. and Ryde, D., "Attenuation of Centimeter and Millimeter Waves by Rain, Hail, Fog and Clouds," GEC Reports No. 8670 (May 1945) No. 7831 (Oct 1941), No. 8516 (Aug 1944).
19. Hines, M. E. "Network Integration Approaches for Multiple-Diode High Power Microwave Generation" *G-MTT Symposium Record,* Detroit, (May 1968) p. 46.

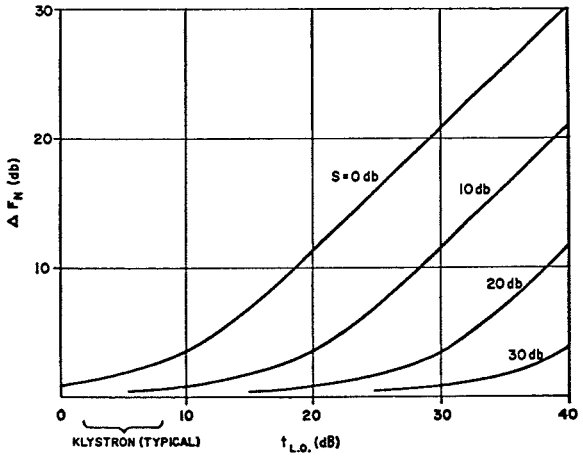

Fig. 15—Mixer noise figure degredation due to local oscillator noise contribution with mixer suppression as a parameter (Ref. 9).

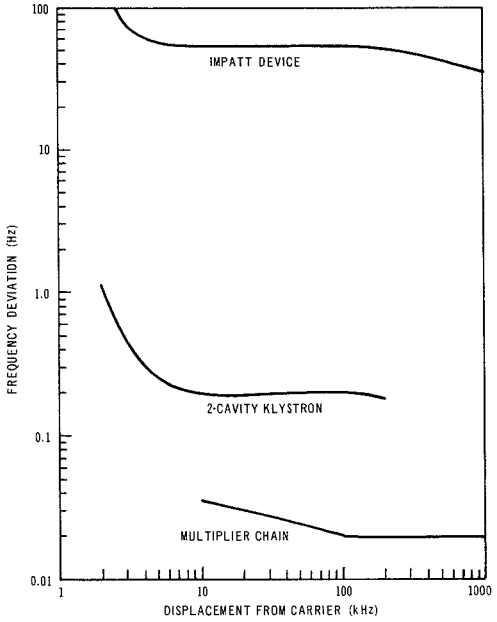

Fig. 16—Typical FM noise for various oscillators measured in a 1-kHz bandwidth.

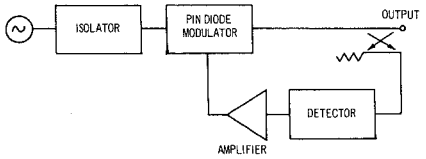

Fig. 17a)—Block diagram of AM noise reduction circuit (Ref. 9).

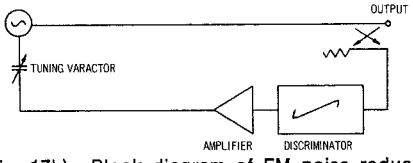

Fig. 17b)—Block diagram of FM noise reduction circuit (Ref. 9).

Modern optics

Dr. A. M. Sutton | C. F. Panati

This article presents a simplified portion of the material normally given in a five-day seminar on Modern Optics* by the RCA Institutes. It demonstrates the manipulative ease of the modern approach to optical problems.

THE ADVENT OF THE laser and the hologram has added new significance to the science of optics. The wealth of new and diverse applications has made it imperative that many scientists and engineers acquire a sound knowledge of this field.

Traditionally, the study of optics has been divided three ways: physics of light, geometrical optics, and physical optics. The tremendous advances of the past decade have led to significant changes in points-of-view. Consequently, the content of optics has been restructured—again into three areas of study: quantum electronics, matrix optics, and Fourier optics.

Each of these contemporary divisions has a huge literature, but is served somewhat unevenly by texts and treatises. This has been most acutely felt in the area of matrix optics. The Institute for Professional Development has attempted to communicate the new matrix methods through a five-day seminar entitled *Modern Optics.*

This seminar is supported by an extensive text written by the authors. The course begins with a matrix review covering some familiar topics, such as eigenvalues and eigenvectors, and some less familiar topics, such as traces and Kronecker products. With these tools, a full-scale treatment of polarization is started. This is done in terms of the Jones-Mueller calculus, the Poincare sphere, and the Stokes parameters. This material covers the first day and a half of the course. The remaining three and a half days are devoted to the analysis and design of general optical systems. Well over 100 problems are posed and solved in the course of the week. These problems show, to full practical advantage, the power and utility of the matrix-vector machinery. While the primary aim of the course is to communicate tools of an advanced practical nature, the course is carefully designed to be consistent with the underlying physics.

Physically what is done is the following: vector photons are considered, and the machinery for handling their polarization is developed. Then the amplitude of their associated quantized waves is studied. Spin and amplitude are then stripped away to leave only the position and momentum of a classical scalar photon. Its propagation through an optical system is then studied in great detail.

It is emphasized throughout the text that it is particles that are being studied and not "rays." In fact, the theory carries over unchanged to electron optics. This model is more akin to physical reality than the traditional approach, and the formulas of geometrical optics take on additional meaning in terms of impulse and momentum. Finally, the course shows how Fourier optics arises as a consequence of quantizing this particle set-up.

The direct method

The Direct Method is the modern approach to tracing photons through optical systems. It is so named because it represents the *direct* use of Snell's law via matrix algebra. It represents an extension into optics of an input-output philosophy. Specifically, it is indebted to the A,B,C,D formalism for electrical two-ports, and to the S-matrix of quantum mechanics. It is especially advantageous for optical systems that are rotational symmetric.

The basic idea of the Direct Method is to follow the motion of a photon through an optical system. As indicated in Fig. 1, we choose an input plane, labeled X_s. The photon pierces this plane to yield a position vector **X** and momentum vector **P** as shown. Of course, this input plane is a mathe-

Reprint RE-15-3-9
Final manuscript received May 22, 1969.
*Since this article was written, the title of the seminar had been changed to *Optical Systems Engineering.*

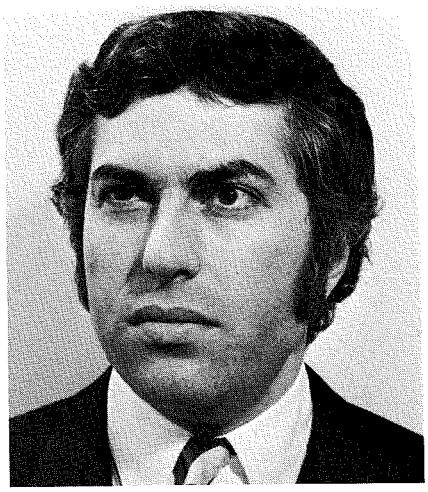

Dr. Albert M. Sutton†
RCA Institutes
New York, N.Y.
received the AB in Mathematics from Harvard College and the PhD in Theoretical Physics from Yeshiva University. He is well known for his fundamental work on spinning particles and is co-author of RCA Institutes' texts, *Digital Communications* and *Modern Optics.* He is presently a member of the RCA Institutes and Leader of the Technical Staff in the area of Optics.

†Since writing this article, Dr. Sutton has left RCA.

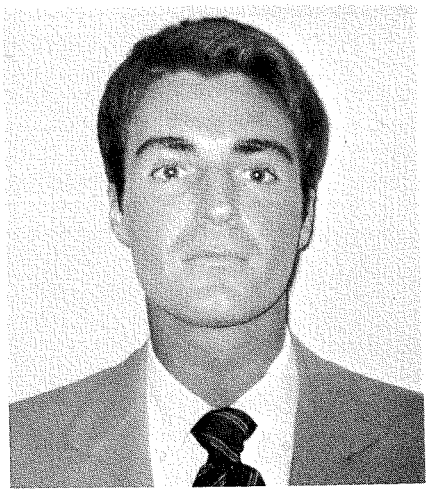

Charles F. Panati
RCA Institutes
New York, N.Y.
received the BS in Physics from Villanova University in 1965. The following year, he received the MS in Physics from Columbia University. For one year, he served as Radiation Physicist to the Columbia Presbyterian Medical Center. Mr. Panati has been a member of the Technical Staff of RCA Institutes since 1967. He is co-author of RCA's texts. *Digital Communications* and *Modern Optics* He is presently Leader of the Technical Staff in the area of Communications.

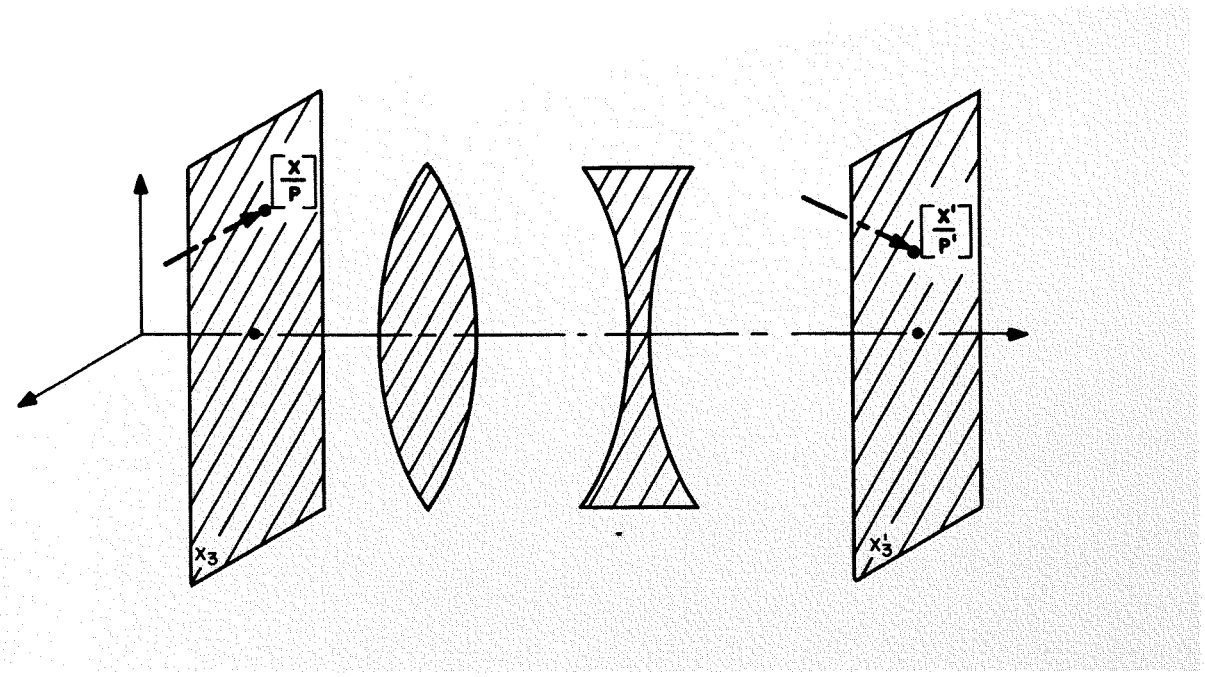

Fig. 1—Transmission through a hypothetical optical system.

matical artifice and may be selected at any convenient location along the optical axis. After leaving this plane, it undergoes a sequence of simple transformations. The nature of these transformations is evident by considering the motion of the photon as it moves down the system. While in a medium of homogeneous index, it executes free particle motion, traveling along in the direction of its momentum. Ultimately, it encounters a discontinuity in the refractive index, for example, when it passes from air to glass. Physically this corresponds to an impulsive force which, by Newton's second law, leads to a change in its momentum. Quantitatively, this change is given by Snell's law.

This primitive operation of refraction may be summarized by a *refraction matrix*. After the refraction has taken place, the particle propagates freely in the new medium, translating along the direction of its new momentum until it hits the next surface. This primitive translation operation may be summarized by a *translation matrix*. After performing the necessary physical refractions and translations, we may carry the photon to a conveniently located mathematical output plane. This yields final position and momentum vectors $\mathbf{X}'$ and $\mathbf{P}'$ as shown.

Thus, we have made plausible that the transformation from any desired input plane to any desired output plane may be written as a cascade of primitive transformations: translate, refract, etc.

System matrices

The preceding paragraphs have stressed the three-dimensional aspects of the position and momentum vectors $\mathbf{X}$ and $\mathbf{P}$. However, this is somewhat redundant. The reason is that as soon as the position of the input plane is specified, we automatically know the X_3 component of the photon position. Thus, only the *transverse* components X_i, $i=1, 2$ need be specified.

A similar conclusion holds for momentum. It may be shown that the momentum of a photon, in appropriate units, may be written as:

$$\mathbf{P}=nL_1\mathbf{i}+nL_2\mathbf{j}+nL_3\mathbf{k} \qquad (1)$$

where n is the index of refraction and L_1, L_2, and L_3 are direction cosines. From this equation, it is clear that $\mathbf{P}^2=n^2$. This may be solved for P_3 to obtain

$$P_3=\pm\sqrt{n^2-(P_1^2+P_2^2)} \qquad (2)$$

Again, we conclude that knowledge of the *transverse* momentum components P_i, $i=1, 2$ suffices. The matrix machinery operates in terms of these transverse position and momentum components.

In terms of these components, the input-output relation enjoys the simple form

$$\begin{bmatrix} X_i' \\ P_i' \end{bmatrix}_{X'_3} = \begin{bmatrix} A & B \\ C & D \end{bmatrix}_{X'_3 X_3} \begin{bmatrix} X_i \\ P_i \end{bmatrix}_{X_3} \qquad (3)$$

Notice a remarkable feature of Eq. 3—it is valid for *either* transverse component, since the A, B, C, D coefficients are independent of which transverse coordinates we choose to look at. For this reason, we may drop the subscript i. Thus, the system matrix which carries the photon from input plane X_3 to output plane X_3' is

$$X'_3S_{X_3} = \begin{bmatrix} A & B \\ C & D \end{bmatrix}_{X'_3 X_3} \qquad (4)$$

Let this be followed by a second transformation from X_3' to X_3'' whose system matrix is

$$X''_3S_{X'_3} = \begin{bmatrix} E & F \\ G & H \end{bmatrix}_{X''_3 X'_3} \qquad (5)$$

Then the transformation of the cascade is

$$X''_3S_{X_3} = X''_3S_{X_3}X'_3S_{X_3} \qquad (6)$$

Thus, the initial and final transverse components are related by

$$\begin{bmatrix} X'' \\ P'' \end{bmatrix}_{X''_3} = \begin{bmatrix} E & F \\ G & H \end{bmatrix}_{X''_3 X'_3} \begin{bmatrix} A & B \\ C & D \end{bmatrix}_{X'_3 X_3} \begin{bmatrix} X \\ P \end{bmatrix}_{X_3} \qquad (7)$$

Gaussian approximation

One might believe that A, B, C, D coefficients are merely functions of the construction parameters of the system, that is, the indices or refraction, radii

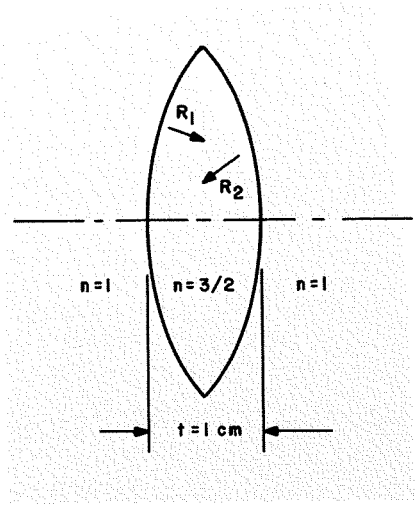

Fig. 2—Convex lens in air.

of curvature, and the inter-vertex separations. However, when the above formalism is applied to concrete examples, a disagreeable fact emerges: the matrix elements are not only dependent upon the construction parameters of the system but also on the input vector $\begin{bmatrix} X \\ P \end{bmatrix}$. To dispose of the non-linearity, we may expand the A, B, C, D coefficients in a MacLaurin series. Taking the lowest order approximation yields Gaussian optics. In this approximation, the general input-output relation becomes

$$\begin{bmatrix} X' \\ P' \end{bmatrix}_{x'_3} = \begin{bmatrix} a & b \\ c & d \end{bmatrix}_{x'_3 x_3} \begin{bmatrix} X \\ P \end{bmatrix}_{x_3} \qquad (8)$$

where a,b,c,d are *constants* depending only on the system's construction parameters.

For example, the translation matrix in the Gaussian approximation is simply

$$T = \begin{bmatrix} 1 & \frac{t}{n} \\ 0 & 1 \end{bmatrix} \qquad (9)$$

This matrix is basically the identity matrix except for an appropriate entry in the *translation slot*. The entry is t/n, where t is the longitudional distance translated, and n is the index of the medium in which the photon is translating. The quantity t/n is called a *reduced* length and will be denoted as z.

The refraction matrix in the Gaussian approximation is simply

$$R = \begin{bmatrix} 1 & 0 \\ \frac{n-n'}{R} & 1 \end{bmatrix} \qquad (10)$$

Note that it too is basically the identity matrix except for an appropriate entry in the *refraction slot*. The entry is $\frac{n-n'}{R}$, where n *and* n' are the indices of the media to the left and right of the refracting surface, and R is its radius of curvature. The quantity $\frac{n-n'}{R}$ is called the *negpower* of the surface. It is the negative of the conventional power.

Some examples

Example 1

For the first example, consider a convex lens in air. Let us compute the system matrix carrying a photon from a plane tangent to the first surface of this lens to the plane tangent to the second surface. The lens has the following specifications: $R_1 = 1\text{cm}, R_2 = -1\text{cm}$, vertex separation $t = 1\text{cm}$, and refractive index $n = 3/2$ (see Fig. 2).

The matrix for the cascade involves a refraction, followed by a translation, followed by another refraction:

$$\begin{bmatrix} 1 & 0 \\ \frac{3/2-1}{1} & 1 \end{bmatrix} \begin{bmatrix} 1 & \frac{1}{3/2} \\ 0 & 1 \end{bmatrix} \begin{bmatrix} 1 & 0 \\ \frac{1-3/2}{1} & 1 \end{bmatrix}$$

Thus, the system matrix is

$$\begin{bmatrix} 2/3 & 2/3 \\ -5/6 & 2/3 \end{bmatrix}$$

Example 2

Let us compute the system matrix for the preceding lens where the vertex separation is zero. The matrix for the cascade is

$$\begin{bmatrix} 1 & 0 \\ -1/2 & 1 \end{bmatrix} \begin{bmatrix} 1 & 0 \\ 0 & 1 \end{bmatrix} \begin{bmatrix} 1 & 0 \\ -1/2 & 1 \end{bmatrix}$$

Thus the system matrix is

$$\begin{bmatrix} 1 & 0 \\ -1 & 1 \end{bmatrix}$$

Note that the resultant c coefficient is merely the sum of the c coefficients of the constitutent surfaces. This corresponds to the fact that the powers of thin lenses are additive.

Example 3

A concave lens operates in air; its specifications are $R_1 = -1\text{cm}$, $R_2 = 1\text{cm}$, vertex separation $t = 1\text{cm}$, and refractive index $n = 3/2$. Compute the system matrix carrying a photon from a plane tangent to the first surface to the plane tangent to the second surface. We leave the detailed calculation to the reader. The resulting system matrix is

$$\begin{bmatrix} 4/3 & 2/3 \\ 7/6 & 4/3 \end{bmatrix}$$

Focusing and magnification

Once one is in possession of the system matrix, a number of important system parameters may be immediately read off. These include focusing properties, magnifications, and the locations of the various cardinal planes.

Consider the following picture.

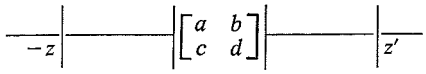

The a,b,c,d matrix operates as a black box between the planes indicated. An object is placed at a reduced distance $-z$ to the left of the input plane of the instrument, and its image is studied on a plane located a reduced distance z' to the right of the final plane of the instrument. Therefore the object-to-image system matrix is obtained by translating from $-z$ to the input plane, passing through the instrument via the a,b,c,d matrix, and then translating to z':

$${}_{z'}S_z = \begin{bmatrix} 1 & z' \\ 0 & 1 \end{bmatrix} \begin{bmatrix} a & b \\ c & d \end{bmatrix} \begin{bmatrix} 1 & -z \\ 0 & 1 \end{bmatrix} \qquad (11)$$

Therefore

$$\begin{bmatrix} X' \\ P' \end{bmatrix}_{z'} = \qquad (12)$$

$$\begin{bmatrix} a+cz' & -az+b-czz'+dz' \\ c & -cz+d \end{bmatrix}_{z'z} \begin{bmatrix} X \\ P \end{bmatrix}_z$$

We will now investigate focusing. Let a point source at z broadcast a bundle of photons. Then X is a fixed number, and P is variable. If this bundle is to reunite to form a focused image, we must obtain a unique X' for each X. This means that X' must be independent of the momentum of any particular photon in the emitted bundle. This can happen only if the b coefficient is zero; that is,

$$-az+b-czz'+dz' = 0 \qquad (13)$$

which may be solved for z' to yield the Focusing Equation

$$z' = -\frac{-az+b}{-cz+d} \qquad (14)$$

This yields the well-known equations of Newton and Gauss as special cases.

When the system is focused, the a coefficient by definition gives the magnification. Therefore

$$m=a+cz' \qquad (15)$$

or using the Focusing Equation (Eq. 14)

$$m=\frac{1}{-cz+d} \qquad (16)$$

Principal planes

It is an easy task to determine the location of the principal planes and the focal planes in terms of the a,b,c,d coefficients.

By definition, the principal planes H and H' are conjugate planes with a magnification of unity. Setting $m=1$ in Eq. 16 yields

$$z_H=\frac{d-1}{c} \qquad (17)$$

Inserting this value into the Focusing Equation (Eq. 14) yields

$$z_{H'}=-\frac{a-1}{c} \qquad (18)$$

Recall that the system matrix for our first example was

$$\begin{bmatrix} a & b \\ c & d \end{bmatrix} = \begin{bmatrix} \frac{2}{3} & \frac{2}{3} \\ -\frac{5}{6} & \frac{2}{3} \end{bmatrix}$$

Therefore the principal planes of this thick lens are located at $z_H=2/5$ cm and $z_{H'}=-2/5$ cm.

Thus, the principal planes lie inside the lens 2/5 cm to the right and left of the first and second surface respectively.

Focal planes

Location of the focal planes is equally simple. An object placed at the object-side focal point will have its focused image appearing at infinity. Thus the denominator of the Focusing Equation (Eq. 14) must vanish. Therefore

$$z_F=d/c \qquad (19)$$

The image-side focal point is the location of the focused image of an object placed infinitely far away. Again from the Focusing Equation,

$$z_{F'}=-\frac{a}{c} \qquad (20)$$

For our first example, the location of the object-side and image-side focal planes is $z_F=-4/5$ cm and $z'_F=+4/5$ cm.

Thus, the focal points lie 4/5 cm to the left of and to right of the first and second surfaces respectively.

The focal length of a system, by definition, is the distance between the principal and focal planes. This yields input and output focal lengths, f and f', given simply by $f=1/c$ and $f'=-1/c$.

For the example we have been considering, the focal lengths are $f=-1\frac{1}{5}$ cm and $f'=1\frac{1}{5}$ cm.

It is equally straightforward to obtain the location of the nodal points, anti-principal points and anti-nodal points of a system. They all follow simply from the matrix:

$$\begin{bmatrix} a & b \\ c & d \end{bmatrix}$$

Telescope problem

We wish to display the working of the above machinery by means of a simple but non-trivial problem:

1) Find the matrix for a system operating between its focal points, denoted ${}_{F'}S_F$.
2) Consider two systems, each referred to their focal points, with the image-side focal point of the first coincident with the object-side focal point of the second. Find the ${}_{F'2}S_{F_1}$ matrix of the cascade. Is the system focused?
3) What is the negpower of the instrument? Where are the focal and principal planes located?
4) What is the momentum magnification? Is the instrument erecting or inverting?
5) What is the position magnification? How is it related to the momentum magnification?
6) Write the Focusing Equation for this instrument.
7) How would you design a constant magnification photographic enlarger?

In answer to the above questions:

1) With respect to some pair of prior planes, the instrument is described by a matrix:

$$\begin{bmatrix} a & b \\ c & d \end{bmatrix}.$$

Shifting the input and output planes to z and z' yields.

$${}_{z'}S_z=\begin{bmatrix} a+cz' & -az+b-czz'+dz' \\ c & -cz+d \end{bmatrix}_{z'}^{z}$$

Letting $z=z_F=d/c$ and $z'=z_{F'}=-a/c$, the system matrix operating between focal planes is

$${}_{F'}S_F=\begin{bmatrix} 0 & -1/c \\ c & 0 \end{bmatrix}$$

2) ${}_{F'2}S_{F_1}=\begin{bmatrix} 0 & -1/c_2 \\ c_2 & 0 \end{bmatrix}_{F'_2}\begin{bmatrix} 0 & -1/c_1 \\ c_1 & 0 \end{bmatrix}_{F_1}$

$$=\begin{bmatrix} c_1/c_2 & 0 \\ 0 & -c_2/c_1 \end{bmatrix}$$

Note that the system is focused since the b coefficient is zero.
3) Since the c coefficient is zero, the focal lengths are infinite. The system is then said to be afocal or telescopic. From the formulas for the principal (Eqs. 17 and 18) and focal (Eq. 14) planes, we see that these planes are located at infinity.
4) The momentum magnification is $-c_2/c_1$. In terms of focal lengths, this becomes f_1/f_2' or f_1'/f_2. When used with the eye, momentum magnification is equivalent to the magnifying power of the instrument. The instrument is clearly erecting or inverting depending upon the relative sign of the focal lengths or negpowers. An erecting instrument requires an opposite relative sign. This may be achieved by a convex lens followed by a concave lens to yield a Galilean Telescope. An erecting instrument may also be obtained by concave followed by a convex lens. Why is this system not practical?
An inverting system may be achieved with two convex lenses to yield the well-known astronomical telescope. However, two concave lenses would also work. Why is this solution not practical?
5) The position magnification is clearly $-c_1/c_2$. In terms of focal lengths, $m=f_2'/f_1$ or f_2/f_1'. The essential point to remember is that it is the reciprocal of the magnifying power.
6) The Focusing Equation for this instrument is

$$z'=\left(\frac{c_1}{c_2}\right)^2 z$$

Thus $z'=\left(\frac{1}{M.P.}\right)^2 z$, where M.P. is the magnifying power.
7) Recall that the magnification is

$$m=\frac{1}{-cz+d}$$

For a telescope $c=0$. Therefore

$$m=\frac{1}{d}$$

which is a constant quite independent of the location of the object. Thus a constant magnification photographic enlarger is a telescope used backwards between finite conjugates.

Reference

Sutton, A. M. and Panatti, C. F., *Modern Optics*. The Institute for Professional Development, RCA Institutes, Inc.

Developing air-vac Si-Ge thermoelectric technology and applications

R. E. Berlin | L. H. Gnau | R. S. Nelson

Thermoelectric power supplies which convert thermal energy directly into electrical energy are gaining greater acceptance for both the sophisticated missions planned by NASA and the DoD for the 1970's and as the workhorse devices for oceanographic and terrestrial applications. Silicon-germanium (Si-Ge) thermoelectrics developed by RCA are strong competitors for these applications. Si-Ge thermoelectric material has been fabricated into a variety of thermocouple configurations depending on the device applications, its available heat source, and the environmental conditions. The air-vac thermocouple, so-called because of its capability to operate in either air or vacuum environment over the full temperature range of the material, has emerged as the most promising concept and is presently receiving extensive developmental support.

THE AIR-VAC THERMOCOUPLE, shown in Fig. 1, takes full advantage of the high-temperature capability and excellent mechanical properties of Si-Ge. The thermocouple operates by radiation heat transfer from a heat source to the heat acceptor plate, or *hot shoe*, which is an alloy of silicon and molybdenum. The two active thermoelements, or legs, of the themocouple are made of suitably doped Si-Ge material and are joined to the hot shoe at the hot junction. Because the hot shoe has a higher thermal conductivity than the Si-Ge thermoelectrics, the radiant thermal energy received at the shoe at a relatively low flux density is concentrated for processing through the active element legs at a much higher thermal flux density. This procedure results in a volume and, therefore, a weight saving.

The thermocouple assemblies are supported in cantilever fashion from the cold end and require no other mechanical structure. The electrical connection at the hot end of each thermocouple is made through the hot-shoe material, which is suitably doped for low resistivity. Each thermocouple must be electrically isolated from the baseplate or radiator structure, and, at the same time, must have good thermal contact between each cold junction and the baseplate (see Fig. 2). These goals are accomplished by a very thin ceramic disk in the "stack" assembly between each thermocouple cold junction and the baseplate. Cold-end electrical interconnections are terminated in this same stack structure.

Two different techniques are presently used to attach the air-vac couple to the baseplate—metallurgical bonding and mechanical attachment. In the former case, as shown in Fig. 2a, the couples with stress isolators are metallurgically bonded to a rigid baseplate. In the mechanical attachment, or fleximod technique, as shown in Fig. 2b, the air-vac couple is bonded to a mount stud, which is subsequently mechanically attached to the baseplate. The key features of the fleximod are the high degree of stress isolation between couples, the wide range of possible configurations, and ease of fabrication.

Fibrous thermal insulation is fitted into the void areas between couples to minimize thermal shunt losses.

Advantages of the air-vac concept

System integration

The air-vac concept permits the design of complete converters which allow for easy insertion and removal of the uncoupled heat source and can be used with a wide range of heat-source designs. The fleximod approach, furthermore, permits a wide range of converter configurations and ease of assembly. In providing for a small building-block structure, the problems associated with maintaining process control are reduced.

Reprint RE-15-3-7 (ST-3916)
Final manuscript received May 21, 1969.

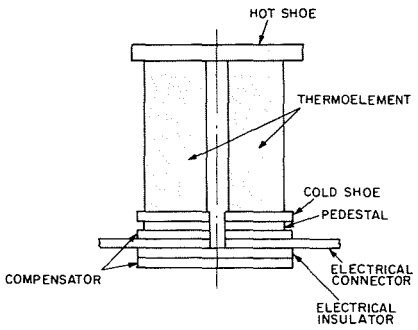

Fig. 1—Air-vac thermocouple

Mechanical integrity

The free hot-plate suspension reduces module design complexity with respect to thermal and mechanical stresses. Furthermore, because of the low weight of the materials used in the thermocouple, the configuration has a relatively low moment of inertia and thus excellent resistance to mechanical shock and vibration. A high degree of stress isolation between couples is achieved by the highly flexible electrical interconnectious.

Environmental capability

The silicon alloys and other materials in the thermocouple structure which are insensitive to the environment allow for fabrication of converters which do not require any encapsulation or substructure to protect them from air or space conditions. No vaporization or sublimation is experienced over the temperature range of operation.

Thermal transformation and transmission

As previously noted, the thermal flux concentration capability of the hot shoe permits coupling to heat sources with low thermal flux density and the ability to optimize couples with respect to weight, volume, and mechanical strength. Another benefit of coupling the heat source to the thermocouples at a low thermal flux is that the ΔT loss is minimized across the radiation path. In addition, an improved thermal transmission coefficient is achieved with the air-vac because losses are minimized. High conversion efficiencies over the full range of heat source temperatures can thus be achieved.

Electrical isolation

The design of generators with practical voltage levels requires that considerable attention be paid to electrical isolation. In systems conductively coupled to the heat source, the thermoelectric

Robert E. Berlin, Mgr.
Thermoelectric Technology Department
Industrial Tube Division
Electronic Components
Harrison, N.J.

received the BSME from the City College of New York in 1956, and the MS in Engineering Science from Rensselaer Polytechnic Institute in 1959. He is presently studying for the PhD in Industrial Engineering at New York University. Mr. Berlin joined the CANEL project of Pratt and Whitney Aircraft in 1956 where he was employed as a Senior Analytical Engineer on the structural design and analysis of high temperature nuclear reactors. In 1960, he joined the New York Office of the AEC where he held successively the positions of Project Engineer, Branch Chief, and, ultimately, Director of the SNAP Program division which was responsible for the technical, contractual, and business management of the AEC-supported SNAP isotope programs. Mr. Berlin joined Thermoelectric Products Engineering at RCA in 1966 and is currently Manager of Thermoelectric Technology Development. He is responsible for advanced thermoelectric technology and new products development. The major program presently under his supervision is the AEC-supported Si-Ge Thermoelectric Material and Module Development Program under which the major part of the technology development reported in this paper has been accomplished. Mr. Berlin is a member of Tau Beta Pi and Pi Tau Sigma, and is a registered Professional Engineer in New York.

Lewis H. Gnau, Ldr.
Thermoelectric Materials Technology
Industrial Tube Division
Electronic Components
Harrison, N.J.

received the BS in Chemistry at Lycoming College in 1950 and the MS in Chemistry at Bucknell University in 1951. From 1951 to 1959 Mr. Gnau was employed by Sylvania as a Product Development Engineer. In 1959 Mr. Gnau joined RCA at the Electron Tube Division in Harrison. In his initial position he was concerned with the application of insulating and emission coatings to electron tube components. In 1961 he was assigned to the general area of new products development. He contributed to the development of a vapor deposition process for the production of superconducting materials. He was responsible for establishing zone leveling techniques for the large-scale production of silicon-germanium thermoelectric alloys used for power generation in the SNAP-10A Program. For this effort he was included in the David Sarnoff Engineering Team Award in 1963. In 1968 he was promoted to Engineering Leader, responsible for the Thermoelectric Materials Technology task of the Silicon Germanium Thermoelectric Materials and Module Development Program. Mr. Gnau is the author of several technical papers and holds a patent in the area of electrophoretic coatings. He is a member of the American Chemical Society and the American Society for Metals.

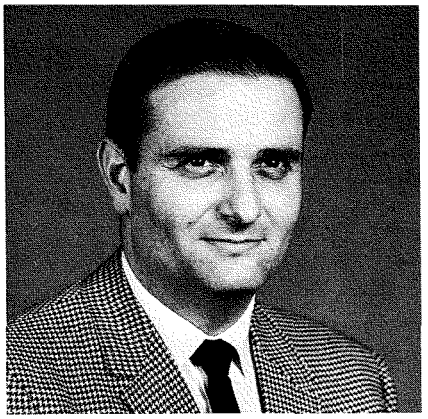

Robert S. Nelson, Ldr.
Thermoelectric Device Development
Industrial Tube Division
Electronic Components
Harrison, N.J.

received the BSEE from the Massachusetts Institute of Technology in 1956. Upon graduation, he joined RCA where he worked in the Advanced Development Engineering Group on Beam Deflection and Nuvistor Vacuum tubes. From 1960 to 1963 he worked in the Receiving Tube Design—New Products activity where he was responsible for the design of Nuvistor triodes, tetrodes and special purpose vacuum tubes. In addition he was responsible for the Design Group's duties regarding maintenance of the line in the nuvistor factory and customer complaint problems and their solutions. In 1963 he joined the Thermoelectric Device Development activity, responsible for the design development, and evaluation of the hot stack for the high-temperature advanced thermoelectric module. In 1965 he was appointed engineering leader for the Quality, Reliability and Test Engineering Group of the Thermoelectric Device Development activities. In 1968 he was responsible for the air-vac module development phase of the Si-Ge thermoelectric materials and module development program where he directed the design, fabrication and testing of air-vac modules and converters. Mr. Nelson is a member of the IEEE.

generator must be isolated at the hot contact through electrical insulators. For high-temperature operation, this requirement places severe limitations on the stack design and the available materials for insulators at the hot contact. The free suspension requires only isolation at the cold-end contact and thus greatly reduces this system design constraint.

Non-magnetic structure

The air-vac couple with an aluminum or other non-magnetic baseplate and radiator is constructed entirely of non-magnetic materials. This feature is of considerable importance in certain space-mission environments. It is also feasible to fabricate the entire converter of non-magnetic materials.

Areas of developmental support

The primary non-RCA source of support for the detailed examination of current air-vac structures and the development of advanced concepts is the "Si-Ge Thermoelectric Material and Module Development Program" funded by the Atomic Energy Commission. This program's broad objective is to optimize the materials, fabrication processes, and design concepts which comprise the air-vac concept; to demonstrate, by the fabrication and testing of couple and module structures, the achievement of improved performance characteristics; and to advance the quality and reproducibility of fabrication to aerospace-oriented hardware in a two-year period. Several NASA facilities, through the procurement of test hardware and the development of advanced concepts, are also participating in the growth of the air-vac approach. In the early stages of application, a considerable amount of work was performed under the cognizance of the Signal Corps and the Navy.

Air-vac materials

The silicon alloys used in air-vac thermocouple construction are particularly suited to stable, high-temperature operation in air and vacuum. The active thermocouple legs consist of 63.5-atomic-% silicon, doped with phosphorus (N-type) and with boron (P-type). Silicon-germanium alloys are prepared by vacuum casting of the elemental constituents and subsequent zone leveling; this process results in homogeneous, uniformly doped polycrystalline materials. The silicon-molybdenum hot shoe serves as a heat-acceptor plate and electrically connects the silicon-germanium thermoelements. The hot-shoe material is prepared by direct vacuum casting of silicon and molybdenum with the suitable dopants.

Silicon-germanium

The silicon-germanium alloys in common use are inherently high-temperature materials. Their superior oxidation resistance permits unprotected operation in air, as well as in vacuum and in fossil-fuel combustion products environments. The low vapor pressure of silicon-germanium results in the capability of the material to withstand high-temperature operation without degradation. Other desirable properties, essential to device construction, are high mechanical strength, low den-

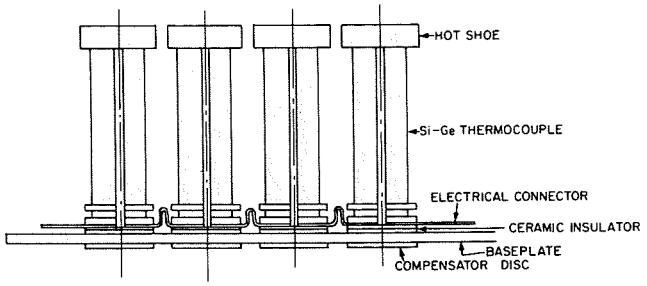

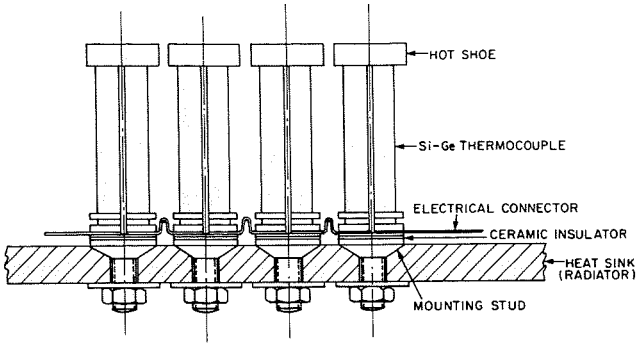

Fig. 2—Air-vac module construction: (left) rigid module; (right) fleximod

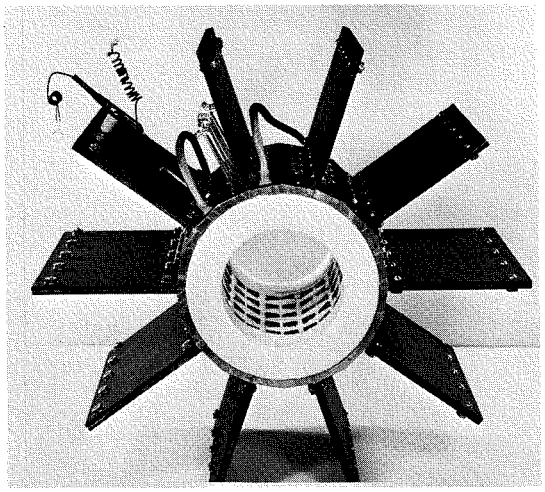

Fig. 3—One-third section of Snapoodle generator which supplies 72 watts under normal operation

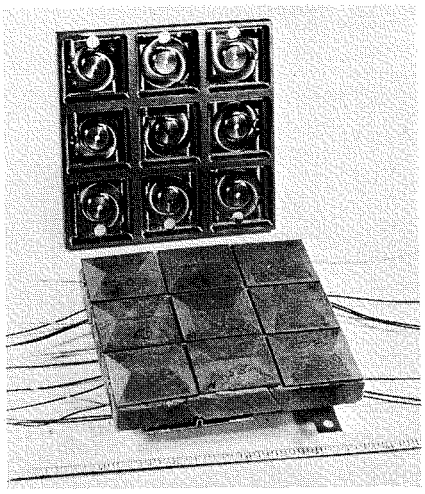

Fig. 4—Solar thermoelectric generator test panel for a 150-watt flat-plate solar thermoelectric generator.

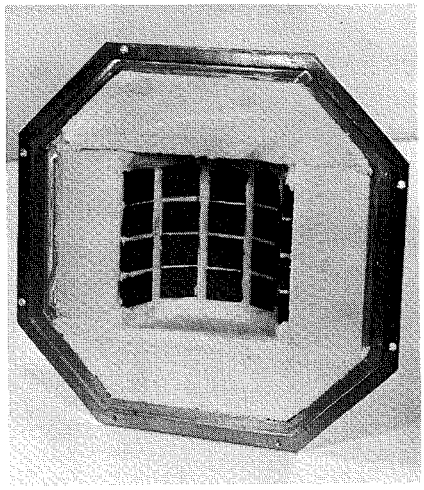

Fig. 5—"Step-II" generator; a 10-watt semicylindrical converter

sity, and the ability to bond to a variety of refractory materials to form stable, low-resistance electrical contacts.

Preliminary work at RCA has shown that the use of thermoelement alloys with compositions between 75- and 85-atomic-% silicon may offer significant advantages over lower-silicon-content alloys in air-vac thermocouples. In addition to a small improvement in electrical performance, higher-silicon-content alloys provide a better thermal expansion match to silicon-molybdenum hot shoes and thus result in a more stable junction at high temperatures. Development of reliable methods for the preparation of the higher-silicon-content materials, optimization of the alloy composition, and the establishment of thermocouple bonding techniques are in process.

The most serious problem encountered during the preparation of materials in the composition range of 75- to 85-atomic-% silicon is the softening of the quartz ampule containing the ingot under process at high temperatures. As a result, ingot yields are low. Initial testing with thick-walled quartz ampules for zone leveling is encouraging. In addition, hot pressing is being investigated as a preparative method for higher-silicon-content alloys.

Determination of the silicon-germanium alloy composition with the highest figure-of-merit is being accomplished by varying alloy composition and dopant concentration until the optimum is reached.

Silicon-molybdenum

The alloy of 85% silicon and 15% molybdenum (by atomic weight) used in hot shoes was developed to provide a material of high mechanical strength which could be doped to a sufficiently low resistivity to minimize electrical losses. The material was expected to perform in a variety of atmospheres, including air, at high temperatures. A close thermal expansion match to silicon-germanium was desired to enhance bond integrity.

The silicon-molybdenum alloy is largely experimental, and has relatively low production yields. The material is sensitive to minor changes in the vacuum casting technique and product reproducibility is difficult to achieve. However, the difficulties of preparing the silicon-molybdenum hot-shoe material are being resolved by a detailed chemical and physical characterization to determine factors contributing to inhomogeniety and structural faults. A specially designed vacuum-casting furnace with facilities for controlling the cooling rate, a major factor in determining ingot quality, will be used to develop improved methods for silicon-molybdenum preparation. Hot pressing is being investigated as a supplementary method for producing high-density, homogeneous silicon-molybdenum alloys.

Alternate hot shoes

The performance of air-vac thermocouples may be improved by the use of hot-shoe materials that have higher thermal conductivities than those currently obtainable with silicon-molybdenum alloys. The present work efforts are designed to develop and evaluate high-conductance metallic, inter-metallic, or composite hot shoes for use in primary rocket-launch or

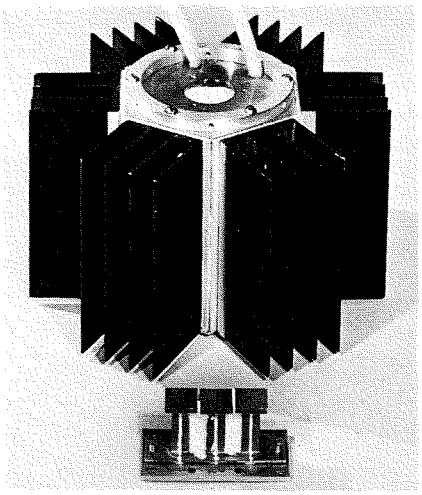

Fig. 6—5-watt generator for potential commercial application

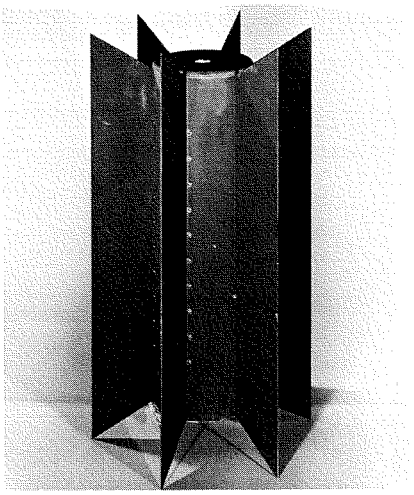

Fig. 7—Reference-design air-vac thermoelectric converter

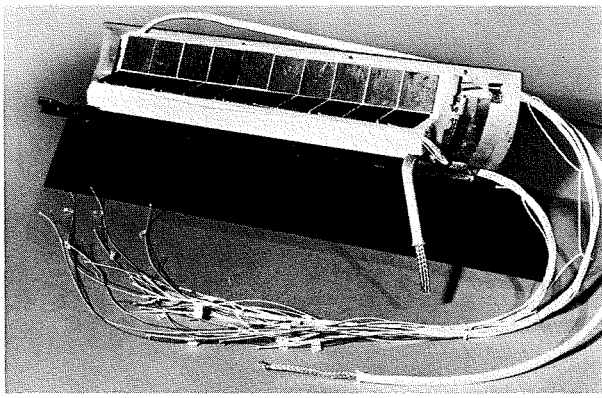

Fig. 8—Reference-design air-vac modular assembly

vacuum environments at temperatures above 900°C. The tasks are concerned with the development of high-temperature, long-life bonds between silicon-germanium and selected hot-shoe materials.

Included with the materials under study as alternates to silicon-molybdenum are silicon carbide and graphite. Both of these materials have coefficients of thermal expansion close to that of silicon-germanium. The thermal conductivities of silicon carbide and graphite are higher than that of silicon-molybdenum; both have acceptably low electrical resistivities.

The result of the materials development effort will be silicon-germanium thermo-electric materials and structures capable of reliable operation at a hot-junction temperature of 1000°C.

Air-vac module and converter

The air-vac couple configuration has been utilized in a variety of module assemblies produced as one-at-a-time feasibility demonstrations of the concept. The module construction has been both of the direct metallurgical attachment type from the cold stack to the base and of the mechanical fleximod attachment. The requirement for many of these modules was to fabricate the hardware, without development, to a specification based on the then-existing limits of technology. Unlike past thermoelectric programs, the current AEC-supported "Si-Ge Thermoelectric Materials and Module Development Program" provides the support for the developmental effort required to optimize the module and converter.

Design and Analyses

A recent RCA-developed computerized analysis provides a highly sophisticated technique for the achievement of optimized designs. This analysis, although in its early stages of application, has been used to optimize a solar generator and a high-performance thermoelectric air-vac converter. This converter has been built and is currently on performance testing under vacuum conditions.

In designing practical high-performance air-vac devices, it is important to account for not only the figure-of-merit of the thermoelectric material and operating temperatures, but also the electrical and thermal losses. The computer analysis technique is constantly being reviewed to better approximate thermal losses associated with heat-shunt insulation. This approximation is concerned not only with the thermal conductivity of various insulations, but also with practical fabrication of devices, e.g., gap losses between the insulation and the thermoelectric material.

Fabrication of air-vac modules and converters

Figs. 3 through 6 show some of the more significant Si-Ge Air-Vac thermoelectric power supplies fabricated during the past few years.

As part of the present air-vac module technology program, a reference-design converter (Fig. 7) has been built using state-of-the-art technology and materials and is being used as a base point to compare improvements in thermoelectric materials and techniques. The assembly is comprised of three pie-shaped modular assemblies (Fig. 8). The twenty-couple module is built as a single unit using the fleximod connection concept. The couples are electrically connected in a series-parallel arrangement to provide redundancy.

An important aspect of the fabrication of thermoelectric devices is the use of heat-shunt insulation to minimize thermal losses. Based on studies of the optimum insulation, the multi-layer metallic foils have the greatest potential to minimize thermal losses and improve device efficiency. Effort is being made to use these foils in high-performance developmental designs.

Test program

Stability test data

The data accumulated to date on various life tests indicate the excellent and predictable stability of air-vac couples as a function of time at temperature (Fig. 9). Performance data from these life tests indicate changes in power levels as a function of time at temperature to be within predictable limits based on material properties of the silicongermanium. A number of these modules are still continuing on life test.

Converter performance testing

The 5-watt air-vac generator shown in Fig. 6 and the reference-design converter shown in Fig. 7 are currently on performance life-testing under vacuum conditions. Although electrically heated, these devices can be considered as closely representing an actual radioisotope thermoelectric system. Fig. 10 shows the power output and device efficiency of the 5-watt converter as a function of hot-shoe temperature. This converter has accumulated more than 3500 hours of operation at a hot-shoe temperature of 1000°C while maintaining a device efficiency of 5.3%.

The reference design converter of Fig. 7 has been mapped for performance at the design and off-design conditions. Performance mapping consisted of

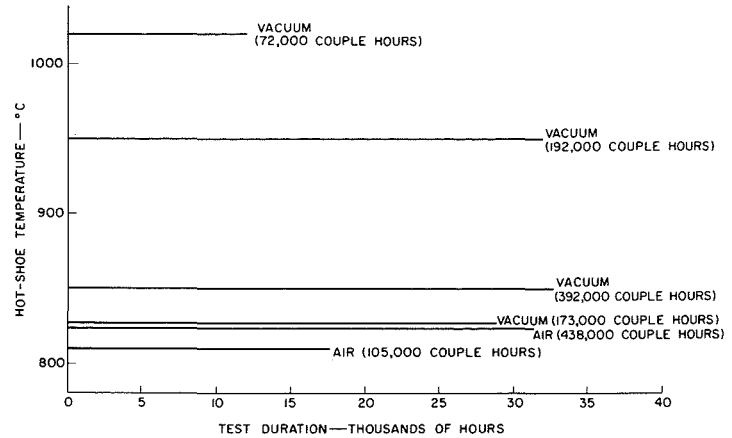

Fig. 9—Longest-duration air-vac module life tests as a function of hot-shoe temperature

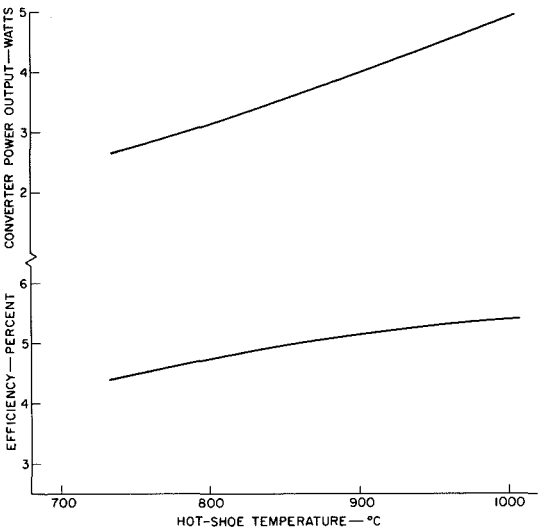

Fig 10—Power output and efficiency of 5-watt air-vac converter as a function of hot-shoe temperature

measuring the electrical and thermal parameters as a function of load current at a constant heat-source power input. Fig. 11 shows a typical "load swing" performance mapping at a nominal hot-shoe temperature of 950°C. Curves of power output and device efficiency as a function of hot-shoe temperature for the reference-design converter are shown in Fig. 12. The converter has accumulated more than 2300 hours to date on stability life test at a hot-shoe temperature of 970°C while maintaining a device efficiency of 5.8%.

Mechanical testing

The mechanical stability of air-vac devices is important in the development of power conversion for space application. To assure reliable operation after launch, air-vac modules and couples have been subjected to specification levels and higher engineering levels of shock and vibration sequences. These sequences not only assure mechanical stability at launch levels of acceleration but also indicate the capability of these devices to be used with other vehicles requiring more stringent mechanical conditions.

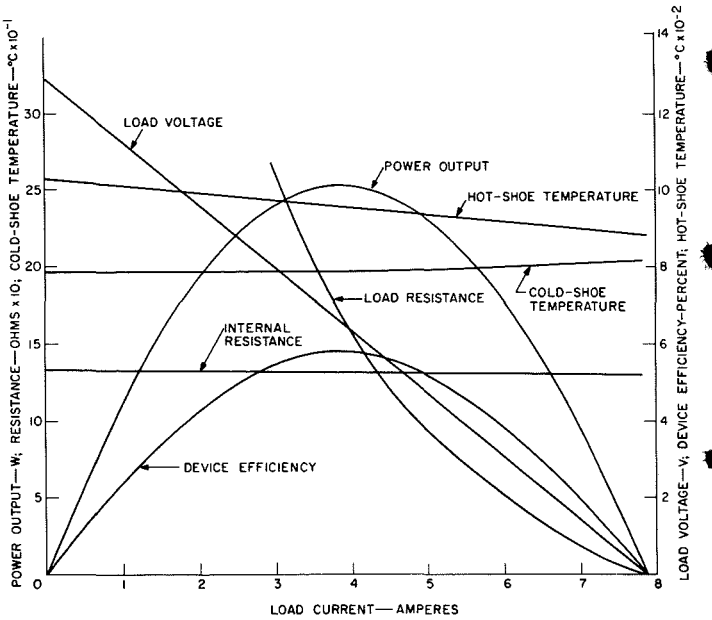

Fig. 11—Reference-design converter performance as a function of load current

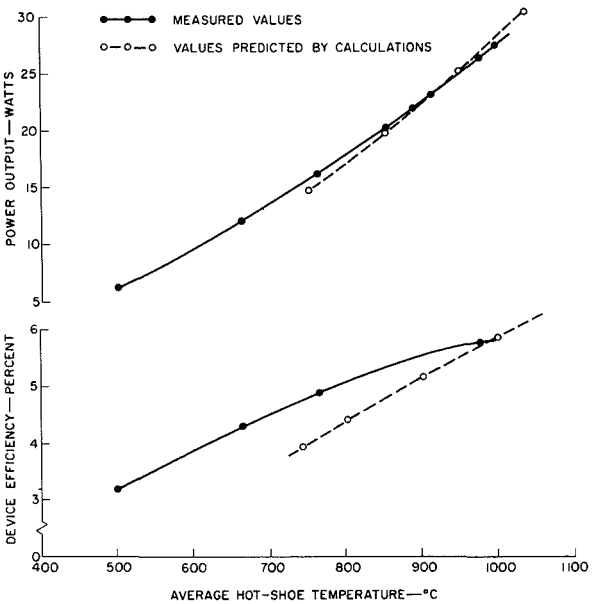

Fig. 12—Power output and efficiency of the reference-design air-vac converter as a function of hot-shoe temperature

Areas of potential applications

At present, the substantial developmental effort being devoted to the air-vac concept is directed toward the ultimate application in radioisotope generators requiring reliable, stable outputs for long-term missions being planned by NASA and the DoD. These aerospace missions may include the projected "Grand Tour" or "New Moons" visits to the outer planets, and future "Voyager" missions to Mars or Venus. In addition, recent work performed for NASA has been directed toward the development of Si-Ge air-vac solar thermoelectric generators for a potential solar probe.

The growing oceanographic field and the Navy and Coast Guard requirements for power supplies for such applications as buoy markers, offshore oil-rig auxiliaries, and remote weather stations offer a potential for application of RCA thermoelectric generators which is yet to be tapped. In addition, numerous terrestrial commercial and Government requirements for remote power supplies capable of extended (up to ten years), maintenance-free operation are being defined. Major growth in this area is projected for the 1970's.

Thus, as the efficiencies of Si-Ge air-vac devices improve, and an increasing backlog of test data is developed, the potential areas of applicability will expand.

New design concepts in thermoelectric generators

V. Raag

Although practical methods of thermoelectric power conversion have existed for over a decade, considerable effort is continuously devoted toward improving the performance capabilities of thermoelectric devices and providing a broader range of applications. The primary emphasis in the development of thermoelectric devices is on greater overall conversion efficiency, enhanced mechanical reliability and electrical stability, and the simplification of fabrication procedures. Reduction of generator weight is another development goal of special importance in space applications. All of these goals are interrelated in that directly or indirectly they all lead to decreased device end costs in practical applications. Achieving these goals involves a combination of basic research to find better thermoelectric materials and innovations in design and technology that largely use existing materials and components to improve device performance. This paper describes a variety of new thermoelectric-device concepts currently under study and/or development in the Thermoelectric Products Engineering Group.

ONE OF THE MORE PRACTICAL thermoelectric-device concepts makes use of RCA-developed silicon-germanium air-vac thermocouples. Although air-vac thermocouples have been treated in detail elsewhere,[1,2] a brief description is in order so that air-vac device design improvements may be discussed meaningfully.

Improved air-vac thermoelectric devices

Fig. 1 shows a cross-sectional diagram of a silicon-germanium air-vac thermocouple. The N- and P-type silicon-germanium thermoelements are bonded on one end to an extended-area heat collector made of a silicon and molybdenum alloy and called the *hot shoe*, and on the other end to a cold-stack assembly. The cold-stack assembly permits mechanical or metallurgical attachment of the air-vac thermocouple to a support frame or radiator without creating undesirable stresses that arise from the differential thermal expansion of silicon-germanium and the frame. Physical contact with the heat-rejection system minimizes the temperature drop between thermoelement cold junctions and the radiator. The stack assembly includes an electrical insulator for purposes of electrical isolation.

The air-vac thermocouple is designed for radiative coupling to a heat source, such as a radioisotope fuel capsule. Radiative coupling eliminates physical contact of the thermocouple to the heat source and thereby prevents possible stress and material incompatibility problems at the hot side. In addition, air-vac thermocouples, because of their cantilever-type construction, are extremely rugged. Because the materials are unreactive with a variety of atmospheres and possess very low values of vapor pressure, air-vac thermocouples are operable, even at high temperatures, in air, vacuum (thus the name air-vac), and the combustion products of fossil fuels.

Although radiative coupling to a heat source eliminates mechanical stress and chemical reactions, it produces a temperature drop between the source and the thermocouple that generally exceeds that obtainable with direct conductive coupling. All extraneous temperature drops are undesirable because a heat source has an upper limit on operating temperature and any decrease in temperature subtracts from the temperature drop across the active thermoelectric material and results in less-than-optimum thermocouple performance. A possible way of minimizing the temperature drop between the heat source and the thermocouple is to reduce the flux of incident radiation. Many heat sources naturally emit at relatively low flux values and therefore the air-vac thermocouple is ideally suited for use with them. Present radioisotope fuels, for example, yield incident heat-flux densities in the range of 0.1 to 3 watts/square centimeter. The resultant range of temperature drops between heat source and thermocouple is from a few degrees to about 100°C. Although low values of incident heat flux provide a reduction in the temperature drop between thermocouples and heat source and therefore an increase in thermocouple hot-side operating temperature, the configuration of the thermocouple legs may in some instances become somewhat extreme in relation to its mechanical strength, as discussed below.

The conversion efficiency of a thermoelectric device is approximately proportional to the temperature difference across the active thermoelectric material. For best performance, therefore, the device must be operated at as high a hot-side temperature and at as low a cold-side temperature as possible. The maximum obtainable hot-side temperature depends on the heat-source temperature and the materials used in the construction of the device. In the case

Reprint RE-15-3-6 (ST-3907)
Final manuscript received May 29, 1969.

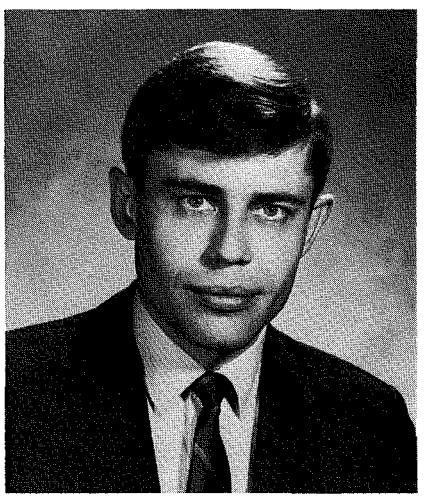

Valvo Raag*
Industrial Tube Division
Electronic Components
Harrison, N.J.

received the BS in Physics from Brown University in 1958. He continued his studies for a year at the University of Helsinki in Finland. He received the MS in Physics from New York University in 1964. Mr. Raag joined the Physics and Electronics unit of the Chemical and Physical Laboratory of RCA in Harrison in 1959. He has been concerned with the kinetics of electron-tube processing and activation, and with the effects of materials on the performance of tubes. More recently, he has been involved in the measurement and interpretation of the thermo-electric properties of silicon-germanium alloys and in the development of techniques for rigorous computerized performance analyses of thermoelectric devices. Mr. Raag has published eight papers in the fields of electron tubes and thermoelectrics. He is a member of Sigma Xi, and the A.S.T.M. Subcommittee on Thermoelectrics.

* Since January of 1969, Mr. Raag has been working for Resalab Inc. as a consultant on energy conversion.

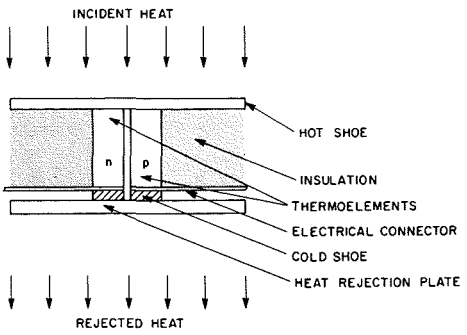

Fig. 1—Cross-section of silicon-germanium air-vac thermocouple.

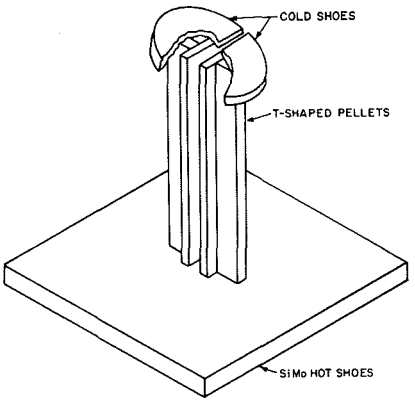

Fig. 2—Thermocouple using T-shaped thermoelements.

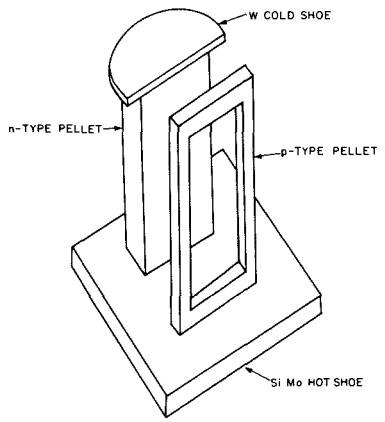

Fig. 3—Window-frame-type air-vac thermocouple.

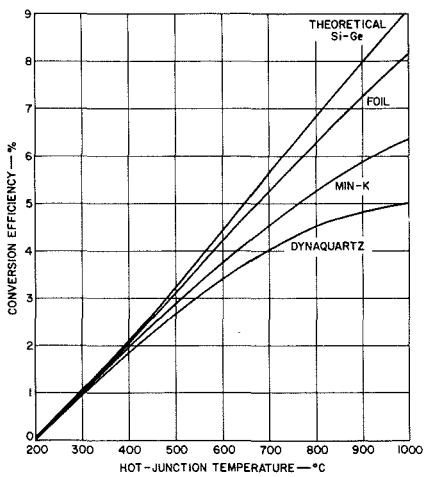

Fig. 4—Performance curves for devices using different types of thermal insulation.

of devices using silicon-germanium air-vac thermocouples, this temperature is of the order of 1000°C. The lowest obtainable cold-side temperatures depend on the method of heat rejection. In the case of space systems in which rejection occurs by radiation, weight limitations usually restrict radiators to sizes that yield cold-side temperatures of the order of 100 to 300°C. Somewhat lower cold-side temperatures are obtainable in terrestrial and hydrospace applications. For most applications, therefore, device operating temperatures are fairly closely defined within the above limits.

Thermocouple configuration

The dimensions of the thermocouple legs and the thermal conductivity of the leg materials primarily determine how much heat is required to yield the desired temperature difference. For leg sizes that are conveniently fabricated and that exhibit good mechanical-strength characteristics, the input-heat requirement dictates the use of the extended-area hot shoe because the necessary heat flux in the thermocouple legs nearly always exceeds the available flux incident on the shoe. The extended area of the hot shoe enables the required amount of heat to be collected and funneled into the thermocouple legs. It is apparent that the lower the incident flux, the larger the hot shoe that is needed to collect the required heat. Because there are limitations on the maximum size to which hot shoes can normally be fabricated, the goal of increased hot-shoe size may also effectively be attained by a reduction in the cross-sectional areas of the thermocouple legs. For a given hot-shoe area, in the limit of very low values of incident heat flux, the thermoelements must be made very slender and consequently they may be subject to mechanical failure as a result of handling or, in the case of space systems, because of shock and vibration experienced during launch.

Other thermocouple-leg configurations have therefore been devised to enhance the mechanical-strength characteristics of air-vac thermocouples when designed for use in applications that require very small cross-sectional element areas. Fig. 2 illustrates a thermocouple design that makes use of thermoelements of T-shaped cross-section.[3] Actual thermocouples that use this leg configuration have been made with silicon-germanium slices that are only 0.020 inch thick. The durability of such thermocouples under shock and vibration conditions exceeds that of conventional couples with identical cross-sectional element areas. Fig. 3 shows another ruggedized air-vac couple in which the P-type element is hollowed into a window-frame-type structure.[3] Only the P-type is hollowed because optimum thermocouple performance results when the cross-sectional areas of the N- and P-type thermoelements are in the approximate ratio of two to one. Because the areas of contact to the hot and cold shoes are larger than the cross-sectional area of the P-type leg, a relatively lower electrical contact resistance in the thermocouple is obtained. Thermocouple leg configurations other than those shown in Figs. 2 and 3 are also being considered in an effort to reduce cross-sectional leg areas while maintaining mechanical strength.

Thermal losses

Another area of improvement in devices that use silicon-germanium air-vac thermocouples concerns the introduction of advanced thermal-insulation materials to minimize direct heat transfer that bypasses the thermoelements between the hot and cold sides of the device. In the air-vac thermocouple shown in Fig. 1, the space between the hot shoe and the cold side not occupied by thermoelements permits direct heat transfer by radiation. Unless this space is thermally insulated, the shunt heat loss may be substantial, especially during operation at elevated temperatures. Until recently, the most suitable fibrous-type thermal insulations were Dynaquartz and Microquartz. Although these insulations reduced thermal shunt losses, the losses were still quite sizable, in some instances being as large as 40 to 50% of the total heat traversing the thermocouple. Within the past several years, however, a new family of fibrous-type thermal insulations, the MIN-K series, has been developed by Johns-Manville.[4] The most valuable of these insulations for use in silicon-germanium thermoelectric devices are MIN-K 2002 and MIN-K 2020. The former has a maximum operating temperature of about 850°C and therefore may be used in some, but not all, silicon-germanium devices. The latter insulation, how-

ever, has been designed for application at temperatures as high as 1000°C and therefore is well suited for most devices that use air-vac thermocouples. The thermal conductivity of MIN-K-type thermal insulations is lower than that of the best older-type insulations by a factor of some three to four. Depending on device design, the use of the new fibrous insulations therefore results in a considerable reduction of thermal shunt losses.

In addition to fibrous insulations, an entirely new concept in thermal insulations has been developed over the past few years and offers even greater possibilities for the reduction of thermal shunt losses in high-temperature thermoelectric devices. This concept involves a sandwich-type arrangement of radiation shields in the form of metallic foils, separated by thin sheets of bulk insulation. Such foil insulations have an effective thermal conductivity nearly an order of magnitude lower than that of the MIN-K fibrous insulations. The foil insulation, however, is not as easily adapted to thermoelectric devices as is the fibrous insulation. The metallic foils are electrically conductive and, unless special care is taken to prevent contact between the foils and the thermocouples, the danger exists of electrically shorting the generator. Fibrous insulation must be added, therefore, as a spacer that separates the foil insulation from the thermocouples. Although the two types of insulation are thermally in parallel (and therefore their combined thermal conductivity is greater than that of the foil insulation alone) projected device performance gains are still significant.

Performance

Fig. 4 compares the performance of thermoelectric devices that use silicon-germanium air-vac thermocouples and different types of thermal insulation. The data in Fig. 4 show device performance in terms of conversion efficiency as a function of hot-junction temperature. The cold junction is assumed to remain fixed at a value of 200°C—a temperature typical of thermoelectric devices used in deep space. Because exact values of conversion efficiency generally depend on detailed device design, the data in Fig. 4, although quite representative, should be considered only approximate. It should be noted that the top curve shows conversion efficiency with no thermal shunt losses and represents the upper performance limit of silicon-germanium devices.

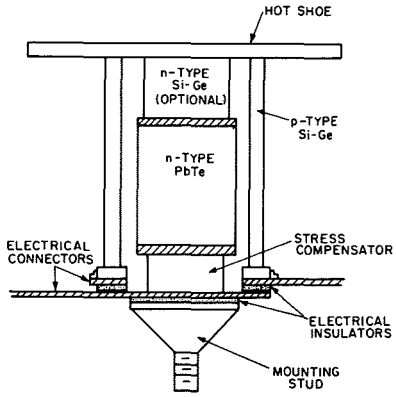

Fig. 5—Hybrid thermocouple using N-type lead telluride and P-type silicon-germanium thermoelements.

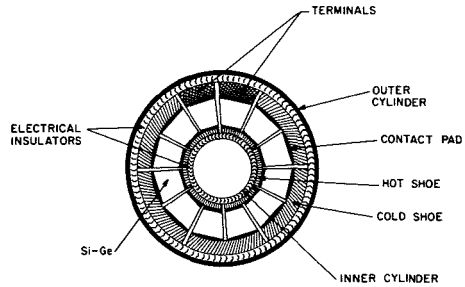

Fig. 6—Cross-sectional drawing of silicon-germanium compression module.

Although the discussion on insulations concerns the reduction of thermal shunt losses in air-vac thermocouples and modules, for maximum performance from a thermoelectric generator all thermal losses must be eliminated. For example, the generator is usually subject to thermal losses at the two ends of a cylindrical generator. The types of insulation discussed above can also be used to reduce these end losses. The advanced fibrous-type thermal insulations have already been incorporated into a few of the latest air-vac thermoelectric devices and have demonstrated their usefulness by enhanced performance values. Effort is presently underway on the practical utilization of foil-type insulations in such devices.

Hybrid thermocouple

Silicon-germanium alloys and alloys of lead and tellurium compounds, of which lead telluride is probably the best known example, are the most widely used thermoelectric materials in energy conversion. Silicon-germanium alloys are characterized by their capability of unprotected high-temperature operation, light weight, and good mechanical strength. Their useful range of operating temperatures for energy-conversion purposes is room temperature to 1000°C. The ability to operate over such an extended range of temperatures is one reason for the attractiveness of silicon-germanium alloys. The stability of the thermoeletric properties is good, although the N-type alloys exhibit a slight modification in electrical resistivity and Seebeck coefficient because of a temperature dependence of the solid solubility of dopant. The tellurides have a smaller range of useful operating temperatures, from room temperature to about 600°C, and must be protected in most applications from the environment. Oxygen has an adverse effect on the thermoelectric properties of the tellurides and, because of their high vapor pressure, they must be sealed in inert gas in vacuum operation. Mechanical strength of the tellurides is not as great as that of the silicon-germanium alloys, and tellurides do not form as reliable a contact to metallic shoes as do the silicon-germanium alloys. Hot-side contacts and in particular the contact to the P-type thermoelement are unreliable. The main attractiveness of tellurides is their excellent ability to convert heat to electricity, reflected by the so-called "figure of merit". Up to temperatures of about 550°C, the tellurides have a higher figure of merit than the silicon-germanium alloys. At higher temperatures the converse is true.

A careful examination of the relative characteristics of lead telluride and silicon-germanium alloys indicates that a combination of N-type lead telluride and P-type silicon-germanium results in a thermocouple that exhibits stable electrical performance, high strength, and good contactability to metal or semiconductor end pieces. The N-type lead telluride has a high figure of merit and good stability when operated at temperatures not exceeding about 550°C (the degradation characteristic of lead telluride thermoelectric devices is primarily caused by the hot-side contact of the P-type thermocouple leg). The high strength and good machinability of silicon-germanium allows the two materials to be combined in such a manner that the silicon-germanium, in addition to serving as the P-type leg of the thermocouple, completely surrounds the N-type lead telluride, sealing it off from the environment. This design eliminates the need for a separate sealing container for the telluride leg.

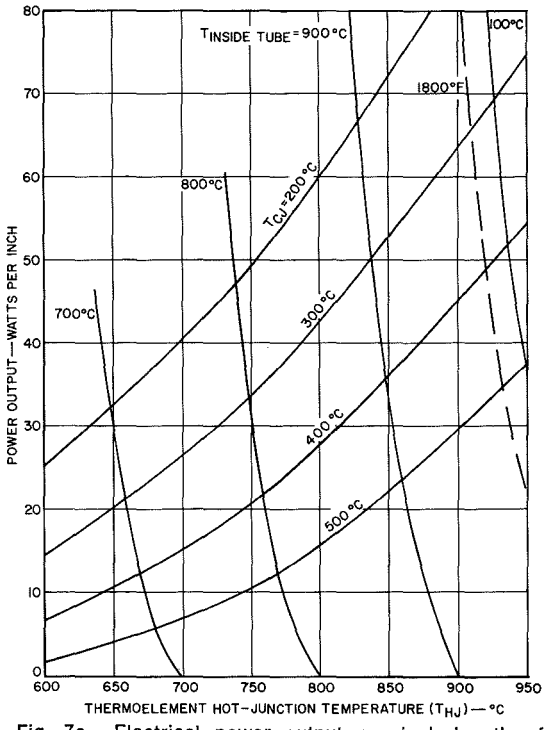

Fig. 7a —Electrical power output per inch length of module.

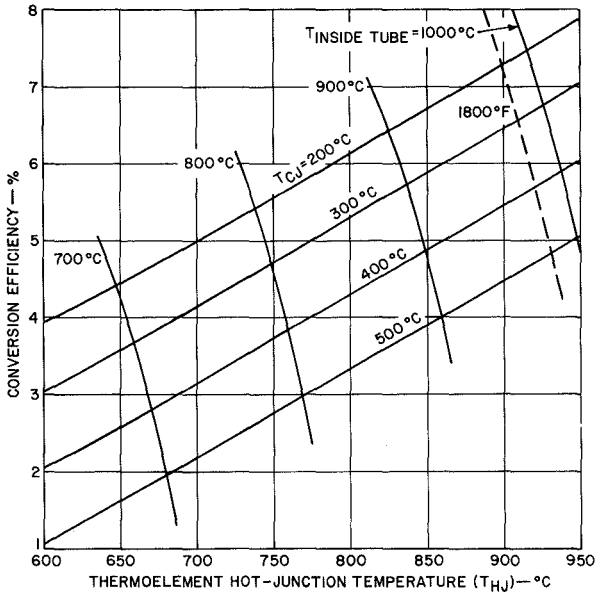

Fig. 7b —Conversion efficiency.

The combination of N-type lead telluride and P-type silicon-germanium into one thermocouple, known as the hybrid thermocouple,[5] is schematically illustrated in Fig. 5. Although the concept is illustrated in terms of an air-vac type thermocouple with its semiconductor hot shoe, it is equally applicable to a conductively coupled system in which the thermocouples are directly joined to the heat source. The hollow cylinder surrounding the N-type lead telluride thermoelement is made of P-type silicon-germanium. Both ends of the silicon-germanium cylinder are metallurgically bonded, one to the silicon-molybdenum hot shoe and the other to the cold-stack assembly. The cold-stack assembly is attached to a tapered stud, including a nut-and-bolt arrangement that permits convenient mounting to a radiator. Two electrical insulators in the cold-stack assembly provide electrical isolation of the two thermocouple legs from each other and from the stud. Each leg is contacted to an electrical connector. The N-type lead telluride thermoelement is contacted to metallic end pieces. The hot-side end piece is contacted to N-type silicon-germanium, which in turn is bonded to the hot shoe. The cold-side lead telluride end piece is bonded through a stress compensator to the cold-stack assembly. The segment of N-type silicon-germanium in series with the lead telluride thermoelement is optional in that it is used only in applications that yield hot-side operating temperatures in excess of those permissible for lead telluride. The silicon-germanium segment, while contributing as an active thermoelement, drops the hot-junction temperature of the lead telluride leg to an acceptable level. In lower-temperature applications, the silicon-germanium segment is not used. The lead telluride thermoelement is metallurgically bonded to the remainder of the thermocouple. Thermal contact and electrical continuity are always assured even though the bond degrades because the lead telluride has a relatively high expansion coefficient which places it under compression. Finally, the space between the P-type and N-type thermoelements is filled with an inert-gas atmosphere to inhibit sublimation of the lead telluride.

Performance

The hybrid thermocouple may be characterized by a high level of performance that remains stable during extended operation. In initial values of conversion efficiency, it outperforms silicon-germanium thermocouples and approaches the performance of lead-telluride thermocouples when compared at identical operating temperatures. It is expected that the hybrid thermocouple will also outperform the lead-telluride couple after extended operation because of the severe degradation with time that is characteristic of many lead-telluride devices. When compared at temperatures above the maximum lead-telluride operating temperature, the hybrid thermocouple outperforms both lead-telluride and silicon-germanium thermocouples. In applications that require operation of the devices for long periods of time, the relative performance of the thermocouples is in the sequence: hybrid, silicon-germanium, and lead telluride.

Preliminary test data on hybrid thermocouples confirm the expectations of good and stable performance. Longest tests to date have been conducted for several thousand hours without any degradation in electrical performance.

Compression module

The highest-temperature applications of silicon-germanium alloys make use of the air-vac thermocouples by radiatively coupling them to a variety of heat sources. At temperatures of the order of 1000°C, radiative coupling is more reliable than conductive coupling obtained by metallurgically bonding the thermocouple to the heat source because material interactions and/or stress are eliminated. Although metallurgical or conductive coupling has been successfully accomplished at lower temperatures, up to about 800°C, most attempts to extend this to the upper-temperature capabilities of silicon-germanium alloys have not been successful. Nevertheless, there are distinct advantages to a conductively coupled high-temperature silicon-germanium thermoelectric system. As discussed above, radiative coupling of air-vac thermocouples to a heat source requires low values of incident heat flux to prevent an excess temperature drop. Low values of heat flux, however, require the use of extended-area hot shoes to collect sufficient quantities of heat to establish a large temperature difference between the hot and cold sides of the thermocouple. The extended-area hot shoe in turn gives rise to thermal shunt losses that in many instances substantially detract from device performance. A conductively coupled system that receives heat at high values of heat flux is not subject to the same shortcomings. Of course, in applications with heat sources that emit at low values of heat flux, it is necessary to concentrate the heat to obtain the desired operating temperatures from the device.

The compression module is the result of attempts to obtain a conductively

coupled silicon-germanium high-temperature thermoelectric device. Fig. 6 shows a cross-section of the device. The thermoelectric circuit consisting of N- and P-type silicon-germanium thermoelements and hot- and cold-side electrical connectors is placed between two hollow metal cylinders. Electrical insulators in the form of cylinder sections isolate the thermoelectric circuit from the metal cylinders. The thermoelements are thermally in parallel and electrically in series when heat flows radially between the cylinders. Input heat is applied to the inner surface of the inside cylinder. After radially traversing the module, it is rejected from the outer surface of the outside cylinder. The resultant temperature gradient across the thermoelements gives rise to a voltage. When a load is connected across the two terminals shown in Fig. 6, the device produces electrical power.

Bonding

There are basically no metallurgical bonds between any of the components of the compression module, although they may be added if desired. Intimate physical contact between adjacent components, needed for minimizing electrical and thermal resistance at interfaces, is obtained by "shrink fitting". A possible fabrication sequence for the device is to machine all parts except the outer cylinder to an exact fit. The inner diameter of the outer cylinder is machined to a value slightly less than the outer diameter of the outer insulator. The interference of diameter precludes the possibility of sliding the outer cylinder over the device after the rest of the components have been assembled. Heating of the outer cylinder to a sufficiently high temperature, however, expands its inner diameter so that it fits around the rest of the components. As the cylinder cools, the whole device is compressed. Depending on the construction materials, operating temperatures, and component dimensions, subsequent operation of the device at high inner-cylinder and low outer-cylinder temperatures can result in still greater compression.

The amount of compression obtained in the device is thus a matter of design and may conveniently be predetermined. The criterion of a desirable compression level depends on the requirements of low electrical and thermal resistances at component interfaces and the necessity of remaining within the elastic limit of all materials in the device. The first requirement dictates the use of high compression; the second requirement places an upper limit on compression.

The compression module may be built around one end of a heat pipe which actually forms the inner cylinder of the device. The other end of the heat pipe is buried in a heat source, such as a radioisotope fuel capsule or a nuclear reactor. Other possible heat sources, depending on the intended application, are a circulating-liquid metal loop or the mantel of a fossil-fuel burner. The heat from the compression module may be rejected by radiation from fins placed on the outer cylinder or by conduction to a coolant loop surrounding the cylinder. The mode of heat rejection selected depends on a given application. The compression module inherently produces electrical power at values of low voltage and high current. Increasing the voltage and decreasing the current are possible by splitting a given-length module into several shorter modules that are electrically series-connected. The module sections fit over a common inner cylinder and are spaced by thin insulator discs. The total power output is unaffected by this procedure.

Features and Performance

The cylindrical construction of the compression module is extremely rugged. The silicon-germanium thermoelements operate under compression and do not serve as supporting structural members as in most other devices. The elimination of metallurgical bonds minimizes the possibility of failure under environmental loading and thermal-cycling conditions. The design minimizes electrical leakage problems because of the relatively small areas of exposed insulator surface. A wide choice of materials and sizes is permitted throughout the device. Because thermal shunt losses are minimized, device performance is enhanced. Because the high-temperature operating limit of the device is that of the silicon-germanium alloys themselves, the full capabilities of silicon-germanium can be utilized. The elimination of metallurgical bonds in the compression module simplifies fabrication and reduces cost. Moreover, practically all of the parts of the module are salvagable. Considerable savings in cost may therefore be projected.

The calculated performance of the compression module is illustrated in Fig. 7 for a variety of hot-junction, cold-junction, and inner-cylinder temperatures. The data represent a compression module that has an outer diameter slightly less than three inches and an inner diameter of the order of one inch. Fig. 7a shows curves of electrical power output per inch length of module as a function of thermoelement hot-junction temperature for a variety of cold-junction and inner-cylinder temperatures. Fig. 7b shows conversion efficiency as a function of the same variables. Because of the higher electrical power and conversion efficiency possible with the compression module, it is especially suitable in applications that require large amounts of electrical power.

Preliminary test data on several compression modules have indicated the feasibility of this concept. However, before the concept is considered fully developed, further effort must be directed to the selection of materials, refinement of design and assembly methods, and the accumulation of more test data.

Summary

The field of thermoelectric energy conversion has attained maturity during the past decade, and RCA has firmly established itself as a recognized contributor to the field. Maintaining and expanding this position requires that improvements be made in device capabilities and the cost of power converted be reduced. These goals can be accomplished by use of design innovations that utilize existing materials and technology. A few such design innovations have been discussed in terms of present effort in the Thermoelectric Products Development group.

References

1. Lawrence, W. F., and Dingwall, A. G. F., "Fossil-Fuel Thermoelectric Generators," RCA reprints PE-171, PE-172, PE-173, PE-174.
2. Berlin, R. E., Gnau, L. H., and Nelson, R. S., "Developing Air-Vac SiGe Technology and Applications," *this issue.*
3. Notarius, H., *private communication.*
4. Collins, J. O., *Develop 1800F—400F Fibrous-Type Insulation for Radiosotope Power Systems,* Phase I Final Report, Volume I, Contract No. AT(30-1)-3633 (Oct. 2, 1967).
5. Caprarola, L. J., *private communication.*

Editor's note: The following is an excerpt of comments made by one of the technical reviewers:

> Many of us have been reading about the enormous problems associated with EMC (Electromagnetic Compatibility) but it is almost always in a context associated with military systems such as missiles, airplanes, fire control and communication. This is, of course, of the utmost importance . . .
>
> But the personal aspect of this paper brings the problem right down to the individual's level. All of us are ill from time to time and require the use of diagnostic devices which are probably severely limited in their usefulness because of EMI. The FCC has had regulations governing the use of such devices for a fair number of years, but these regulations are principally concerned with very bad offenders such as diathermy machines and X-ray machines. The authors pinpoint the problem when they note that "as operating rooms fill with devices, they can be expected to be more complex, and concurrently, weaker signals will need to be monitored and more electrical service equipment to be installed in hospitals." This is recognition of the same problem which harassed the military as their use of electronic devices has increased.
>
> One must look at this paper as an early study which concerns itself with a little recognized and growing problem. Data is presented and it is important because such data is almost non-existent in the literature. It is hoped that additional work is done along the following lines:
>
> 1) More measurements and tests be performed to provide an interference profile of a typical hospital.
> 2) A model suitable for prediction purposes should be developed so that some insight can be realized into potential EMI problems as new devices are developed.
> 3) The entire problem must be studied from a system viewpoint.
> 4) The EMI specification as presented, although worthwhile considering the limited information, must be expanded to deal effectively with the complexities of the problem.
>
> At least one trade magazine, the *Electronic Engineer* has asked the electronic engineer to help and work with the physician. This paper underlines this thought very elegantly. —**R. Ficchi,** DCSD, Camden, N.J.

EMI problems in the hospital

U. A. Frank | R. T. Londner

Electromagnetic interference (EMI) is a prime concern in the proper design of electronic medical equipment. However, no industry or government specification can be found. To form the basis of such a specification, a survey of the EMI environment in two modern American hospitals was made. The survey dealt with conducted and radiated emissions and susceptibility tests covering frequency ranges of: conducted 30 Hz to 100 MHz; radiated magnetic field 30 Hz to 30 KHz; and radiated electric field 14 kHz to 10 GHz. Some sources of strong EMI were identified, and the EM spectrum in several hospital locations was recorded. Based on these environments, design guidelines were formulated and preliminary specifications established.

WITH THE INCREASINGLY LARGE NUMBER of complex medical electronic devices in hospitals, the disturbing effects of electromagnetic interference (EMI) has now assumed serious consequences. For example, during surgical operations depend upon automatic, vital-sign monitors, which simply cannot be utilized during intervals of severe EMI. As the multiplicity of biomedical instrumentation increases, and as the dependence on this instrumentation increases, this deplorable condition will deteriorate further. It is hoped that this article will be a significant first step in providing an industry-wide specification delineating the maximum permissible emission of EMI generators, and limits on vulnerability (susceptibility) of sensitive components.

As the operating room fills with devices, they can be expected to become more complex, and concurrently, weaker signals will need to be monitored and more electrical service equipment to be installed in hospitals. All this helps to make medical electronics a real growth industry; but it turns the EMI status into a dilemma.

It is recognized that FCC specifications govern the test procedures and limits for emitted signals. However, these specifications define radiation limits over specific frequency ranges at specific distances and for specific types of equipment. The FCC specifi-

Reprint RE-15-3-8

R. T. Londner*
Standards Engineering
Medical Electronics
Trenton, N.J.
received the BSEE from Drexel Institute of Technology in 1959. Upon graduation he joined the Airborne Systems Division of RCA. In 1963 he transferred to the Special Projects Laboratory at the David Sarnoff Research Center, Princeton, New Jersey working on large scale system studies for the Air Force and the Navy. In February of 1967 he transferred to the Medical Electronics group in Trenton, New Jersey, and is presently working in the Standards Engineering group there.

*When this paper was written, the authors were with RCA Medical Electronics which has since been sold to Hoffman-LaRoche.

Ulrich A. Frank*
Medical Electronics
Trenton, N.J.
graduated from the University of New Hampshire in 1947 with the BA, the BSME and the Dean's Award. His graduate work was done at Johns Hopkins University in the field of Instrumentation. He then joined NACA (now NASA) as a Research Scientist. Since joining RCA M&SR in 1959 he has been Lead Engineer on tactical radars and on instrumentation of underground nuclear tests. As Principal Project Engineer on the Two-Pound Radar he received, along with other team members, the David Sarnoff Outstanding Achievement Award in Engineering. He is a Senior Member of IEEE and Chairman of its GPMP Chapter, a frequent contributor to this and other magazines, and holds several patents. In 1967 he transferred to RCA Medical Electronics.

Table I—EEG waveshapes.

Name of wave	*f (Hz)*	*amplitude, μV_{p-p}*	*electrode location*	*characteristic activity*
Alpha	8 to 13	50	occipital region	eyes closed, resting
Beta	14 to 50	5-80	parietal region	intense thought
Theta	4 to 7	——	parietal & temporal	stress, frustration
Delta	0.5 to 3.5	5-70	cortex	sleep

Table II—ECG wave components.

Component	*Typical duration (ms)*	*Typical amplitude (mV)*
P	90	0.1
Q	10	0.03
R	83	0.98
S	10	0.01
T	130	0.20

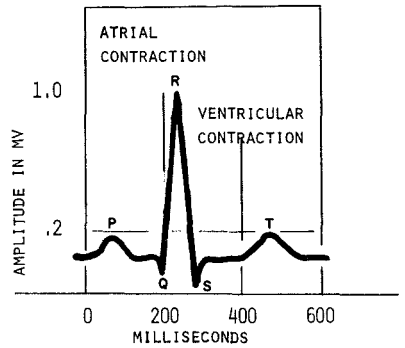

Fig. 1—Normal ECG signal.

cations do not consider the results of several sensitive medical instruments and devices operating adjacent to one another. The special considerations of medical electronics necessitate some other means of EMI evaluation.

Typically, early hospital electrical wiring was designed for the two-wire line cord, common to home lamp fixtures. These outlets did not provide an earth ground unless a pigtail lead was connected to the outlet. This, of course, is not conducive to mobility of equipment, thus, it is fairly safe to assume that the pigtail would never get connected. However, for patient safety, a ground must be provided for electronic equipment. The newer hospital wings now have 3-prong receptacles.

Yet, ground loops, lack of power-line isolation between wings, floors, and rooms cause conducted interfering signals to be transmitted to almost any part of the hospital. These interfering signals originate from generators and other equipment connected to the line, or from radiated signals impressed upon the power lines and then conducted throughout the hospital.

Biopotentials

One of the basic considerations in any discussion on EMI is the level and frequency of the electrical signals generated by the body, called biopotentials. Biopotentials are generated in excitable cells (nerve and muscle) by the migration of sodium and potassium ions across the cell membrane. The body activities of these cells cause disturbances in the equilibrium across the membrane which causes the ion exchange, resulting in currents. These disturbances cause "ion ripples" to be formed adjacent to the membrane and successively to greater distances. They are greatly attenuated through the impedance of the body tissues and fluids, eventually reaching the surface where electrodes may be attached.

Biopotentials range from a very few microvolts to several millivolts and the source impedances from a few hundred ohms to several hundred megohms. Much of this impedance occurs at the electrode/tissue interface. To lower this impedance, surface preparations such as conductive gels or subcutaneous electrodes are used. Such subcutaneous electrodes have many disadvantages, but their use demonstrates the length to which the medical profession is prepared to go to obtain usable monitoring signals. It is of interest to look in detail at some of the more important electrical signals from the body.

The electroencephalogram (EEG)

The EEG is a signal of the electrical activity in the brain. Unfortunately the biopotential of a single nerve fiber is difficult to obtain, and the EEG reflects the synchronous activity of thousands of neurons. For brain waves to be meaningful, some synchronizing action, such as muscle movement, must occur. Cerebration is associated with asynchronous neural activity and therefore results in attenuation and

Table III—Other biopotentials.

Signal	*Amplitude, (mV)*	*Frequency (Hz)*	*Duration (sec)*
Electromyograph (EMG)	0.1 to 5 p-p	20 to 5000	2 to 15
Electrooculograms (EOG)	1.0	DC	——
Electroretinograph (ERG)	0.5 p-p	——	1000+

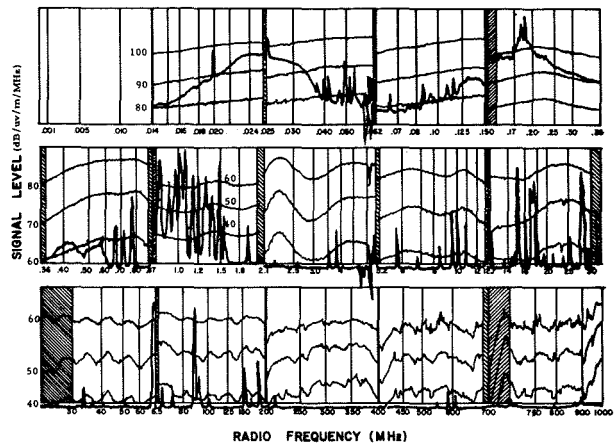

Fig. 2—Radiation broadband and CW in operating room.

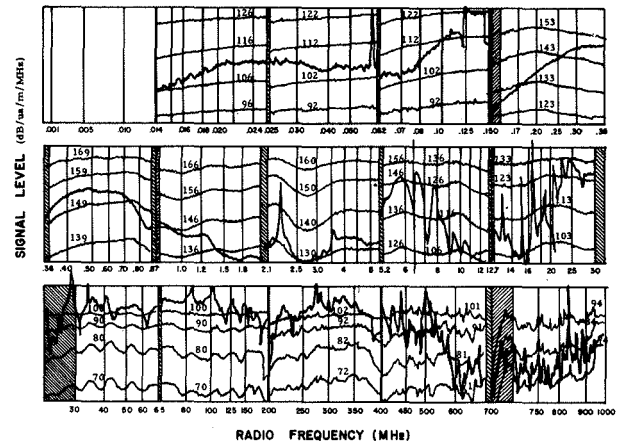

Fig. 3—Broadband radiated (electric cautery device).

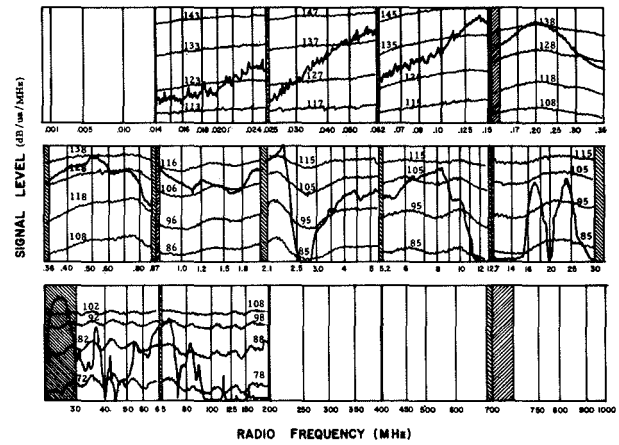

Fig. 4—Power line conducted (electric cautery device).

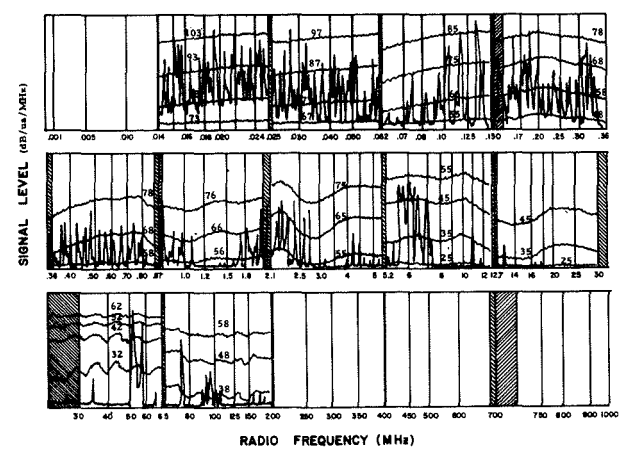

Fig. 5—Power line conducted.

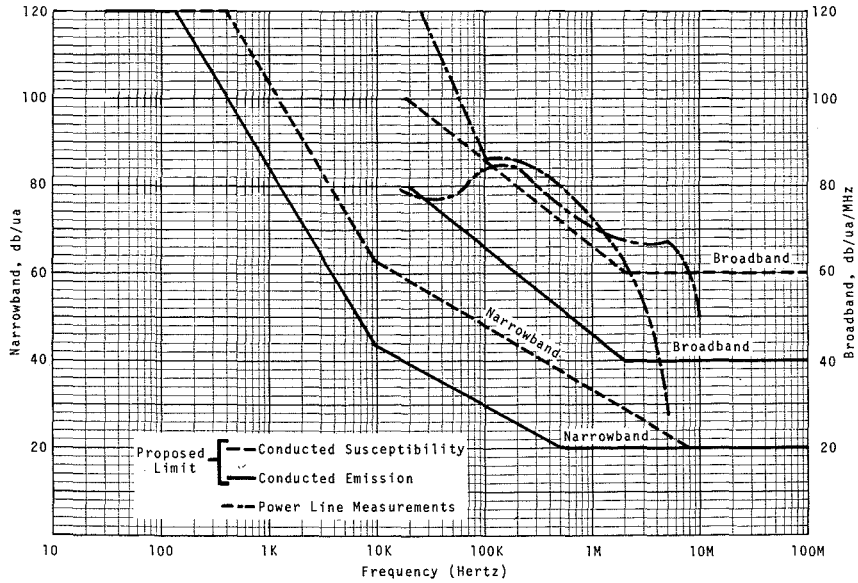

Fig. 6—Conducted emission and susceptibility, power lead (narrowband and broadband).

disorganization of the EEG. Several distinct waveshapes are associated with the EEG (Table I).

The electrocardiogram (ECG)

The ECG detects the electrical signals from the heart. A signal from a normal heart is shown in Fig. 1. The *P* wave represents atrial depolarization and the *QRS* complex occurs as a result of ventricular depolarization. The repolarization of the ventricles occurs during the *T* wave. The ECG wave components are given in Table II.

Fetal electrocardiograms

Heart signals of the fetus have been recorded. This is of particular importance during delivery where a temporary interference with blood flow can cause permanent damage. In the trace derived from the mother's abdomen, the fetal signals are superimposed on the mother's signals. Moreover, the amplitude ratio (maternal to fetal) may be 30 to 1 with the average maternal peak to peak signal showing 1200 μv. The major portion of the energy in the mother's ECG is below 20 Hz, and the fetal *Q*, *R* and *S* wave peak power content is near 30 Hz.

Other biopotentials

Significant signals have been obtained from other muscle fibers (see Table III).

Levels of interfering signals

The originating source of the interfering signal (noise source) can be considered to be either primary equipment (designed as radiators); or secondary (equipment intended to perform some function other than the radiation of RF signals). Examples of the former are diathermy equipment and x-ray equipment, and the latter, motors, sliding contacts, elevators, and spark-gap cutting devices.

The radiating levels of diathermy, x-ray, etc., equipment are regulated by the Federal Communications Commission (FCC). As known radiating devices, controls are included in their design to limit radiation of all frequencies other than the design operating frequency. These controls included directional radiators, shielding, and filtering. With the secondary noise sources, however, a different problem is encountered. Here the noise sources are switch closures and openings, motor commutators, the make and break of sliding contacts, and electro-surgical instruments such as those used to cut, and coagulate or cauterize. The noise generated by these devices appear throughout the RF spectrum either as a noise spike or broadband levels (Fig. 2). Fig. 3 shows the broadband radiated noise level of an electrosurgical unit, identified as one of the worst EMI generators. Fig. 4 indicates the noise levels impressed upon the power lines by the unit, and Fig. 5 the noise encountered on the hospital power lines without the unit.

Fig. 7—Radiated emission susceptibility, electric field (narrowband and broadband).

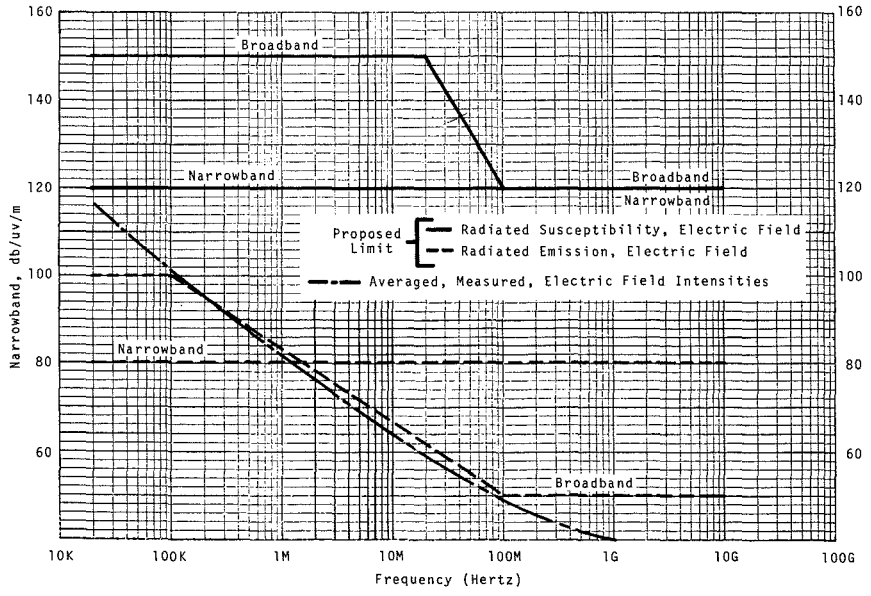

Techniques of measurement

The measurement techniques used were typical of those methods specified in the various military specifications for EMI, such as MIL STD 826. Discrete data as well as data derived from automated equipment scans were used to obtain both qualitative and quantitative data at various times.

Measurements were made at a "quiet" time of the day as well as "noisy" in order to obtain comparative data. When possible, measuring antennas were erected in operating rooms during operations as well as in unused operating rooms for additional comparative data. The RF noise is usually identified by frequency, spectral characteristics (broadband and CW), and means of transmission (conducted and radiated).

Emission and susceptibility tests

Tests were performed in two hospitals. Data was taken in and near the operating rooms because it was felt that here interfering signals would cause the greatest potential patient hazard, i.e., where the greatest number of different pieces of electronic equipment would be utilized simultaneously.

Conducted emission on power leads, 30 Hz to 100 MHz (broadband, narrowband)

The curves (long-and-short dashes in Fig. 6), result from measurements made on three of the main power lines to the operating room suites taken at the distribution panel nearest the op-

erating room. The proposed curve, identifying both narrow and broadband noise, is shown by the heavy line. This curve is based upon the ambient emission levels measured. It is 10 to 15 dB below measured ambient levels, to provide some assurance that no *single* device will significantly raise the ambient level to an uncontrollable point.

Conducted emission on control and signal loads, 30 Hz to 100 MHz

The same limits specified for power lead conducted emission (Fig. 6) hold here. The need for a separate category results from the different test setup and procedures used for each test.

Conducted susceptibility via power lines, 30 Hz to 100 MHz

Fig. 6 also shows the proposed limits for narrow and broadband conducted susceptibility on power leads. The meaning of a broadband measurement becomes less significant when the lower frequency regions are considered. Thus, the broadband limits cut off at 14 kHz. The curves represent a statistical average of points taken on a White Electromagnetic Model 120-A Automatic Scan System.

Radiated emission—electric field, 14 kHz to 10 GHz

The curves in Fig. 7 again represents the suggested specified levels and are the statistical averages of a series of measurements made in both hospitals. Narrowband measures omit peaks due to local TV and radio transmission and electrical-surgical equipment. These peaks range from 60 to 120 db/microvolt/meter.

Radiated susceptibility—electric field, 14 kHz to 10 GHz

Fig. 7 was developed based on measurements and least-square calculations. These curves, too, show the suggested limits to which equipment used in a hospital should be designed.

Radiated emission and susceptibility—magnetic field, 30 Hz to 30 kHz

Measurements were made over the frequency range of 30 Hz to 30 MHz. (It should be noted that normally these measurements are not taken above 30 kHz). Fig. 8 shows the statistical average of these measurements, a result of data taken from five locations at both hospitals.

Conducted susceptibility via power leads, line voltage spike

Fig. 9 represents the proposed limit for a voltage spike on the power leads.

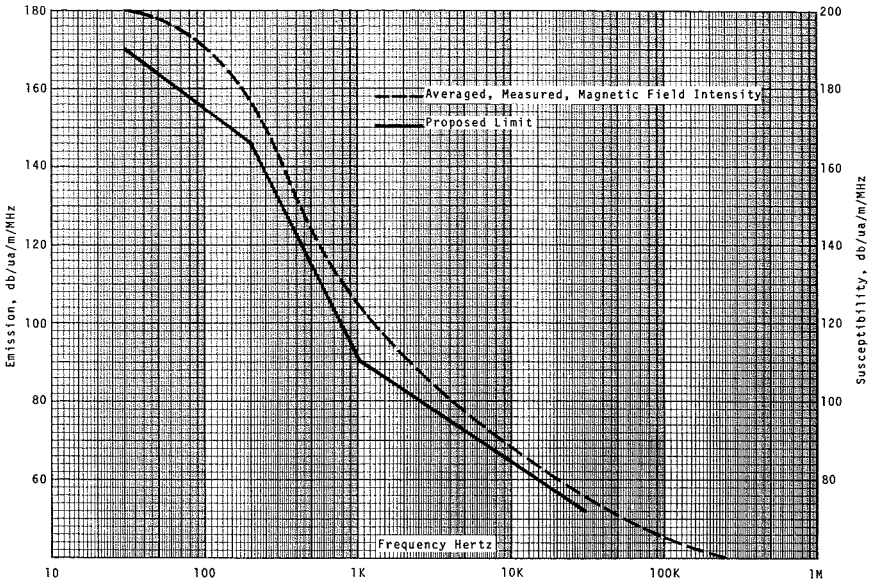

Fig. 8—Radiated broadband magnetic field (emission and susceptibility).

The data was taken by sampling the line current, using a current probe, and is a result of the averaging of data taken at both hospitals. These spikes can occur anywhere over the frequency spectrum. Their shape and amplitude must be considered if there is any possibility of their falsely triggering the patient monitoring/measuring equipment.

These spikes may be caused by variation in power requirements resulting from the switching in and out of equipment. A sample of the line voltage variation in each hospital during a 24-hour period is tabulated below:

Time	*Hospital 1*	*Hospital 2*	*Floor*
2:00 AM	129 VAC	119±2 VAC	A
2:00 PM	118 VAC	119±2 VAC	A
2:00 AM	119 VAC	119±2 VAC	B
2:00 PM	109 VAC	119±2 VAC	B

Rationale used to establish limits

Although the number of hospitals sampled was less then desirable, the following assumptions were made:

1) A safe limit is defined as that level at which the equipment does not interfere with other equipment, nor is susceptible to interference by other equipment.
2) A spread of 20 to 30 dB should be placed between emission and susceptibility levels to achieve the safe limit. This amounts to an emission limit of 10 to 15 dB below the measured ambients and a susceptibility limit of 10 to 15 dB above the measured limits.

Hospital equipment must be tested to the above considerations. A reasonable approach for new equipment design is to specify that the new equipment does not add any noise to the environment (emission) nor be affected by existing noise levels (susceptibility). In order for this approach to be meaningful, the magnitude of typical ambient levels must be ascertained. We have begun to do just that.

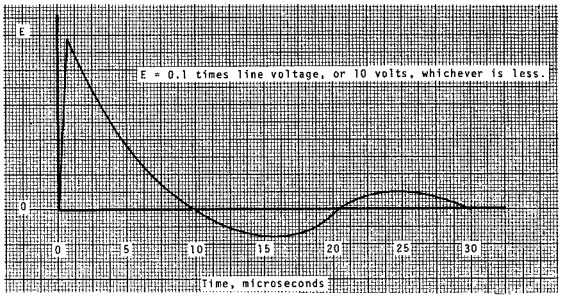

Fig. 9—Limit for conducted susceptibility, power leads, spike.

Conclusion

We have started to look at the problem of Electromagnetic Interference in modern hospitals. The main emphasis has been on the levels of electromagnetic signals from "inner space", the noises of outer space, and their implication to medical electronic equipment design. The data presented will also be of interest to architects of hospitals and in the specification of electric service equipment. The study had been started because no industry or government specification could be found. It is hoped that this paper may represent a step in the formulation of such an industry-wide specification.

Our conclusions stress the need for additional work in this area. A recommendation is made to work toward industry-wide EMI standards, that include effects of radiated and conducted, electric and magnetic fields levels. Then, as EMI offensive devices become outdated, lesser interference can be hoped for among the increasing sophisticated number of devices.

TV monitoring of satellite antenna-boom position

J. R. Staniszewski | W. Putterman

The Radio Astronomy Explorer—Antenna Aspect System (RAE-AAS) is the lightest-weight two-vidicon instrumentation system, complete with PCM formatter, designed for space applications to date. The development of a ½-inch vidicon with white-going, temperature-stable reticles, the development of a magnetic focus and deflection yoke weighing less than 80 grams, and the development of analog camera circuits in hybrid micro-electronic configuration for the RAE-AAS are the significant advances which will benefit future space-oriented camera designs. The paper includes discussions of the system concept, the mechanical design concepts, and the circuit implementation.

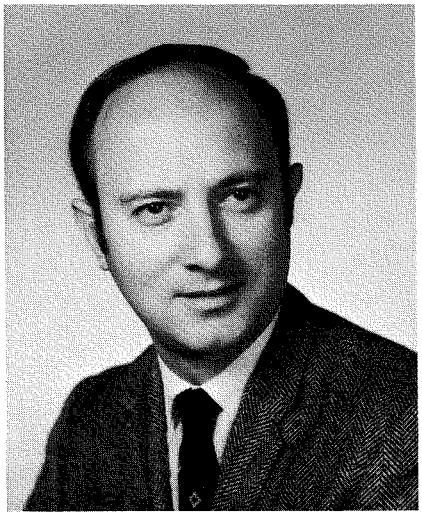

William J. Putterman*
Sensor and Display Engineering
Astro-Electronics Division
Princeton, N.J.

received the BEE from the Brooklyn Polytechnical Institute in 1958 and presently is enrolled in a graduate program at Rutgers University. From 1958 until 1961, he worked at the Missile & Surface Radar Division, where he designed display circuitry for the BMEWS and Tradex projects. In 1961, he transferred to the Astro-Electronics Division, with the television design group. Mr. Putterman has worked on a variety of television system designs, including circuitry for the cameras of the Orbiting Astronomical Observatory, and TIROS spacecraft. He has also participated in systems analysis for the TIROS-APT "wheel" spacecraft, the TIROS M spacecraft, Surveyor Lunar Rover Vehicle, and classified projects. Mr. Putterman's most recent assignments have been as lead engineer on the Antenna Aspect System cameras for the Radio Astronomy Explorer satellite and as design engineer for the Dynamic Beam Current Regulator for the 2-Inch Return Beam Vidicon.

* Since this article was written, Mr. Putterman has transferred to NBC.

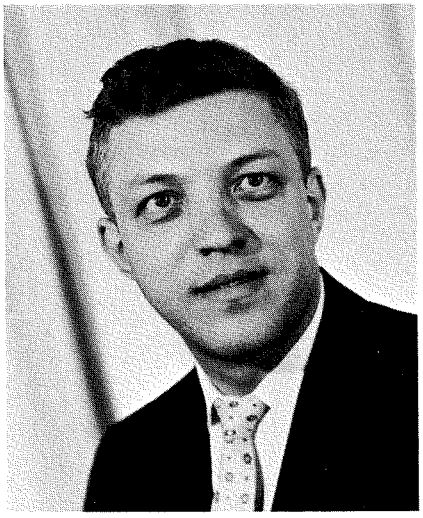

Joseph R. Staniszewski, Mgr.
Program Management
Astro-Electronic Division
Princeton, N.J.

received the BS in Physics from the Carnegie Institute of Technology in 1950 and subsequently did graduate work at the University of Pennsylvania. From 1950 to 1953 he worked as a radar instructor in the Netherlands. In 1953 he joined RCA and was initially assigned to the design and development of automatic tracking circuits for the Mod II Shoran. He also developed a tracking radar simulator, using analog computer techniques. He participated in the design and development of a closed-loop television system utilizing a sensitive image orthicon for military airborne applications. Mr. Staniszewski transferred to the Astro-Electronics Division in 1958 and worked on the development of a miniature television camera for space vehicles. In 1961, he joined the Ranger Project and became an engineering group leader in that project in 1963. He participated in definition studies for the Apollo Command Module, Pallett, and the Lunar Scientific Survey Module. In 1966, he became Project Manager for the Antenna Aspect System Cameras for the Radio Astronomy Explorer Satellite. He presently is Program Manager of a classified project. He is a member of the IEEE and has presented papers on the space applications of television at the American Astronautical Society, the Franklin Institute, and the IEEE Symposium on Military Electronics.

Reprint RE-15-3-17
Final manuscript received May 8, 1969.

EXPLORER 38, the Radio Astronomy Satellite, was launched from Vandenberg AFB, the West Coast Missile range on July 4, 1968, and placed into a 3,640-mile, retrograde orbit. This satellite measures radio signals from within the solar systems and from cosmic sources as a function of frequency, direction, and time. The frequency band measured is from 0.5 to 10 MHz; observation in this range of frequencies from galactic emitters has been denied to earth-based radio telescopes because emissions below 10 MHz are reflected back into space by charged particles in the atmosphere. Expectations are high that new observations of the Galaxy will be added to the literature of astronomy, with this new radio-frequency-window opened for the first time.

The receiving equipment carried in this satellite consists of nine-step Ryle Vonberg Radiometers and associated antenna systems. The receivers measure nine different frequencies: 0.45, 0.7, 0.9, 1.3, 2.2, 3.9, 4.7, 6.55, and 9.2 MHz. There is an antenna system and associated radiometer to observe galactic emissions and an antenna and radiometer to observe emissions from the earth's magnetosphere. The success and feasibility of the mission depended upon the long, tubular, extensible booms, shown in Fig. 1, that make up the antenna systems. (The horizontal booms seen in Fig. 1 are associated with other functions, and are of no interest to the present discussion.) The two *V* antennas atop and below the satellite have been extended to their full 750-foot length.

The pairs of booms extend at a 60° included angle. Each of the booms is monitored by a slow-scan television camera using a ½-inch vidicon. The cameras measure antenna deployment and bending through the use of a five-point reticle. They also provide position data on the antenna boom tips, which is used to derive antenna aspect information and, ultimately, to locate low-frequency radio emissions received through the upper array.

After launch and stabilization of the satellite, the downward-looking camera showed an image of the earth's disc. As shown in Fig. 2, the downward-looking antenna booms are somewhat obscured by the background of the earth. It is, however, indicative of

the satellite's stability. At a boom extension of 450 ft., the upward-looking vidicons showed the root of the boom and the small video signal of the boom tip (Fig. 3).

TV camera system

The television system, designated the Antenna Aspect System (AAS), utilizes the first of a new class of ultra-miniature television cameras which incorporate microelectronic circuits and ½-inch vidicons in the basic design. The system consists of two dual-camera heads, each using two ½-inch electro-magnetic-focus vidicons contained in one integrated camera housing, as shown in Fig. 4. Each vidicon is equipped with a 5.5 mm, f/1.8 lens, a sun sensor, and a sun-shield shutter. Each vidicon-lens combination can view the tip of one of the 750-foot-long antenna booms (at full extension) as it sways within a 60° field of view. The camera housing is designed to maintain a pre-set pointing angle to within ±0.1°, referenced to the mounting surface. Contained within the camera housing are video pre-amplifiers and amplifiers for each vidicon, deflection generators and amplifiers, and focus-current and beam-current regulators. A separate camera-electronics assembly contains power-conditioning circuits, camera-programming circuits, and data-processing circuits.

A precise 10-kHz tuning-fork-oscillator clock and counting circuits provide the basic timing for raster formation and camera programming. The analog video from each vidicon is processed through an analog-to-digital converter and a PCM formatter. The Antenna Aspect System provides a 10 kilobit/second, split-phase PCM output which is delivered directly to the satellite's high-power transmitter on demand.

The camera housing assembly and the camera electronics assembly weigh a total of 5.25 pounds and require an average power of 6.5 watts from the 18-volt DC spacecraft bus. The approximate volume of the camera housing assembly is 86 cubic inches.

Camera programming

The camera head viewing the upward-looking antenna booms normally is connected to the camera electronics. A manual command sent before the programming sequence will connect the downward-looking cameras instead.

The system is put into operation by two spacecraft commands. The first command—ABLE POWER ON—excites the sun sensors and the power-sensing circuit. The second command—SYSTEM POWER ON—puts all of the camera circuits into operation. Application of the 18-volt system power is the signal for the solenoid-operated shutter to open, providing the sun is not in the field of view of the sun sensors. The field of view of the sun sensor is slightly larger than the vidicon's field of view so that a shutter-actuation signal is generated as the sun enters the field of view of the sensor.

With the shutter open, a nominal 60° circular field of view is imaged, inscribed on the 6.3 x 6.3-mm vidicon format. The vidicon has a solid-porous-solid (SPS) photoconductor; a five-point reticle array is etched into the photoconductive layer. The typical residual signal of an SPS photoconductor after one scanning frame is approximately 5% of the initial signal. The white-going reticle pattern provides an accurate and invariant position calibration for antenna booms when imaged against the dark field of space. The one-to-one aspect image of the vidicon is scanned with a linear array of horizontal lines. There are 256 lines scanned in a 13.56 second frame. The camera electronics provides automatic sequencing of the two vidicons such that four frames are read out from vidicon one, followed by four frames from vidicon two. The sequence is repeated until the system power is commanded off by the manually initiated commands: ABLE POWER OFF and SYSTEM POWER OFF, in that order.

Boom-position determination

A 3-inch-diameter Lexon ball is attached at the end of each antenna boom. Lexon is a plastic product of the General Electric Co. The transmissive and reflective properties of the Lexon ball are such that the brightness is nearly constant as a function of the sun-ball-camera angle. The worst-case brightness is expected to be 800 foot-lamberts. The ball is imaged on the photoconductor as a point-source diffraction pattern which is smaller than a resolution element. However, the scanning beam aperture is designed to

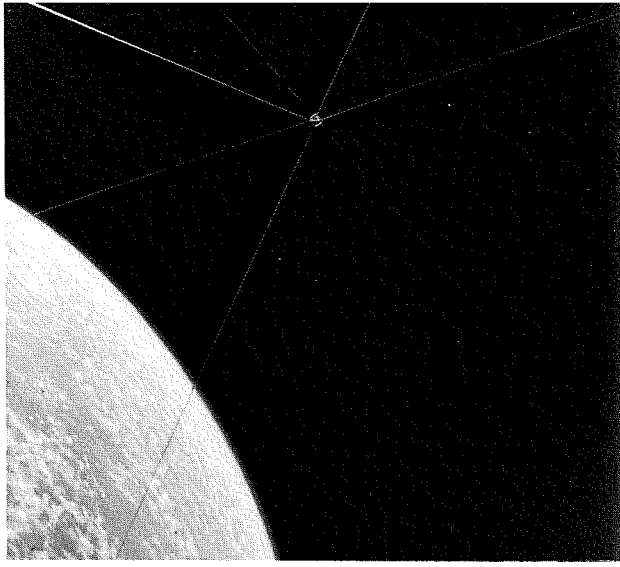

Fig. 1—Radio Astronomy Explorer Satellite (artist's concept) with antenna booms deployed.

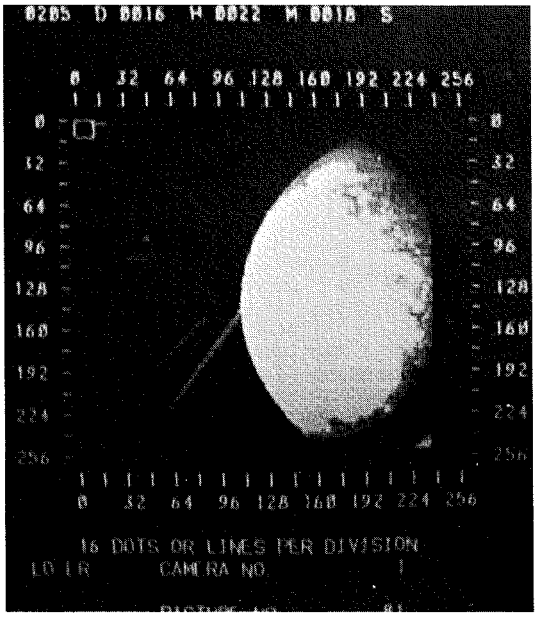

Fig. 2—TV picture of earth-facing booms (with earth in background).

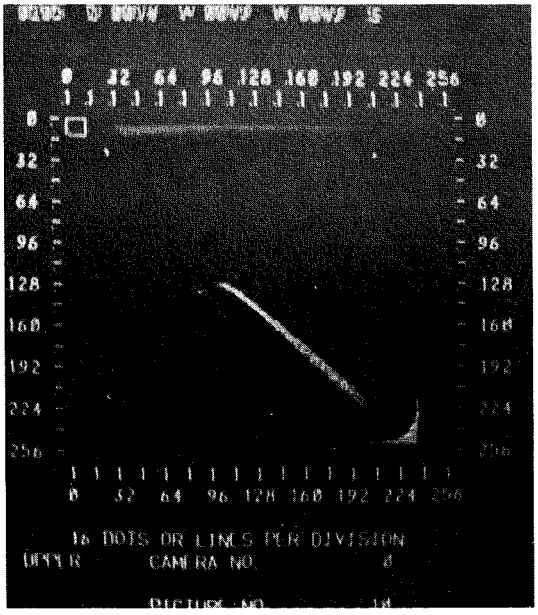

Fig. 3—TV picture of space-facing booms, showing boom root and tip.

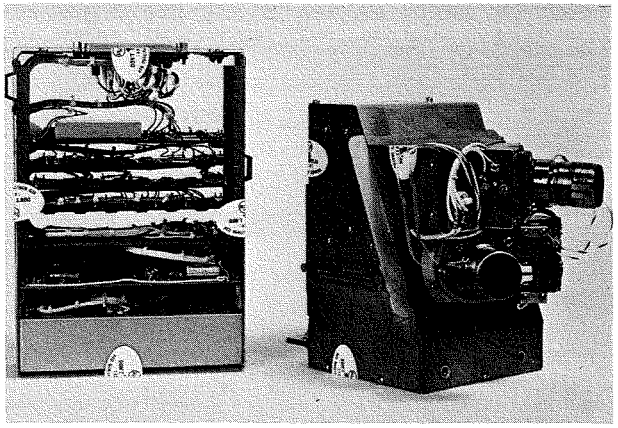

Fig. 4—Antenna Aspect System dual-camera head and associated electronics (before encapsulation.)

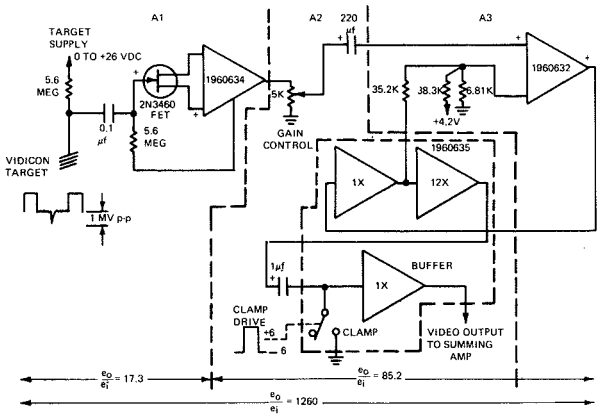

Fig. 5—Video preamplifier and amplifier.

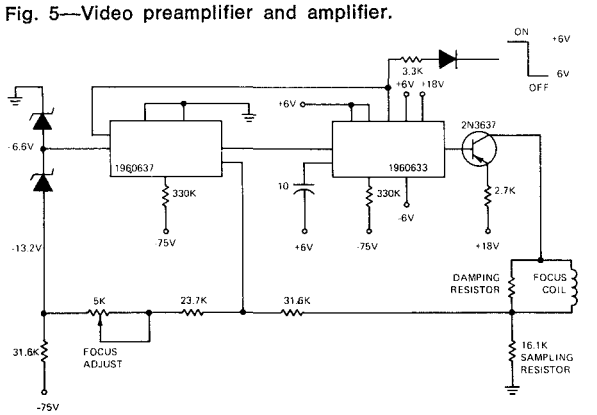

Fig. 6—Focus-current regulator.

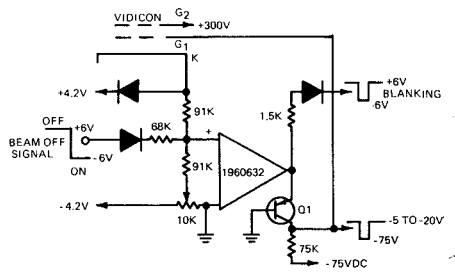

Fig. 7—Beam-current regulator.

cause the energy in the point source to spread over an area about three elements in length by three lines in width.

The TV system has sufficient resolution capability to detect 0.25° changes in boom-tip position and to locate a point to within ±0.5° in a 60° field of view.

Imaging techniques

The sensitivity of the vidicon and its unique electron-beam scanning aperture provide the means for imaging the three-inch ball when the boom attains its maximum extension distance of 750 feet. The vidicon's electron optics are controlled to provide a scanning aperture which has an electron distribution which is approximately Gaussian.

The ability to satisfactorily image the "point-source" target also depends on its luminous intensity. With a solar input of 13,400 foot-candles, the computed brightness of the target ball will vary from 900 foot-lamberts to 4500 foot-lamberts. For this range of brightness, the SPS vidicon operates in a slow-scan mode with a 13-second frame time and produces a signal exceeding the minimum signal-to-noise ratio of three-to-one required for the detectivity threshold.

Position calibration

The viewed area of interest is calibrated by superimposing an imaginary grid on a plane perpendicular to the vidicon's optical axis. The grid configuration is based on the number of scanning lines and the number of samplings per line required at the vidicon for the specified accuracy of position determination. Fragmenting the 60° field on the vidicon by 252 lines and 240 samples/line resulted in the desired 0.25 degrees/line and 0.25 degrees/sample element, forming a grid box or "cell" which provides ±0.5° position determination.

The scanning system is a standard television raster development, whose timing source is an accurate clock. The clock is counted and, at appropriate times, horizontal and vertical sync signals are generated which initiate linear-deflection waveforms (that are accurately related to one another as a function of time) to be applied to the vidicon yoke. The deflection waveforms are so applied as to cause the electron beams to scan the vidicon's faceplate and a linear array of horizontal lines is laid down on the vidicon until the 6.3-mm-high image format has been covered by 252 lines. The accurate timing used to recycle the beam deflection and the care taken to ensure a linear displacement of the electron beam per unit time are the principle *a priori* information used to convert scan-line number and element-sample number to an angular location, referenced to the optical axis. A linear vertical-deflection waveform will ensure that each line has a dip of exactly 1/252 of the raster height during the time the horizontal deflection is taking place. The sampling of the video information, which is occurring as the horizontal deflection is scanning the width of the raster, is performed in the analog-to-digital converter at a 5-kHz rate, and each new element is sampled as the deflection beam progresses across 1/240 of the line width. The combination of these timing waveforms and timed samplings partition the plane which contains a projection of the circular field-of-view into the more than 60,000 location "cells." The deflection is so applied so that the first information cell in the upper left-hand corner is the first to be sampled. All the cells in the first horizontal line are sampled in sequence. This is followed by a sampling of line 2, line 3, and each succeeding line, until the bottom of the raster (line 252) has been sampled. During the time of an additional four horizontal lines (lines 253 to 256) the tube is blanked off and the vertical deflection is retraced, and the sampling procedure is repeated.

TV camera configuration

The camera assembly is machined from a solid block of magnesium with tolerances held to one mil to ensure system accuracy at mounting interfaces. The yoke assembly supports the ½-inch vidicon in the electromagnetic deflection and focus fields. The vidicon can be rotated within the yoke before being locked in place; the end of the yoke housing is machined into a ball which fits into a socket held in place by the housing and provides a convenient means for two degrees of freedom for optical alignment. Two such yoke assemblies, containing ruggedized vidicons are supported within the camera housing. The lens, a nine-element, Schneider-Cinegon, mounts to the yoke along with a sun-shield shutter and a *CdS* sun sensor. In addition to the electro-optical assemblies, the camera head contains video, deflection, sun-shutter, and telemetry circuits.

The camera electronics are contained in an aluminum shell with one third of the volume devoted to the power supply and regulators, a second third of the volume for the clock and counters, and the final third for the analog-to-digital converter and signal-output

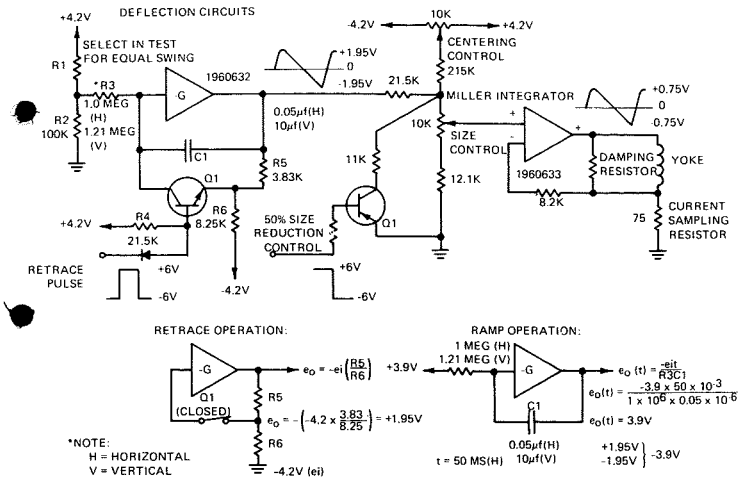

Fig. 8—Sawtooth generator and sweep amplifier.

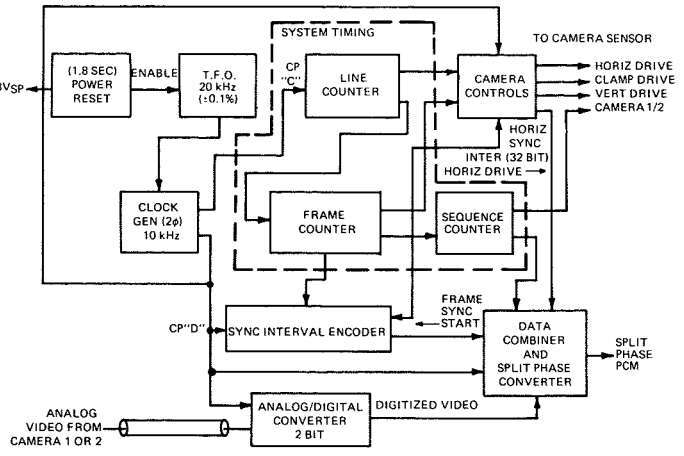

Fig. 9—Oscillator and countdown logic.

stage. The saturable reactor for DC-to-DC conversion is mounted on a printed-circuit board along with transistor drivers and is enclosed in an 18-mil mu-metal enclosure. A top it fitted on the mu-metal container, which fits into the end of the aluminum bracket. Electrical connections are made to the regulator board through feed-through filters and terminals. The regulator circuits are on a printed-wiring board which is located next to the power convertor and an aluminum bulkhead. The remaining four circuit boards are multi-layered and provide the interconnections for the digitally processed controls and data management. These boards are each made up of four printed layers separated by insulating material and bonded into the multi-layered form. Two layers are used for signal paths, one layer for the distribution of the B supply, and the third layer for the power supply return. The entire assembly is foam-encapsulated with a solder-spray coat applied to external foam surfaces for electrostatic shielding.

Camera electrical design

Video circuits

The video-amplifier and high-level-drive video circuits (shown in Fig. 5) consist, mainly of one field-effect transistor and three hybrid integrated circuits. The first field-effect, hybrid-circuit combination provides a transformation from the high source impedance to a low output impedance with an approximate gain of 17. The second and third hybrid circuits are combined into a feedback amplifier with an overall gain of 70. A portion of the second hybrid circuit performs dark-current clamping and inhibits video output whenever the alternate vidicon is on the line. The composite video from each sensor is combined in an operational amplifier and coupled to the analog-to-digital converter located in the electronics assembly.

Focus- and beam-current regulators

The focus-current regulator combines hybrid integrated circuits and a power transistor output stage into an operational amplifier configuration. This circuit is shown in Fig. 6. The focus output is determined by the closed-loop gain, which is controlled by means of a potentiometer located in the feedback loop. The nominal focus current is 110 milliamps with *G3-G4* of the vidicon at +175 volts and *G2* at +318 volts. To conserve power, the regulator associated with the tube that is not in use is cut off. The beam-current regulator schematic is shown in Fig. 7. The unique feature of this circuit is that the vidicon's *G1* and cathode elements are connected into the feedback loop of the regulator. The circuit maintains a constant current at a pre-set level over the operational lifetime of the vidicon. The range of beam current control is zero to 46 microamperes. Horizontal and vertical blanking pulses are inserted at the output stage of this regulator. During blanking, the beam is cut off by moving the *G1* potential to −75 volts. During the period when the vidicon is off line for four frames, an additional signal is gated in at this point to cut off the beam current.

Shutter control

A shutter assembly, two solenoids, and a *CdS* sensor are associated with each vidicon in a protective system for preventing direct solar inputs to the vidicon. One solenoid pulls the shutter into the open position and the other solenoid pulls it into the closed position. As the sun enters the field of view of the *CdS* sensor, a hybrid IC comparator circuit changes state and closes the shutter. Conversely, the shutter will open when the sun leaves the sensor field of view. A third hybrid IC comparator is used to sense system power. The shutters will automatically open, provided the sun is not in the field of view of either of the vidicons, whenever the SYSTEM POWER ON command is given to the Antenna Aspect System (and providing that the ABLE POWER ON command, which activates solenoid driver, *CdS* logic, and power logic and switches, has already been given).

Deflection circuits

Six hybrid IC's and four discrete transistor switches make up the horizontal and vertical deflection circuits, and a precisely linear current ramp is generated in a Miller-type integrator. These circuits are shown in Fig. 8. The Miller integrator provides the input for the yoke driver. Four drivers are available for the horizontal and vertical coils of each vidicon yoke. Each driver has amplitude and centering controls, and when the particular vidicon is off-line, the optical stages reduce the peak-to-peak amplitude of the deflection to half to conserve system power.

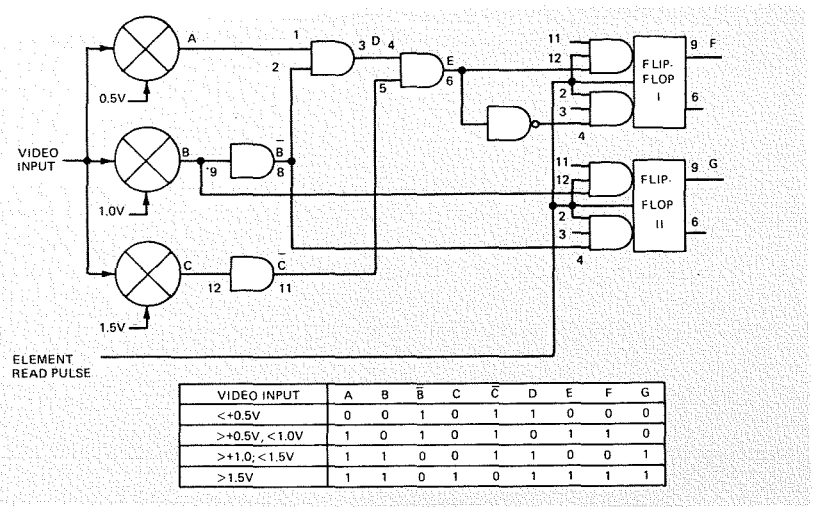

VIDEO INPUT	A	B	$\bar{B}$	C	$\bar{C}$	D	E	F	G
<+0.5V	0	0	1	0	1	1	0	0	0
>+0.5V, <1.0V	1	0	1	0	1	0	1	1	0
>+1.0; <1.5V	1	1	0	0	1	1	0	0	1
>1.5V	1	1	0	1	0	1	1	1	1

Fig. 10—Analog-to-digital converter.

Camera timing and control

The Antenna Aspect System is automatically programmed after the power turn-on command is received to read out four frames from camera one, followed by four frames from camera two. This sequence is repeated until the POWER OFF command is received. This programming function is performed by four hybrid IC's and three transistors in the camera-control programmer circuit. One of the hybrid IC's is a flip-flop, which is associated with the sequencing of the two cameras. The camera 1 and camera 2 ON commands from the electronic assembly are coupled to the flip-flop. The commands are DC levels, four frames in duration. When the level for one command is high, the second is low. A high-level command indicates that its associated camera is to be gated through to the analog-to-digital converter. In addition, the flip-flop controls the turning on and off of the beam and focus current regulators and the horizontal and vertical deflection size for the two cameras.

The heart of the basic timing system is a 20-kHz tuning-fork oscillator which has a short term accuracy of ±0.1% (see Fig. 9). The oscillator is self-contained in a hermetically sealed mu-metal can. The 20-kHz signal is used to generate the 10-kHz clock signals, 180° out of phase. These two 10-kHz signals are designated as CP—C and CP—D. The CP—C signals start the system timing counter chain; the CP—D signals clock the data generation and readout functions in the analog-to-digital converter, the sync interval encoder, and the data combiner. They also trigger the camera control signals.

The system timing is generated in a 20-stage serial (ripple-carry) counter chain functionally divided into: a 9-stage line counter, an 8-stage frame counter, and a 3-stage sequencer counter. The line counter provides 512, 100 μs bit periods per line, the frame counter provides 256 lines/frame, and the sequence counter provides a repetitive sequence of four camera-1 frames and four camera-2 frames. The counting sequence is initiated 1.8 seconds after system power is applied and repeats until system power is removed.

The vertical drive, clamp drive, camera-1 and camera-2 drive signals, and the horizontal sync interval (32 bits) are generated by synchronous (S-R) operation flip-flops. The horizontal drive signal to the vidicon is derived from the shift register in the sync interval encoder.

The analog-to-digital converter, shown in block form in Fig. 10, accepts the analog video signal from the video combiner amplifier and converts it to a 2-bit binary signal at the 5-kHz sampling rate. This provides 240 samples per active line period (48 milliseconds). To resolve four quantum levels in the simultaneous sample analog-to-digital converter, the analog signal is continuously applied to three thresholding comparator circuits. Then, depending on which of the comparators is activated, the relative amplitude of the input video signal is identified. The comparator outputs are encoded to provide the instantaneous two-bit binary equivalent of the video amplitude.

The resultant binary signals present at the output of two synchronously operated flip-flops during the sampling aperture are stored and read out serially in real time to the data combiner.

The sync-interval encoder generates the timing signals for deriving the 23-bit pseudo-random code signal for the horizontal (minor frame) synchronization and for serial readout of the camera identification (1 bit) and line number identification (8 bits) during the horizontal sync interval, the first 32 bits of each scan line. These sync codes and line and camera identifiers are generated in a three-stage shift register and a six-stage shift counter supplying timing signals to five NAND-gate and nine NAND-gate "wired OR" decoders at the start of each horizontal line.

The data combiner is a three NAND-gate "wired-OR" configuration for serial formatting of the vertical sync interval (the first four lines of each frame coded to all logical ones during the active line period), horizontal sync code, camera and line number, and video data in a non-return-to-zero (NRZ) form, which is presented to the split-phase generator. The final-output is a split-phase PCM signal which is generated by combining the NRZ data signal with a 10-kHz symmetrical square wave in an exclusive-OR gate.

Conclusion

A new ultra-miniature television camera system is being used on the Radio Astronomy Explorer satellite to view the position of four extensible boom antennae that are 750 feet long. The camera system incorporates one-half inch vidicons with individual lens assemblies and video processing circuits. Hybrid integrated circuits are used for the camera programming and to convert analog video into the 10 kilobit, biphase PCM data stream. Transmission is in real time with the data stream either displayed on a kinescope or processed in a computer. The antenna boom position is determined to within ±0.5° in a 60° field of view by imaging a three-inch-diameter ball attached at the end of each antenna boom. The complete equipment installed on the satellite weighs 5.25 lbs and requires 6.5 watts of power from the spacecraft's 18-volt bus when in operation.

Engineering and Research Notes

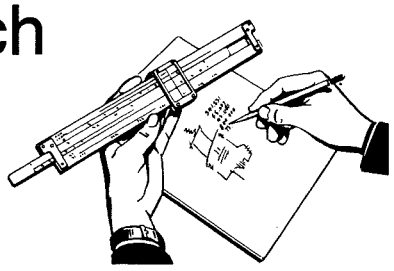

Brief Technical Papers of Current Interest

New maser packaging approach

G. G. Weidner | D. J. Miller
Applied Physics
Advanced Technology
Laboratories
Camden, N.J.

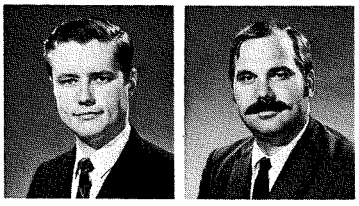

Weidner Miller

Advanced Technology Laboratories (ATL) has achieved significant improvements in maser packaging techniques through a reduction in the size and weight of superconducting magnets. Previously only one maser-magnet combination could be packaged in the limited volume of a closed-cycle refrigerator (CCR). The reduction in magnet size for comparable performance has enabled packaging multiple masers in the same CCR. This new versatility in packaging promises to extend the applications of masers. Immediate applications include 1) a wide-tuning-range amplifier system with masers tuned to adjacent bands, 2) broadband, fixed-tuned masers (e.g., 150 MHz, 30-dB gain each at C-band) covering different bands, and 3) very broadband, fixed-tuned masers (e.g., 400 to 500 MHz, 10-dB gain each) in cascade.

ATL has applied this technique in the development of a wide-tuning-range, low-noise amplifier system for Cassegrain antenna mounting, consisting of three maser-magnet configurations in a single CCR. The amplifier tunes from 1.8 to 6.2 GHz in three separate bands with 25-dB minimum gain and 15°K maximum noise temperature. It is operable in any orientation. Tuning is completely electronic, with only two controls required to adjust frequency. Fig. 1 shows the amplifiers and refrigerator removed

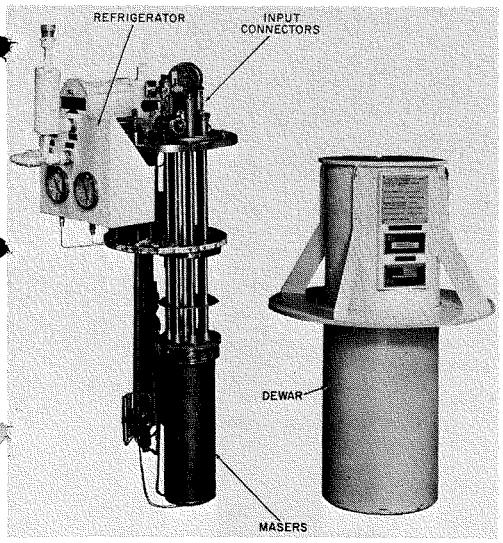

Fig. 1—Maser amplifiers and refrigerator.

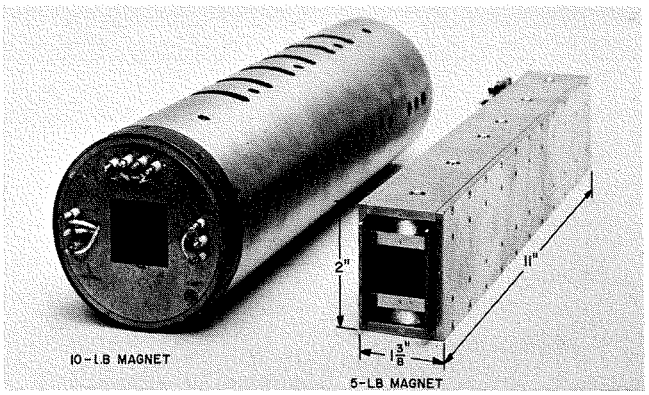

Fig. 2—Reduction in magnet size.

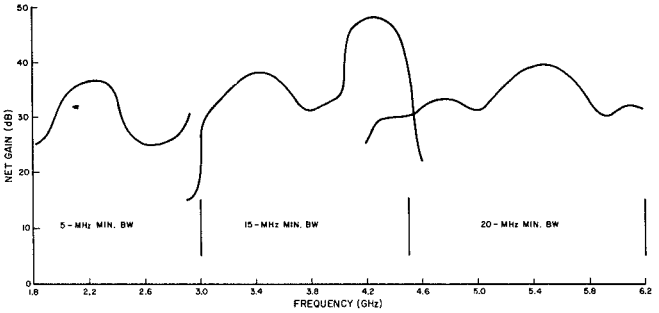

Fig. 3—Gain across the tunable range for minimum instantaneous bandwidth in each band.

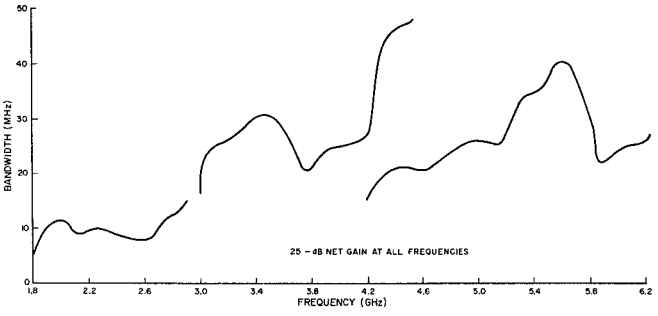

Fig. 4—Minimum instantaneous bandwidth for 25-dB net gain across the tunable band.

from the outer dewar. The input structure has three pairs of coaxial input/output lines and three separate pump waveguides, allowing independent operation of any combination of the three maser amplifiers.

All three amplifiers use rutile as the active material, coupled to printed circuit meander-line slow-wave circuits. The design approach was developed in a laboratory-model tunable S-band maser[1], and the basic packaging/mounting approach was developed for an antenna-mounted, liquid-helium-cooled amplifier tunable from 1.9 to 3.1 GHz.[2]

The requirement for a strong, uniform magnetic field has traditionally limited the practical packaging of maser amplifiers for field use. However, in this design, typical superconducting magnet weight was reduced from 10 to 5 lb.—primarily by eliminating overdesign and shortening magnetic paths. The relative magnet sizes can be seen in Fig. 2.

Strong, stable pump power is provided by Hughes type 381 backward-wave-oscillator (BWO) tubes, the only non-solid-state portion of the system. The BWO tubes are operated well below rated power output and have integral miniature vacuum ion pumps for increased life. Experience to date gives an expected operating life of 5000 to 10,000 hours.

Fig. 3 shows the measured net gain available from each of the three amplifiers for the indicated minimum bandwidths. Fig. 4

shows the measured instantaneous bandwidth of 30-dB net gain. Adjustable staggering of magnetic fields allows the exchange of gain for bandwidth at any frequency in the tunable band, with control settings favoring gain yielding the data in Fig. 3, and favoring bandwidth the data in Fig. 4. Characteristics are summarized in Table I.

Table I—Characteristics of wide-tuning-range maser.

Gain	25 dB minimum
Instantaneous bandwidth	5 MHz minimum, 1.8 to 3.0 GHz 15 MHz minimum, 3.0 to 4.5 GHz 20 MHz minimum, 4.5 to 6.2 GHz
Noise temperature	15°K maximum
Dynamic range	−60 dBm input for 1-dB compression
Input VSWR	2.5:1 maximum
Gain stability	±0.1 dB/30 min

References

1. Morris, L. C. and Miller, D. J., "A Broad Tunable Bandwidth Traveling-Wave Maser", *IEEE Trans. on Microwave Theory and Techniques* (Jul 1964) pp. 421-428.
2. Miller, D. J. and Weidner, G. G., "Wide Tuning Range S-Band Maser", *Proc. IEEE* (Apr 1969).

Reprint RE-15-3-24 | Final manuscript received May 1, 1969.

New carbon-dioxide laser lines in the 9.4 and 10.6 micrometer vibrational-rotational bands

T. R. Schein
Aerospace Systems Division
Burlington, Mass.

Using an echelon diffraction grating as the totally reflective cavity mirror (first described by Mueller and Rigden[1] and more recently by Jacobs and Snowman[2]) within a 3.3-meter-active-length 35-mm-bore carbon-dioxide-laser cavity, we have been able to obtain continuous oscillation on the greatest number of carbon-dioxide laser lines from the $C^{12}O^{16}$ isotope yet reported in the literature. The totally reflecting mirror consisted of a Bausch and Lomb number-3553-08-96 gold-plated plane eschelle grating with 75 grooves/mm blazed for a first-order Littrow wavelength of 12±1.2 μm. The output mirror was a germanium plano-concave substrate coated for minimum reflectivity at 10 μm on the outer surface and gold coated, except for a 0.5-cm diameter central spot, on the inner cavity side. This modified hole-coupling configuration producing a transmitted spot size approximately 60% of the theoretical diameter of the fundamental mode is a compromise between high output power and cavity gain.

The following gas mixture was used at a flow rate of about 3 ft³/hr: CO_2: 7.3; N_2: 17; He:74; H_2:1.4; O_2:0.4. The total pressure measured at the exhaust port was 5 torr. The current density was maintained at 4.7 mA/cm³ during the power measurements—about 50% less than that producing maximum radiation intensity, to protect the epoxy replica grating surface from overheating.

The grating was rotated at 1.9 x 10^{-5} rev/sec using a synchronous timing motor with a precision gear reducer. The total angle subtended in covering the 9.13 to 11.29 μm bandwidth was 4.93°.

The emission lines were identified using a Jarrell Ash Model 78460 Czerny-Turner 1 meter spectrophotometer using a 10-μm blazed eschelle grating. The detector was an unimmersed germanium bolometer whose chopped output was amplified, rectified, and fed to a chart recorder. The resolution of the instrument was approximately 4 Å over the spectral range covered. Power was simultaneously monitored using a self-calibrating thermal detector which deflected 5% of the radiant power into a special thermistor element forming one leg of a dynamic Wheatstone bridge. The square of the current required to heat an identical thermistor element to achieve balance yielded an analog of the radiant power.

Table I summarizes the experimental results. In the interest of brevity, the reader is referred to the wavelength tables given by Laures and Ziegler[3] for the wavelengths and numbers of specific $P(J)$ and $R(J)$ lines. However Table II identifies 12 additional lines with their approximate wavelengths and wavenumbers not reported by Laures and Ziegler. In all cases the expected gain of these lines is low as extrapolated from the data presented by Djeu, et al.[4]

Table I—Summary of vibrational rotational lines identified using grating-tuned 3.3-meter flowing-gas carbon-dioxide laser.

Band	*Branch*	*Inclusive J values**	*Wavelength span (μm)*	*Ave. separation between lines (A)*	*(MHz)*
00^01 to 02^00	R	4 to 52	9.13 to 9.37	95	
	P	4 to 62	9.43 to 9.96	188	
00^01 to 10^00	R	2 to 58	10.01 to 10.37	120	
	P	2 to 56	10.42 to 11.02	220	
00^01 to 03^30	P	14 to 45	10.92 to 11.29	6 18.3	14.5** 44.2

*J values are even integers only except in the 00^01 to 03^30 band where both odd and even integer values are permitted.
**Last entry is double since adjacent lines are grouped in pairs.

Table II—New low-gain CW laser lines in the 3 primary carbon-dioxide-laser bands.

Band	*Line designation*	*Wavelength* (μm)*	*Wavenumber (cm^{-1})*
00^01 to 02^00	P(2)	9.414	1062.24
	P(62)	9.972	1002.80
00^01 to 10^00	R(2)	10.381	963.30
	R(56)	10.051	993.34
	R(58)	10.042	992.75
	P(2)	10.458	956.21
00^01 to 03^30	P(14)	10.921	915.67
	P(15)	10.930	914.91
	P(16)	10.942	913.91
	P(17)	10.952	913.07
	P(20)	10.987	910.17
	P(21)	11.008	908.43

*Wavelength accurate to ±0.002 μm

Fig. 1 shows the chart recorded output from the power monitor as the grating was being continuously swept through the emission band. Several dominant lines are identified in each band

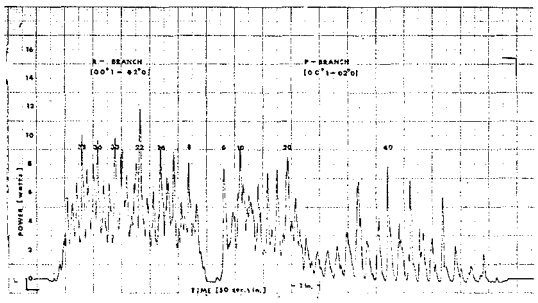

Fig. 1a—Spectral intensities of the (00°1 to 02°0) vibrational—rotational transitions in a grating-tuned CO_2 laser.

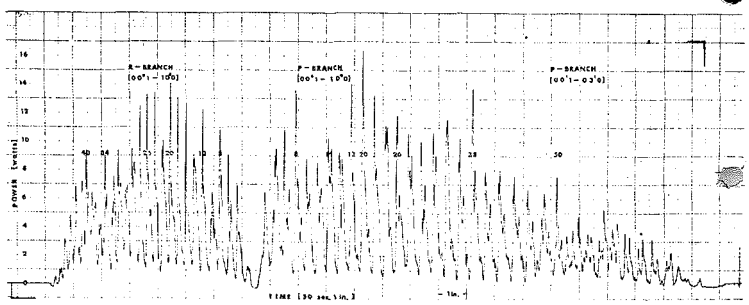

Fig. 1b—Spectral intensities of the (00°1 to 10°0) and (00^01 to 03^30) vibrational rotational transitions in a grating-tuned CO_2 laser.

head. It is of interest to note that considerable output power can be achieved on lines of much less gain than the dominant (00°1 to 10°0) $f(16)$ *to* $P(22)$ lines obtained when an inner-cavity grating is not used. Single-line output power of the dominant lines was nearly two-thirds the power obtained for the same current density when the grating was replaced by a plane mirror resulting in multiline output. In general, the highest intensity lines are found near the center of each branch since the gain is greatest here but this is not always the case as Fig. 1 indicates. Repeated scans show some intensity shifts among the lines. Some lines seem to split. This is caused by the simultaneous appearance of the adjacent line as the grating revolves toward the optimum position for the next line.

References

1. Mueller, G. and Rigden, J. D., *App Phys Lett* Vol 8 No. 2 (1 Feb 1966) p 69.
2. Jacobs, G. B. and Snowman, L. R., *IEEE Journ Quantum Elect* Vol QE-3 No. 11 (11 Nov 1967) p 603.
3. Laures, P. and Ziegler, X., *Jour Chem Phys* Tome 64 (1967) p 99.
4. Djeu, N., Ican, T. and Wolga, G. T., *IEEE Journ Quantum Elect* Vol QE-4 No. 5 (May 1968) p 256.

Reprint RE-15-3-24 | Final manuscript received May 14, 1969.

Analog rate comparator for frequency-difference measurements

P. DeBruyne
Technical Staff
Aerospace Systems Division
Burlington, Mass.

It is often necessary to measure the difference in counting rates of two detector channels, or the difference between two frequencies. While scalers are available that indicate the total of accumulated counts, the time-dependent difference rate can be conveniently and directly determined by employing a ratemeter whose output is a function of the frequency difference to be measured. This method has definite advantages over application of the more accurate events-per unit-time meter, which does not provide for separate count-up and count-down inputs.

An operational amplifier, used in conjunction with a diode current-pump circuit, as shown in Fig. 1, can produce a ratemeter output. The output sensitivity is controlled by the "bucket" capacitors. C_3 and C_4, and the feedback resistor, R_1. The two input terminals are connected to two diode pump circuits of opposite polarity. This circuitry permits the frequency difference between the two signals to be measured.

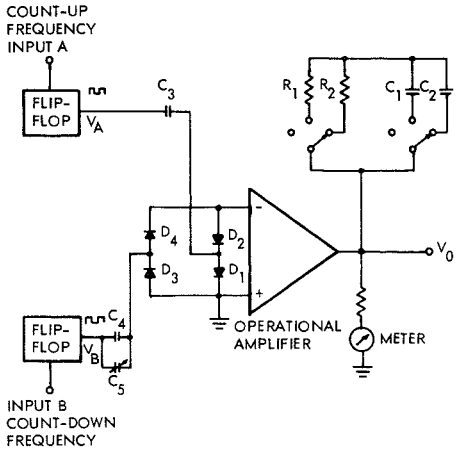

Fig. 1—An operational amplifier and a diode current-pump circuit combine to provide ratemeter output.

The operational characteristics of the count-up and count-down sections of the diode pump are identical except for their output polarity. The operation of each section functioning by itself will serve as an illustration.

The count-up section flip-flop establishes the voltage reference levels for the diode pump circuit, which consists of the "bucket" capacitor, C_3, and the diodes, D_1 and D_2. Fig. 1 shows that one side of C_3 is connected to the summing point of the operational amplifier via the diode D_2, and to the reference (non-inverting) input via diode D_1. For an unsaturated condition both input voltages are very nearly equal; as one is grounded, the other will also be at ground potential. The waveforms of this circuit are illustrated in Fig. 2. If we assume a peak driving current, i_A, available from the flip-flop, we see that at each voltage transition a charge, C_3V_a, is alternately drawn from the reference input (which is at ground potential) and dumped into the summing point, which, due to feedback from the output, remains at ground potential. The output voltage is thus developed in increments, V_x, such that

$$V_x = V_a \frac{C_1}{C_3}$$

With R_1 switched out of circuit, the output voltage, V_0, after n pulses, will be $V_0 = nV_x$. With R_1 in the circuit, the feedback current that flows through R_1 is equal to the driving current, i_a, and the resulting voltage output increment, V_a, is equal to $-i_aR_1$. The output voltage for a rate of s pulses per second, with the driving charge of C_3V_a, will be $V_0 = sR_1C_3V_a$.

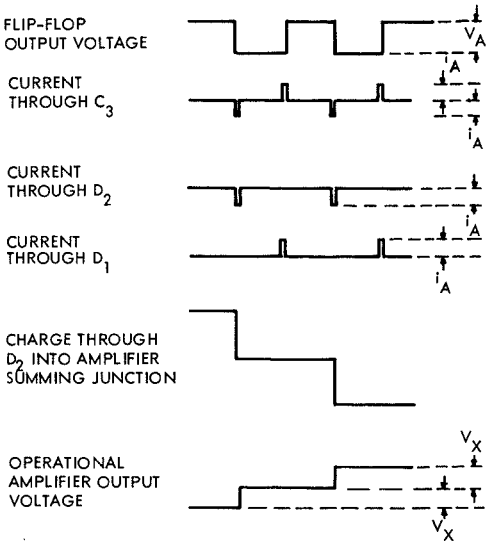

Fig. 2—Waveforms for comparator circuit.

The capacitor, C_1, in the feedback path integrates the input from the two diode pump circuits. The time constant, R_1C_1, can be adjusted to provide the required smoothing of the output voltage at the required sensitivity by using separate controls for R_1 and C_1.[1]

Calibration for equal sensitivities can be obtained by connecting the two inputs together and observing the effect of an input signal. Output drift is balanced out by adjusting C_5. The diode pump circuits are driven from identical flip-flops, operating from a regulated power supply. The sensitivity is proportional to the output amplitude of the flip-flops. Changes in normal ambient temperature do not affect the balance sensitivity of the two channels, since they employ the same components. A calibration accuracy of 2% can be achieved, which is adequate for this application. This was verified by applying the same input frequency to both channels and measuring the output voltage drift with R_1 switched out of the circuit.

Reference

For a more complete discussion of current-pump circuits, refer to *Applications Manual for computing Amplifiers,* published by Philbrick/Nexus Research.

Reprint RE-15-3-24 | Final manuscript received July 15, 1969.

ALERT—a new technical information service for RCA scientists and engineers

E. R. Jennings, Mgr.
Technical Information Systems
Corporate Engineering Services
Camden, N.J.

An important task for many scientists and engineers is the regular scanning of current literature sources for new developments in their fields. This time-consuming task has become virtually impossible to do thoroughly, because of the thousands of journal articles, technical reports, and conference papers issued every month.

Another problem in this current awareness task frequently arises when an engineer must apply the advanced or specialized techniques of disciplines other than his own. Many times, an engineer familiar with one discipline or speciality will not be sufficiently familiar with the literature of another speciality to know where such information might be found.

To cope with these problems, RCA Technical Information Systems, Corporate Engineering Services, is now making available a new information service called ALERT.

How ALERT works

ALERT is a computer technique for screening newly issued papers, reports, and other world-wide information sources and automatically notifying the engineer or scientists of those specific items pertinent to his current work.

To use ALERT, an engineer first describes (in his own words) an information need using an "interest profile" form. An individual may have one, or many interest profiles—depending on his needs. All such profiles are individually analyzed by an information specialist on the staff of RCA Technical Information systems, then encoded and entered into the computer. The computer then compares the interest profile with thousands of descriptions of newly issued information sources. Where the match is sufficient, the computer prints out notifications that are sent to the engineer (see Fig. 1). After reviewing such notifications, he may selectively order the full text of the journal articles, reports, etc. from his local RCA Technical Library.

Advantages of ALERT

The individualized ALERT interest profiling technique offers:

Assured awareness of current progress in specific fields of interest;

Reduction of time spent keeping abreast of new information sources;

Announcement of new technical innovations in sources not ordinarily seen;

An effective way to set up and maintain personal files of reference material; and

Identification of otherwise unknown technical effort as an aid in planning new projects.

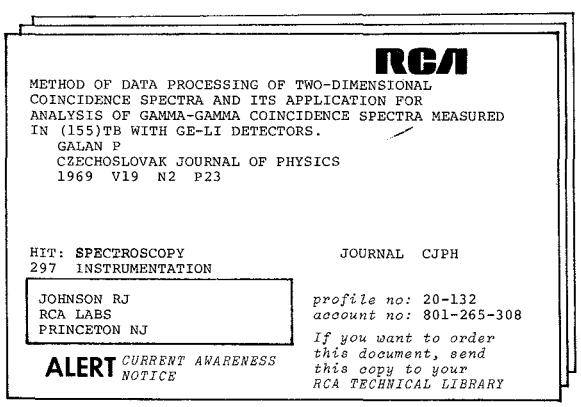
RCA

METHOD OF DATA PROCESSING OF TWO-DIMENSIONAL COINCIDENCE SPECTRA AND ITS APPLICATION FOR ANALYSIS OF GAMMA-GAMMA COINCIDENCE SPECTRA MEASURED IN (155)TB WITH GE-LI DETECTORS.
GALAN P
CZECHOSLOVAK JOURNAL OF PHYSICS
1969 V19 N2 P23

HIT: SPECTROSCOPY JOURNAL CJPH
297 INSTRUMENTATION

JOHNSON RJ
RCA LABS
PRINCETON NJ

profile no: 20-132
account no: 801-265-308

If you want to order this document, send this copy to your RCA TECHNICAL LIBRARY

ALERT *CURRENT AWARENESS NOTICE*

Fig. 1—This sample ALERT notification identifies a journal article and may be sent to the Library as an order form. A second part of this form duplicates the information shown here and may be retained by the user for personal reference—perhaps used to maintain a "personal" file to relevant literature.

What ALERT covers

Every two weeks, a new magnetic tape file containing some 8,000 descriptions of newly issued information sources (technical reports, papers, etc.) is entered into the computer. This biweekly update allows over 200,000 different items to be screened for the engineer each year, including:

1) Articles from over 2,000 technical journals, as soon as published (over 120,000 articles/year).
2) Newly published technical books (6,000/year).
3) Government unclassified R&D technical reports issued by the DOD, AEC, and NASA (35,000/year as announced by the U.S. Government Clearinghouse).
4) New internal RCA information sources, such as RCA reports, papers, patent information, and R&D projects.

This data base and means for improving it will regularly be evaluated and adjusted to keep ALERT most effective.

ALERT notifications

Once his ALERT interest profile is "in the system," the engineer receives biweekly notifications (Fig. 1) that the computer identified as "matching" his interest profile. The engineer may then . . .

1) Review the set of notices, and select those which are sufficiently pertinent to justify ordering the full text of the item from his local RCA Technical Library.
2) For those selected, he may detach the order portion of the notice and return it to his local RCA Technical Library. (If there is a special source for the item other than the library, the ALERT notice will specify this.)
3) Retain the file-copy portion of the pertinent notices for reference. Note that he can readily use this portion of the notice to set up and maintain a reference file.

Generally, an interest profile, once adjusted for optimum matching, will return some 10 to 20 notices for review every two weeks. If the profile is well-designed, some 50% to 80% of these will be relevant. The *ALERT Users Guide* provides guidelines on how the engineer may most effectively prepare his interest profile to gain the best results from the service.

How to subscribe to ALERT

ALERT is available on a subscription basis to any RCA scientist or engineer. An RCA technical group can also subscribe, in cases where several members of the group have very similar information needs. However, ALERT is a technique for handling specific, detailed expressions of information needs. A broad, general-interest profile intended to serve the varied interests of a group may (at the discretion of TIS) be separated into several, more-specific profiles for most effective operation of the system.

After completing an interest profile form for each profile desired, following the guidelines noted in the *ALERT Users Guide,* the form is returned to the librarian, who checks it for completeness and forwards it to Technical Information Systems.

Interest-profile forms and the *User's Guide* are available from any RCA Technical Library; if your location does not have an RCA Library, contact RCA Technical Information Systems directly (2-8-1, Camden; 609-963-8000, PC-3119).

ALERT is operated by RCA Technical Information Systems, Corporate Engineering Services, in cooperation with the RCA Technical Libraries. Because it is an RCA-operated service, it can be monitored to provide an effective, individualized, information service for RCA scientists and engineers Corporate wide.

RCA Reprint RE-15-3-24 | Final manuscript received September 22, 1969.

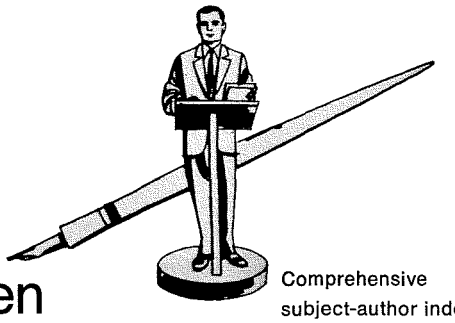

Pen and Podium

Comprehensive subject-author index to Recent RCA technical papers

Both published papers and verbal presentations are indexed. To obtain a published paper, borrow the journal in which it appears from your library, or write or call the author for a reprint. For information on unpublished verbal presentations, write or call the author. (The author's RCA Division appears parenthetically after his name in the subject-index entry.) For additional assistance in locating RCA technical literature, contact: **RCA Staff Technical Publications, Bldg. 2-8, RCA, Camden, N.J. (Ext. PC-4018).**

This index is prepared from listings provided bimonthly by RCA Division Technical Publcations Administrators and Editorial Representatives—who should be contacted concerning errors or omissons (see inside back cover).

Subject index categories are based upon the Thesaurus of Engineering Terms, Engineers Joint Council, N.Y., 1st Ed., May 1964.

Subject Index

Titles of papers are permuted where necessary to bring significant keyword(s) to the left for easier scanning. Author's division appears parenthetically after his name.

AMPLIFICATION

AVALANCHE DIODE FM SIGNAL AMPLIFIER, Performance of an—A. Schwarzmann (DCSD, Cam) International Conference on Communications, National Bureau of Standards and IEEE Chapter on Communications, Boulder, Colorado; 6/9-11/69; *Proceedings*

INTEGRATED PARAMETRIC AMPLIFIERS With IMPATT Diode Pumping—P. Bura, S. Yuan, W. Y. Pan (DCSD, W. Windsor) Int'l Microwave Symposium, Dallas, Texas; 5/5-8/69

CHECKOUT

DIGITAL MESSAGE GENERATOR AND RECEIVER for ATE, Programming Dynamic—G. W. Wong (ASD, Burl) St. Louis ATE, St. Louis, Mo.

TEST PROGRAM, Organizing, Staffing and Initiating a—D. R. Williams (AED, Pr) AMA Test Engineering Management Seminar, New York, N.Y.; 6/9/69

CIRCUIT ANALYSIS

ANALOG DELAY LINE, Integrated MOS—R. A. Mao, K. R. Keller, R. W. Ahrons (EC, Som) *IEEE J. of Solid State Circuits;* 8/69

DIGITAL MESSAGE GENERATOR AND RECEIVER for ATE, Programmable Dynamic—G. W. Wong ASD, Burl St. Louis ATE, St. Louis, Mo.

DIPNET, A General Distributed Parameter Network Analysis Program—W. N. Parker (EC, Lanc) *IEEE Trans. on Microwave Theory and Techniques;* 8/9

EXPERIMENTAL SYNC SEPARATOR and Associated Circuitry in Integrated Form—R. Feryszka, J. O. Preisig (EC, Som) *IEEE J. of Solid State Circuits;* 8/69

FREQUENCY MIXING AND SPURIOUS ANALYSIS, Design Handbook for—D. H. Westwood (DCSD, Cam) 7/69

LINEAR AMPLIFIER, Operation and Construction of a Hybrid, 5-Ampere, 75-Volt—W. R. Peterson (EC, Som) WESCON, San Francisco, Calif.; 8/19-22/69; *WESCON Preprint;* 8/69

LINEAR FREQUENCY TRANSLATION Utilizing Schottky Barrier Diodes, Aspects of—H. M. Goldberg (DCSD, Cam) Master's Thesis, Univ. of Penna., Phila., Pa.; 5/69

REACHABILITY MATRIX of a Directed Linear Graph, An Algorithm for Finding the—S. H. Unger (Labs., Pr) *IEEE Trans. on Circuit Theory,* Vol. CT-16, No. 1; 2/69

CIRCUITS, INTEGRATED

ANALOG DELAY LINE, Integrated MOS—R. A. Mao, K. R. Keller, R. W. Ahrons (EC, Som) *IEEE J. of Solid State Circuits;* 8/69

EXPERIMENTAL SYNC SEPARATOR and Associated Circuitry in Integrated Form—R. Feryszka, J. O. Preisig (EC, Som) *IEEE J. of Solid State Circuits;* 8/69

INTEGRATED MICROWAVE CIRCUITS, Notes on—H. Sobol (EC, Som) University of Michigan Summer Lecture Series; 8/69

MICROSTRIP LINES in Microwave Integrated Circuits, Approximate solutions for a Coupled Pair of—A. Schwarzmann (DCSD, Cam) *Microwave Journal;* 5/69

COMMUNICATIONS COMPONENTS

AVALANCHE DIODE FM SIGNAL AMPLIFIER, Performance of an—A. Schwarzmann (DCSD, Cam) International Conference on Communications, National Bureau of Standards and IEEE Chapter on Communications, Boulder, Colorado; 6/9-11/69; *Proceedings*

INTEGRATED MICROWAVE CIRCUITS, Notes on—H. Sobol (EC, Som) U. of Michigan Summer Lecture Series; 8/69

MICROSTRIP LINES in Microwave Integrated Circuits, Approximate solutions for a Coupled Pair of—A. Schwarzmann (DCSD, Cam) *Microwave Journal;* 5/69

COMMUNICATIONS SYSTEMS

COHERENT PSK AND NON-COHERENT FSK in a Multipath Environment, A Comparative Study of—J. C. Blair (AED, Pr) U. of Penna., Doctoral Dissertation; 6/69

MULTIPLE ACCESS Communication Systems, Coding for—N. Macina (DCSD, W. Windsor) Master's Thesis, Polytechnic Institute of Brooklyn, New York; 6/69

COMPUTER APPLICATIONS

DIPNET, A General Distributed Parameter Network Analysis Program—W. N. Parker (EC, Lanc) *IEEE Trans. on Microwave Theory and Techniques;* 8/69

HYPHENATE ENGLISH WORDS, A Program to—W. A. Ocker (GSD, Dayton) Master's Thesis, University of Penna., Phila., Pa.; 7/69

LORENTZ-FIELD AMPLIFICATION in a Bounded Semiconductor Medium, Computer Solutions of—J. R. Golden, K. K. N. Chang (Labs., Pr) *J. of Applied Physics,* Vol. 14, No. 4; 3/69

SUBSCRIPTIONS TO BIBLIOGRAPHIC FILES in Magnetic Tape Form, Potential Use of—A. DeStephen (CS, Cam) Drexel Institute, Phila., Pa:; 4/26/69

TRANSISTOR ANALYSIS AND DESIGN—A Regional Approach, Computer-Aided—R. B. Schilling (EC, Som) McGraw-Hill Seminar on Device Modeling, Los Angeles, Calif.; 8/5/69

WHERE is Technology Leading Communications?—J. C. Phillips (CS, Cam) *IEEE-EWS Symposium Proceedings;* 8/7/69

COMPUTERS, PROGRAMMING

HYPHENATE ENGLISH WORDS, A Program to—W. A. Ocker (GSD, Dayton) Master's Thesis, University of Penna., Phila., Pa.; 7/69

COMPUTER STORAGE

LAMINATED FERRITE MEMORY SYSTEM for Aerospace Applications, Design of a—P. Holtzman, B. D. Schubert (AED, Pr) University of Penna., Master's Thesis; 6/69

CONTROL SYSTEMS

AUTOMATED INTERFACE DESIGN for ATE—J. Fay (ASD, Burl) ASSC, St. Louis, Mo.

AUTOMATION IN TV—J. K. Hamalainen (CESD, Cam) Montreux Festival, Montreux, Switzerland; 5/69

CONTROL OF MULTIPLE DRONE AIRCRAFT, An Automatic System for the—P. Z. Peebles, B. E. Keiser (MSR, Mrstn) *IEEE Trans. on AES;* 5/69

DISPLAYS

AUTOMATION IN TV—J. K. Hamalainen (CESD, Cam) Montreux Festival, Montreux, Switzerland; 5/69

LARGE AREA ELECTRO-OPTIC DISPLAY SYSTEM, Gamma Correction for a—M. Barron (ATL, Cam) Master's Thesis of Science & Engineering, Univ. of Penna., Phila., Pa.; 6/25/69

LIQUID CRYSTAL Matrix Displays—B. J. Lechner (Labs., Pr) IEEE 4.10 Committee Meeting, Sanibel Island, Florida; 7/1/69

DOCUMENTATION

AVOID POSSIBLE LEGAL PROBLEMS, How an Author Can—H. K. Mintz (ASD, Burl) 12th Annual Institute in Technical and Industrial Communication, Colorado State University, Ft. Collins, Colo.; 7/20-25/69

HYPHENATE ENGLISH WORDS, A Program to—W. A. Ocker (GSD, Dayton) Master's Thesis, University of Penna., Phila., Pa.; 7/69

SUBSCRIPTIONS TO BIBLIOGRAPHIC FILES in Magnetic Tape Form, Potential Use of—A. DeStephen (CS, Cam) Drexel Institute, Phila., Pa.; 4/26/69

WHERE is Technology Leading Communications?—J. C. Phillips (CS, Cam) *IEEE-EWS Symposium Proceedings;* 8/7/69

EDUCATION

CONTINUING ENGINEERING EDUCATION, The Nuts and Bolts of—W. C. Morrison (CS, Cam) AMA Course on Engineering Management, Chicago, Ill.; 8/19/69

ENGINEERING MANAGER TRAINING, A Continuing Education Program—Dr. J. M. Biedenbach (CS, Cam) *IEEE Spectrum;* 11/68

INDUSTRIAL VIDEO TAPE APPLICATIONS to Continuing Engineering Studies Programs—Dr. J. M. Biedenbach (CS, Cam) American Society for Engineering Education National Meeting, Penn State University, University Park, Pa.; 6/23/69

ELECTRO-OPTICS

HIGH-RESOLUTION SYSTEM—O. H. Schade (EC, Hr) Summer Program on Photo-Electronic Imaging Devices, University of Rhode Island; 7/28-8/8/69

ENVIRONMENTAL ENGINEERING

WIRE AND CABLE, High Temperature—F. M. Oberlander (CS, C. H.) *Electronic Products;* 8/69

GRAPHIC ARTS

WHERE is Technology Leading Communications?—J. C. Phillips (CS, Cam) *IEEE-EWS Symposium Proceedings;* 8/7/69

LABORATORY TECHNIQUES

INTERNAL PHOTOEMISSION for Characterizing Dielectric Films, Use of—A. M. Goodman (Labs., Pr) *J. of Vacuum Science and Technology,* Vol. 6, No. 1; 1&2/69

LOGIC THEORY

INTEGRATED THRESHOLD LOGIC—J. Beinart, D. Hampel, K. Prost, L. Micheel (DCSD, Cam) NAECON, Dayton, Ohio; 5/19-21/69; *NAECON Conference Record*

MANAGEMENT

CONTINUING ENGINEERING EDUCATION, The Nuts and Bolts of—W. C. Morrison (CS, Cam) AMA Course on Engineering Management, Chicago, Ill.; 8/19/69

ENGINEERING MANAGER TRAINING, A Continuing Education Program—Dr. J. M. Biedenbach (CS, Cam) *IEEE Spectrum;* 11/68

INDUSTRIAL ENGINEERING, Fundamentals of—A. G. Cattell (DCSD, Cam) AMA, New York, N.Y.; 6/25-27/69

MATHEMATICS

ADAPTIVE EQUALIZING with a Second-Order Gradient Algorithm—C. Devieux (AED, Pr) Polytechnic Institute of Brooklyn, Doctoral Dissertation; 6/69

FALLACIES AND FRAUDS in Mathematics—M. S. Corrington (ATL, Cam) Research Society of America, Franklin Institute, Phila., Pa.; 6/18/69

LORENTZ-FIELD AMPLIFICATION in a Bounded Semiconductor Medium, Computer Solutions of—J. R. Golden, K. K. N. Chang (Labs., Pr) *J. of Applied Physics,* Vol. 14, No. 4; 3/69

REACHABILITY MATRIX of a Directed Linear Graph, An Algorithm for Finding the—S. H. Unger (Labs., Pr) *IEEE Trans. on Circuit Theory,* Vol. CT-16, No. 1; 2/69

MECHANICAL DEVICES

WIRE AND CABLE, High Temperature—F. M. Oberlander (CS, C.H.) *Electronic Products;* 8/69

OPTICS

HIGH-RESOLUTION SYSTEM—O. H. Schade (EC, Hr) Summer Program on Photo-Electronic Imaging Devices, University of Rhode Island; 7/28-8/8/69

PARTICLE BEAMS

SCATTERING of Highly Focused Kilovolt Electron Beams by Solids—R. W. Nosker Labs., Pr) *J. of Applied Physics, Vol.* 40, No. 4; 3/69

PROPERTIES, MOLECULAR

CHROMIUM CHALCOGENIDE SPINELS, Systematics of the Hyperfine and Exchange Interactions in the—S. B. Berger, J. I. Budnick, T. J. Burch (Labs., Pr) *The Physical Review,* Vol. 179, No. 2; 3/10/69

EXCHANGE INTERACTIONS in Mn Sc_2S_4—P. J. Wojtowicz, L. Darcy, M. Rayl (Labs., Pr) *J. of Applied Physics,* Vol. 40, No. 3, *Magnetics Conference Issue;* 3/1/69

LARGE-AREA MICROPLASMA-FREE P-N JUNCTIONS in GaAs and $GaAs_{1-x}P_x$—R. E. Enstrom, J. R. Appert (Labs., Pr) *Proc. of the Symp. on GaAs;* 1968

SEEBECK COEFFICIENT in N-Type $CdCr_2Se_4$—A. Amith, G. L. Gunsalus (Labs., Pr) *J. of Applied Physics,* Vol. 40, No. 3; 3/1/69

SINGLE CRYSTALLINE SILICON from Silane, Low Temperature Epitaxial Growth of—D. Richman, R. H. Arlett (Labs., Pr) *J. of the Electrochemical Soc.,* Vol. 116, No. 6; 6/69

ZONE MELTING PURIFICATION of Gallium Trichloride by a Radiotracer Method, Investigation of—W. Kern (Labs., Pr) Chapter in a book, *Purification of Inorganic and Organic Materials,* Marcel Dekker, Inc., N.Y.; 1969

PROPERTIES, SURFACE

MACROSCOPIC SURFACE IMPERFECTIONS in Vapour-Grown GaAs, The Origin of—J. J. Tietjen, M. S. Abraham, A. B. Dreeben, H. F. Gossenberger (Labs., Pr) *Proc. of Symp. on GaAs;* 1968

PROPERTIES, CHEMICAL

PRESSURE SINTERING of Gallium Arsenide—W. P. Stollar, H. I. Moss (Labs., Pr) *J. of American Ceramic Soc.,* Vol. 52, No. 4; 4/69

VIRIAL THEOREM and Cohesive Energy and Monovalent Metals—A. Rothwarf (Labs., Pr) *Physics Letters,* Vol. 29A, No. 3; 4/21/69

PROPERTIES, OPTICAL

INFRARED PHOTOEMISSION from Si-Al_2O_3-GaP:Cs Structures—E. D. Savoye (EC, Pr) Conference on Photoelectric and Secondary Emission, University of Minnesota; 8/27-28/69

PHOTOCHROMIC $SrTiO_3$ Doped with Fe/Mo and Ni/Mo, Optical and EPR Studies of—B. W. Faughnan, Z. J. Kiss (Labs., Pr) *IEEE J. of Quantum Electronics,* Vol. QE-5; No. 1; 1/69

PHOTOCHROMIC MATERIALS for Quantum Electronics—Z. J. Kiss (Labs., Pr) *IEEE J. of Quantum Electronics,* Vol. QE-5, No. 1; 1/69

PHOTOEMISSIVE MATERIAL for the Visible Spectrum, $GaAs_{1-x}P_x$ as a New High-Quantum-Yield—R. E. Simon, A. H. Sommer, J. J. Tietjen, B. F. Williams (EC, Pr) Conference on Photoelectric and Secondary Emission, University of Minnesota; 8/27-28/69

RADAR

PARALLEL PROCESSING for Phased-Array Radars—J. E. Courtney, H. M. Halpern (MSR, Mrstn) Symposium on Parallel Processor Systems, Technologies & Application, Navy Post Graduate School, Monterey, Calif; 6/25-27/69

PHASE MODULATED CORRELATION RADAR AN/PPS-9 Radar Set, Development of a—R. A. Van Olst (MSR, Mrstn) Navy Post Graduate School, Monterey, Calif.; 6/17-19/69; 15th Annual Tri-Service Radar Symposium

RECORDING, IMAGE

INDUSTRIAL VIDEO TAPE APPLICATIONS to Continuing Engineering Studies Programs—Dr. J. M. Biedenbach (CS, Cam) American Society for Engineering Education National Meeting, Penn State University, University Park, Pa.; 6/23/69

RELIABILITY

THRESHOLD AND FAILURE ANALYSIS, Improving Computing Equipment Reliability Through—N. R. Wheelock (DCSD, Cam) IEEE, Philadelphia Chapter, all day seminar, Phila., Pa.; 5/22/69; Proceedings of Seminar

SOLID-STATE DEVICES

AVALANCHE DIODES, Induced DC Negative Resistance in—A. S. Clorfeine, R. D. Hughes (Labs., Pr) *Proc. of IEEE,* Vol. 57, No. 5; 5/69

AVALANCHE DIODE FM SIGNAL AMPLIFIER, Performance of an—A. Schwarzmann (DCSD, Cam) International Conference on Communications, National Bureau of Standards and IEEE Chapter on Communications, Boulder, Colorado; 6/9-11/69; *Proceedings*

INTEGRATED PARAMETRIC AMPLIFIERS with IMPATT-Diode Pumping—P. Bura, S. Yuan, W. Y. Pan (DCSD, W. Windsor) Int'l Microwave Symposium, Dallas, Texas; 5/5-8/69

LINEAR FREQUENCY TRANSLATION Utilizing Schottky Barrier Diodes, Aspects of—H. M. Goldberg (DCSD, Cam) Master's Thesis, U. of Penna., Phila., Pa.; 5/69

MICROWAVE POWER TRANSISTORS—H. C. Lee (EC, Som) U. of Michigan Summer Lecture Series; 8/69

TRANSISTOR ANALYSIS AND DESIGN—A Regional Approach, Computer-Aided—R. B. Schilling (EC, Som) McGraw-Hill Seminar on Device Modeling, Los Angeles, Calif; 8/5/69

SPACE COMMUNICATIONS

SHF Tactical Satellite Earth Terminals—E. F. Bailey (DCSD, Cam) AFCEA, Washington, D.C.; 6/5/69

SPACECRAFT

LEM—RCA's Role—F. J. Gardiner (ASD, Burl) Fels Planitarium, Franklin Institute, Philadelphia, Pa.; 7/18/69

TELEVISION BROADCASTING

AUTOMATION IN TV—J. K. Hamalainen (CESD, Cam) Montreux Festival, Montreux, Switzerland; 5/69

JCIC ad hoc COMMITTEE ON COLOR TV, A Status Report from the Transmission Subcommittee of the—W. C. Morrison (CS, Cam) IEEE Group on Broadcasting Symposium, Washington, D.C.; 9/19/69

LIVE COLOR CAMERA DESIGN—Chromacomp, An Advance in—N. L. Hobson, R. A. Dischert, J. F. Monohan (CESD, Cam) Montreux Festival, Montreux, Switzerland; 5/19/69

TRANSMISSION LINES

MICROSTRIP LINES in Microwave Integrated Circuits, Approximate solutions for a Coupled Pair of—A. Schwarzmann (DCSD, Cam) *Microwave Journal;* 5/69

TUBES, ELECTRON

NEW IMAGE ISOCON—E. M. Musselman (EC, Lanc) Summer Program on Photo-Electronic Imaging Devices, University of Rhode Island; 7/28-8/8/69

TELEVISION CAMERA TUBES, Transfer Characteristics and Spectral Response of—L. D. Miller (EC, Lanc) Summer Program on Photo-electronic Imaging Devices, U. of Rhode Island; 7/28-8/8/69 and Soc. of Photo-Optical Instrumentation Engineers, San Francisco, Calif.; 8/11/69

Author Index

Subject listed opposite each author's name indicates where complete citation to his paper may be found in the subject index. An author may have more than one paper for each subject category.

ASTRO-ELECTRONICS DIVISION

Blair, J. C. communications systems
Devieux, C. mathematics
Holtzman, P. computer storage
Schubert, B. D. computer storage
Williams, D. R. checkout

AEROSPACE SYSTEMS DIVISION

Fay, J. control systems
Gardiner, F. J. spacecraft
Mintz, H. K. documentation
Wong, G. W. checkout
Wong, G. W. circuit analysis

ADVANCED TECHNOLOGY LABORATORIES

Barron, M. displays
Corrington, M. S. mathematics

COMMERCIAL ELECTRONIC SYSTEMS DIVISION

Dischert, R. A. television broadcasting
Hamalainen, J. K. control systems
Hamalainen, J. K. displays
Hamalainen, J. K. television broadcasting
Hobson, N. L. television broadcasting
Monohan, J. F. television broadcasting

CORPORATE STAFF

Biedenbach, J. M. education
Biedenbach, J. M. management
Biedenbach, J. M. recording, image
DeStephen, A. computer applications
DeStephen, A. documentation
Morrison, W. C. television broadcasting
Morrison, W. C. education
Morrison, W. C. management
Oberlander, F. M. environmental engineering
Oberlander, F. M. mechanical devices
Phillips, J. C computer applications
Phillips, J. C. documentation
Phillips, J. C. graphic arts

DEFENSE COMMUNICATION SYSTEMS DIVISION

Bailey, E. F. space communication
Beinart, J. logic theory
Bura, P. amplification
Bura, P. solid-state devices
Cattell, A. G. management
Goldberg, H. M. circuit analysis
Goldberg, H. M. solid-state devices
Hampel, D. logic theory
Macina, N. communications systems
Micheel, L. logic theory
Prost, K. logic theory
Pan, W. Y. amplification
Pan, W. Y. solid-state devices
Schwarzmann, A. amplification
Schwarzmann, A. communications components
Schwarzmann, A. solid-state devices
Schwarzmann, A. circuits, integrated
Schwarzmann, A. transmission lines
Westwood, D. H. circuit analysis
Wheelock, N. R. reliability
Yuan, S. amplification
Yuan, S. solid-state devices

ELECTRONIC COMPONENTS

Ahrons, R. W. circuit analysis
Ahrons, R. W. circuits, integrated
Feryszka, R. circuit analysis
Feryszka, R. circuits, integrated
Lee, H. C. solid-state devices
Keller, K. R. circuit analysis
Keller, K. R. circuits, integrated
Mao, R. A. circuit analysis
Mao, R. A. circuits, integrated
Miller, L. D. tubes, electron
Musselman, E. M. tubes, electron
Parker, W. N. circuit analysis
Parker, W. N. computer applications
Peterson, W. R. circuit analysis
Preisig, J. O. circuit analysis
Preisig, J. O. circuits, integrated
Savoye, E. D. properties, optical
Schade, O. H. electro-optics
Schade, O. H. optics
Schilling, R. B. computer applications
Schilling, R. B. solid-state devices
Simon, R. E. properties, optical
Sobol, H. circuits, integrated
Sobol, H. communications components
Sommer, A. H. properties, optical
Tietjen, J. J. properties, optical
Williams, B. F. properties, optical

GRAPHIC SYSTEMS DIVISION

Ocker, W. A. computer applications
Ocker, W. A. computers, programming
Ocker, W. A. documentation

LABORATORIES

Abrahams, M. S. properties, surface
Amith, A. properties, molecular
Appert, J. R. properties, molecular
Arlett, R. H. properties, molecular
Berger, S. B. properties, molecular
Budnick, J. I. properties, molecular
Burch, T. J. properties, molecular
Chang, K. K. N. computer applications
Chang, K. K. N. mathematics
Clorfeine, A. S. solid-state devices
Darcy, L. properties, molecular
Dreeben, A. B. properties, surface
Enstrom, R. E. properties, molecular
Faughnan, B. W. properties, optical
Golden, J. R. computer applications
Golden, J. R. mathematics
Goodman, A. M. laboratory techniques
Gossenberger, H. F. properties, surface
Gunsalus, G. L. properties, molecular
Hughes, R. D. solid-state devices
Kern, W. properties, molecular
Kiss, Z. J. properties, optical
Kiss, Z. J. properties, optical
Lechner, B. J. displays
Moss, H. I. properties, chemical
Nosker, R. W. particle beams
Rayl, M. properties, molecular
Richman, D. properties, molecular
Rothwarf, A. properties, chemical
Stollar, W. P. properties, chemical
Tietjen, J. J. properties, surface
Unger, S. H. circuit analysis
Unger, S. H. mathematics
Wojtowicz, P. J. properties, molecular

MISSILE AND SURFACE RADAR DIVISION

Courtney, J. E. radar
Halpern, H. M. radar
Keiser, B. E. control systems
Peebles, P. Z. control systems
Van Olst, R. A. radar

Professional Meetings

Dates and Deadlines

Be sure deadlines are met—consult your Technical Publications Administrator or your Editorial Representative for the lead time necessary to obtain RCA approvals (and government approvals, if applicable). Remember, abstracts and manuscripts must be so approved BEFORE sending them to the meeting committee.

Calls For Papers

JAN. 19-21, 1970: **AIAA 8th Aerospace Sciences Meeting,** Statler-Hilton Hotel, New York, New York. **Deadline info: (abst), 8/18/69; 12/8/69 (papers to:** Robert A. Gross, School of Engineering and Applied Science, Columbia University, New York, N.Y. 10027.

FEB. 4-6, 1970: **AIAA Advanced Space Transportation Meeting,** Cocoa Beach, Fla. **Deadline info: 9/4/69 (abst); 10/15/69 (ms) to:** Alfred C. Draper, Air Force Flight Dynamics Lab. (FDM), Wright-Patterson Air Force Base, Ohio 45433.

MARCH 6-7, 1970: **AIAA Fighter Aircraft Conference,** St. Louis, Missouri. **Deadline info: (abst.) 10/30/69, (ms) 1/12/70 to:** Robert W. Bratt, Advanced Aircraft Systems, Norair/Northrop Corp., 3901 West Broadway, Hawthorne, Calif.

APRIL 1-3, 1970: **AIAA Test Effectiveness in the 70's Conference,** Palo Alto, Calif. **Deadline info: (abst.) 11/3/69 to:** Co. Frank Borman USAF, Room 342, Building CB, NASA Manned Spacecraft Center, Houston, Texas 77058.

APRIL 6-8, 1970: **AIAA 3rd Communications Satellite Systems Conference,** International Hotel, Los Angeles, Calif. **Deadline info: 2/2/1970 (papers) to:** Nathaniel E. Feldman, The Rand Corporation, 1700 Main Street, Santa Monica, Calif. 90406.

APRIL 12-16, 1970: **16th Annual Meeting Institute of Environmental Sciences,** Sheraton Boston Hotel, Boston, Massachusetts. **Deadline info: (abst) 10/15/69; (papers) 2/16/70 to:** Technical Program Committee, Institute of Environmental Sciences, 940 East Northwest Highway, Mt. Prospect, Illinois 60056.

APRIL 14-16, 1970: **Conference on Automatic Test Systems,** Birmingham, Warwickshire, England. **Deadline info: (syn) 10/31/69 to:** The Secretary, Organizing Committee for the Conference on Automatic Test Systems, The Institution of Electronic and Radio Engineers, 8-9, Bedford Square, London, W. C. 1, England.

APRIL 14-16, 1970: **Computer Graphics International Symposium,** Brunel Univ., Uxbridge, Middlesex, Eng. **Deadline info: (syn) 9/30/69 to:** IEE, Savoy Place, London, W. C. 2 England.

APRIL 14-17, 1970: **International Geoscience Electronics Symposium,** Marriott Twin Bridges Motor Hotel, Washington, D. C. **Deadline info: (abst) 12/1/69 to:** Ralph Bernstein, IBM Corp., 18100 Frederick Pike, Gaithersburg, Md. 20760.

APRIL 16-18, 1970: **1970 Carnahan Conference on Electronic Crime Countermeasures,** Carnahan House, University of Kentucky, Lexington, Kentucky. **Deadline info: (abst.) 11/15/69, (papers) 2/15/70 to:** Prof. J. S. Jackson, Department of Electrical Engineering, University of Kentucky, Lexington, Kentucky 40506.

APRIL 21-24, 1970: **International Magnetics Conference (INTERMAG),** Statler Hilton Hotel, Washington, D. C. **Deadline info: (abst) 12/12/69 to:** D. S. Shull, Bell Telephone Labs., 3300 Lexington Ave., Winston-Salem, N.C. 27102.

APRIL 22-24, 1970: **AIAA/ASME 11th Structures, Structural Dynamics, and Materials Conference,** Denver, Colo. **Deadline info: (abst.) 9/12/69, (ms) 3/9/70 to: Structures,** Roger A. Anderson, Structures Research Division, Mail Stop 188, NASA Langley Research Center, Langley Station, Hampton, Va. 23365; **Materials,** Dr. Edward Epremian, Carbon Products Division, Union Carbide Corp., 270 Park Avenue, New York, N.Y. 10017; **Structural Dynamics,** Dr. H. M. Voss, Mail Stop 8R-34, The Boeing Co., P. O. Box 3999, Seattle, Washington 98124; **Other areas,** Dr. H. M. Voss, Mail Stop 8R-34, The Boeing Co., P. O. Box 3999, Seattle, Wash. 98124.

APRIL 22-24, 1970: Southwestern IEEE Conference & Exhibition (SWIEEECO), Memorial Auditorium, Dallas, Texas. **Deadline info: (sum) 12/1/69, (ms) 3/1/70 to:** Professor Andrew P. Sage, Technical Program Chairman, 170-SWIEEECO, Information and Control Sciences Center, SMU Institute of Technology, Dallas, Texas 75222.

MAY 4-5, 1970: **Transducer Conference, Nat'l Bureau of Standards,** Washington, D. C. **Deadline info: (papers) 11/1/69, (ms) 2/15/70 to:** Dr. Robert B. Spooner, IMPAC Instrument Service, 201 East Carson Street, Pittsburgh, Pennsylvania 15219.

MAY 4-5, 1970: **Transducer Conference,** NBS & Governor's House, Gaithersburg, Maryland. **Deadline info: (abst) 11/1/69, (ms) 2/15/70 to:** H. P. Kalmus, Harry Diamond Labs., Dept. of the Army, Wash., D.C.

MAY 4-7, 1970: **4th Conference on Aerospace Meteorology (AMS/AIAA/IES),** Las Vegas, Nev. **Deadline info: (abst.) 9/1/69, (papers) 12/15/69 to:** Norman Sissenwine, AFCRL (CREW), L. G. Hanscom Field, Bedford, Mass. 01730- **meteorological studies;** William W. Vaughan, NASA Marshall Space Flight Center, Code: S&E-AERO-Y, Huntsville, Ala. 35812-**engineering studies.**

MAY 5-6, 1970: **Appliance Technical Conference,** Leland Motor Hotel, Mansfield, Ohio. **Deadline info: (syn) 10/1/69, (ms) 1/10/70 to:** R. G. LaBudde, Westinghouse Elec. Corp., 246 E. 4th Street, Mansfield, Ohio 44902.

MAY 13-15, 1970: **AIAA Atmospheric Flight Mechanics Conference,** Tullahoma, Tenn. **Deadline info: (abst.) 10/15/69 to: Missiles,** Lester L. Cronvich, Applied Physics Lab., Johns Hopkins University, 8621 Georgia Ave., Silver Spring, Md. 20910; **Ordnance,** Warren H. Curry, Experimental Aerodynamics, Division 9322, Sandia Labs, Albuquerque, N. Mex. 87115; **V/Stol,** John Zvara, Kaman Corp., 2nd Avenue, Northwest Industrial Park, Burlington, Mass. 01803; **Entry Vehicles,** Victor Stevens, Mail Stop 229-3, NASA Ames Research Center, Moffett Field, Calif. 94035; **Aircraft,** Martin T. Moul, NASA Langley Research Center, Hampton, Va. 23490; **Other areas,** C. J. Schueler von Karman Gas Dynamics Facility, Arnold Engineering Development Center. Arnold Air Force Station, Tenn. 37389.

MAY 13-15, 1970: **Electronic Components Conference,** Statler Hilton Hotel, Washington, D.C. **Deadline info: (abst) 11/15/69 to:** Mr. Burks, Sprague Electric Company, Marshall Street, North Adams, Mass., 01247, (papers) 1/1/70, (ms) 3/1/70.

MAY 18-20, 1970: **AIAA 5th Aerodynamic Testing Conference,** University of Tennessee Space Institute, Tullahoma, Tenn. **Deadline info: (abst.) 9/8/69, (papers) 11/15/69 to:** Dr. Hans K. Doetsch, Arnold Engineering Development Center (AELR), Arnold Air Force Station, Tenn. 37389.

MAY 19-21, 1970: **Conference on Signal Processing Methods for Radio Telephony,** London, England. **Deadline info: (ms) 12/29/69 to:** IEE Office, 345 East 47th Street, New York, N.Y. 10017.

MAY 19-21, 1970: **Conference on Signal Processing Methods for Radio Telephony,** London, England. **Deadline info: (ms) 12/29/69 to:** IEEE Office, 345 East 47th Street, New York, N.Y. 10017.

JUNE 15-19, 1970: **Sixth U.S. National Congress of Applied Mechanics,** Harvard University, Cambridge, Massachusetts 02138. **Deadline info: (paper) 1/1/70 to:** Professor George F. Carrier, Chairman, Papers Committee, Sixth U. S. National Congress of Applied Mechanics, Pierce Hall, Cambridge, Massachusetts 02138.

JUNE 16-18, 1970: **International Computer Conference,** Washington Hilton Hotel, Washington, D.C. **Deadline info: (ms) 11/15/69 to:** G. L. Tucker, Off. of Sect'y of Defense, Rm. 3E1014, The Pentagon, Washington, D.C. 20301.

JUNE 21-25, 1970: **Design Automation Workshop,** Sherton Palace Hotel, San Francisco, Calif. **Deadline info: (abst) 1/5/70 to:** H. Freitag, IBM Watson Rec. Ctr., POB 218, Yorktown Hgts., N.Y. 10598.

JUNE 24-26, 1970: **Joint Automatic Control Conference,** Georgia Inst. of Tech., Atlanta, Georgia. **Deadline info: (papers) 11/15/69 to:** Prof. J. B. Lewis, Department of Electrical Engineering, Pennsylvania State University, University Park, Penna. 16802.

JULY 14-16, 1970: **Electromagnetic Compatibility Symposium,** Grand Hotel, Anaheim, Calif. **Deadline info: (sum) 11/15/69, (ms) 4/1/70 to:** J. C. Senn, Technical Program Chairman, P.O. Box 1970, Anaheim, California 92803.

JULY 20-24, 1970: **Conf. on Dielectric Materials, Measurements & Applications,** Univ. of Lancaster, Lancaster, England. **Deadline info: (syn.) 5/30/69, (papers) 1/1/70 to:** IEEE, Savoy Place, London W. C. 2 England.

SEPT. 2-4, 1970: **Seoul Int'l Electrical & Electronics Engineering Conference,** Korean Inst. of Sci. & Tech., Seoul, Korea. **Deadline info:** S. K. Chung, c/o KIST, POB 131, Cheong Ryang, Seoul, Rep. of Korea.

SEPT. 15-18, 1970: **Conference on Gas Discharges,** London, England. **Deadline info: (syn) 12/1/69 to:** IEE Office, 345 East 47th Street, New York, N.Y. 10017.

Meetings

OCT. 21-24, 1969: **International Conference on Quality Control,** Tokyo, Japan. **Prog info:** American Society for Quality Control, 161 West Wisconsin Avenue, Milwaukee, Wisconsin 53203.

OCT. 27-29, 1969: **Electronic & Aerospace Systems Convention (EASCON),** Sheraton Park Hotel, Washington, D.C. **Prog info:** H. P. Gates, Jr., Sect'y of Army for SE Asia Matters, The Pentagon, Washington, D.C. 20310.

OCT. 27-29, 1969: **Jt. Materials Handling Engineering Conference,** Sheraton Motor Inn, Portland, Oregon. **Prog info:** Max Frey, c/o Cascade Corp. POB 7587, Portland, Ore. 97220.

OCT. 27-29, 1969: **Machine Tools Technical Conference,** Detroit Hilton Hotel, Detroit, Michigan. **Prog info:** James Lewelling, Ex-Cell-O Corp., Numera-Grol Work Ctr., 13001 Capital, Oak Pk., Michigan 48010.

OCT. 29-31, 1969: **Int'l Electron Devices Meeting,** Sheraton Park Hotel, Washington, D.C. **Prog info:** M. M. Atalla, Hewlett-Packard Labs., Palo Alto, Calif.

OCT. 29-31, 1969: **Nuclear Science Symposium,** Sheraton Palace Hotel, San Francisco, Calif. **Prog info:** R. C. Maninger, L-121, Lawrence Rad. Lab., POB 808, Livermore, Calif. 94550.

NOV. 3-5, 1969: **Symposium on Automatic Support Systems for Advanced Maintainability,** Chase Park Plaza Hotel, St. Louis, Missouri. **Prog info:** M. F. Mayer, Sta. 2608, Emerson Elec. Co., 8100 Florissant Av., St. Louis, Mo. 63136.

NOV. 5-6, 1969: **Symp. of the Affiliation of North Carolina Sections,** Greensboro, N. Carolina. **Prog info:** Leo Schenker, Bell Telephone Labs., 3300 Lexington Rd., Winston-Salem, N. Carolina 27102.

NOV. 5-7, 1969: **Northeast Electronics Research & Engineering Meeting** (NEREM), Sheraton Boston Hotel, War Mem. Aud., Boston, Mass. **Prog info:** IEEE NEREM Office, 31 Channing St., Newton, Mass.

NOV. 17-21, 1969: **The Lubrication Division of ASME,** Biltmore Hotel, Los Angeles, Calif. **Prog info:** Lubrication Division, The American Society of Mechanical Engineers, 345 East 47 Street, New York 17, New York.

NOV. 17-19, 1969: **Symposium on Adaptive Processes,** Penn. State Univ., University Park, Penna. **Prog info:** Dr. John B. Lewis, IEEE, inc. 345 East 47th Street, New York, N.Y. 10017.

NOV. 18-20, 1969: **EIA-Commerce Department Laser Colloquium,** Paris, France. **Prog info:** Mrs. Jane Davis, EIA Headquarters, 2001 Eye Street, N.W., Washington, D.C. 20006.

NOV. 18-20, 1969: **Fall Joint Computer Conference,** Convention Ctr., Las Vegas, Nev. **Prog info:** Eugene Grabbe, TRW Svs., Bldg. R3, Rm. 2070, One Space Pk., Redondo Beach, Cal. 90278.

NOV. 18-21, 1969: **Magnetism and Magnetic Materials Conference,** Benlamin Franklin Hotel, Phila., Penn. **Prog info:** Brooks Harris, Univ. of Penna., Phila., Penna. 19104.

NOV. 19-21, 1969: **1969 Annual Meeting of the USA Standards Institute,** Statler Hilton Hotel, Detroit, Michigan. **Prog info:** Dorothy Hogan, News, USASI, 10 East 40th Street, New York, N.Y. 10016.

NOV. 19-21, 1969: **IEEE Region 3 Convention,** Sheraton Motor Inn, Huntsville, Ala. **Prog info:** J. P. Hallowes, Jr., 8107 Warden Dr., S. E., Huntsville Alabama 35802.

DEC. 3-5, 1969: **Eighteenth International Wire and Cable Symposium** (primary emphasis on cable TV) Shelburne Hotel, Atlantic City, New Jersey. **Prog info:** F. Oberlander, RCA Corp., 204-1, Cherry Hill, N.J. 08110.

DEC. 4-5, 1969, **Vehicular Technology Conference,** Sheraton-Columbus Motor Hotel, Columbus, Ohio. **Prog info:** R. E. Fenton, Ohio State Univ., 2015 Neil Ave., Columbus, Ohio 43210.

DEC. 8-9, 1969: **Symposium on Consumer Electronics,** Conrad Hilton Hotel, Chicago, Illinois. **Prog info:** Charles Hepner, Zenith Radio Corp., 6101 W. Dickens Ave., Chicago, Ill. 60639.

DEC. 8-10, 1969: **Conference on Applications of Simulation,** Int'l Hotel, Los Angeles, Calif. **Prog info:** P. J. Kiviat, Simulation Assoc. Inc., 10884 Santa Monica Blvd., L. A., Calif.

DEC. 8-10, 1969: **Int'l Symposium on Circuit Theory,** Mark Hopkins Hotel, San Francisco, Calif. **Prog info:** R. A. Rohrer, Fairchild Semiconductors, 4001 Junipero Serra Blvd., Palo Alto, Cal. 94304.

DEC. 8-10, 1969: **National Electronics Conference,** Conrad Hilton Hotel, Chicago, Illinois. **Prog info:** Nat'l Elec. Conference, Oakbrook Exec. Plaza #2, 1121 W. 22 St., Oak Book, Ill. 60521.

DEC. 8-12, 1969: **IEEE G-AP Int'l Symp. & Fall USNC/URSI Meeting,** Villa Capri Hotel, Austin, Texas. **Prog info:** A. H. LaGrone, Engrg. Sci. Bldg. 502, Univ. of Texas, Austin, Texas 78712.

DEC. 9-11, 1969: **Symposium on Application of Magnetism in Bio-engineering,** Wiezman Inst. of Science, Rehovot, Israel. **Prog info:** Weizmann Inst. of Sci., G-EMBK G-MAG, Israel Soc. Bioengrg.

DEC. 10-12, 1969: **Asilomar Conference on Circuits & Systems,** Asilomar Hotel, Pacific Grove, Calif. **Prog info:** Shu-Park Chan, Univ. of Santa Clara, Santa Clara, Calif.

Engineering News and Highlights

Dr. R. G. Groshans named to Corporate engineering staff

Dr James Hillier, Executive Vice President, RCA Research and Engineering, appointed **Dr. Russell G. Groshans** as a Staff Engineer, Product Engineering. Dr. Groshans' responsibilities cover technical management liaison between Dr. Hillier's office and the RCA operating divisions. His office is at the David Sarnoff Research Center in Princeton, N.J.

Dr. Groshans received the BS from the U.S. Military Academy in 1953. His graduate work in Physics was done at Georgetown University, where he received the MS in 1963 and the PhD in 1967. Prior to his appointment to Dr. Hillier's staff, Dr. Groshans worked for two years as a Systems Engineer, Advanced Programs and Plans, at the RCA Astro-Electronics Division in Hightstown, N.J. His main activities were engineering and feasibility studies on advanced spacecraft systems, environmental sensing techniques, and computer simulation for spacecraft interactions with the upper atmosphere. From 1953 to 1967, Dr. Groshans served as an officer in the U.S. Air Force. In addition to being a pilot, he held positions as Air and Staff Operations Officer, Squadron Commander, and Staff Physicist for Headquarters, Officer of Aerospace Research. Dr. Groshans is a member of the American Geophysical Union and the IEEE.

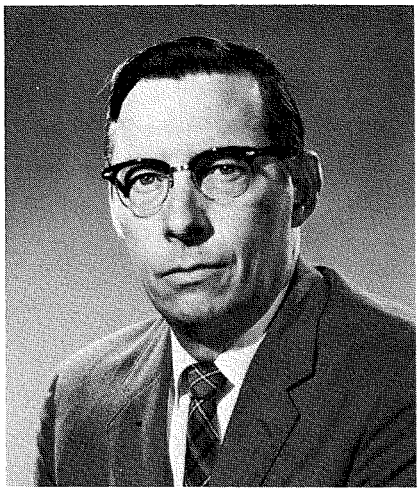

Arch Luther elevated to Fellow of SMPTE

The Board of Governors of the Society of Motion Picture and Television Engineers (SMPTE) upon the recommendation of the Fellow Membership Award Committee, has conferred the distinguished grade of Fellow Member upon **Arch C. Luther, Jr.,** Manager, Video Tape Engineering, Commercial Electronic Systems Division, Camden, N.J.

A fellow of the Society is one who is no less than 30 years of age and who has, by his proficiency and contributions, attained an outstanding rank among engineers or executives of the motion picture, television, or related industries.

Mr. Luther received the BSEE from the Massachusetts Institute of Technology. He has worked on the design and development of sync generators, camera control equipment, monitors, switching equipment and other items of television studio equipment. He is now Manager of the Tape Equipment, Projector and Scientific Instruments Engineering Department, responsible for TV tape recorders, magnetic heads, TV film projectors and electron microscope engineering. He holds twenty-five United States Patents and has published numerous papers. Mr. Luther is affiliated with Eta Kappa Nu, the Society of the Sigma Xi and the IEEE.

Manger named Chief Engineer

C. S. Constantino, Division Vice President and General Manager, Astro-Electronics Division appointed **Dr. Warren P. Manger** as Chief Engineer. Dr. Manger, formerly Manager of Advanced Systems and Technology, will be responsible for the design and engineering of spacecraft and space systems.

Dr. Manger received the BS, MS, and PhD from the Massachusetts Institute of Technology. Since joining Astro-Electronics Division in 1958, he has been instrumental in many space projects, including the development of TIROS weather satellites, the three-axis stabilization systems for TIROS M, and lunar and planetary exploration systems.

Before joining RCA, Dr. Manger was Chief Physicist with Farrel-Birmingham, Inc. He began his engineering career as a staff member of the MIT Radiation Laboratories in 1943.

Dr. Manger, a member of the American Institute of Aeronautics and Astronautics, is a contributing author to the *Theory of Servo-mechanisms* published by the MIT Radiation Laboratories and to the volume *Peaceful Uses of Outer Space* published by the International Federation of Automatic Control.

Kessler and Kreuzer elected Executive Vice Presidents

Robert W. Sarnoff, President, recently announced the election of **Irving K. Kessler** as Executive Vice President, Defense Electronic Products, and **Barton Kreuzer** as Executive Vice President, Commercial Electronic Systems; **W. Walter Watts** is relinquishing his duties as Senior Executive Vice President, Defense and Commercial Systems, in anticipation of his retirement next spring. Mr. Watts, who has remained active in RCA management past the normal retirement age at the request of Mr. Sarnoff, will continue on the Staff of the President as Executive Vice President.

Degrees granted

D. F. Ruggieri, MSR, Mrstn. .....BS, Business Admin., LaSalle University; 6/69
J. V. Hess, MSR, Mrstn. .....BS, Business Admin., Rutgers University; 6/69
F. G. Adams, MSR, Mrstn...MS, Mechanical Engineering, Drexel Institute of Tech; 6/69
B. J. Giancola, MSR, Mrstn. .....MS, Physics, University of Delaware; 6/69
A. L. Dietz, MSR, Mrstn. .....MSEE, Drexel Institute of Technology; 6/69
M. Stoll, MSR, Mrstn. .....BS, LaSalle University; 6/69
J. L. Arensberg, MSR, Mrstn. .....MS, University of Pennsylvania; 5/69
R. L. Burke, MSR, Mrstn. .....MSEE, Drexel Institute of Technology; 6/69
R. R. Kowalczyk, MSR, Mrstn. .....MS, Electrical Physics, LaSalle University; 6/69
P. W. Schirmer, MSR, Mrstn. .....BSEE, Drexel Institute of Technology; 6/69
J. F. O'Brien, MSR, Mrstn. .....MSE, University of Pennsylvania; 8/69

Promotions

As reported by your Personnel Activity during the past two months. Location and new supervisor appear in parentheses.

RCA Global Communications, Inc.

J. W. Cuddihy from Design Engineer to Group Leader, Satellite and Radio Engineering (J. M. Walsh, New York)

J. Muller from Design Engineer to Group Leader, Mechanical Design Group, Equipment Design (S. N. Friedman, New York)

M. P. Rosenthal from Senior Member Technical Staff, RCA Defense Advanced Communications Lab., W. Windsor Township, N. J. to Group Leader, Engineering Services (E. J. Williamson, New York)

L. Spann from Project Engineer to Group Leader, Equipment System Group, Equipment Design (S. N. Friedman, New York)

DEP Missile and Surface Radar Division

W. Kinslow from A Engineer to Ldr. D&D, Info. Sys. & Human Factors (Dr. Ireland, Moorestown)

A. Reich from AA Engineer to Ldr., Eng. Sys. Project, ALCOR (W. Scull, Moorestown)

L. Saffitz from AA Engineer to Ldr., Sys. Engrg., E. W. Systems (M. Etengoff, Moorestown)

W. S. Sepich from AA Engineer to Mgr., Equip. Des & Dev., Mech. Engrg. & Radiation Equipment (P. Levi, Moorestown)

T. S. Stecki from A Engineer to Ldr., D&D, Engrg. Depot Engrg. (R. M. Fisher, Moorestown)

B. Stockwell from A Engineer to Ldr., Sys. Engrg., Ground Tactical Systems (E. Roberts, Moorestown)

Information Systems Division

L. Limbaugh from Ldr. Tech. Staff to Mgr. Communications & Special Design Engineering (H. N. Morris, West Palm Beach)

Electronic Components
Solid State and Receiving Tube Division

S. Katz from Associate Engineer, Product Develop. to Eng., Ldr., Product Develop. Advanced Applications and Devices Department (Dr. F. Sterzer, Somerville)

W. Lawrence from Eng. Ldr., Prod. Develop., Harrison to Mgr., Engineering in the Liquid Crystal Program (Norman Freedman, Somerville)

Television Picture Tube Division

M. I. Jefferson from Engineer, Manufacturing to Manager Production Engineering (N. R. Meena, Marion)

R. L. Leigh from Engineering Leader, Product Develop. to Mgr., Chemical and Physical Laboratory, (D. J. Ransom, Marion)

R. L. Whitlock from Engineer, Manufacturing to Manager, Production Engineering (N. Meena, Marion)

DEP Defense Engineering

J. Friedman from A Engineer to Ldr., Des. & Dev. Eng., Advanced Technology (M. G. Pietz, Camden)

Commercial Electronics Systems Division

N. Nikolayuk from AA Engineer to Ldr. Design & Development Engineers, Pylon Antenna Design Group (R. L. Rocomora, Camden)

Staff Announcements

Defense Electronic Products

I. K. Kessler, Executive Vice President, Defense Electronic Products, appointed **M. L. Long** as Division Vice President and General Manager, Defense Communications Systems Division, and **P. A. Piro,** Division Vice President and General Manager, Missile and Surface Radar Division.

J. F. Burlingame, formerly Division Vice President and General Manager, Defense Communications Systems Division appointed **M. Goldman** as Manager, Programs Management.

Operations Staff

Chase Morsey, Jr., Executive Vice President has appointed **R. C. Bitting** as Program Director, PREVS (Pre-Recorded Electronic Video Systems.

B. V. Dale, Manager, Automatic Test and Measurement Systems has appointed **J. L. Miller** as Manager, International Test and Measurement Systems.

RCA Laboratories

H. R. Lewis, Director, Materials Research Laboratory has appointed **B. Abeles** as Head, General Research, Materials Research Laboratory.

C. C. Foster, Manager, Technical Information Services, has announced the organization of Technical Information Services as follows: **R. F. Ciafone,** Editor, *RCA Review;* **Miss F. I. Cloak,** Librarian; **S. F. Dierk,** Administrator, Documentation and Reports; **C. W. Sall,** Administrator, Technical Publications.

L. R. Weisberg, Director, Semiconductor Device Research Laboratory has appointed **H. Kressel** as Head, Semiconductor Optical Devices Research.

Electronic Components

J. B. Farese, Executive Vice President, Electronic Components has appointed **L. Gillon** as Division Vice President and General Manager, Television Picture Tube Division.

D. D. Van Ormer, Manager, Color Picture Tube Engineering, has appointed **A. J. Torre** as Manager, Application and Reliability Engineering Laboratory.

K. A. Thomas, Manager, Photo-Tube Manufacturing, has appointed **E. J. Vresilovic** as Engineering Leader, Manufacturing (Photo Tube).

R. A. Nolan, Manager, Development Shop —Color, has appointed **G. R. Fadner** as Engineering Leader, Product Development—Color Development Shop.

R. L. Klem, Manager, Safeguard Program has appointed **G. J. Andeskie** as Manager, Quality and Reliability Assurance; **W. N. Lewis** as Engineering Leader—Wafer Preparation; and **J. A. Schramm** as Manager, Manufacturing.

Information Systems Division

J. R. Lenox, Division Vice President, Manufacturing and Engineering, has appointed **B. W. Pollard** as Manager of the newly created organization, New Product Line Systems Development.

Professional activities

Aerospace Systems Division

A. W. Sinkinson was a session chairman at the NEPCON East Symposium in Philadelphia, Pa., on June 10-12, 1969.

RCA leads in IR-100 Awards for 1969

RCA was the top winner in this year's Annual IR-100 Competition sponsored by *Industrial Research* magazine. Seven technical developments originating at the David Sarnoff Research Center were selected among the 100 most significant new technical products in 1969. The awards were announced at a banquet held at the Museum of Science and Industry, Chicago, Ill., where displays of the prize winners remained on exhibit from mid-September to mid-October.

The seven RCA developments which won are:

1) Mixed liquid crystal storage display;
2) Reversible holographic storage medium;
3) Single-stage lumped-element 2-GHz 1-watt amplifier;
4) Sonic film memory;
5) High efficiency series-operated Gunn device;
6) Digitally scanned image-sensor array; and
7) Close-confinement injection laser.

The *RCA Review* is published quarterly. Copies are available in all RCA libraries. Subscription rates are as follows (rates are discounted 20% for RCA employees):

	DOMESTIC	FOREIGN
1-year	$4.00	$4.40
2-year	7.00	7.80
3-year	9.00	10.20

RCA develops color-TV tape player using lasers and holography

SelectaVision—a low-cost color TV tape player destined for home use in the early 1970's—was demonstrated and plans for its production were outlined recently at RCA Laboratories.

In commercial form, the tape player is expected to be the first consumer product to employ lasers, and will be designed to attach to the antenna connections of any standard color television set. It will play full-color programs recorded on low-cost clear-plastic tapes.

The tapes are scratch-proof, dust-proof, and virtually indestructible under conditions of normal use. They will have countless replay capabilities, be able to be run in slow motion, or be able to be stopped and started at will. The player will be compact and as easy to operate as a modern cartridge player.

Present plans call for production of SelectaVision players to commence in 1972. Shortly thereafter they will be offered for sale to the public at a target price of under $400 per unit. At the same time, a library of 100 original program albums in the half-hour to hour category will be offered for use with the players. Their target price is about $10 per half-hour program (much less expensive than present videotape or other proposed film-replay media).

At present, SelectaVision tapes are not made directly from life, but from movie films. The film is converted by a laser to a series of holograms (optical interference patterns) recorded on a plastic tape coated with photoresist—a material that hardens to varying degrees depending on the intensity of the light striking it.

Next, the tape is developed in a chemical solution that eats away the portions of the photoresist not hardened by the laser beam. The result is a relief map of photoresist whose hills and valleys, and the spacing between, represent the original color TV program in coded form. This is called the hologram master. This master is plated with a thick coating of nickel and stripped away, leaving a nickel tape with the holograms impressed as a series of engravings. This is called the nickel master. Finally, the nickel master is fed through a set of pressure rollers along with a transparent vinyl tape of similar dimensions, and the holographic engravings on the master are impressed on the smooth surface of the vinyl as holographic reliefs, producing a SelectaVision program tape ready for home use. The nickel master can be used to press thousands of SelectaVision tapes in this way without degradation.

Playback of such a tape requires only that the beam from a very low-powered laser pass through it into a simple, low-cost TV camera which sees the images reconstructed by the laser directly, and their colors as coded variations in those images. The playback mechanism, the laser, and the TV camera are all housed in the SelectaVision player, which is attached to the antenna terminals of a standard color TV set for actual program viewing. (SelectaVision programs are fully compatible, and may also be viewed on black-and-white sets without color.)

The principal elements of the SelectaVision player are: 1) a helium-neon laser, 2) a vidicon TV camera, and 3) a simple tape transport.

Specifications of the demonstration-model SelectaVision player are as follows:

Tape speed	7½ in./sec.
Tape width	½ in.
Tape thickness	2 mil.
Laser wavelength	6328 Å
Laser power	2 mW
Luminance bandwidth	3 MHz
Chrominance bandwidth	0.5 MHz
Playing time	½ hour
Reel diameter	6 in.

Awards

Aerospace Systems Division

Ronald P. Gallagher of Electro-Optics and Controls Engineering has been selected as Engineer of the Month of June for his contributions to the proposal for the Manned Space Station.

The team of **Martin D. Brazet, Richard de Pierre, Donal W. Fogg, Norman G. Hamm, Robert P. Morin, Donald A. Panaccione, Russell F. Wade, Wilfred J. Wagner,** and **Gerald J. Zerfas** from RF Engineering has been chosen for a Team Award for June. The team was selected for its outstanding work on the LM RRBTC program.

Carl A. Heldwein of Radar Engineering, has been selected as Engineer of the Month for May. The selection recognizes his outstanding work in the system engineering of the Pulsed Doppler Radar.

The team of **J. E. Larmand, W. H. Neve, J. N. Ostis, W. J. Perreault, J. A. Rhynd,** and **S. P. Skinner** from Systems Support Engineering has received a team award for the month of May. The team is recognized for its outstanding work in the Category I tests of AN/TSW-7 system at Otis Air Force Base.

Frank A. Barnes of Systems Development and Applications has been selected as Engineer of the Month for July for his outstanding work in the development of a novel gunflash detection system.

The team of **Allan A. Alaspa** and **Dennis G. Tachnick** from RF Engineering has received a team award for the month of July for outstanding work in the application of PMOS technology to the design of the logic circuits of the APN-194 Radar Altimeter.

A Department of Defense achievement award is presented to the RCA Service Company, represented by J. F. Murray (center) Division Vice President of Government Services, and W. D. Russell, Manager of Administrative Controls and Systems. The presentation was made by Lt. Col. E. B. Turner, U. S. Army Commander of the Camden Defense Contract Administrative Services District. The award was given in recognition of the company's efforts in cost reductions on government contracts. Since 1964 the RCA Service Company has achieved approximately $30 million in cost savings on Department of Defense contracts.

Seminars in Modern Optics and Digital Communications

The Institute for Professional Development, RCA Institutes, has developed two unique short courses—Digital Communications and Modern Optics. These five-day intensive seminars are offered to engineers and stress practical approaches to actual design situations.

Modern Optics is addressed to two classes of professionals: the engineer newly entering optics, and the experienced opticist trained in classical methods. The past twenty years have seen a dramatic revival in the field of optics, due to greatly improved theoretical and experimental techniques (refer to the Sutton, Panati article, p. 64).

The objectives of the Digital Communications seminar are: 1) to develop an understanding as to how signals may be extracted from heavy noise; 2) to determine under what conditions certain coding schemes are optimum; 3) to provide practical applications of information theory; 4) to examine the types of distortion inherent in digitizing an analog signal; 5) to investigate the advantages of digital over analog transmission in the noisy channel; 6) to examine various modulation techniques in the context of information theory; and 7) to convey practical design criteria for the digital hardware at either end of a data link.

For further information on either of these seminars, contact: RCA Institutes, Inc. Institute for Professional Development, P.O. Box 962, Clark, New Jersey 07066.

Editorial Representatives

The Editorial Representative in your group is the one you should contact in scheduling technical papers and announcements of your professional activities.

Defense and Commercial Systems

Defense Electronic Products

Aerospace Systems Division
D. B. DOBSON* Engineering, Burlington, Mass.

Electromagnetic and Aviation Systems Division
R. J. ELLIS* Engineering, Van Nuys, Calif.
J. McDONOUGH Engineering, West Los Angeles, Calif.

Astro-Electronics Division
I. M. SEIDEMAN* Engineering, Princeton, N.J.
S. WEISBERGER Advanced Development and Research, Princeton, N.J.

Missile & Surface Radar Division
T. G. GREENE* Engineering, Moorestown, N.J.

Defense Communications Systems Division
A. LIGUORI* Engineering, Camden, N.J.

Defense Engineering
M. G. PIETZ* Advanced Technology Laboratories, Camden, N.J.
M. R. SHERMAN Defense Microelectronics, Somerville, N.J.
E. J. PODELL Systems Engineering, Evaluation, and Research, Moorestown, N.J.
J. E. FRIEDMAN Advanced Technology Laboratories, Camden, N.J.
J. L. KRAGER Central Engineering, Camden, N.J.

Commercial Electronics Systems Division

D. R. PRATT* Chairman, Editorial Board, Camden, N.J.
N. C. COLBY Mobile Communications Engineering, Meadow Lands, Pa.
C. E. HITTLE Professional Electronic Systems, Burbank, Calif.
R. N. HURST Studio, Recording, & Scientic Equip. Engineering, Camden, N.J.
K. C. SHAVER Microwave Engineering, Camden, N.J.
R. E. WINN Broadcast Transmitter & Antenna Eng., Gibbsboro, N.J.

Industrial and Automation Systems
H. COLESTOCK Engineering, Plymouth, Mich.

Information Systems

Information Systems Division

M. F. KAMINSKY* Engineering, Camden, N.J.
M. MOFFA Engineering, Camden, N.J.
S. B. PONDER Palm Beach Engineering, West Palm Beach, Fla.
R. J. McLAUGHLIN Engineering, Marlboro, Mass.

Magnetic Products Division
A. G. EVANS Development, Indianapolis, Ind.

Memory Products Division
L. A. WOOD Engineering, Needham, Mass.

Graphic Systems Division
J. GOLD* Engineering, Dayton, N.J.

Research and Engineering

Laboratories

C. W. SALL* Research, Princeton, N.J.

Consumer Products and Components

Electronic Components

C. A. MEYER* Chairman, Editorial Board, Harrison, N.J.

Solid State and Receiving Tube Division
M. B. ALEXANDER Solid State Power Device Engrg., Somerville, N.J.
R. W. MAY Commercial Receiving Tube and Semiconductor Engineering, Somerville, N.J.
I. H. KALISH Solid State Signal Device Engrg., Somerville, N.J.
J. KOFF Receiving Tube Operations, Woodbridge, N.J.
T. J. REILLY Semiconductor and Conversion Tube Operations, Mountaintop, Pa.
R. J. MASON Receiving Tube Operations, Cincinnati, Ohio
J. D. YOUNG Semiconductor Operations, Findlay, Ohio

Television Picture Tube Division
J. H. LIPSCOMBE Television Picture Tube Operations, Marion, Ind.
E. K. MADENFORD Television Picture Tube Operations, Lancaster, Pa.

Industrial Tube Division
J. M. FORMAN Industrial Tube Operations, Lancaster, Pa.
H. J. WOLKSTEIN Microwave Tube Operations, Harrison, N.J.

Technical Programs
D. H. WAMSLEY Engineering, Harrison, N.J.

Consumer Electronics Division

C. HOYT* Chairman, Editorial Board, Indianapolis, Ind.
D. J. CARLSON Advanced Devel., Indianapolis, Ind.
R. C. GRAHAM Procured Products Eng., Indianapolis, Ind.
P. G. McCABE TV Product Eng., Indianapolis, Ind.
J. OSMAN Electromech. Product Eng., Indianapolis, Ind.
L. R. WOLTER TV Product Eng., Indianapolis, Ind.
R. F. SHELTON Resident Eng., Bloomington, Ind.

Services

RCA Service Company

B. AARONT EDP Service Dept., Cherry Hill, N.J.
W. W. COOK Consumer Products Service Dept., Cherry Hill, N.J.
M. G. GANDER* Consumer Product Administration, Cherry Hill, N.J.
K. HAYWOOD Tech. Products, Adm. & Tech. Support, Cherry Hill, N.J.
W. R. MACK Missile Test Project, Cape Kennedy, Fla.

RCA Global Communications, Inc.

W. S. LEIS* RCA Global Communications, Inc., New York, N.Y.

National Broadcasting Company, Inc.

W. A. HOWARD* Staff Eng., New York, N.Y.

Record Division

M. L. WHITEHURST* Record Eng., Indianapolis, Ind.

RCA International Division

C. A. PASSAVANT* New York, N.Y.

RCA Ltd.

W. A. CHISHOLM* Research & Eng., Montreal, Canada

Education Systems

Instructional Systems

E. M. MORTENSON* Instructional Systems Engineering, Palo Alto, Cal.

*** Technical Publication Administrators listed above are responsible for review and approval of papers and presentations.**